Florida Department of Transportation

Title

# EFFECTS OF VIBRATION AND SOUND DURING THE INSTALLATION OF DEEP FOUNDATIONS

Part of State Project No. 99700-3361-010, WPI No. 0510794


Dr. D. V. Reddy
Principal Investigator
Professor and Director
Center for Marine Structures and Geotechnique
Department of Ocean Engineering
Florida Atlantic University
Boca Raton, FL

Dr. K. Tawfiq
Subcontractor
Associate Professor and Associate Chairman
Department of Civil Engineering
Florida State University
Tallahassee, FL

Dr. S. Putcha
Contractor Monitor
State Geotechnical Construction Engineer
Florida Department of Transportation
Tallahassee, FL


August 2000

## ACKNOWLEDGEMENTS

The Principal Investigator, Dr. D. V. Reddy, and the Subcontractor, Dr. K. S. Tawfiq, would like to thank the Florida Department of Transportation (State Project # 99700-3361-010, Work Program # 0510794 Contract # BA 510) for its generous financial support. Gratitude is expressed to the Contract Monitor Dr. S. Putcha, State Construction Geotechnical Engineer, Construction Division, FDOT, Tallahassee, FL, for his continued interaction with invaluable input, encouragement, and guidance.

Thanks are due to following agencies/companies for their participation and support :

| | |
|---|---|
| Florida Department of Transportation, District Two (Mr. Dan Turner) | 1901, South Marion Street, Lake City, FL 32025 |
| Law Engineering and Environmental Services, Inc. (Mr. K. McIntosh) & Mr. B. Kinney, Jr) | 3901, Carmichael Ave. Jacksonville, FL 32207<br>2104, Corporate Drive, Boynton Beach, FL 33426 |
| Williams Earth Sciences, Inc. | 11329, Distribution Avenue West Jacksonville, FL 32356 |
| Technos, Inc. | 3333, Northwest 21st Street Miami, FL 33142 |
| Goble Rausche Likins and Associates, Inc. | 8008, S.Orange Ave. Orlando, FL 32809 |
| Coastal Caisson, Inc. | 12290, US 19 N Clearwater, FL 34624 |
| Curry Industries, Inc. | 3020, NE 188th Street, Miami, FL 33180 |
| Environmental Noise Control | 4402, Southwest 74th Avenue,Miami, FL 33155-4408 |

Appreciation is expressed to Mr. C. S. Gonzalez- Mier, former Graduate Assistant at FAU, who was the principal contributor for the field investigation on drilled shafts with his M.S. thesis based on the project, and Mr. R. Ruiz, former Research Engineer at FSU, who helped with the laboratory testing . Other graduate students at FAU, who participated, were Mr. B. Butul, Mr. B. Carratt, Mr. C. Cazagnaire, Ms. K. Surles, Mr. F. Navarette, and Mr. T. Pierro. Mr. T. Pierro was the principal contributor for the laboratory and field investigation of pile noise.

The administrative support of Dr. S.E. Dunn, Professor and Chairman, Department of Ocean Engineering, and Dr. J. T. Jurewicz, Dean of Engineering, Florida Atlantic University, is gratefully acknowledged.

# EXECUTIVE SUMMARY

This project addresses two frequent construction problems associated with deep foundation installation: i) The effect of vibrations induced during the installation of drilled shafts, on "green concrete", defined as freshly placed and maturing concrete within 24 hours after initial placement, and ii) Noise levels during pile driving due to the low threshold of human perception.

The laboratory investigation addressed the determination of the damage threshold particle velocity by shake table vibration testing of concrete cylinders at predetermined time delays (0,1,2,3,4, and 24 hours), ultrasonic testing for compression moduli before compressive strength testing, and testing of cored cylinders from full scale drilled shafts.The principal finding from laboratory testing was that construction vibrations that produce particle velocities less than 8 in./sec would not have any effect on the compressive strength or compression modulus of the concrete aged between the time of placement to the first 24 hour.

In the field investigation, the peak particle velocities during drilled shaft were monitored to determine their effect on "green concrete". The principal findings from the field study are as follows: i) Vibrations, with peak particle velocities of upto 2.5 in./sec do not cause damage to the "green concrete" at a distance of two times the shaft diameter and beyond. ii) In general, a spacing of three times the shaft diameter would be a safe specification to ensure no concrete damage due to shaft vibration.

In Part 2, the propagation of noise generated from the driving of concrete piles was measured and the effect of mitigation though the use of an acoustic curtain evaluated. This project focused on the use of an acoustic curtain constructed of a combination of absorptive and reflective materials to provide a complete enclosure of the source to mitigate the propagation of the inherent noise. In the field, a full-scale experiment was conducted by evaluating noise levels generated from the installation of concrete piles, with and without the aid of the acoustic curtain, a reinforced polyvinyl chloride outer shell for added mass, with a specially developed inner lining of 2in. thick fiber glass acoustic insulation (1.5 $lb/ft^2$). The results indicated that noise levels were reduced by up to 10dB, with the curtain enclosing the diesel hammer. Further research is recommended.

# SUMMARY

This project addresses one of the frequent construction problems associated with deep foundation installation. The primary concern is the effect of vibrations on "green" concrete, where, "green" concrete as defined in this paper refers to freshly placed and maturing concrete within 24 hours after initial placement. And the noise levels during pile during due to the low threshold of human perception.

The project is divided into two parts. Part 1 addresses the" Effects of Vibrations Induced During the Installation of Drilled Shafts" and Part 2, the " Effects of Sound Induced During the Installation of Piles". Part 1 comprises Field and Laboratory Investigations. The field work was carried out by Florida Atlantic University, FAU laboratory at four sites-two preliminary tests at FAU, one in Delray Beach, FL, and the other in Clearwater, FL. The laboratory investigation was done by Florida State University, FSU. Part 2, a minor component of the research project, was mainly a field investigation with a component of laboratory work, all of which was carried out by FAU.

In Part 1, a review of the characteristics of construction vibration is followed by a laboratory investigation to determine the peak particle velocity by shake table vibration testing of concrete cylinders at predetermined time delays (0,1,2,3,4, and 24 hours) and their compressive strength testing at 3, 7, 14, and 28 days. The input signals were based on field acceleration records transformed from the time domain to the frequency domain by using the Fast Fourier Transform(FFT). The measurements also included ultrasonic testing for compression moduli before compressive strength testing. Core samples from full-scale drilled shafts were also tested in the laboratory. The field investigation addressed the monitoring of drilled shaft installation-induced vibrations (peak particle

velocities) in the ground and their effect on "green concrete". Sets of two shafts 24" (unreinforced) and 36" (reinforced) were installed. The purpose of the smaller shaft was to determine the effect on the integrity and strength of a shaft within a three diameter distance from the vibrating source. The instrumentation consisted of subsurface triaxial accelerometers attached to the steel casing, surface accelerometers in the ground, and geophones at varying depths in a circular array around the vibrating steel casing. Both control concrete and cored concrete cylinders were tested for compressive strength. The Pile Integrity Testing (PIT)- a combination of the Pulse Echo Method (PEM) and the Transient Response Method (TRM), and Cross-Hole Sonic Logging (CSL) were the Nondestructive Testing Methods used. Additionally, Geophysical Logging was carried out with neutron-neutron (porosity) and gamma-gamma (density) measurements.

Vibrations, with peak particle velocities of up to 2.5in./sec did not cause damage to the "green concrete". The PIT and CSL tests also indicated no damage, although the data at the Clearwater site was incomplete for the upper thirds of the shaft poured. The recommendation is made for using strains, rather than particle velocities, to monitor damage in "green concrete", as the same velocity would produce different strains amplitudes in different materials and in different structures. The principal findings are as follows: 1) a spacing of 3 times the diameter of a shaft, between shafts, seems to be generally conservative, 2) concrete cured upto 24 hours is not damaged due to vibrations due to particle velocities upto 2.5 in/sec.

In Part 2, the propagation of noise generated from the driving of concrete piles was measured and the effect of mitigation though the use of an acoustic curtain evaluated. This project focused on the use of an acoustic curtain constructed of a

evaluated. This project focused on the use of an acoustic curtain constructed of a combination of absorptive and reflective materials to provide a complete enclosure of the source to mitigate the propagation of the inherent noise.

Tests were conducted in a laboratory chamber, with a sample acoustic curtain, indicated noise level reductions more than 16 dB, identifying the strong need for field testing. In the field, a full-scale experiment was conducted by evaluating noise levels generated from the installation of concrete piles, with and without the aid of the acoustic curtain, a reinforced polyvinyl chloride outer shell for added mass with a specially developed inner lining of 2in. thick fiber glass acoustical insulation (1.5 $lb/ft^2$). The results indicated that noise levels were reduced by up to 10dB, with the curtain enclosing the diesel hammer. Further research is recommended.

# Table of Contents

## Part I

## Effects of Vibration Induced during The installation of Drilled shafts


**Chapter 1: Introduction**

| | | |
|---|---|---|
| 1.1 | Statement of the Problem | 1 |
| 1.2 | Background | 3 |
| 1.3 | Scope of the Work | 3 |
| 1.4 | Report Organization | 5 |
| 1.5 | Objectives and approach-6 | 5 |

**Chapter 2: Background**

| | | |
|---|---|---|
| 2.1 | Characteristics of Construction Vibrations | 8 |
| 2.1.1 | Peak Component and True Vector Sum | 18 |
| 2.1.2 | Propagation Velocity | 20 |
| 2.1.3 | Strains from Particle Velocities | 22 |
| 2.2 | Response of Cohesion less Soil Deposits Under Construction Vibrations | 23 |
| 2.2.1 | Comparison of Values of $(K_2)_{max}$ for Sands Determined by Laboratory and Field Tests | 26 |
| 2.3 | Concrete Vibration | 33 |

**Chapter 3: Laboratory Testing**

| | | |
|---|---|---|
| 3.1 | Introduction | 39 |
| 3.2 | Test Methodology | 41 |

**Chapter 4: Site Characterization and Field Testing**

| | | |
|---|---|---|
| 4.1 | Site Characterization | 47 |
| 4.2 | Field Vibration Testing | 48 |
| 4.2.1 | Field No.1 (FAU, Boca Raton, FL) | 48 |
| 4.2.1.1 | Site Preparation | 49 |
| 4.2.1.2 | Instrumentation and Vibratory Excitation | 49 |
| 4.2.1.3 | Monitoring of Vibrations | 50 |
| 4.2.2 | Field Test No.2 (FAU, Boca Raton, FL) | 51 |
| 4.2.2.1 | Site Preparation, Procedures and Monitoring of Ground Vibration | 52 |
| 4.2.2.2 | Drilled Shaft Configuration and Installation Procedures | 53 |
| 4.2.3 | Field Test No.3 (Delray Beach, FL) | 55 |
| 4.2.4 | Field Test No. 4 (Clear water, FL) | 56 |
| 4.2.5 | Vibration Data | 56 |
| 4.3 | Testing of Control Concrete cylinders | 56 |
| 4.4 | Non-Destructive Testing | 57 |
| 4.4.1 | Pile Integrity Testing (PIT) | 57 |
| 4.4.2 | Cross-Hole Sonic Logging (CSL) | 57 |

| | | |
|---|---|---|
| 4.5 | Concrete Coring of the Drilled Shafts and Compression Testing | 57 |
| 4.6 | Geophysical Logging | 58 |
| 4.6.1 | Neutron-Neutron Radiation | 58 |
| 4.6.2 | Gamma- Gamma Radiation | 58 |

**Chapter 5: Analysis of Results and Discussion**

| | | |
|---|---|---|
| 5.1 | Laboratory Test Results | 86 |
| 5.2 | Analysis of Field Results | 87 |
| 5.2.1 | FAU Field Test #1 | 87 |
| 5.2.2 | FAU Field Test #2 | 120 |
| 5.3 | Field Monitoring of Induced Ground Motion | 135 |

**Conclusion:** 160

**References:** 164

**Part II**

**Effects of Sound Induced during the Installation of Piles**

**Chapter 1: Pile Driving Noise Mitigation Through Use of an Acoustic Curtain**

| | | |
|---|---|---|
| 1.1 | Background | 167 |
| 1.2 | Laboratory Testing | 167 |
| 1.2.1 | Test Setup | 167 |
| 1.2.2 | Test results | 168 |
| 1.3 | Field Testing | 168 |
| 1.3.1 | Field Test setup | 168 |
| 1.3.2 | Pile Driving | 170 |
| 1.3.3 | Noise Measurements | 171 |
| 1.3.4 | Acoustic Curtain | 172 |
| 1.3.5 | Discussion and Conclusions | 177 |

**References:** 177

**Appendix A** A1-A24

**Appendix B** B1-B7

**Appendix C** C1-C35

**Appendix D** D1-D3

**Appendix E** E1-E10

**Appendix F** F1-F11

**Appendix G** G1-G4

**Appendix H** H1-H16

**Appendix I** I1-I10

**Appendix J** J1-J41

## FIGURES

### PART I


| | Page |
|---|---|
| 1.1 Effect of vibration on freshly placed concrete | 7 |
| 2.1 Construction vibration generating compression waves | 10 |
| 2.2 Generation and propagation of surface and body shear waves due to a driven casing | 11 |
| 2.3 Constructional vibration generating Rayleigh waves | 12 |
| 2.4 Vertical, longitudinal and traverse mode of steel casing vibrations | 14 |
| 2.5 Operating principle of vibrator with dual rows of eccentric mass | 19 |
| 2.6 Principal wave types and particle displacement paths during the passage of surface waves | 27 |
| 2.7a Shear moduli of sands at different void rations | 28 |
| 2.7b Shear moduli at different relative densities | 29 |
| 2.8 Variation of shear modulus with shear strain for sands | 30A |
| 2.9 Variation of shear modulus with shear strain for sands | 30B |
| 2.10 Vibratory cracking of curing concrete | 38 |
| 3.1 Shacking table used in the study | 42 |
| 3.2 Ultrasonic testing for concrete samples | 44 |
| 3.3 Concrete samples subjected to different level of vibration amplitudes and at various delay Times | 46 |
| 4.1a Testing setup for each borehole | 59 |
| 4.1b Recording steel easing and ground responses using FFT Analyzer | 60 |
| 4.1c Accelerometer layout | 61 |
| 4.1d Traces 15 and 16 showing accelerometer #1 for the vibrating casing, and the ground surface accelerometer #2 at 15' away from the testing | 62 |
| 4.1e Traces 7 and 8 showing accelerometer #1 on the vibrating casing, and the ground surface accelerometer #2 at 10' away from the casing | 63 |
| 4.2 FAU Field Testing showing the arrangement of the geophones and the driven steel Casing | 64 |
| 4.3 Arrangements of geophones in PVC tubes at FAU test site | 65 |
| 4.4 The extraction process of the steel casing | 66 |
| 4.5a Configuration and instrumentation of the shafts at the Delray Site | 67 |
| 4.5b Layout of Delray Testing Site | 68 |
| 4.6 Geophone locations in the drilled shaft(Delray Beach) | 69 |
| 4.7 Placing of steel reinforced with instrumentation set no.4 (Delray Beach.Florida) | 70 |
| 4.8 Dropping the tremmie in the hole,Set no.4 (Delray Beach,Florida) | 71 |
| 4.9 Pulling of steel casing after pouring of the concrete, Set no.4 (Delray Beach,Florida) | 72 |
| 4.10 CSL tubes and settlement plant,$\phi$36" drilled shaft, Set no.1 (Delray Beach,Florida) | 73 |
| 4.11 Geophone data acquisition system, (Delray Beach,Florida) | 74 |
| 4.12 Layout of clearwater testing site | 75 |
| 4.13 Installation of the 24-inch diameter steel casing(Clearwater,FL) | 76 |
| 4.14 Installation of the 36-inch diameter steel casing(Clearwater,FL) | 77 |
| 4.15 Steel cage with geophone and cross-hole sonic logging instrumentation (Clearwater,FL) | 78 |

4.16 Placing the steel cage in the drilled shaft(Clearwater,FL) 79
4.17 Vibration of casing adjacent to freshly poured shafts(Clearwater,FL) 80
4.18 Surface placement of cylinders exposed to 2-hr vibration (Clearwater,FL) 81
4.19 PIT on shaft(Clearwater,FL) 82
4.20 CSL tubes and geophones in place on the steel reinforcing cage. 83
4.21 CSL recording equipment (Delray Beach,Florida) 84
4.22 Cored drilled shaft(Delray Beach,Florida) 85

5.1 Compressive strength of concrete samples subjected to acceleration of 88
5.2 Compressive strength of concrete samples subjected to acceleration of 14g 89
5.3 Compressive strength of concrete samples subjected to acceleration of 30g 90
5.4 Compressive strength of concrete samples after 3 days 91
5.5 Compressive strength of concrete samples after 7 days 92
5.6 Compressive strength of concrete samples after 14 days 93
5.7 Compressive strength of concrete samples after 3 days; vibration amplitude =30g 94
5.8 Compressive strength of concrete samples after 7 days; vibration amplitude-30g 95
5.9 Compressive strength of concrete samples after 14 days; vibration amplitude-30g 96
5.10 Compressive strength of concrete samples after 28 days; vibration amplitude=30g 97
5.11 Compressive strength vs. velocity amplitude for all the tested samples 98
5.12 Compression modulus of concrete vs. velocity amplitude for all the tested sample 99
5.13 Compression modulus of concrete vs. velocity amplitude for the time delay used in testing 100
5.14 Vibratory drilled shaft casing generating shear waves in the surrounding soil 106
5.15 Time-history record of the steel casing at an accelerometer 5 ft from the ground 107
5.16 Time-history record of the steel casing at an accelerometer 5 ft from the ground 108
5.17 Time-history record of the steel casing at an accelerometer 5 ft from the ground 109
5.18 Time-history record of the steel casing at an accelerometer 5 ft from the ground 110
5.19 Time-history record of the steel casing at an accelerometer 5 ft from the ground 111
5.20 Time-history record of the steel casing at an accelerometer 5 ft from the ground 112
5.21 Time-history record of the steel casing at an accelerometer 5 ft from the ground 113
5.22 Time-history record of the steel casing at an accelerometer 5 ft from the ground 114
5.23 Frequency content of a 40 ft drilled shaft steel casing driven to 1.5 ft in sandy soil 116
5.24 Frequency content of a 40 ft drilled shaft steel casing driven to 5 ft in sandy soil 117
5.25 Frequency content of a 40 ft drilled shaft steel casing driven to 8 ft in sandy soil 118
5.26 Frequency content of the steel casing due to 10 ft penetration 119
5.27 Dominant frequency of the steel casing at penetration depth of 1.Sft 121
5.28 Dominant frequency of the steel casing at penetration depth of5 ft 122
5.29 Dominant frequency of the steel casing at penetration depth of8 ft 123
5.30 Predominant frequency of the steel casing at penetration depth of 10 ft in the ground 124
5.31 Frequency content of the ground surface vibration due to an 8 ft casing penetration 125
5.32 Dominant frequency of the ground surface due to 8 ft casing penetration 126
5.33 Frequency content of the ground surface due to casing penetration of 10 ft 127
5.34 Predominant frequency of the ground due to a casing penetration of 10 ft 128
5.35 Dominant frequency of the ground surface due to 12 ft casing penetration 129
5.36 Drop in the ground level after completing the driving process 130
5.37 Grain size distribution of sand obtained from FAU site 131

5.38 Shear wave velocity vs. depth at FAU Site 137
5.39 Standard penetration test results of boring #1 at FAU site 138
5.40 Standard penetration test results of boring #2 at FAU site 139
5.41 Shear wave velocity vs. depth using laboratory test results and SPT blow countvalues 140
5.42 Shear wave velocity vs. depth using laboratory test results and SPT blow count values for the second boring log 141
5.43 Shear wave velocity vs. depth using laboratory test results and SPT blow count values for the Delray Site 142
5.44 Shear wave velocity vs. depth using laboratory test results and SPT blow count value for the Delray site boaring # 2 143
5.45 Shear wave velocity vs. depth 144
5.46 Shear wave velocity vs. depth in uniform, fine sand 145
5.47 Shear wave velocity vs. Depth in rock 146
5.48 Variation of Rayleigh wave velocity with depth-Eglin Field Site 147
5.49 Particle velocity vs. Penetration depth of the steel easing 149
5.50 Factor vs Penetration Depth of the Drilled Shaft Casing 150
5.51 Factor vs. Penetration Depth of the Drilled Shaft Casing 151
5.52 Change in the particle velocity with penetration depth of drilled shaft Casing 152
5.53 Vibration levels at individual geophones during driving ranges 153
5.54 Average recorded vibration for different depths of drivings 154
5.55 Compressive strength of control samples 155
5.56 Compression strength of cored samples 156

**PART II**

1. Enclosed chamber with no reverberation 167
2. Site selection 169
3. Field test setup 170
4.a Pile driving 171
4.b 20 ft concrete piles 171
4.c Pile extraction 171
5.a Setting up for noise measurements at 50 ft. 172
5.b Quest 2900 SL meters 172
5.c 10 ft measurement pole with meter 172
6. Curtain and frame assembly (courtesy of ENC) 173
7.a Assembling the curtain from rectangular panels connected together by Velcro and rope 174
7.b Attaching the completed curtain to the crane with steel leads to the frame 174
7.c Erecting the pile-driving frame with the curtain attached 175
7.d Adjusting the frame to ensure the pile will be driven vertically and at the proper location 175
7.e Curtain swung open for pile installation and setup 175
7.f Attaching the skirt to the bottom of the curtain to minimize sound propagation along the ground 176
7.g Final field-test setup showing noise measurement poles and the acoustic curtain completely enclosing the pile driving apparatus. 176

## Tables


| | | |
|---|---|---|
| 2.1 | Estimated Propagation Velocities | 21 |
| 2.2 | Shear Modulus of Sand Based on Field Shear Wave Velocity Measurements | 31 |
| 5.1 | Florida Atlantic University Test Site | 102 |
| 5.2 | Analysis of Time and Frequency Domain of the Particle Velocity | 103 |
| 5.3 | Soil Properties of Samples Obtained from FAU Site on 7/31 | 104 |
| 5.4 | Determination of Shear Wave Velocity in the Sandy Soil Layer in FAU Site | 105 |
| 5.5 | Particle Velocities vs. Penetration Depth and Vertical Effective Stress | 148 |

# PART 1

# EFFECTS OF VIBRATION INDUCED DURING THE INSTALLATION OF DRILLED SHAFTS

# CHAPTER I

# INTRODUCTION

## 1.1 STATEMENT OF THE PROBLEM

Construction of drilled shafts often induces ground vibrations with varying intensities. The generation of the vibration is usually caused by the process of driving the exterior casings needed to stabilize the boreholes, in addition to the other construction related vibrations. The casing method of construction is very common in Florida, especially for deep foundations in waterways. The casing method in drilled shaft construction may be used on a temporary or permanent basis. Specifications of the Florida Department of Transportation (FDOT) require that all drilled shaft casings be removed except for those intended to be permanently placed in the boreholes ***(FDOT Specifications 455-15.4 and 455-15.5)***. If the permanent casing method is specified for certain site conditions, then the deeper shafts have to be constructed to compensate for the less of skin friction due to the presence of the casings. Another situation, where casings may become permanent, occurs due to the difficulty of withdrawing the casing from the excavations. Such situations should be assessed by the project engineer, and the contractors are usually compensated for the extra cost. On the other hand, temporary casings are removed during concrete placement in the shaft, when the concrete cures a workable condition.

Current specifications provide regulatory procedures for protection of existing structures from the drilled shaft construction induced vibrations. Under article ***455-1.1,*** structures within a distance of ten shaft diameters or the estimated shaft depth, whichever is greater, should be monitored for settlement, and for possible development of

structural cracking. Existing footings within a distance of three times the depth of the excavation, should also be monitored. The vibration monitoring equipment should be capable of detecting velocities of 2.5 mm/sec (0.1 in./sec) or less. It is mandatory that the source of vibrations cease immediately when structural settlement reaches 1.5 mm (0.06 in.)vibration levels reach 13 mm/sec (0.5 in./sec), or damage to existing structures occurs.

However, the current specifications do not provide acceptable levels of construction induced vibrations for drilled shafts with freshly placed concrete. A waiting period of about 12 to 24 hours may be required before construction proceeds. Although the FDOT specifications do not necessitate such a time span for every project, the delay periods are usually set by the project engineers at the sites. The rationale behind these restrictions is to allow additional curing time for the freshly placed concrete to avoid any possibility of changes in the physical or mechanical properties of the concrete.

Despite the fact that uncontrolled vibrations are usually not allowed during concrete placement, such restrictions have been considered by contractors as subjective and unsubstantiated.

## 1.2 BACKGROUND

In recent years, Florida has undergone a significant growth in its population. Consequently, the infrastructure of the state's roadways has been expanding to accommodate the traffic load accompanying the population growth. Continuous efforts are now underway to increase the vehicular capabilities of the roads. The greatest challenge posed is in the construction of new bridges or lane widening of existing ones or overpasses.

Some of the Florida DOT construction projects use deep foundations because of the following advantages:

- Very high load carrying capacities.
- Applicability to a wide variety of load conditions.
- Large resistance to lateral and uplift forces.
- Significant resistance to scour.

This research project addresses one of the frequent construction problems associated with deep foundation installation. The primary concern is the effect of vibrations on "green" concrete, where, "green" concrete as defined in this report refers to freshly placed and mafuring concrete within 24 hours after initial placement. The investigation addresses the effect of the stress waves due to the installation process with respect to their frequency and the peak particle velocity, and on the integrity of adjacent foundations.

## 1-3 SCOPE OF THE WORK

Several concerns have often been raised by engineers and practitioners regarding the effect of construction induced vibration during drilled shaft installation. These concerns can be listed as follows:

1 **What is the magnitude of construction vibration that can be generated without**

**affecting the properties of a freshly poured shafts?**

2 **What is the minimum allowable distance between the shafts that construction induced vibration would not adversely impact the concrete properties?**

3 **What is the minimum allowable distance between the shafts that construction induced vibration would not adversely impact the general performance of the shafts?**

4 **If there is any effect of the construction vibration at one site, is it possible that changing the site conditions may negate or augment these effects?**

The extent of these questions has necessitated the current investigation. The effect of construction -induced vibrations on the overall performance of drilled shafts involves full scale load testing and settlement monitoring setups.

To investigate the effect of the induced vibration on drilled shafts with the freshly placed concrete, it was decided that the work be divided into three parts. These parts are comprised of the following:

**Laboratory study of the effect of vibration on the compressive strength and the compression modulus of a fresh concrete. This task was needed to predetermine the thresholds of the velocity amplitudes and to assess the time delay required to avoid any changes in the properties of the concrete.**

**Full scale field testing to determine the nature of the vibrations generated by a driven steel casing and to record the patterns of the propagated waves as the casing penetrates the ground.**

**Field investigation of a typical simulated construction procedure of full scale drilled shafts subjected to construction vibrations with different time delays.**

Although the source of the vibration in drilled shaft installation is limited to certain waveforms, attempts have been made in this study to collect time-history records directly from a full scale casing driven in the ground and to correlate the generated waves to those propagated in the vicinity of the shafts. Since a search of the literature has not revealed any prior work related to the vibration of drilled shaft casing, it was decided in this study

to attach a special type of shock accelerometer to a steel casing to record the generated signals in the longitudinal direction along the shaft length. The accelerometer was positioned at predetermined locations along the casing and records were collected at various depths.

The above stated tasks were distributed between the two the principal investigators, Florida Atlantic University and Florida State University. The laboratory testing was conducted at the Civil Engineering Department at Florida State University, and the full scale field tests were performed by Florida Atlantic University at sites located at the Boca Raton campus, Delray, Miami, and Clearwater. Florida State University participated in all the field testing activities and carried out all the laboratory and field analysis of results. **Figure 1.1** presents a detailed schematic of the scope of work and all the efforts devoted to accomplish this study.

## 1-4 REPORT ORGANIZATION

The following chapters present in detail all the tasks involved in this study preceded by a thorough literature review describing relevant subject matters such as: (1) general characteristics of construction vibrations, (2) response of cohesionless soil to construction vibrations, and (3) responses of concrete to vibrations. Findings and conclusions of the study are presented in a separate chapter. Recommendations needed for the Florida Department of Transportation's construction vibration specifications are listed at the end of this report.

## 1.5 OBJECTIVES AND APPROACH

The objectives of the study were the following:

i. To monitor the vibration levels during the installation of drilled shafts.

ii. To monitor the settlement of adjacent structures due to installation.

iii. To evaluate the effect of vibrations on the cracking associated with the setting of concrete.

iv. To determine the distance and time at which vibratory effects become insignificant.

v. To perform maturity testing of the concrete.

vi. To carry out non-destructive testing, pile integrity testing (PIT), and cross-hole sonic logging (CSL) of the drilled shaft concrete.

Ten drilled shafts were designed and constructed according to the Florida Department of Transportation (FDOT) Specifications 455. The selection of the monitoring equipment and instrumentation was chosen primarily as a function of the portability and the robustness.

The scope of the investigation is presented in a flow chart, Fig. 1.1

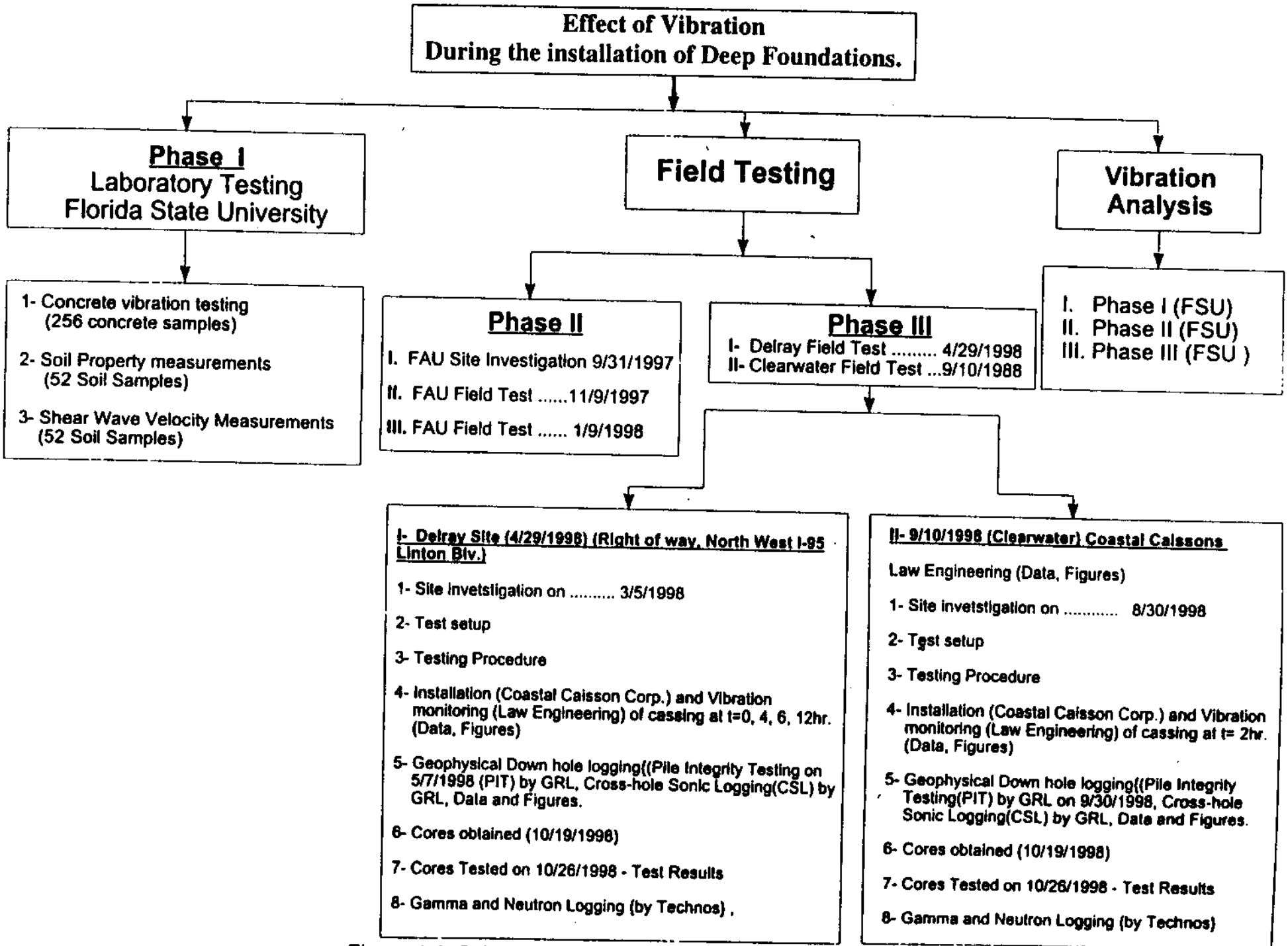


Figure 1.1: Schematic diagram of tasks performed in this study

# CHAPTER II

# BACKGROUND

## 2-1 CHARACTERISTICS OF CONSTRUCTION VIBRATIONS

Vibration from drilled shaft construction will generally be temporary, but the disturbance it could cause may result in permanent damage to the surrounding shafts and specifically to the freshly poured ones. This unpredictable damage may lead to restraints on the working method that result in additional costs or even curtailment of activities.

Vibration-induced damage thresholds are usually expressed in terms of peak particle displacement, velocity or acceleration, and sometimes include a frequency-dependent factor. If construction vibrations comprise of harmonic waves, the characteristics of these waves can be described by any two of the following parameters: frequency, peak particle displacement, peak particle velocity, or peak particle acceleration. The peak particle characteristic indicates that it is the maximum value associated with the motion of a particle at a point in the ground (or on structure) that is being considered. Usually the peak particle velocity (**PPV**) is used, because it has been found to be the best correlated with case history data of damage occurrence and because it has a theoretical underpinning in as much as the strain induced in the ground is proportional to the particle velocity. Although **PPV** is widely used to quantify the damaging potential of a vibration, it must be recognized that velocity of itself, cannot induce damaging forces. Such forces are generated in structures by both:

1. ***Differential displacements, which give rise to distortion as the structures follows movement of the ground upon which it is found, and***
2. ***Change in the ground particle velocity vector (magnitude or direction), which produce internal forces upon the structure.***

In the case of transient vibrations, the peak particle velocity or acceleration would be of a short duration depending on the loading function. Unless the peak value is detected, the prediction of the maximum peaks in random vibrations require statistical analysis which involve the application of the theory of "extrema". For drilled shaft construction, the generated vibrations are more deterministic harmonic signals than random. Thus, converting motions from acceleration to velocity or displacement can be accomplished through direct integration of the functions. In some cases, however, the generated vibrations do not possess the harmonic waveforms. Such vibrations were recorded in this study and were dealt with based on the assumption of a narrow band stationary Gaussian process. Additional cases were encountered in this study where the maximum values of particle velocities were recorded. Considering such values in deciding about the severance of the vibrations may be questionable because of the short duration of peaks. Guidelines for selecting the maximum particle velocities in such cases do not exist. The common practice is to still consider these peak values.

In practice, any structural element will be subjected to both distortion and internal mechanisms at the same time, and these will be superimposed upon pre-existing stresses and strains from other causes. Damage may occur when the combined effects exceed the tolerance of the structure. In the case of freshly placed concrete in a drilled shaft, construction vibrations may directly or indirectly alter the specified concrete properties. Such changes may occur in the strength of the stiffness properties. Other changes may influence the density or the porosity of the matrix which in turn may change the permeability characteristics and hence the concrete durability.

Construction induced vibrations can be divided into three main types: compressive, ***P***, distorsional (shear), ***S***, and surface, ***R*** **(Figures 2.1 to 2.3 ).** To describe the vibration response,

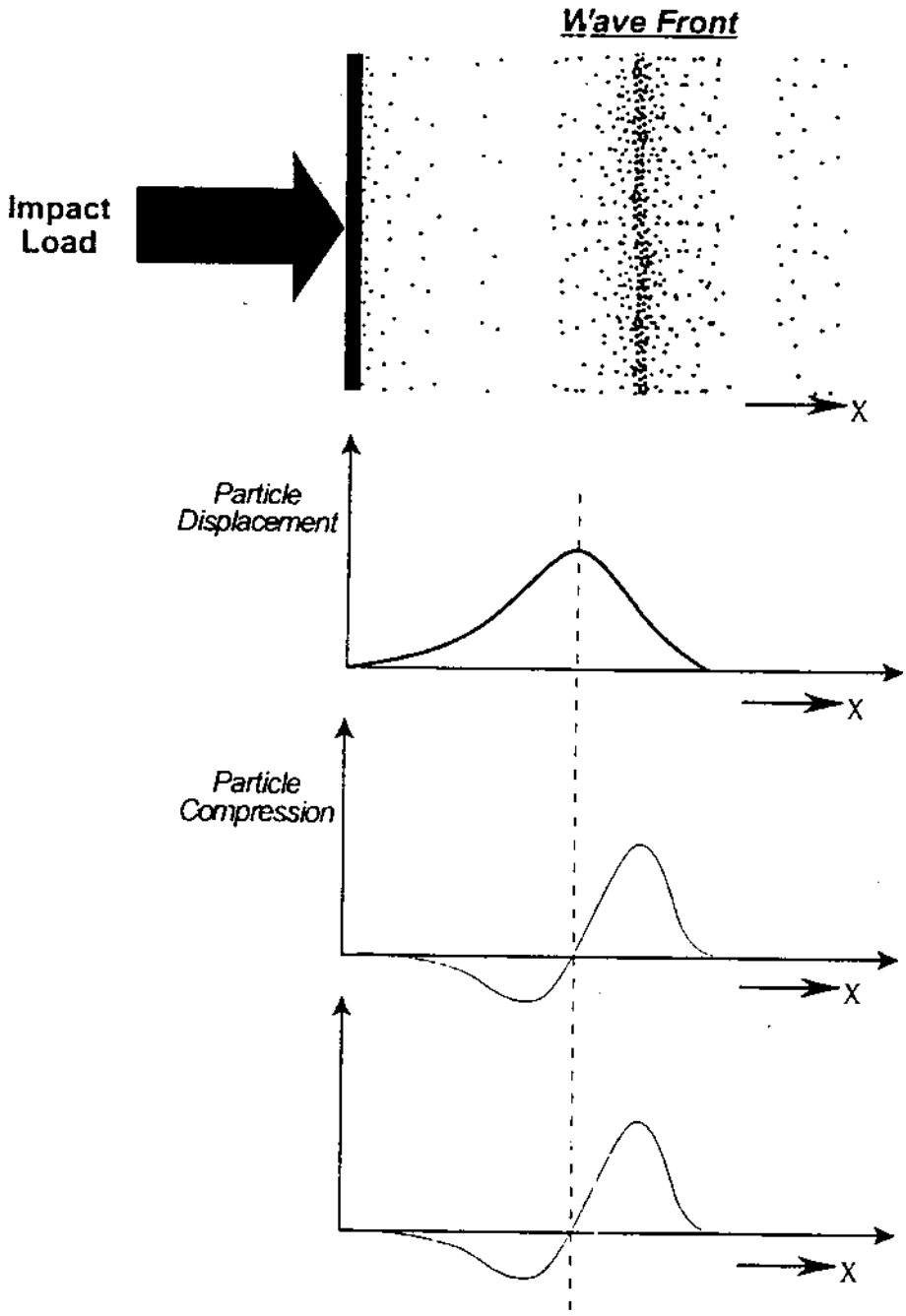


Figure 2.1: Construction vibration generating compression waves.

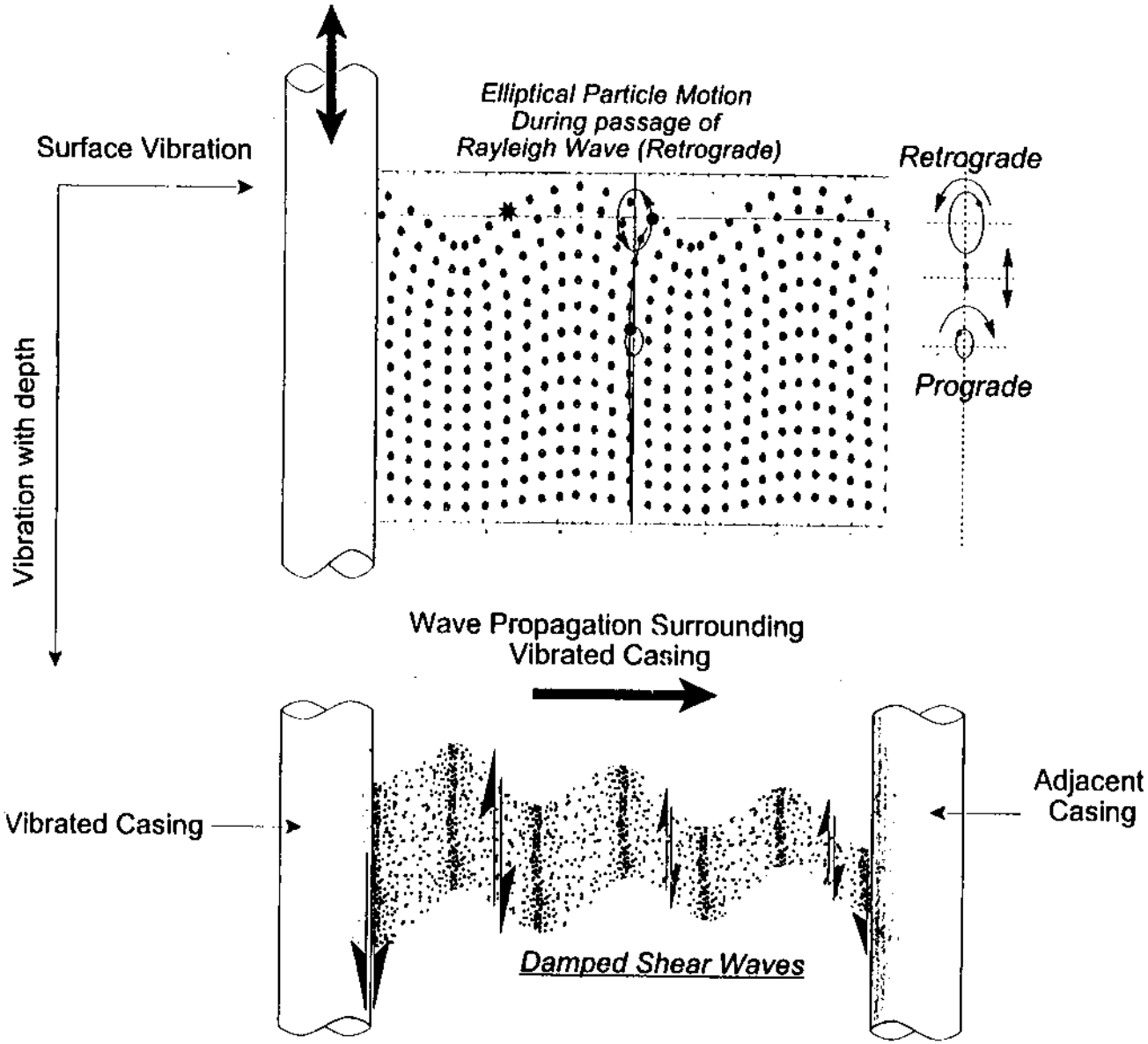


Figure 2.2: Generation and propagation of surface and body shear waves due to a driven casing.

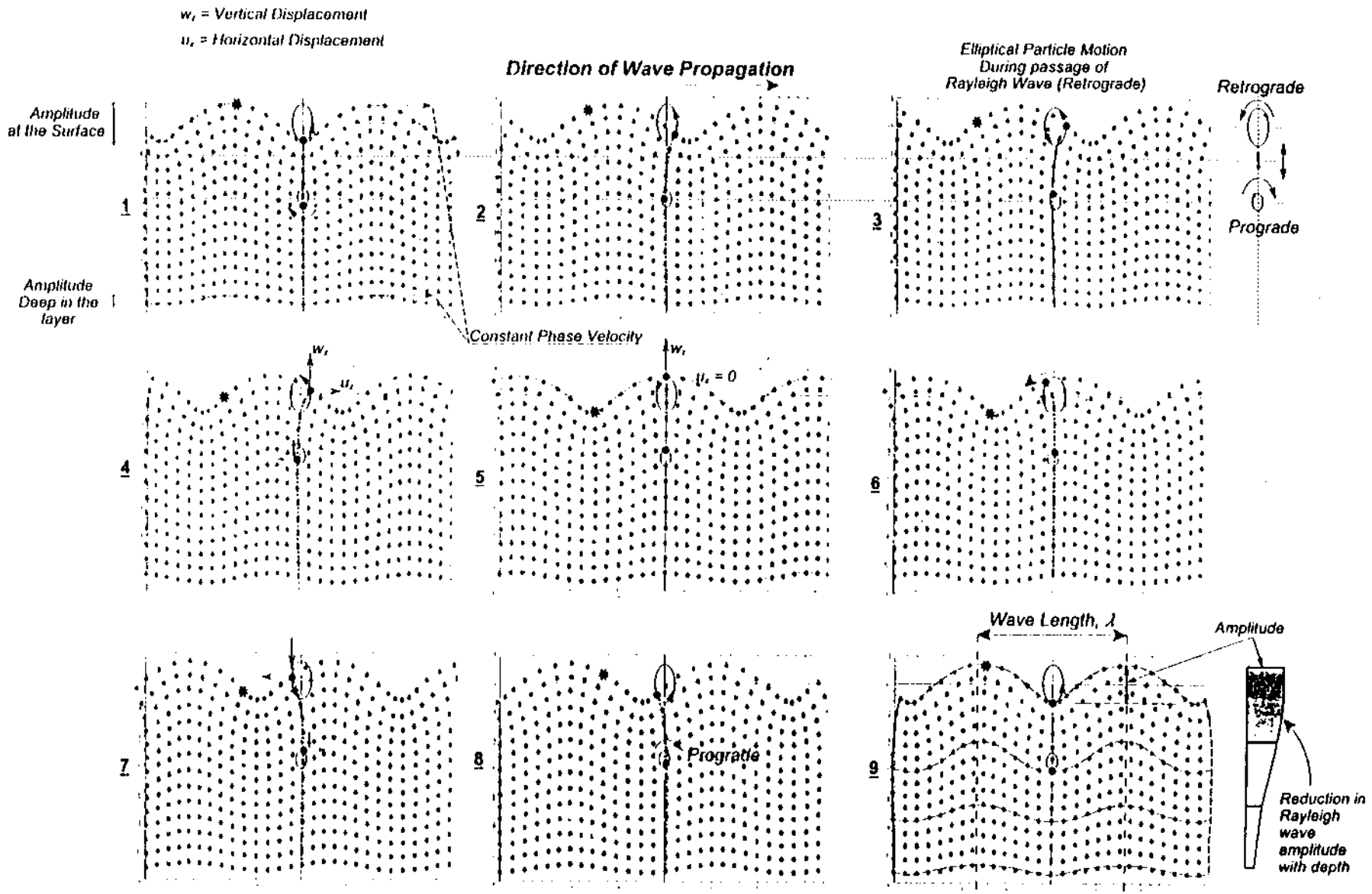


Figure 2.3: Rayleigh waves from construction vibration

three perpendicular components of motions must be measured. The longitudinal component, L is usually oriented along a horizontal radius of the vibration source. It follows, then, that the two perpendicular components will be vertical, **V**, and transverse, **T**, to the radial direction (**Figure 2.4**).

The three main wave types can be encompassed in two different wave categories: body waves which include compressive and shear waves and propagate in the soil, and surface waves, which are transmitted along a surface (usually, the upper ground surface). The surface waves are often described by Rayleigh waves (the most complicated) which produce motions both in the vertical direction and parallel to the direction of propagation. The shear waves in turn are divided into horizontal shear waves, $S_H$, and vertical shear wave, $S_V$. The dominance of any mode of vibration, whether it is $P$, $S_H$, or $S_V$, depends on the polarization of the waves and on the source of the vibration.

Transient impact loads below the ground surface produce predominately body waves at small distances. These body waves propagate outward in a spherical manner until they intersect at a boundary such as another layer (rock or soil) or the ground surface. At this intersection, shear and surface waves are produced, and the reflected surface (Rayleigh) waves become important at larger transmission distances. At small distances, all three wave types will arrive together and greatly complicate wave identification, whereas at large distances, the more slowly moving shear and surface waves begin to separate from the compressive wave and allow identification. Most construction impacts produce a single dominant pulse with trailing subsidiary reflections. Drilled shaft construction produces more deterministic harmonic than random vibrations. The vibratory devices that are used to drive the steel casings are operated by hydraulic motors, which means that they have the potential to operate at a wide range of

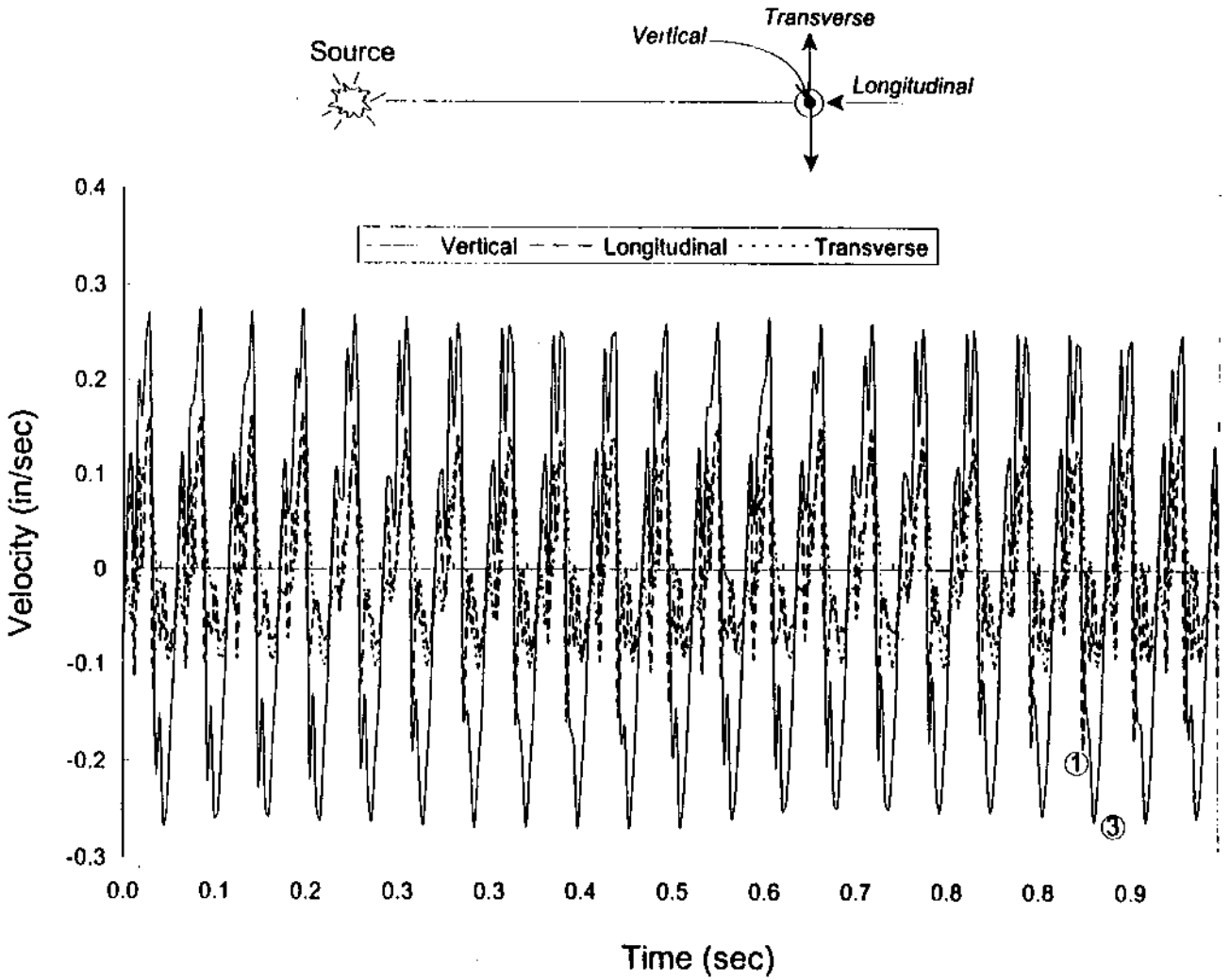


Figure 2.4: Vertical, Longirudinal and Transverse mode of steel casing vibrations

frequencies. As for driven pile, when a steel casing or a pile is driven by a steady-state vibrator, the energy per cycle of vibration may be much less than the energy per blow from an impact load situation. However, it has been observed in practice that the ease or difficulty of vibratory casing driving depends on the characteristics of the soil as well as the characteristics of the casing and the vibratory driver. and is true because two of the three potential resonances that occur during vibratory driving involve soil properties and layer thicknesses. For optimum efficiency, the casing and the soil should not be vibrating "in phase," that is, the casing and the driver must not move together with the surrounding soil, or no penetration occurs.

The following are the three distinct frequencies that affect vibratory casing driving:

1. ***Driver-casing resonant frequency, which results in maximum particle velocity at the casing top;***
2. ***Soil-casing-driver system resonant frequency, which results in maximum displacement of the soil surrounding the casing: and***
3. ***Soil stratum resonant frequency, which is a function of stratum thickness and properties.***

The first is the optimum frequency for driving because the relative motion between the soil and the casing is maximum. The integration of this relative motion gives the casing penetration. The casing is most efficiently driven by vibrations when the combination of mass of driver and casing and the frequency of vibration combine to produce a driver-casing resonance. As long as the frequency of this resonance does not coincide with a resonant frequency of any nearby target or the stratum frequency of the site, large ground vibrations do not occur and damage is unlikely to happen.

Maximum ground vibration amplitude adjacent to the casing during vibratory driving will be encountered when the vibratory casing driver is operating at the resonant frequency of the soil-casing-driver system; this frequency is dependent on properties of the soil stratum that the

casing is penetrating. The amplitude of motion under these conditions will also depend on the force generated by the vibratory driver, the mass of the system, and the stiffness of the soil. However, at this frequency the casing and soil are "in phase or are moving together" and all penetration stops. Also, the ground motion is maximum, exacerbating transmission of vibrations to the neighborhood.

The third resonance involves the soil stratum that the casing is currently penetrating and may change throughout the driving process. At this resonant frequency, the stratum resonates generating large ground motion that very efficiently transmits vibrations throughout the neighborhood. Soil layers or strata will selectively transmit and amplify specific frequencies depending on $V_p$, $V_S$, and strata thicknesses $H$. The resonant frequency of a soil layer can be estimated from Richart et al. (1970) as follows:

$$f = V/4H \tag{1}$$

where $f$ = frequency; $V$ = seismic velocity of layer, $P$-wave. or $S$-wave depending on motion observed; and $H$ = layer thickness.

A potential hazard with vibratory drivers exists in the form of matching the frequency of a soil layer. Vibrators often operate in the range of 20 to 30 Hz. For soils with shear wave velocities of 120 to 600 m/sec, this frequency range may spell a hazard for layers between about 1 and 5 m thick, not uncommon in nature. This phenomenon points out the advantage of providing a vibratory hammer with completely variable frequency, and hammers like this are available. Not only can one optimize the driving by adjusting the frequency, but also minimize damage due to accidental resonance of the ground itself. A similar situation may arise for impact-driven casings, but the opportunity for resonance is much less because the impact is not

associated with only a single frequency; and only a few cycles of any given frequency occur so resonance does not develop.

Ideally, it is possible to compute all resonant frequencies, but for real field conditions, it is not realistic to do so. if one were to use a completely frequency-variable vibrator, all frequencies could be determined in situ by starting the vibrator at zero frequency and increasing frequency until all resonances have been identified by observing the amplitude of casing motion and ground motion near (within 1 m) the casing. Usually the stratum frequency will be lower than the system frequency, which is lower than the driver-casing frequency. The stratum frequency would be encountered first in the run-up of frequency from zero, and, if the force amplitude associated with the vibrator is great, large ground motion may be generated and transmitted away from the casing. The effect is similar for the pile-driver system frequency. It would be better if the force amplitude of the vibrator could be varied so that stratum and soil-casing-driver resonances could be approached and passed with low power or force. Then, when the casing-driver system frequency is found, the force level could be increased to optimize driving. This kind of vibrator now exists.

Not only can the state-of-the-art vibrators vary the frequency of operation, but they can vary the force amplitude by changing the static moment. A vibratory driver, that can do this, is shown schematically in **Figure 2.5** (Massarsch and Westerberg, 1995). The two sets of eccentric masses are arranged in two rows. By changing the orientation of the eccentric masses of one row, compared to the other row, the static moment can be changed, thereby changing the force at all frequencies. With this type of vibrator, the first two resonances associated with vibratory driving can be passed through with low static moment and then, when casing-driver resonance is reached, the static moment can be increased, therefore, increasing the force level to

drive the casing efficiently. For some hammers, the optimum static moment can be monitored and adjusted on the basis of the amperage consumed by the electric motors driving the hydraulic pumps.

### 2-1-1 Peak Component and True Vector Sum

Passage of construction vibrations forces the ground particles to move in an elliptical manner in three dimensions. A two-dimensional representation of displacements produced by pile driving is shown in **Figure 2.6.** While the retrograde motion is symptomatic of a surface wave, the radial motion dominates and gives way to vertical (compression) dominance at a greater distance. To define this motion, three mutually perpendicular components are measured [transverse, longitudinal (radial), and vertical]. Comparison of a typical three-component time history from a transient impact vibration **(Figure 2.4)** shows that:

1. ***Many peaks are present in all cases.***
2. ***The peak component varies (i.e.. it is radial for one case and transverse for another).***
3. ***The peak amplitude in the longitudinal direction, ③, does not occur at the same time as in the transverse direction, ①.***
4. ***Shear and compression waves may not be distinguishable from the three components.***

The difference between the three components results from the presence of the various wave types in the vibration wave trains. Variation of motion with each component has led to difficulty in determining which component is more critical. Peak motions should always be reported as either the peak component or the peak true vector sum. Another measure, the maximum vector sum, is frequently reported but is conservative and not directly related to a maximum velocity at a particular time. In general, the maximum of each component is used regardless of the time when it occurs. Also, the maximum particle velocities are utilized in the field assessments without considering the mode of vibration.

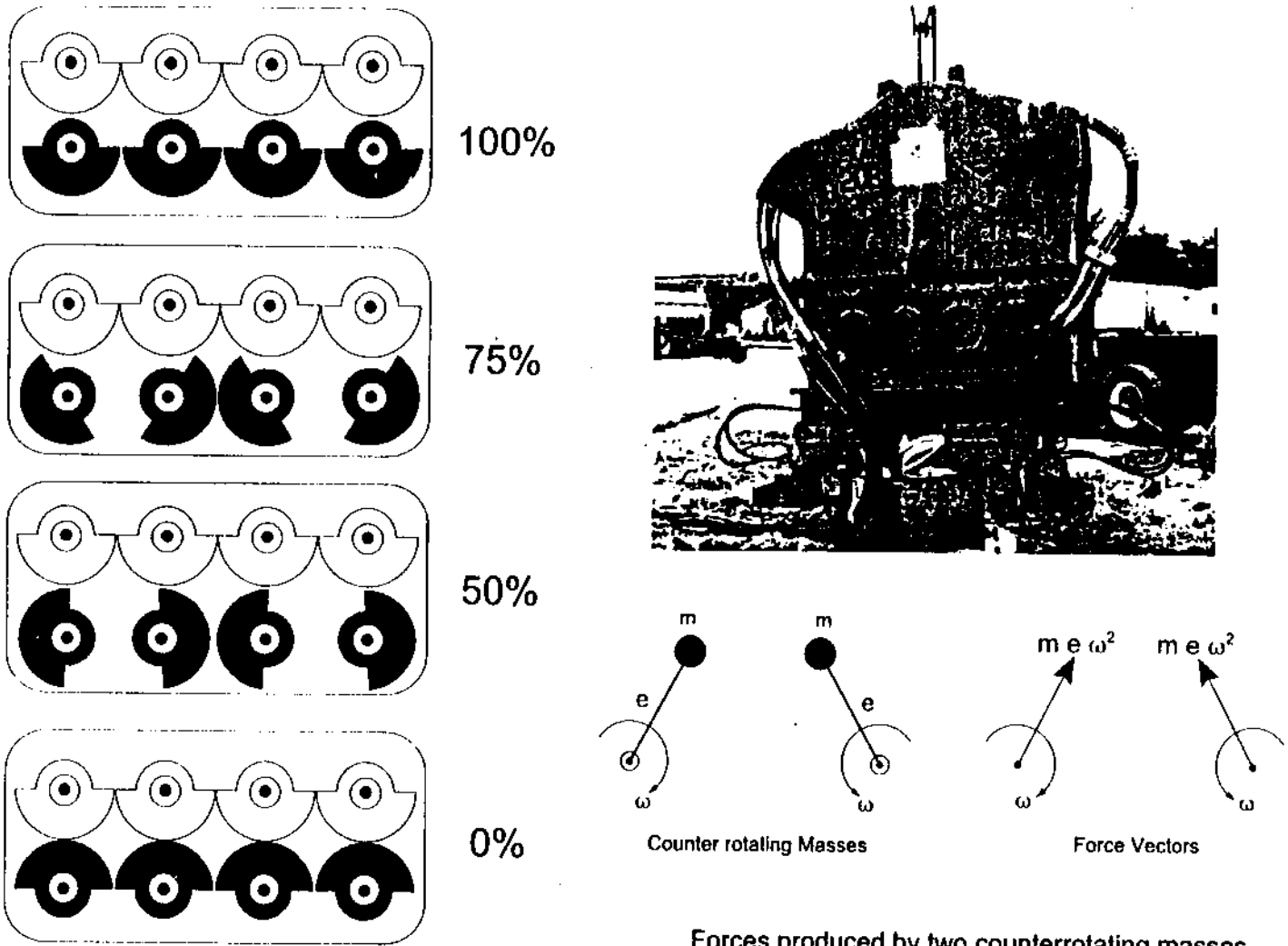


Figure 2.5: Operating principle of vibrator with dual rows of eccentric mass, allowing variation of static moment (displacement amplitude) (Massarsch and Westerberg, 1995)

This type of assessment is insufficient to analyze the consequences of the effect of construction vibration. In other words, underground structures are more vulnerable to compressive waves than above ground structures which are susceptible to distorsional waves. Therefore, it is necessary in some applications to distinguish between the modes and the components of the construction vibration.

### 2-1-2 Propagation Velocity

Propagation velocity is an important factor because it is an indirect measure of soil properties that affect decay of peak particle velocities as well as wavelength. It is important to keep in mind the distinction between the particle and the wave velocities when dealing with seismic wave propagation. The speed of transporting the input energy from point to point in a solid medium is called the wave velocity and it remains the same for the same material. The speed at which a solid particle is being displaced or disturbed at a point is called the particle velocity. Wave velocities are expressed in thousands of meters per second, while particle velocities are expressed in millionths of a meter per second. Particle velocity may be equal to the seismic wave velocity only at a very close distance from the source of the energy.

Geophones on a ground surface record the particle velocities at pertaining points. Knowing the distance between two geophones and the time taken by a seismic wave to travel between the geophones, the wave velocity of the surface layer can be determined. For a decayed vibration in a homogenous elastic solid medium, the velocity of the seismic wave remains unchanged and this corresponds to the stiffness of the material, while particle velocities decrease along the wave propagation path (**Figure 2.2**).

As discussed earlier, the propagation velocities of compressive, shear, and Rayleigh waves vary. Propagation through rock and soil provides a greater wave velocity contrast, as shown by the comparison in **Table 2.1**. The range of velocities for a particular soil type, such as sand, is greater than for rock because of the great variation in stiffness caused by density and overconsolidation ratio for sand and clay, respectively.

**Table 2.1 Estimated Propagation Velocities**

| Material | Wave Velocity (m/s) | |
|---|---|---|
| | Compression | Shear |
| Limestone | 2000 - 5900 | 1000 –3100 |
| Metamorphic rocks | 2100 - 3500 | 1000 –1700 |
| Basalt | 23000 - 4500 | 1100 – 2200 |
| Granite | 2400 - 5000 | 1200 – 2500 |
| Sand | 500 - 2000 | 250 – 850 |
| Clay | 400-1700 | 200-500 |

As shown in **Table 2.1**, the compressive (first arrival) propagation velocity varies greatly for one material type because of differences in densities. In soils the proper propagation velocities should be matched with the appropriate wave type (e.g., compressive with compressive, shear with shear, etc.) to compute frequency and strain. This correlation is important since the shear wave is much more sensitive to changes in soil properties for

propagation below the water table. This sensitivity is a result of the inability of the shear wave to propagate through water. Thus it propagates predominately through the soil matrix.

Below the water table, the compressive wave is much less influenced by the soil density or modulus. because it can propagate through the water itself. The compression modulus values are in turn affected by the presence of the water table and the rate of loading. Higher rates of loading may result in higher moduli values.

### 2-1-3 Strains From Particle Velocities $\dot{u}$

Ground strain, possibly one of the most important parameter in construction vibration.. It can be calculated directly from the mathematical description of the displacement, $u$, caused by a plane-wave traveling in positive direction, and from the particle velocity, $\dot{u}$, which is expressed as

$$\dot{u} \quad \frac{du}{dt} = -cU \quad \cos(x - ct) \tag{2.2}$$

In engineering terms, strain is usually defined as the change in length, $\Delta l$, divided by the original length $l$, or $\Delta l/l$. This ratio is the same as the change in displacement per unit distance. Therefore, in a manner similar to the particle velocity derivation, the first derivative of the displacement, $u$, with respect to position $x$ yields the strain

$$\varepsilon \quad = \frac{du}{dx} \quad = U \cos(x - ct) \tag{2.3}$$

The strain can be defined in terms of the particle velocity, $\dot{u}$, and propagation velocity, c, by substituting Equation 3 into the Equation 2.

$$u = -c\cos(x - ct) = -c\varepsilon \text{ and } \varepsilon = \frac{\dot{u}}{-c} \qquad (2.4)$$

Positive particle velocities toward the right then produce negative strains. Therefore, negative strains are compressive. Thus for plane waves, ground strains can be calculated directly from the particle velocities if the compressive-wave propagation velocity is known or can be estimated.

## 2-2 RESPONSE OF COHESIONLESS SOIL DEPOSITS UNDER CONSTRUCTION VIBRATIONS

For ground response involving no residual soil displacements, the response is determined mainly by the moduli values and damping characteristics.. In such cases, analyses are often made using the equivalent linear analysis method in which the moduli and damping factors used in the analysis are compatible with the strains developed in the soil deposit or earth structure. Values of soil moduli can be determined using laboratory or field testing techniques. Advantages and disadvantages of these techniques have been reported in the literature (Marshall, 1981; Tawfiq, 1987,). Several useful empirical relationships were suggested to obtain shear and compression modulus from physical soil properties of cohesionless soils.

A comprehensive survey of the factors affecting the shear moduli and damping factors of soils and expressions for determining these properties have been presented by Hardin and Drnevich (1970). In these studies it was suggested that the primary factors affecting moduli and damping factors are: strain amplitude, $\gamma$, effective mean principal stress, $\sigma'_m$, void ratio, e, number of cycles of loading, N. Factors with minor influence include: Octahedral shear stress, $\sigma_{oct}$, overconsolidation ratio, OCR, effective stress strength parameters, c' and $\phi'$.

Relationships developed by Hardin and Drnevich (1970) showed clearly that modulus values for sands are strongly influenced by the confining pressures, the strain amplitude, and the void ratio (or relative density) , but not significantly by variations in grain size characteristics or other factors. The expression suggested for maximum shear modulus was as follows:

$$G_{max} = 14760 \frac{(2.973-e)^2}{1+e} (OCR)^a (\sigma'_m)^{1/2} \quad (2.5)$$

where $G_{max}$ = maximum shear modulus, in psf,
e = void ratio
OCR = overconsolidation ratio
a = a parameter that depends on the plasticity index of the soil
$\sigma'_m$ = mean principal effective stress in psf.

The value of 'a' can be obtained from the following table:

| PI | a |
|---|---|
| 0 | 0 |
| 20 | 0.18 |
| 40 | 0.30 |
| 60 | 0.41 |
| 80 | 0.48 |
| ≥100 | 0.50 |

For practical purposes, a convenient relationship between the shear modulus and the confining pressure was provided by the simplified equation (Seed and Idriss, 1970):

$$G = 1000\ K_2\ (\sigma_m')^{1/2} \text{ in } (lb/ft^2) \quad (2.6)$$

where $\sigma_m'$ = mean principal effective stress in psf.
$K_2$ = soil modulus coefficient

The effect of the void ratio and the strain amplitude can be expressed by their influence on the ***soil modulus coefficient, $K_2$.*** For any sand, this coefficient has a maximum value $(K_2)_{max}$ at very low strains of the order of $10^{-4}$ percent. The influence of other factors such as angle of

friction, $\phi'$, effective vertical stress, $\sigma_v'$, coefficient of lateral stress at rest, $K_o$, and void ratio, e, on the computed relationships between $K_2$ and strain amplitude, $\gamma$, can be summarized as follows:

***(a) At very low strains ($\gamma < 10^{-3}$ percent), $K_2$ depends only on the void ratio, e.***
***(b) At intermediate strains ($10^{-3} < \gamma < 10^{-1}$ percent), the variation of $K_2$ with strain is only slightly influenced by the vertical stress and very slightly by variations in $\phi'$ and $K_o$. The values of $K_2$ are still influenced strongly by the void ratio however.***
***(c) At very high strains ($\gamma > 10^{-1}$ percent), the values of $K_2$ are slightly influenced by the vertical stress but they are essentially independent of $K_o$, $\phi'$ and e.***

Thus for practical purposes, values of $K_2$ may be considered to be determined mainly by the void ratio, e, or relative density, $D_r$, and the strain amplitude, $\gamma$. This conclusion has also been shown in studies by Kuribayashi et al. (1974) and Krizek et al. (1974).

Yoshimi et al. (1977) suggested that **Equation (5)** is more applicable for sands with angular grains and proposed the following equation for sands with rounded grains :

$$G_{max} = \frac{8400(2.17-e)^2}{1+e}(\phi_m)^{1/2} \qquad kN/m^2 \qquad (2.7)$$

The Yoshimi et al. equation represents the upper bound limit of similar relationships suggested by Hardin and Black (1968). According Hardin and Black, the maximum shear modulus at low amplitudes ($\gamma \leq 1 \times 10^{-4}$) can be determined from:

$$G_{max} = \frac{6908(2.17-e)^2}{1+e}\sigma_o^{-1/2} \qquad kN/m^2 \quad (round-grained) \qquad (2.8)$$

and

$$G_{max} = \frac{3230(2.97-e)^2}{1+e}\sigma_o^{-1/2} \qquad kN/m^2 \quad (angular-grained) \qquad (2.9)$$

where

propagation methods in the field, and then reducing this value for other strain levels in accordance with the results indicated by the average (dashed) line in **Figure 2.8.**

The studies by Prakash and Puri, 1981, using in-situ tests, indicate that for silty sands the modulus attenuation curve may be slightly flatter than that shown in **Figure 2.8**, but the difference is relatively small. It should also be noted that the Hardin-Drnevich equations and the experimental results of Shibata and Soelarno (1975) and Iwasaki et al.(1976) show that the modulus attenuation curve for sands is influenced slightly by the confining pressure. The experimental results of Iwasaki et al. are presented in **Figure 2.9**. Thus, where more refined analyses are required, it may be more appropriate to use a family of curves similar to those shown in **Figure 2.9** to evaluate the response of sand deposits.

### 2-2-1 Comparison of Values of $(K_2)_{max}$ for Sands Determined by Laboratory and Field Tests

The values of $K_2$ shown in **Figure 2.** are based on laboratory tests on sands. It may be seen that for relatively dense samples, the values of $(K_2)_{max}$ determined at very low strains for laboratory test specimens are typically in the range of 50 to 75. The results of a number of determinations of shear moduli for sands at very low strain levels by means of in-situ shear wave velocity measurements are summarized in **Table 2.2**:

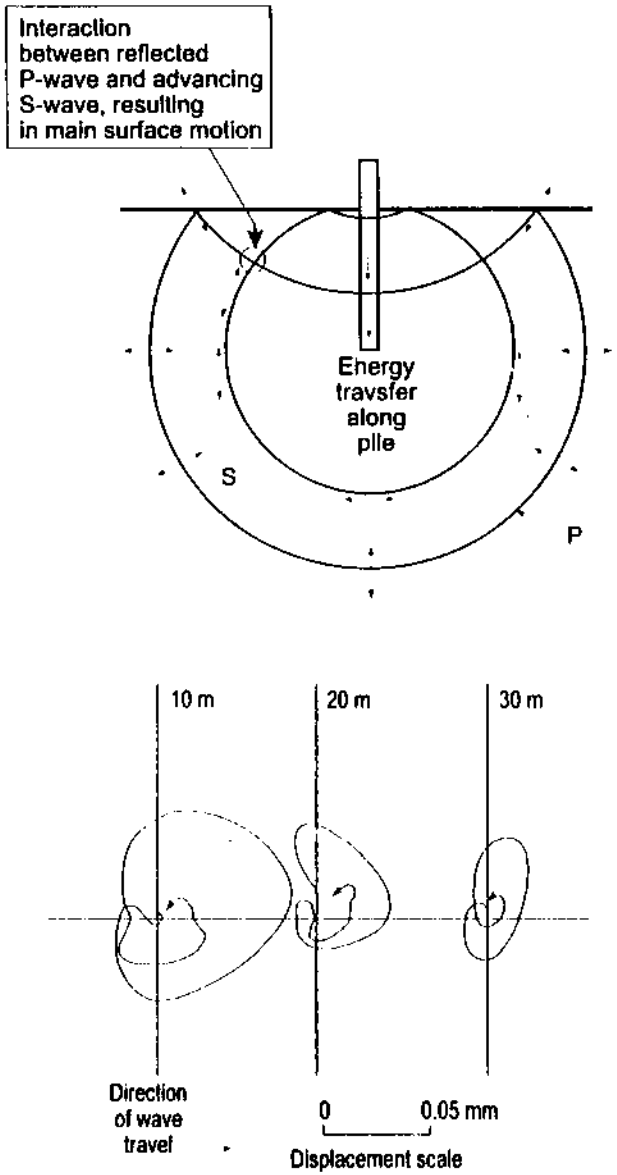


Figure 2.6: Principal wave types and particle displacement paths during passage of surface waves produced by sheaet pile driving (Attewell & Farrer (1973).

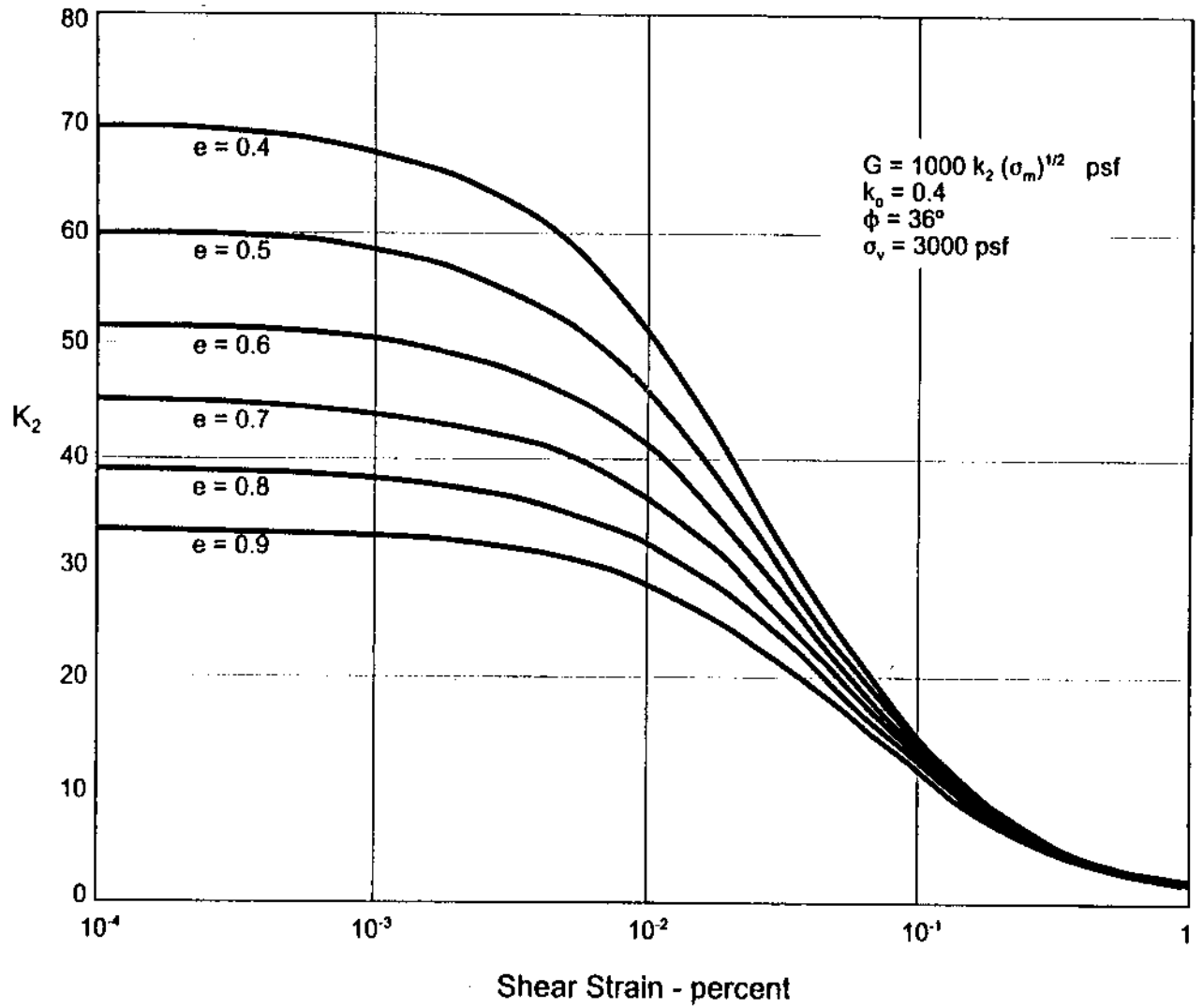


Figure 2.7a: Shear moduli of sands at different void rations (Based on Hardin - Drnevich expressions)

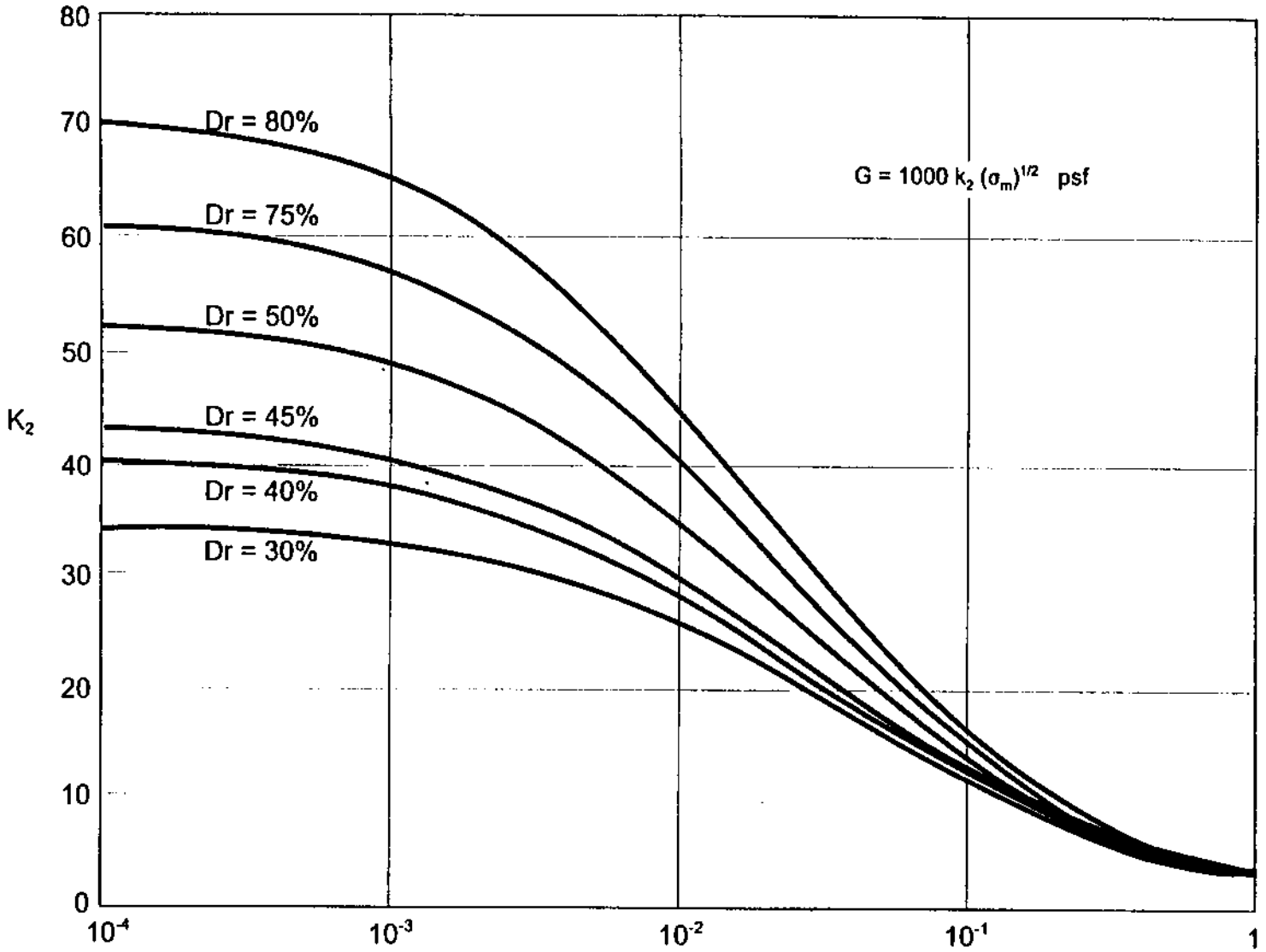


Figure 2.7b: Shear moduli of sands at different relative densities

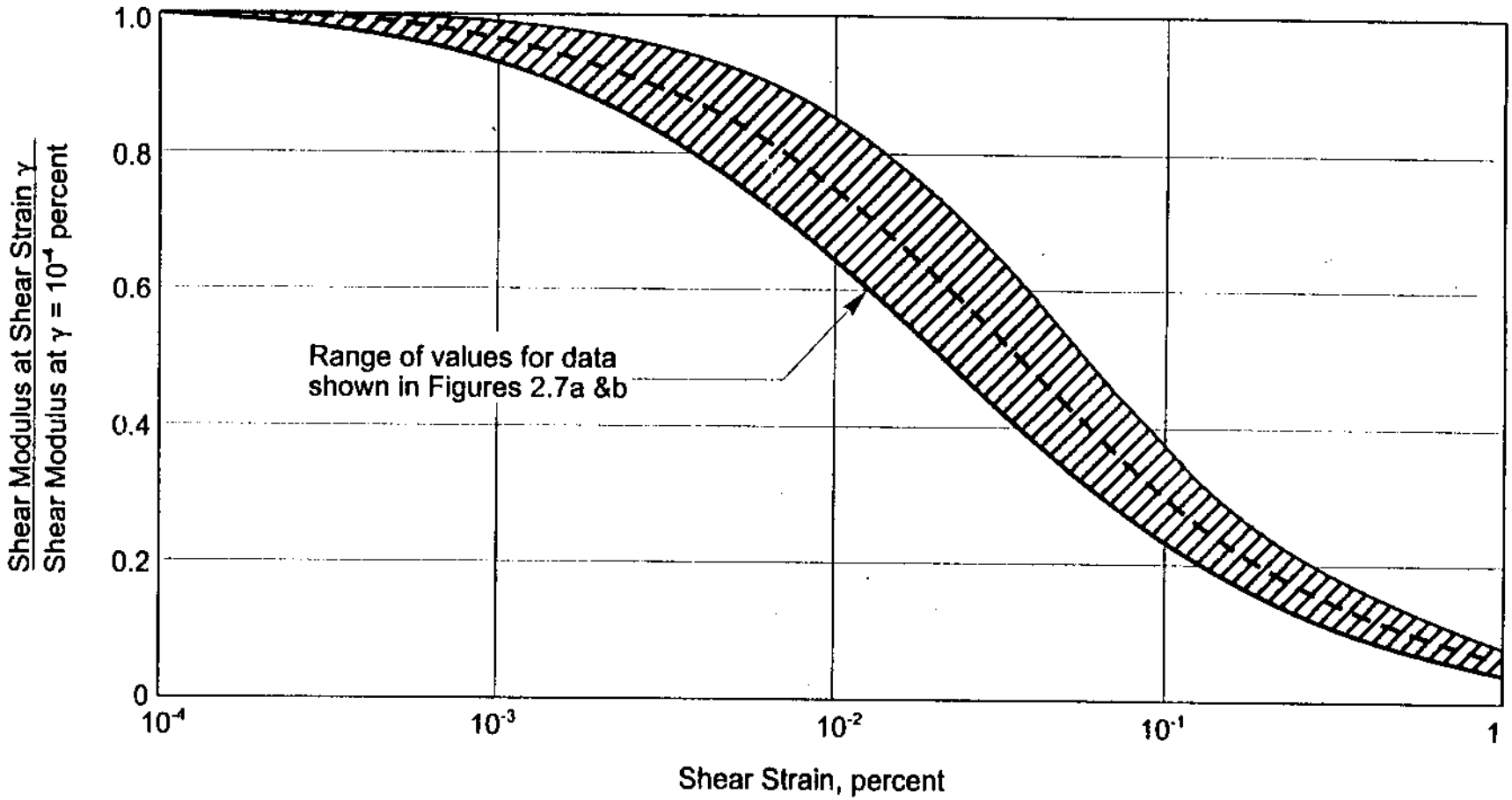


Figure 2.8: Variation o shear modulus with shear strain for sands (Seed and Idriss, 1970)

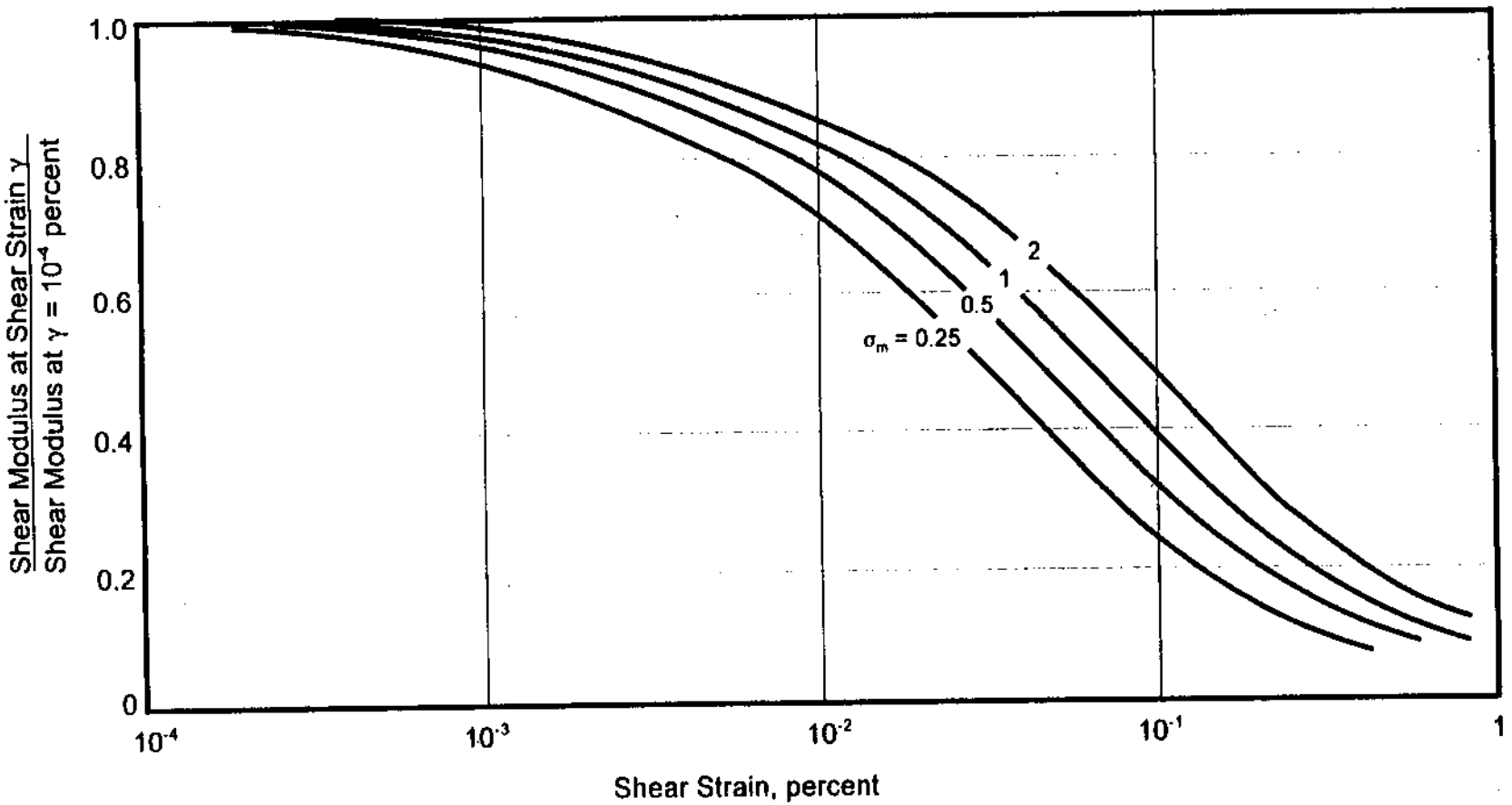


Figure 2.9: Variation o shear modulus with shear strain for sands (Iwasaki, et al', 1976)

**Table 2.2** Shear modulus of sand based on field shear wave velocity measurements (Seed et al., 1984).

| Soil | Location | Depth (ft) | $k_2$ |
|---|---|---|---|
| Loose moist sand | Minnesota | 10 | 34 |
| Dense dry sand | Washington | 10 | 44 |
| Dense saturated sand | South California | 50 | 58 |
| Dense saturated sand | Georgia | 200 | 60 |
| Dense saturated silty sand | Georgia | 60 | 65 |
| Dense saturated sand | South California | 300 | 72 |
| Extremely dense silty sand | South California | 125 | 86 |
| Dense dry sand (slightly cemented) | Washington | 65 | 166 |
| Moist clayey sand | Georgia | 30 | 119 |

The six investigations for dense to extremely dense sands (excluding clayey and partly cemented sands) give values for $(K_2)_{max}$ ranging from 44 to 86. Thus there appears to be good general agreement between the results of laboratory and in-situ investigations.

Further evidence of this result is provided by studies by Ohta and Goto (1976). On the basis of numerous shear wave velocities measured in the field, these investigators presented the following equation:

$$v_s\,(m/s) = 69\, N_j^{0.17}\, D^{0.2}\,(m) \,.\, F_1 \,.\, F_2 \qquad (2.10)$$

where:

$N_j$ = SPT N-value as measured in Japanese practice
D = depth of soil below ground surface
$F_1$ = a factor, depending on the nature of the soil, having a value of 1 for alluvial deposits and 1.3 for diluvial deposits
$F_2$ = a factor, depending on the nature of the soil as follows:

| Soil Type | Factor $F_2$ |
|---|---|
| Clay | 1.0 |
| Fine sand | 1.09 |
| Medium sand | 1.07 |
| Coarse sand | 1.14 |
| Sandy gravel | 1.15 |

| | |
|---|---|
| Gravel | 1.45 |

Thus for sands and sandy gravel deposits, the average value of $F_1$ is about 1.15 and the average value of $F_2$ is close to 1.1 so that the product of $F_1F_2$ is typically very close to 1.25. Converting the results to fps units, **Equation (8)** reduces to

$$v_s = 220\ N_{60}^{0.17}\ D^{0.2} \quad \text{(ft/sec)} \tag{2.11}$$

where:

$N_{60}$ = N-value measured in SPT test delivering 55% of the theoretical free-fall energy to the drill rods and

D = depth of soil in feet.

Actually, due to the small power of $N_j$ in the original equation, the difference in SPT N-values can be neglected for all practical purposes.

Since $G_{max} = \gamma/g\ (v_s)^2$ (2.12)

**Equation (11)** provides a correlation between $G_{max}$ and SPT N-value, based on field test data as follows. Assuming $\gamma = 120$ psf, substitution of **Equation (11)** in **Equation (12)** leads to:

$$G_{max} = 180\ .\ 10^3\ .\ (N_{60})^{0.34}\ .\ D^{0.4} \tag{2.13}$$

If the water table is at a relatively shallow depth below the ground surface, the effective stress at depths below 10 feet may be expressed approximately by:

$$\sigma_o' \simeq 62.5\ D \tag{2.14}$$

Thus $D \simeq \sigma_o'/62.5$ (2.15)

Substituting **Equation ( 15)** into **Equation (13)** leads to

$$G_{max} \simeq 35\ .\ 1000\ N_{60}^{0.34}\ (\sigma_o')^{0.4} \tag{2.16}$$

Noting that $N = N_1 / C_N$ leads to

$$G_{max} \simeq 35\ .\ 1000\ (N_1)_{60}^{0.34}\ \frac{(\sigma_o')^{0.4}}{C_N^{0.34}} \tag{2.17}$$

It can readily be shown that with a high degree of accuracy for effective stresses up to 6000 psf:

$$\frac{(\sigma_o')^{0.4}}{C_N^{0.34}} \simeq 0.47\ (\sigma_o')^{0.5} \qquad (2.18)$$

Thus, **Equation (17)** may be rewritten as:

$$G_{max} \simeq 16.5\ .\ 1000\ (N_1)_{60}^{0.34}\ (\sigma_o')^{0.5} \qquad (2.19)$$

For normally consolidated deposits, $\sigma_m' \simeq 0.65\ \sigma_o'$ ,therefore

$$G_{max} \simeq 1000\ .\ 20\ (N_1)_{60}^{0.34}\ (\sigma_m')^{0.5} \qquad (2.20)$$

It may be noted that this equation has the same form as **Equation (6)**, provided:

$$(K_2)_{max} \simeq 20\ [(N_1)_{60}]^{1/3} \qquad (2.21)$$

Values of $(K_2)_{max}$ determined from **Equation (21)** for $N_1$ values ranging from $N_1 = 5$ (loose sands) to $N_1 = 44$ (very dense sands) are as follows:

| $(N_1)_{60}$ | $(K_2)_{max}$ |
|---|---|
| *5* | *34* |
| *8* | *40* |
| *10* | *43* |
| *18* | *52* |
| *28* | *61* |
| *44* | *71* |

These values for $(K_2)_{max}$ are in the same range as those shown in **Figure 2.7** providing further confirmation of the similarity in values of $(K_2)_{max}$ for laboratory and field determinations.

## 2-3 CONCRETE VIBRATION

Importance of vibration of the consolidation of fresh concrete has been covered in many studies since the development of the vibratory machines in 1930's. In 1936, an ACI Committee 609 reported the benefits of vibrators but failed to explain the effect of vibrations on a fresh

concrete. The frequencies of the early vibrators were limited to 3000 - 5000 cycles per min (50-80 Hz). In 1948, L'Hermite and Tournon reported their fundamental research into the mechanism of consolidation. They found that friction between aggregates is the most important factor preventing consolidation (densification) of fresh concrete, but that this friction is practically eliminated when concrete is in a state of vibration. Meissner (1953) summarized previous research studies and reviewed the state of the art on available equipment and its characteristics. The 1960 ACI Committee 609 gave specific recommendations for vibrator characteristics applicable to different types of construction and field practices. Walz (1960) described the various types of vibrators: internal, surface form, and table and their applications. He also showed that the reduction in internal friction is primarily the result of acceleration produced during vibration. Olsen (1987) used accelerometers to measure the rate of movement of fresh concrete and was able to establish the minimum energy level required to achieve a degree of consolidation of 97 percent or more.

In drilled shaft construction, freshly placed concrete can be subjected to either overvibration or revibration. The difference between the two occurrences is the time delay involved in vibrating the concrete. Overvibration of concrete results from subjecting the concrete mix to a long duration of vibration, or due to the use of grossly oversized equipment and vibration the concrete many times over the recommended amount. Revibration occurs by subjecting the concrete to additional vibration cycles at successive time delays.

Accordingly, fresh placed concrete during drilled shaft construction may be subjected to overvibration, if the surrounding vibrations due to construction activities continue to be generated for a long period during concrete placement, or the fresh concrete is exposed to additional cycles of construction vibrations at different time levels.

Overvibration may result in segregation, or sand streaks. In the same shaft, concrete segregation, can produce different densities with the depth. This variation in the densities may adversely affect the design capacity of the drilled shaft and the durability performance of the concrete. Keeping in mind that the unfavorable subsurface conditions in Florida, durability represents one of the major parameters in designing any underground concrete structures. The problem of concrete overvibration has been discussed by Forssblad and Sallstrom (1995), Alemo and Grandas (1993) and Stark (1986). Forssblad and Sallstrom (1995) suggested that the duration vibration in concrete to amount 60 to 70 percent of the total casting time or the vibration effort can be obtained as follows:

$$V_e = 1800/C \qquad (2.22)$$

where Ve = vibration effort $s/m^3$
C = casting capacity $m^3/hr$

They also found that the optimum vibration effort ranged between 200 $s/m^3$ to 325 $s/m^3$. Using this relationship, a drilled shaft with 4 ft diameter an 20 ft depth can sustain 50 min of continuous vibration, without inducing any changes in the concrete density or compressive strength.

On the effect of revibration of fresh concrete, literature did not present any conclusive evidence that construction-induced vibration would significantly affect concrete properties. However, Tuthill (1977) reported that revibration may produce benefits, particularly for the wetter mixtures, in eliminating water gain under reinforcing bars, reducing bugholes, especially in the upper portion of deep lifts, all of which increase the strength of the concrete. Simulating a field blast condition, Esteves (1978) conducted laboratory testing in concrete prisms subjected to transient impact loading. At different intervals of curing time, he observed the development of microcracks versus the amplitude of the particle velocities (**Figure 2.10**). Surface cracks were

noticed on concrete prisms subjected to impact compression waves at 10 hr of curing time. The particle velocities that produced these cracks reached a level of 9.8 in/sec (250 mm/sec).

If the longitudinal-wave propagation velocity of fully cured concrete is assumed to be 3,000 m/s (10,000 ft/sec), the plane-wave strain associated with the minimum velocity for cracking will be

$$\varepsilon = \frac{\dot{v}}{c} = \frac{150\,mm/\sec}{3000\,m/\sec} = 50\mu \qquad (2.23)$$

Other studies have shown that during curing, the modulus, and, therfore, the compressive-wave velocity, are much lower than the final value. Thus, the strain calculated with this larger propagation velocity is a lower bound.

Esteves (1978) results indicted that there is a period of greater susceptibility to vibration cracking (between 10 and 20 hours); however, the high threshold during this period (150 mm/s) explains why other studies have also shown that there is no loss of final strength from transient vibration (Howes, 1979; Oriard and Coulson. 1980). Hulshizer (1996), suggested some vibration acceptance levels for freshly placed and maturing concrete. In general, Hulshizer found that a value of 5.0 in/sec would represent an average value for an acceptable particle velocity during field construction. This limit may increase or decrease depending on the typw of vibration (Impact or harmonic) and on the duration of the vibration (short period or continuous).

Two of the pile vibration tests conducted by the Michigan and California Highway Departments on in-situ curing of concrete are of special interest. The first involved driving through sand within 0.75 m (30 in.) of 5 m (15 ft)-long-cast-in-place piles some 5 to 6 hours after pouring. After 46 days, these piles were extracted and cored to determine the strengths. The

ground motions produced by pile driving show that the vibration levels at these piles may have been as high as 100 mm/s. Also, piles subjected to vibration were statistically stronger than the nonvibrated comparison pile. The second case involved vibrating in-place cylinders by driving two 11 meter Raymond step taper piles over a curing time span similar to that reported by Esteves (1978). Particle velocities at distances of 2.5, 5, 10, 20, and 40 ft from the vibrating piles recorded amplitudes of 3.9, 1.97, 0.5, 0.3, and 0.12 in/s, respectively. Once again, these California results showed that vibratory excitation by adjacent piling, even during the critical 12 to14 hour period, did not reduce the strength of cast-in-place concrete piles.

It is apparent that enough has been learned about concrete vibration during the past *50* years to insure that low slump concrete can be placed successfully. However, a better understanding of the interaction of vibration and fresh concrete is still desirable. Knowledge gained from past experiences on this subject will be utilized in the current study to investigate the extent of the effect of construction vibration on the concrete performance. The investigation will also address the determination of the minimum distance where vibration in the vicinity of a freshly poured drilled shaft should not be allowed.

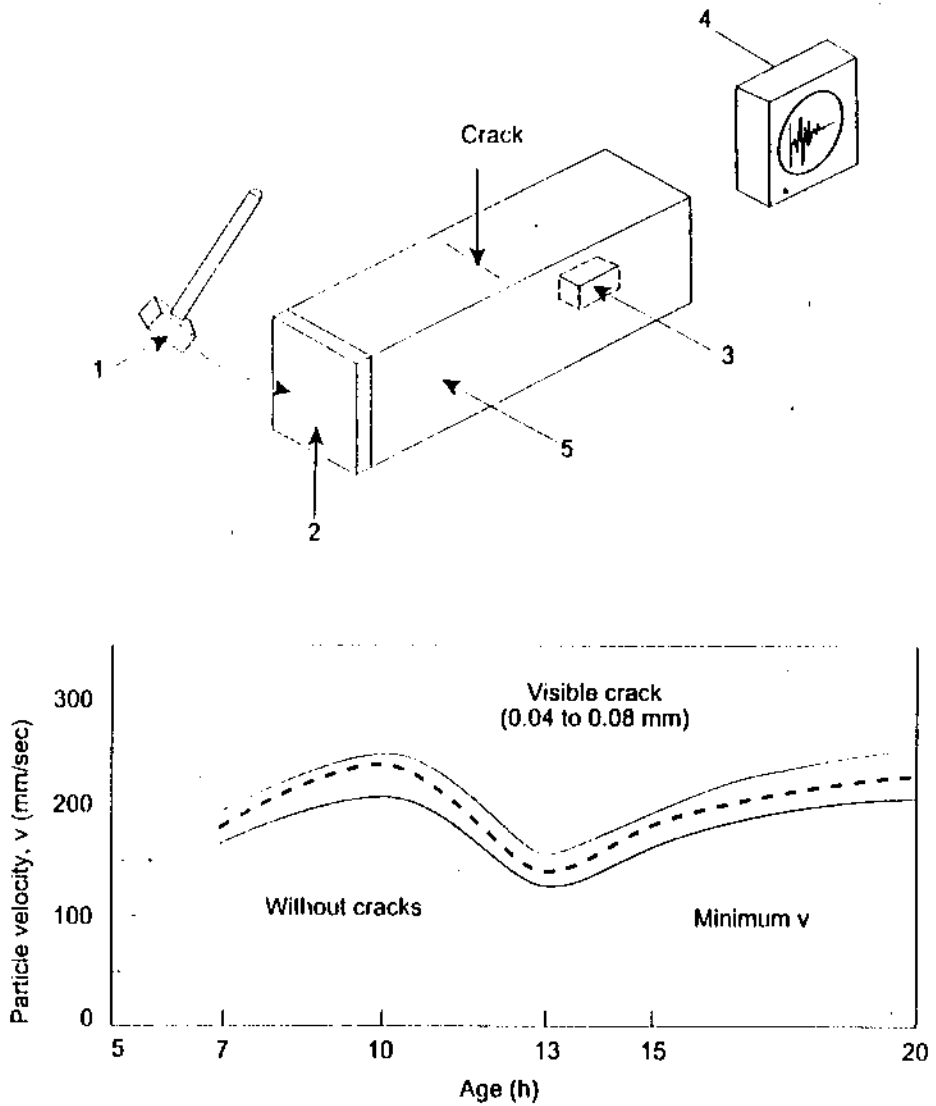


Figure 2.10: Vibratory cracking of curing concrete. (a) Schematic of the test:1, hammer 6 kg; 2 iron plate; 3 geophone; 4, records;.4, recorder; 5, concrete prism with 0.20 x 0.20 x 0.85 m. (B) Critical velocity level (Esteves, 1978)

# CHAPTER III

## LABORATORY TESTING

### 3-1 INTRODUCTION

The test program involved in this study was divided into three phases. These phases were set so that certain parameters such as vibration amplitude and curing time for concrete were first investigated under controlled laboratory conditions. Then results from the first phase were utilized to set up the second and the third phases. Before commencement of the full scale drilled shaft construction and testing, which constituted the third phase, a decision was made to monitor and record simulated construction vibrations produced by a full scale driven casing of 3 foot diameter by 40 foot height. This intermediate stage was considered as the second phase of the test program and was given particular attention, since results from this phase would determine the pattern of instrumentation, and the type of measurements needed for the full scale in-situ testing. This was done because of the lack of any standard testing procedure to conduct such a field test. Most of the published studies on construction vibration were limited to the effect of pile driving, sheet pile construction, and other blast vibrations on adjacent structures or ground settlement. The in-situ test procedure and the instrumentation setup to evaluate the effect of construction vibration on freshly placed concrete have not been covered in the literature. The maximum particle velocities from the second phase were used to arrange the ground and embedded geophones for the full scale drilled shafts. Additional information was gathered from the field testing in the second stage to specify certain driven depths by the steel casing and the time intervals needed to record the sensor outputs.

Various destructive and nondestructive testing methods were used in the test program to obtain strength, stiffness, density, and porosity measurements as related to induced construction vibrations. Laboratory results were used to establish guidelines for the thresholds of vibration amplitudes and permissible curing time spans. In-situ field testing addressed the effect of the severance of construction vibration on the density and porosity of the installed shafts. Additional sets of compression tests were performed on core samples obtained from the full-scale drilled shafts.

Since soil properties were among the parameters considered in this study, the decision was made to limit the investigation to sandy soil layers only. The reason for this selection was: (1) the casing method in drilled shaft construction is typically followed in caving soils, and (2) Soil configurations in Florida are predominantly sandy soils. Also, the presence of shallow ground water tables at the selected testing site provided further information about the effect of effective octahedral stresses ($\sigma_o$ ) on the shear wave velocities ($v_s$) and on the damping characteristics (D%) of the soil layers. About 60 soil samples were obtained from the Florida Atlantic University (FAU) site were classified and tested for water content, unit weight, and void ratio. Grain size distribution analyses were performed on representative samples obtained from the site.

The following sections describe in detail the steps carried out in the testing program to meet the objectives of this study. Since the laboratory and the full scale field testing were conducted at three different stages, concrete samples obtained for each stage were prepared using the same proportions of materials in each case. Requirements given in ***Sections 346 and 455*** of the FDOT Standard Specifications for drilled shaft concrete were followed in the testing program.

## 3-2 TEST METHODOLOGY

A large number of concrete samples were prepared to investigate the effect of vibration amplitudes on the strength and stiffness properties of concrete. Taking into account the reproducibility of the compression test results and the different time delay for vibrating the concrete samples, a test was conducted on a total of 216 concrete cylinders (6 in. x 12 in.). The mixing and curing time was scheduled in a way so that the sequence of vibration testing was started for some sets immediately after pouring the cylinders (t = 0).

Three levels of vibration amplitudes were selected for this segment of the testing program. The vibration amplitudes were designated low, medium, and high. Although there were no guidelines for this designation, the amplitudes were found to increase as the frequencies in the readout box increased.

A **FMC Syntron (Model 04A)** vibration table was used in this study. This model has a variable frequency counter (**Figure 3.1**). However, this shaking table, as in any other multipurpose commercial tables, did not have control over the vibration frequency and amplitude at the same time. It was noticed that as the reading on the frequency counter increased, the amplitudes of the vibrations increased, accordingly. Therefore, before the vibration of concrete samples began, the decision was made to identify the signals generated by the shaking table, including waveforms, frequencies and amplitudes. Also, since the electric vibrating motor was mounted at the center of the table, the vibration identification could be conducted at two different locations, the center, and at the edge of the table.

After recording the generated waves using two accelerometers **(PCB, Model 353-B04)** connected to a two channel oscilloscope, the vibration amplitudes increased with the frequency.

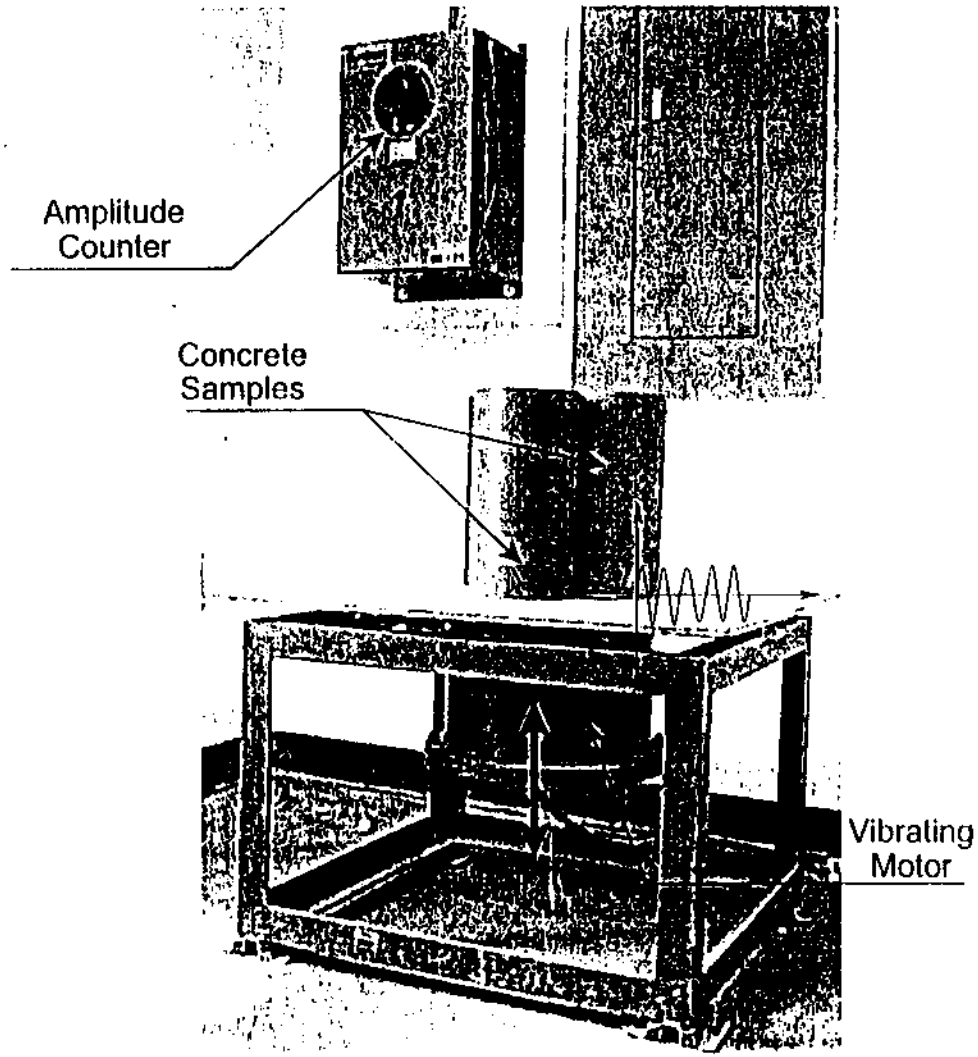


Figure 3.1. Shaking table used in the study.

The frequency increment, however, did not exceed 300 Hz after attaining an acceleration of about 15g.

Using the generated sinusoidal wave forms, the velocity amplitudes selected for this study were 0.128 in./sec, 2.58 in./sec and 8.3 in./sec; these were used for all the tested samples. The concrete samples were subjected to vibration at predetermined time delays. The time delay intervals were 0 hour, 1 hour, 2 hour, 3 hour, 4 hour, and 24 hour. A set of three samples was tested at the same time to obtain the average measurements. Measurements of the compressive strength, f'c, for the concrete samples were taken at 3 days, 7 days, 14, days, and 28 days.

Before the compression testing, each sample was tested using the ultrasonic testing method **(ASTM C-597)** to determine the compression modulus of the material **(Figure 3.2)**. An ultrasonic concrete tester **Model PUNDIT CT-330** was used for the testing. As for the compression test, the ultrasound testing method, necessitates full contact between the exciter and the concrete surface. This contact was achieved by using high vacuum grease to ensure the transfer of the high frequency pulses (54 kHz) through the concrete sample. Any variations in the arrival time of the high frequency signals can drastically affect the determination of the wave velocities and, hence, the compression modulus values.

Of particular concern is that measuring compression modulus using the ultrasound testing method may result in stiffness values that are higher than those obtained from the standard method for determining the static modulus of elasticity (***ASTM C469***). The main reason for this increase in the stiffness values is the very small strain levels produced by the ultrasound pulses. Despite the difference in the compression modulus values, the consistency in the ultrasound testing procedure provided comparable variations in the stiffness values of the concrete samples.

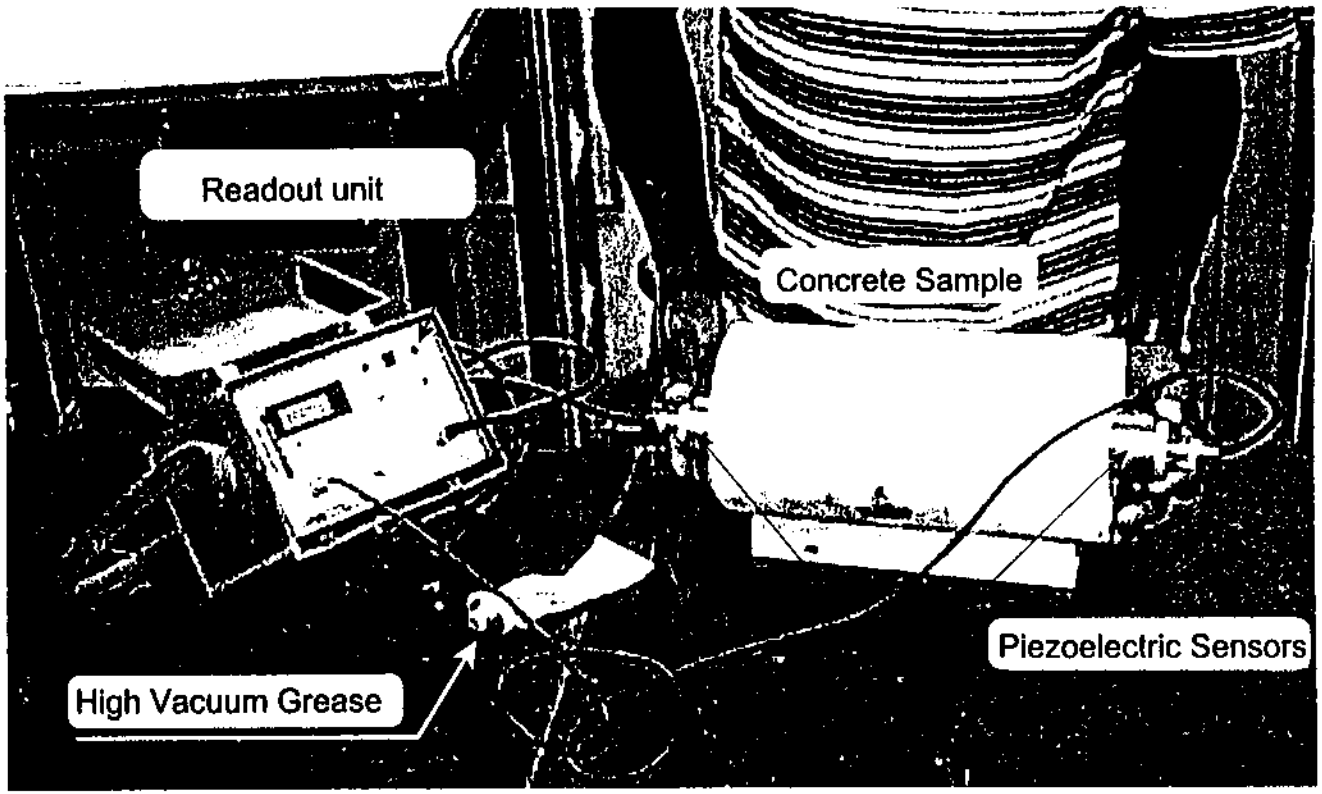


Figure 3.2: Ultrasonic Testing For Concretre Samples

Therefore, the effect of parameters, such as vibration amplitude and time delay from revibration, could be studied from ultrasound testing.

After concluding the stiffness measurements, concrete samples were prepared for the compression testing according to the ***ASTM C-39*** specifications. All the samples were carefully monitored during load applications for any unusual behavior that the samples could exhibit. The compressive strength tests did not reveal any uncommon patterns of failure associated with vibrations. However, some concrete cylinders exhibited increased surface voids when they were visually examined (**Figure 3.3**). These cylinders were obtained from sets subjected to high vibration amplitudes (8.3 in/sec) after three hours from concrete placement. It was difficult to establish the increased void content at the cut surfaces of the laboratory samples and cores from the field, as compared to those subjected to lower vibration amplitudes. Similar observations were recorded for core samples obtained from the full scale drilled shafts at the Delray Beach and Clearwater sites. These cores were obtained from shafts subjected to vibrations after two to four hours from placement.

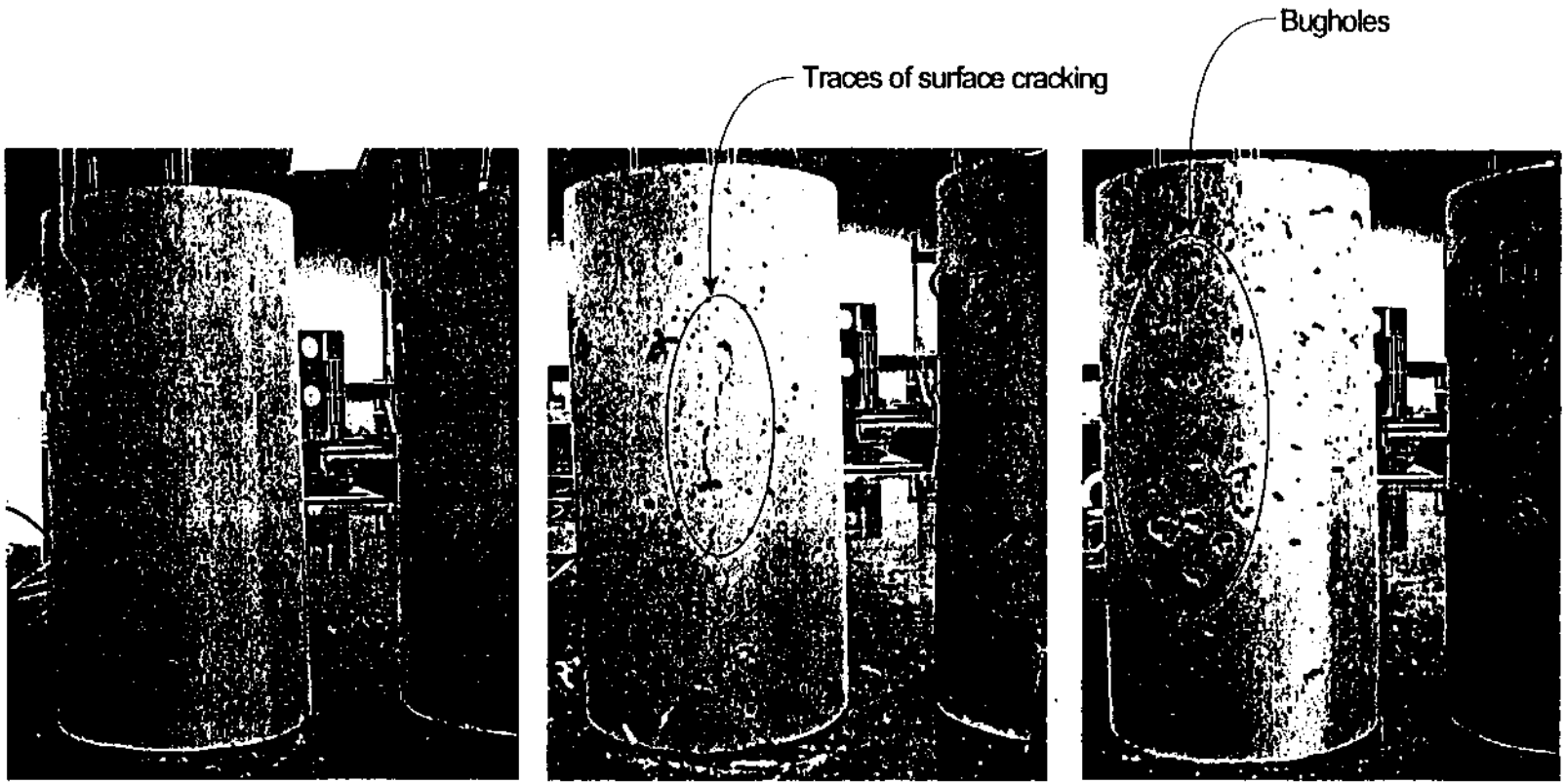


Figure 3.3: Concrete samples subjected to different levels of vibration amplitudes and at various delay time; (A) Low vibration amplitude at zero time, (B) High vibration amplitude at two hours, (C) High vibration amplitude at three hours.

sites. In each boring, a slurry mix was used to prevent caving in the bored hole. The soil samples obtained with the split-spoon methods at FAU were analyzed for their properties at FAMU/FSU, the details of which are covered later in the chapter on laboratory testing. On-site visual inspection of the soil samples showed some very thin layers of crushed shells; however, these layers of shell were far and in between, and went unnoticed in the SPT blow count records. Soil samples were not taken at the other two sites, rather their existing records were analyzed and compared with the samples taken at the FAU North Campus Site; their similarity did not dictate any further testing.

## 4.2 FIELD VIBRATION TESTING

### 4.2.1 FIELD TEST NO. 1 (FAU, BOCA RATON, FL)

In view of the cost of installing deep foundations, it was necessary to conduct a preliminary installation of a steel casing during which the vibration levels in the subsurface would be observed and analyzed. The purpose was to gain an understanding of the dynamic properties of the subsurface and the amplitude of the generating source of vibration that would be used during installation of the drilled shafts.

To gather the data needed to generate a profile of the vibration travel in a 3-D environment, two tests were undertaken at the North Campus of FAU. On December 3, 1997 the profile of the range of displacements at the surface and subsurface was determined in the laboratory to predict the effect of these vibrations on the integrity and strength of the field shafts.

Before starting the field testing, representative soil samples were obtained on August 27, 1997, from two soil borings drilled to about 41 feet. The two boring logs showed that the soil layers at the site were predominantly light tan to dark sandy soil. The obtained samples were then transferred to the **FAMU-FSU** College of Engineering in Tallahassee for further testing.

During the preliminary investigation, the driving subcontractor vibrated the 36-in. steel casing into the subsurface. The installation was achieved using an MKT vibratory hammer. The steel casing was vibrated using the maximum frequency of the hammer's output. These frequencies ranged between 1800-2000 rpm. The steel casing was introduced into the ground at a steady rate in increments of five feet. This increment was decided based on the need to remount the accelerometer attached to the steel casing, which measured the actual displacement of the casing from a distance of five feet above ground level, until it reached the surface of the soil. In addition to the monitoring of the displacement, surface vibrations were successfully recorded and the nature of these will be discussed later.

#### 4.2.1.1 SITE PREPARATION

The ground water table at the site was at about 6.5 feet from the surface. This shallow water table caused some difficulties in installing the triaxial geophones needed to monitor the propagation of the vibrations. The triaxial geophones **(MARK, Model A020793)** inserted in the designated boreholes were buried in the ground once the casing started to vibrate. Recovering the sensors from the ground resulted in a significant time delay which necessitated the postponement of this segment of testing.

#### 4.2.1.2 INSTRUMENTATION AND VIBRATORY EXCITATION

Only casing and surface vibrations could be monitored and recorded from this trial. The sensor attached to the steel casing was of a special type of shock accelerometers **(PCB Model 370A02)** and was placed at a five foot depth from the ground surface. After driving the 36 inch diameter casing into the ground, the accelerometer was relocated at

the same depth from the surface **(Figure 4.1a)** . To provide a proper coupling, the surface accelerometer **(PCB Model 353 B04)** was attached on a steel rod which was inserted in the ground **(Figure 4.1b)**. Vibration measurements were taken at distances of five, ten and ten foot consecutively from the vibrating casing **(Figure 4.1c)**. Signals from the accelerometers were captured by a two channel FFT analyzer. **Figures 4.1d and 4.1c,** Measurements were then stored on a floppy disk for further analysis.

Dimensions of the steel casing used during this investigation:

| | | |
|---|---|---|
| Thickness | = | 0.5 in. |
| Length | = | 40.0 ft. |
| Diameter | = | 36.0 in. |

### 4.2.1.3 MONITORING OF VIBRATIONS

During the installation of the steel casing, vibration levels were monitored at three different locations, which are discussed below:

Steel Casing

The steel casing is the medium through which the vibrations are translated into the subsurface. Thus attaching a PCB accelerometer to the casing generated a history of the displacement of the casing through its penetration into the ground. The accelerometer was placed five feet above ground on the steel casing. Once the accelerometer reached ground level the vibration was stopped and the accelerometer relocated to five feet above the ground. The amplitude obtained during the oscillation of the steel casing were used to determine the attenuation of the subsurface material and these records are compared with the laboratory results in Chapter V.

Surface

Motion at ground level has the potential to produce the largest displacements. The surface is a 'free-end', thus its range of motion is not confined as deepening layers. Using a Wilcox Research accelerometer on the surface at varying distances during the installation of the steel casing, the vibration levels in the surface layer were monitored and recorded. In similar fashion, these records were used to determine the attenuation factors in the working soil.

Subsurface

The recordings were limited and for all practical purposes not useful to interpretation. Therefore, the need for a more comprehensive investigation into the subsurface was identified and is addressed in the next section. The limitations imposed were due to an interface problem with the triaxial accelerometer.

### 4.2.2 FIELD TEST NO. 2 (FAU, BOCA RATON, FL)

In actual field conditions, the generation of vibration during the installation of the steel casing would be significantly similar to a seismic condition generated by blasting or a natural geological event. Seismic methods involve the measurements of the travel-time of seismic waves from the surface, or generating source, to interface geophones. The travel-time would be controlled by the soil conditions, as the seismic velocity in the soil is a function of its elastic constant and density. However, the soil conditions in this investigation were site-specific, and no extensive processing of this data was done beyond what was needed to meet the objectives of the project. When evaluating the concrete strengths, these recordings enabled the correlation of possible damage with the ensuing peak particle velocities. These vibrations are those experienced by a freshly

poured concrete drilled shaft from the vibration due to the installation of a neighboring drilled shaft.

#### 4.2.2.1 SITE PREPARATION, PROCEDURES, AND MONITORING OF GROUND VIBRATION

To reproduce a complete picture of the vibration levels, that would be experienced by a nearby freshly poured shaft during the installation of a neighboring shaft, a 'virtual shaft' was constructed in the field. The 'virtual shaft' enabled the placement of eight geophones at varying depths. The depth of the geophones varied in five feet increments from 0-40 feet in a circular array around the vibrating steel casing at nine feet of 3D, where D is the diameter of the vibrating steel casing, Figure 4.2. The bored holes were cased with PVC pipes to withstand caving of the surrounding soil mass. The geophones were lowered onto their intended depths and restrained, ensuring proper contact with the surrounding soil.

The same steel casing and vibrating hammer, as used in Field Test No. 1, were utilized in this test, on January 9, 98. The actual location of some of the field geophones did not meet the intended depths due to backwash (approximately five feet) in the PVC pipes at depths greater than 10 feet; however, the variation in location was not believed to be a detriment. The measurement points in the 'virtual shaft' were sufficient to provide an accurate account of the vibrations experienced at the recording depths during the installation of the steel casing. The depth locations, 5 and 40 feet, were measured twice: these two points indicated the upper and lower limits of the location of the geophones. During the installation, the remaining geophones in the circular array provided

intermediate data between the upper and lower limit points. However, the geophones, 92 to 97 were at distances greater than 3D for the second drilled shaf(vibrating casing).

The sampling rate was 200 samples per second using the data acquisition system. The recordings were conducted in series, one geophone at a time in one-second intervals. The steel casing was centrally located in the center of a nine feet diameter circle bounded by the eight boring holes. Vibration of the steel casing was increased from 2000rpm at 20 feet to 3000rpm up to a depth of 40 feet. This procedure was repeated twice to validate the data.

Vibrations were recorded on a multichannel seismograph at a rate of sampling equal to 300 sample/seconds. Although it was not particularly high, the rate of sampling and the sequence of signal recording would correspond with the nature of the induced vibrations. The generated waveforms were supposed to be sinusoidal with frequencies ranged from 20 to 40 Hz. The data acquisition system collected a time-history record of one second length for each channel. The recording process was in a sequential order, which means the second time history record for the same channel would be collected after eight seconds. For three consecutive time-history records from each channel, the vibration had to last for about 24 seconds.

#### 4.2.2.2 DRILLED SHAFT CONFIGURATION AND INSTALLATION PROCEDURES

The configurations of the shafts installed are shown in **Figure 4.3**. Two different diameter shafts were used, i.e. 24" and 36". The instrumentation of the shaft would provide a record of the levels of vibrations that the freshly poured drilled shafts

experience. The layout of a single shaft set up is shown in **Figure 4.4**. A set comprised two shafts, one of ϕ24" and the other of ϕ36". The larger diameter shaft ϕ36" was reinforced, and designed to duplicate actual construction conditions. The purpose of the smaller shaft was to determine the vibrations and their possible effect on the integrity and strength of a shaft installed within a 3D distance from the vibrating source, where D is the diameter of the vibrating source, in this case the steel casing.

Installation Procedure in the Field:

1. Set up of equipment and instrumentation.
    a. Geophones.
    b. Temperature sensor.
    c. PVC tubes.
    d. Vinyl ties.
    e. Protecting Foam.
    f. # 9 Re-bars.
    g. # 3 Ties.
2. Construct steel cages.
3. Install instrumentation as specified by design and manufacturer recommendations.

Field Installation of the Steel Casings.

1. Obtain digging permit for the site.
2. Clear surface debris.
3. Record dimensions of the steel casing.
4. Drive steel casings to desired depth.

5. Check levels of the casing.
6. Auger soil from the shafts.
7. Record soil material.
8. Check depth of drilling.
9. Continue to check the shaft for desired length.
10. Remove any foreign material introduced into the shaft.

The steel casing was then extracted from the ground using the same vibration technique. Time-history records were gathered during withdrawal in the same manner as for the driving stage. The extraction process was accomplished by connecting one side of the casing to the vibrator using a steel cable (**Figure 4.4**). Although this method is a common practice when extracting the steel casings, vibrations generated from this operation may not necessarily be similar to those obtained during the driving process. The main reason for this descrepancy is the method by which the casing was driven and extracted. As can be seen from **Figure 4.4**, the casing was pulled out in an asymmetrical manner. This mode of vibration application resulted in generating vibration components that were different from those produced during driving.

### 4.2.3 FIELD TEST NO. 3 (DELRAY, FL)

A total of eight drilled shafts were installed at the site allocated by FDOT on the right of way of the off-ramp from I-95 onto Linton Blvd heading west. A layout of the shafts is shown in **Figure 4.4**. Installation and instrumentation of the drilled shafts is shown pictorially in **Figures 4.4 to 4.17**.

### 4.2.4 FIELD TEST NO. 4 (CLEARWATER, FLORIDA)

The 2-hr test data was not monitored at the Delray Site due to equipment problems. Therefore, the testing was done for a single shaft set at the Clearwater site, to save costs, the installation procedures were similar to those carried out in Field Test No. 2 with the use of a single drilled shaft set. The pictorial presentation is in Figures 4.12 to 4.20. This site differed somewhat in terms of geology as demonstrated from the SPT blow counts, however, the difference was minimal and for practical purposes the comparison between vibration levels can be considered reasonable.

### 4.2.5 VIBRATION DATA

The peak particle velocity(PPV) vs time records were obtained for the Field Tests No.3 and No.4 at Delray Beach and Clearwater, respectively. See Appendix B.

## 4.3 TESTING OF CONTROL CONCRETE CYLINDERS

To evaluate the effect that vibrations had on the freshly poured concrete, samples were taken from the concrete poured in the field. The cylinders were cured and tested at fourteen and twenty-eight days. The compressive strength results are shown in Appendix C.

## 4.4 NON - DESTRUCTIVE TESTING

### 4.4.1 PILE INTEGRITY TESTING (PIT)

The PIT method uses the compressive wave stress signal generated by a hand held hammer striking the top of the drilled shaft to determine the integrity of the shaft. Non-uniformity in the foundation or the shaft toe will reflect the stress wave; this reflection can be observed at the top by using a combination of the Pulse Echo Method (PEM) and Transient Response Method (TRM). For further details on the PIT method of NDT see Appendix D.

The PIT results served to verify the actual concreted depth of the shafts. Although, no cracks or major defects are identified with the PIT, the limitation of the theory does not make this conclusive.

### 4.4.2 CROSS-HOLE SONIC LOGGING (CSL)

Sonic logging is used to detect defects in concrete structures. Some of the anomalies that can be detected in a structure and crucial in this study are the segregation of concrete, cracks due to shrinkage, and non-uniformity of shaft due to collapsing of the wall after withdrawing of a temporary casing. Pulses generated by the ultrasonic pulse generator are converted into ultrasonic waves by the transmitter probe and received by the receiver probe. After conditioning, signals are digitized and stored. Additional details of the operation and procedures are shown in Appendix E.

## 4.5 CONCRETE CORING OF THE DRILLED SHAFTS AND COMPRESSION TESTING

One of the additional tests used to determine the integrity of the drilled shafts, was the compression testing of cored concrete samples. The field shafts were cored to obtain samples at various depths by Law Engineering, Miami Lakes, for the Delray Site,

Figure 4.1a. Testing setup for each borehole.

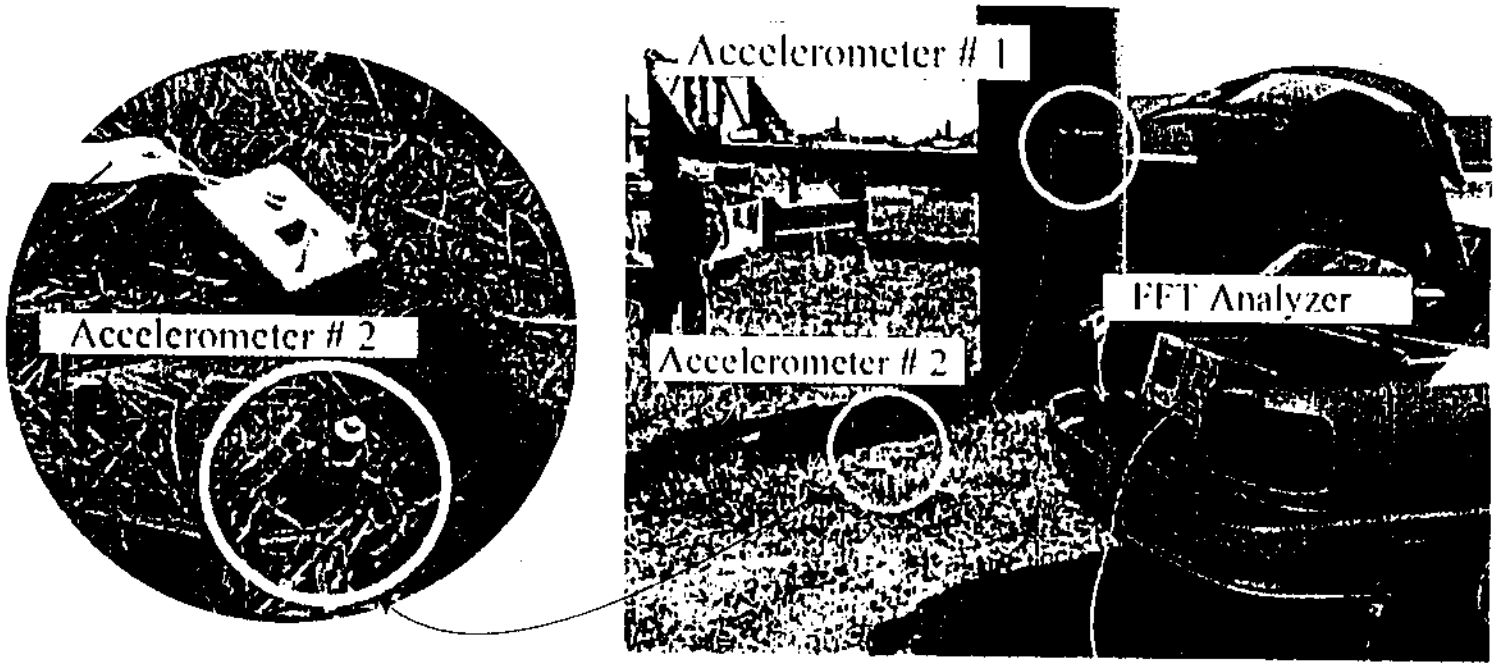


Figure 4.1b. Recording steel casing and ground responses using FFT Analyzer.

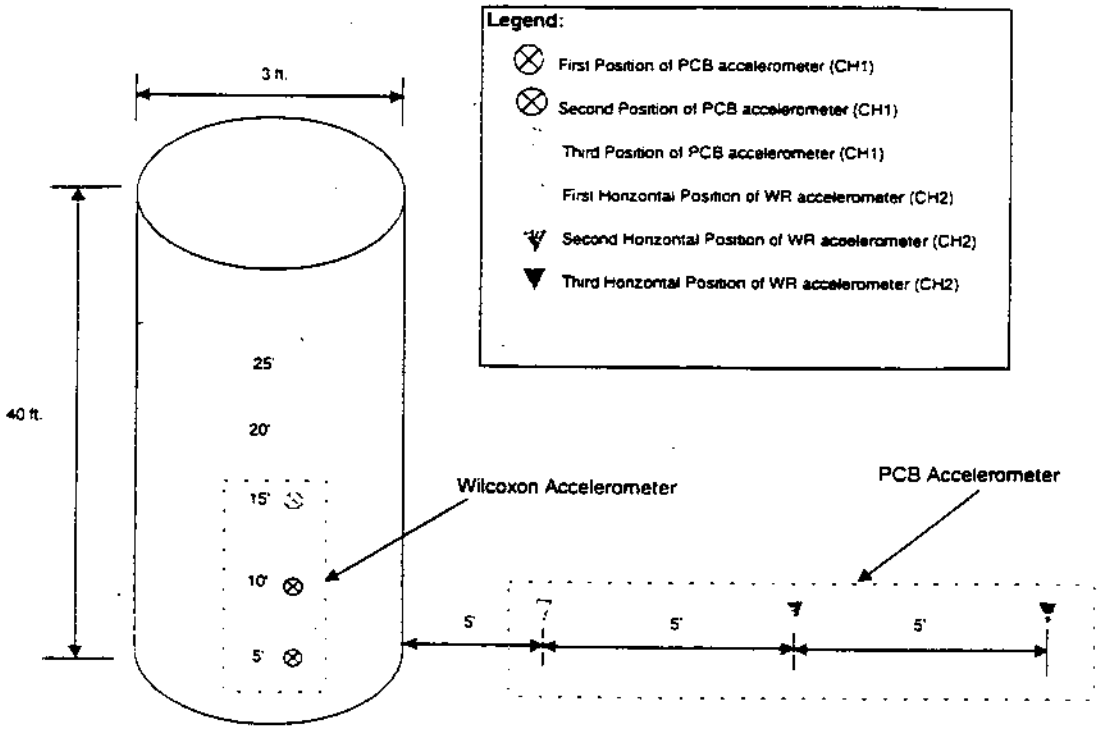


Figure 4.1c Accelerometer Layout

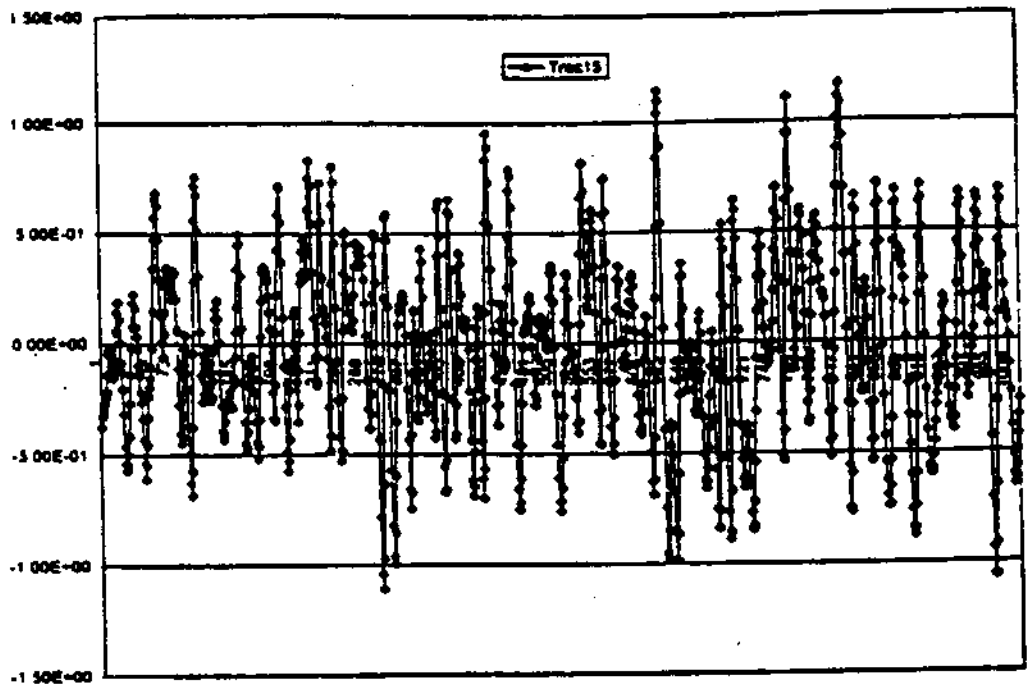


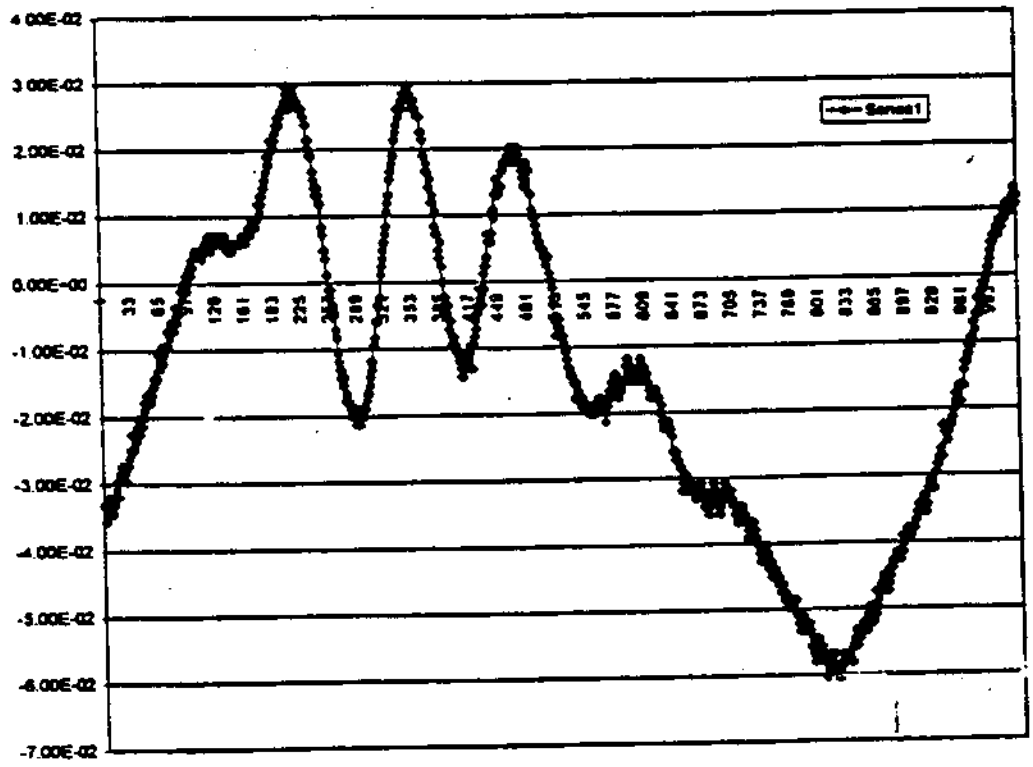


**Fig.4.1D. Traces 15 and 16 showing accelerometer #1 for the vibrating casing, and ground surface accelerometer #2 at 15' away from the casing**

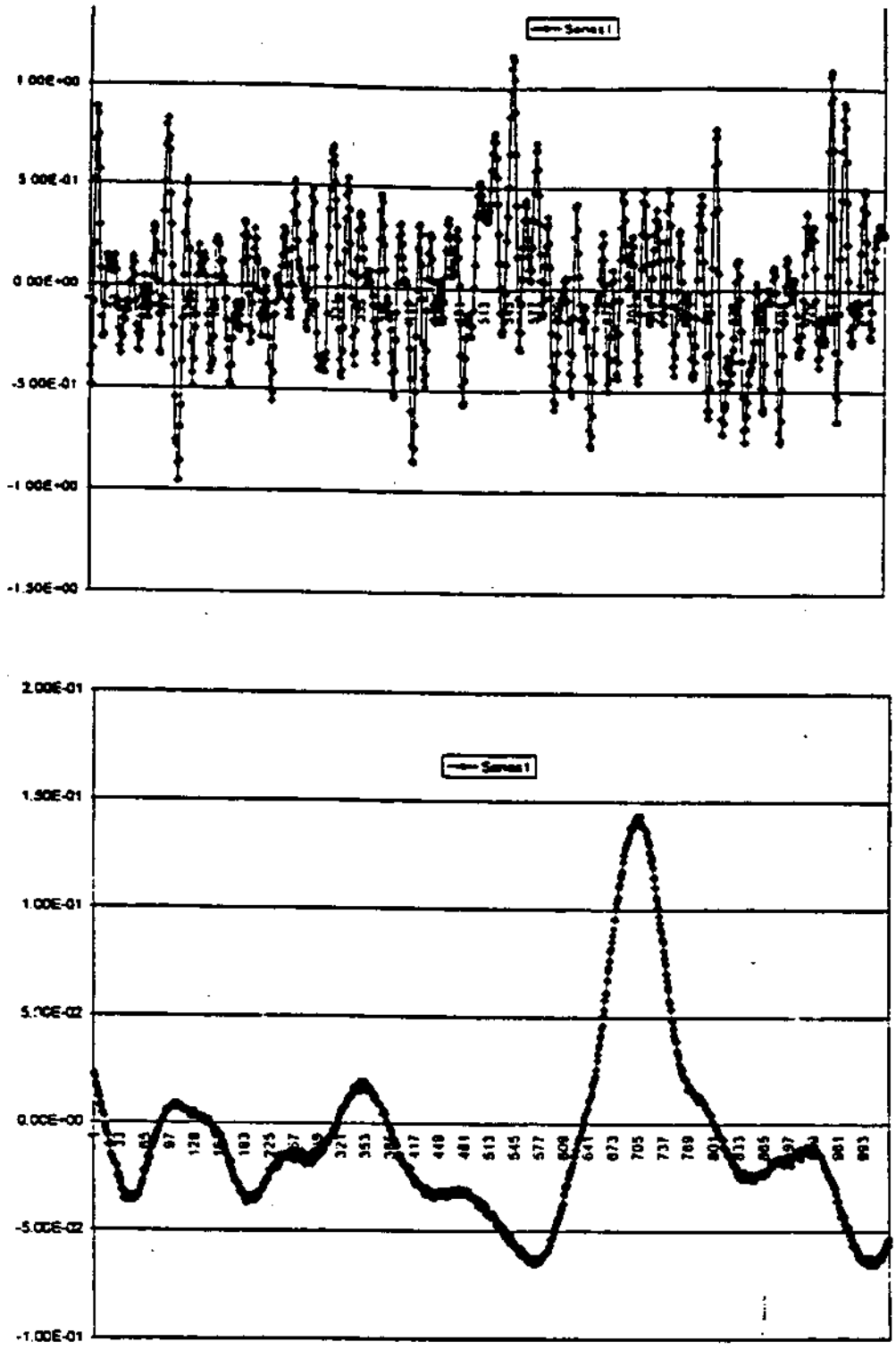


**Fig.4.1e. Traces 7 and 8 showing accelerometer #1 on the vibrating casing, and the ground surface accelerometer #2 at 10' away from the casing**

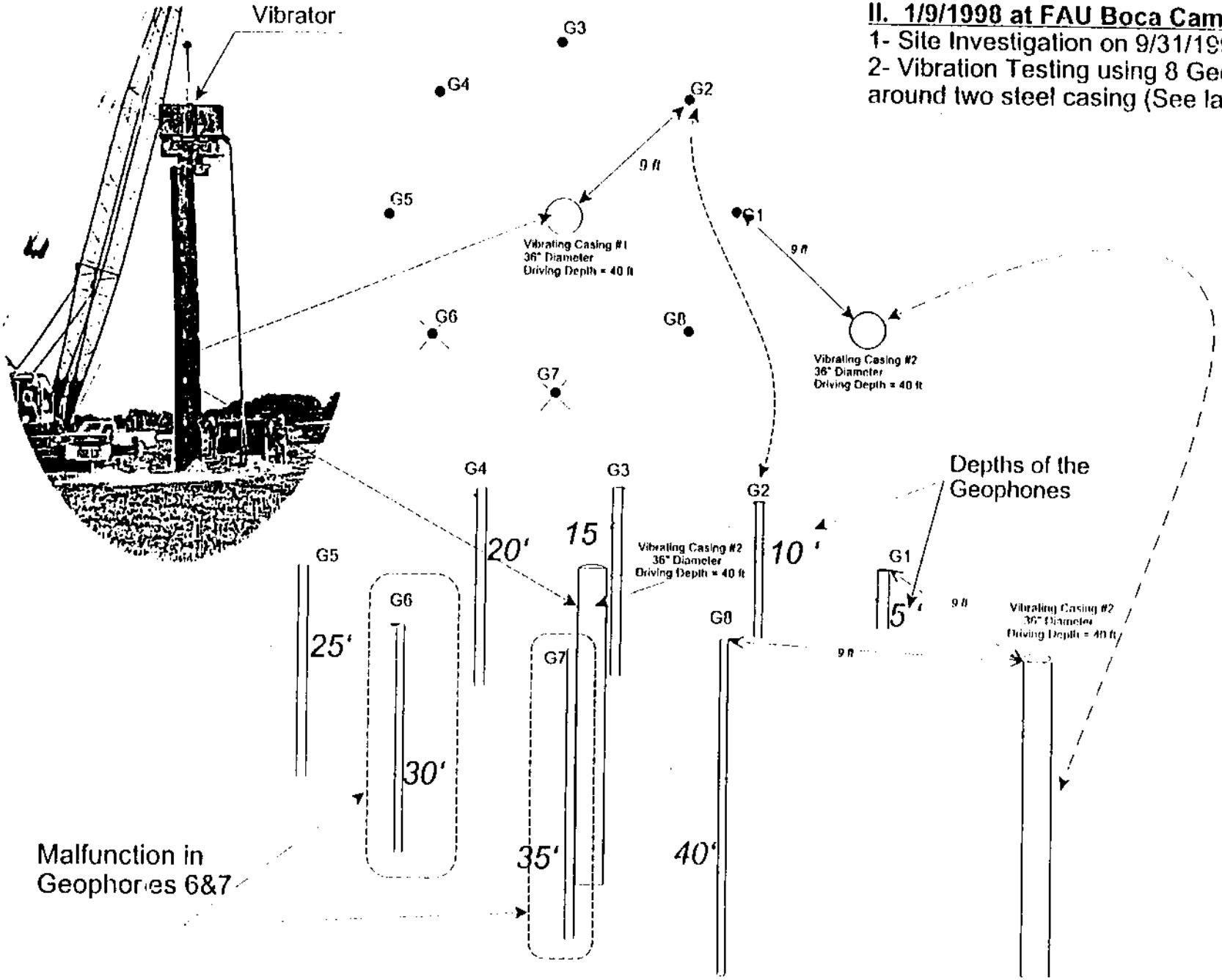


Figure 4.2 FAU Field testing showing the arrangement of the geophones and the driven steel casing.

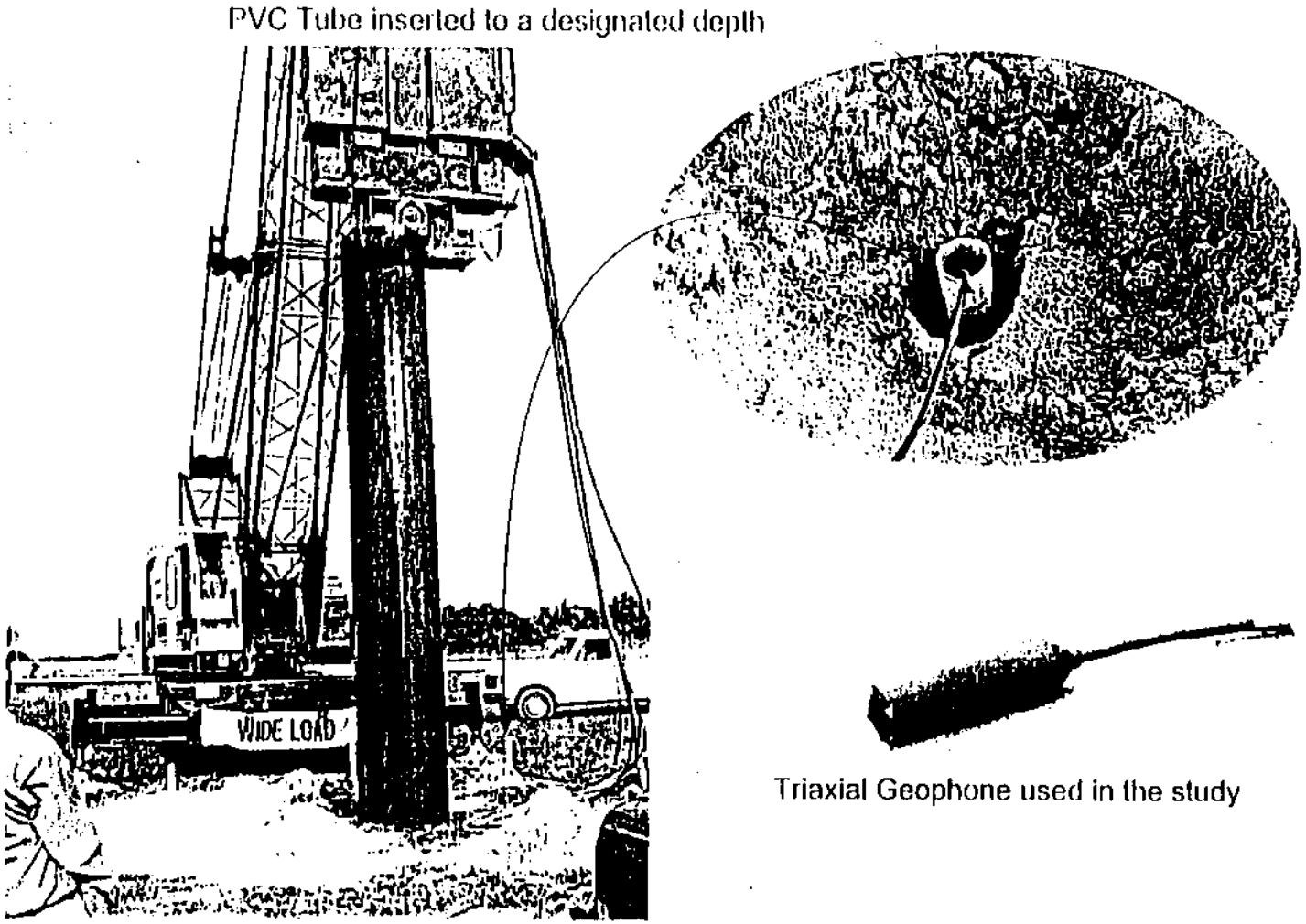


Figure 4.3. Arrangement of geophones in PVC tubes at the FAU test site.

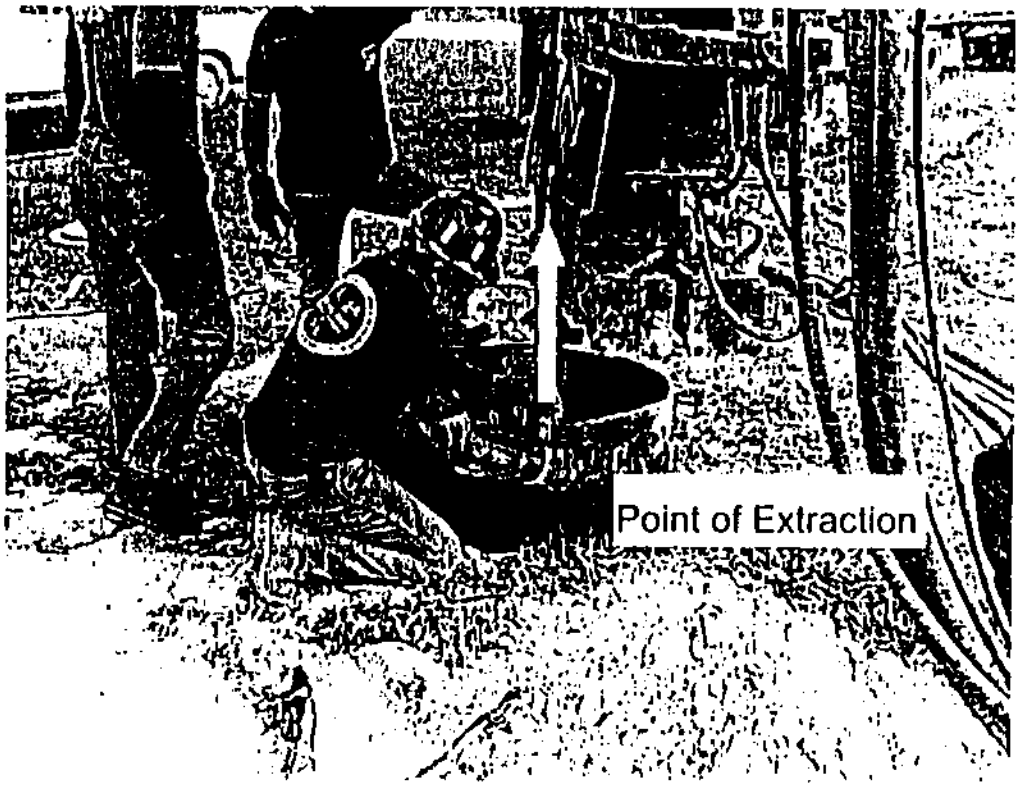


Figure 4.4. Extraction of the steel casing.

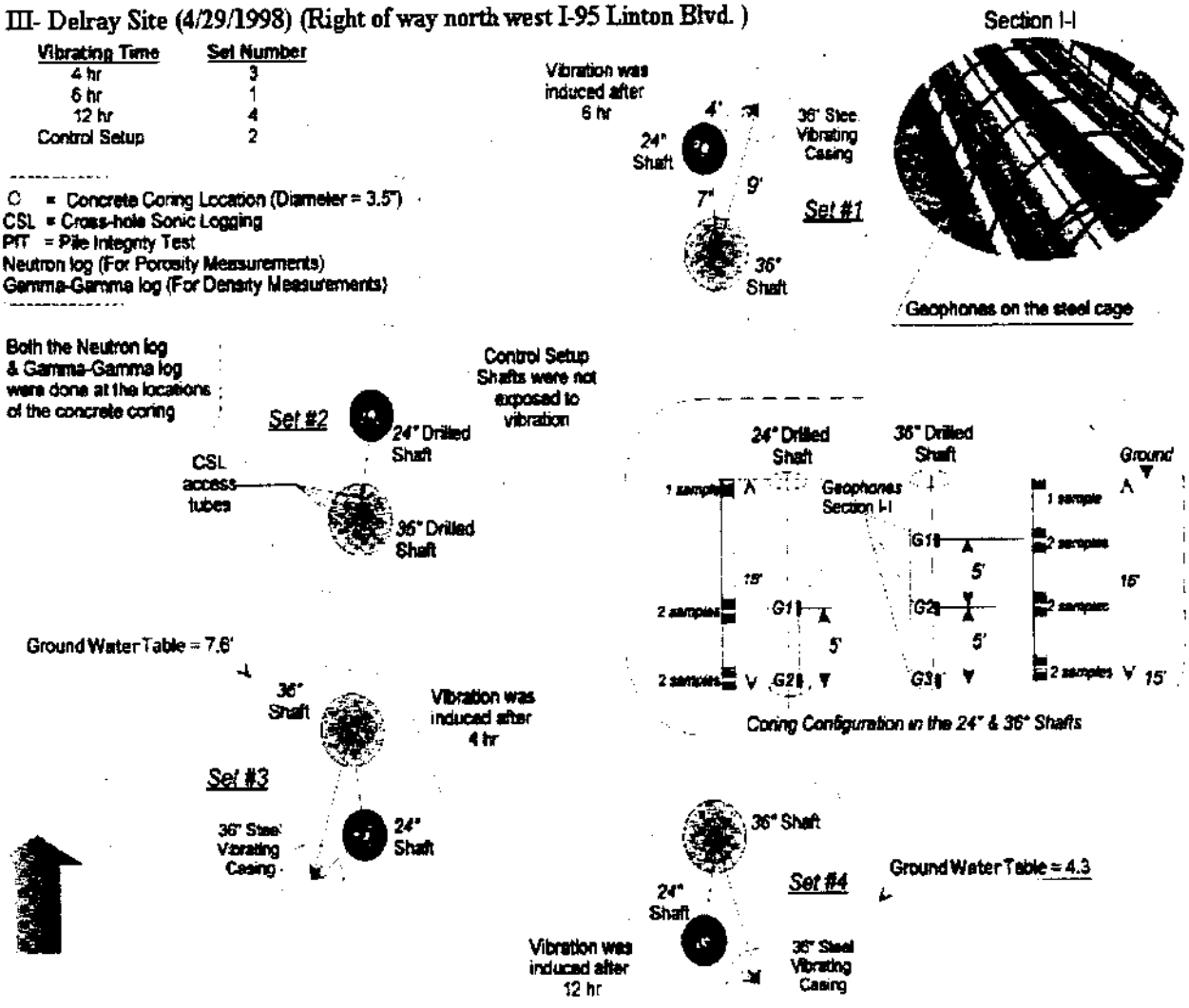


Figure 4.5 a. Configuration and instrumentation of the shaft at the Delray Site

III- Delray Site (4/29/1998) (Right of way north west I-95 Linton Blv.)

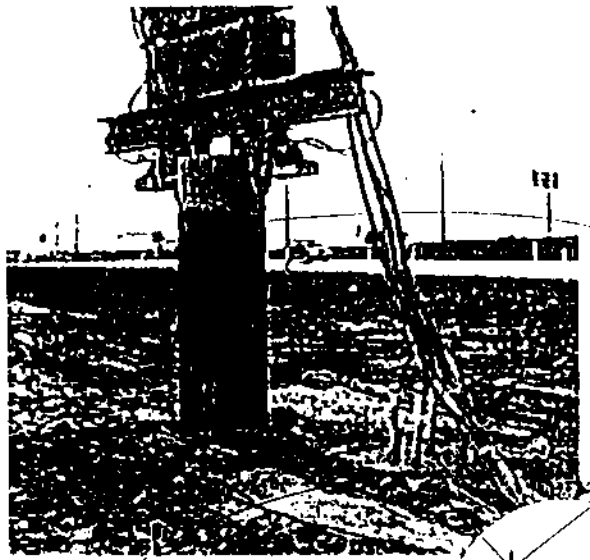





Figure 4.5b. Layout at the Delray Testing Site.

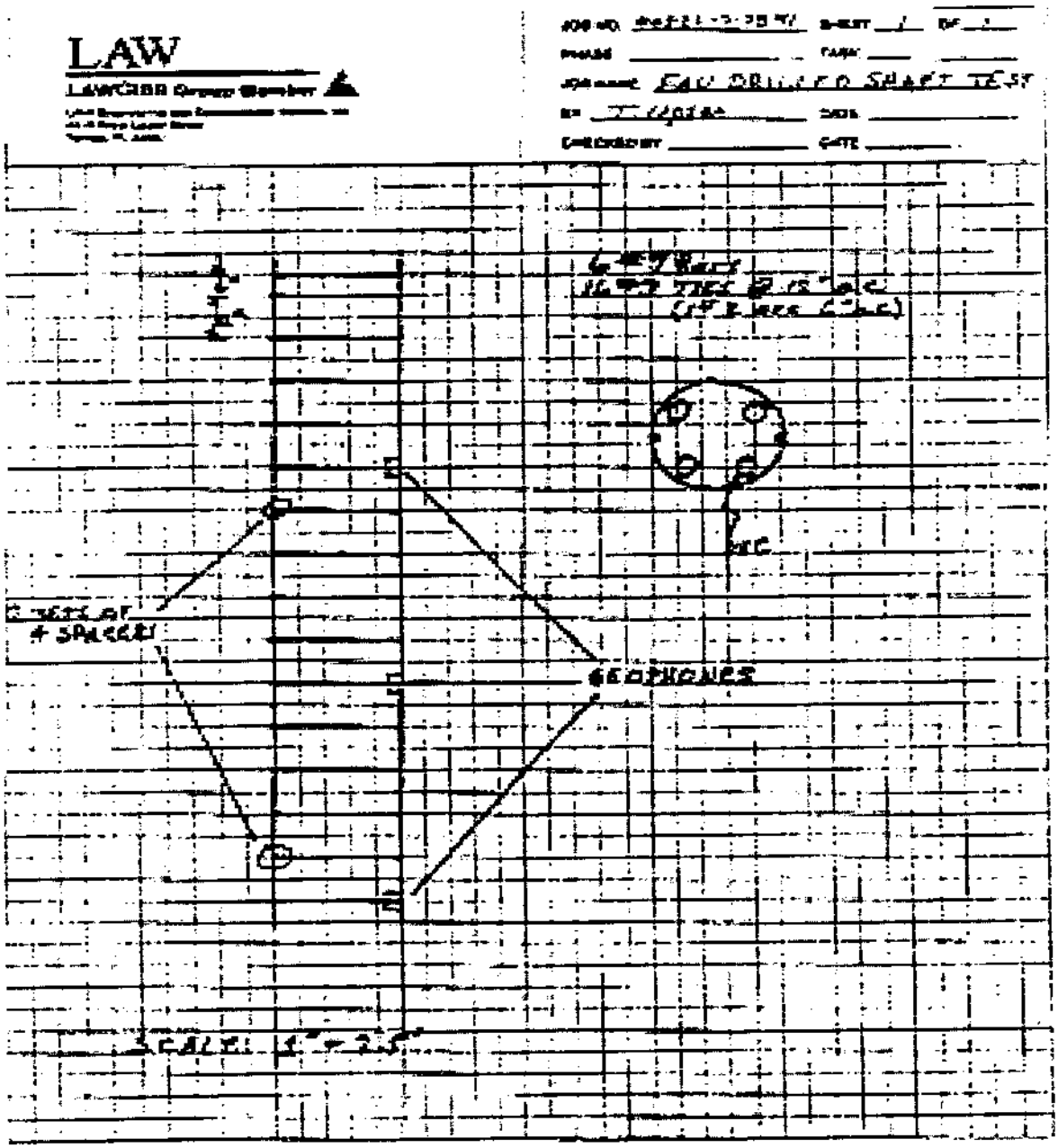


**Figure 4.6. Geophone locations in the drilled shaft (Delray Beach, FL).**

**Figure 4.7. Placing of steel reinforcement with instrumentation Set no.4 (Delray Beach, FL)**

**Figure 4.8. Dropping the tremmie in the hole, Set no. 4 (Delray Beach, FL).**

**Figure 4.9. Pulling of steel casing after pouring of the concrete, Set no. 4 ( Delray Beach, FL)**

**Figure 4.10. CSL tubes and settlement plate, ϕ36" drilled shaft, Set No. 1 (Delray Beach, FL).**

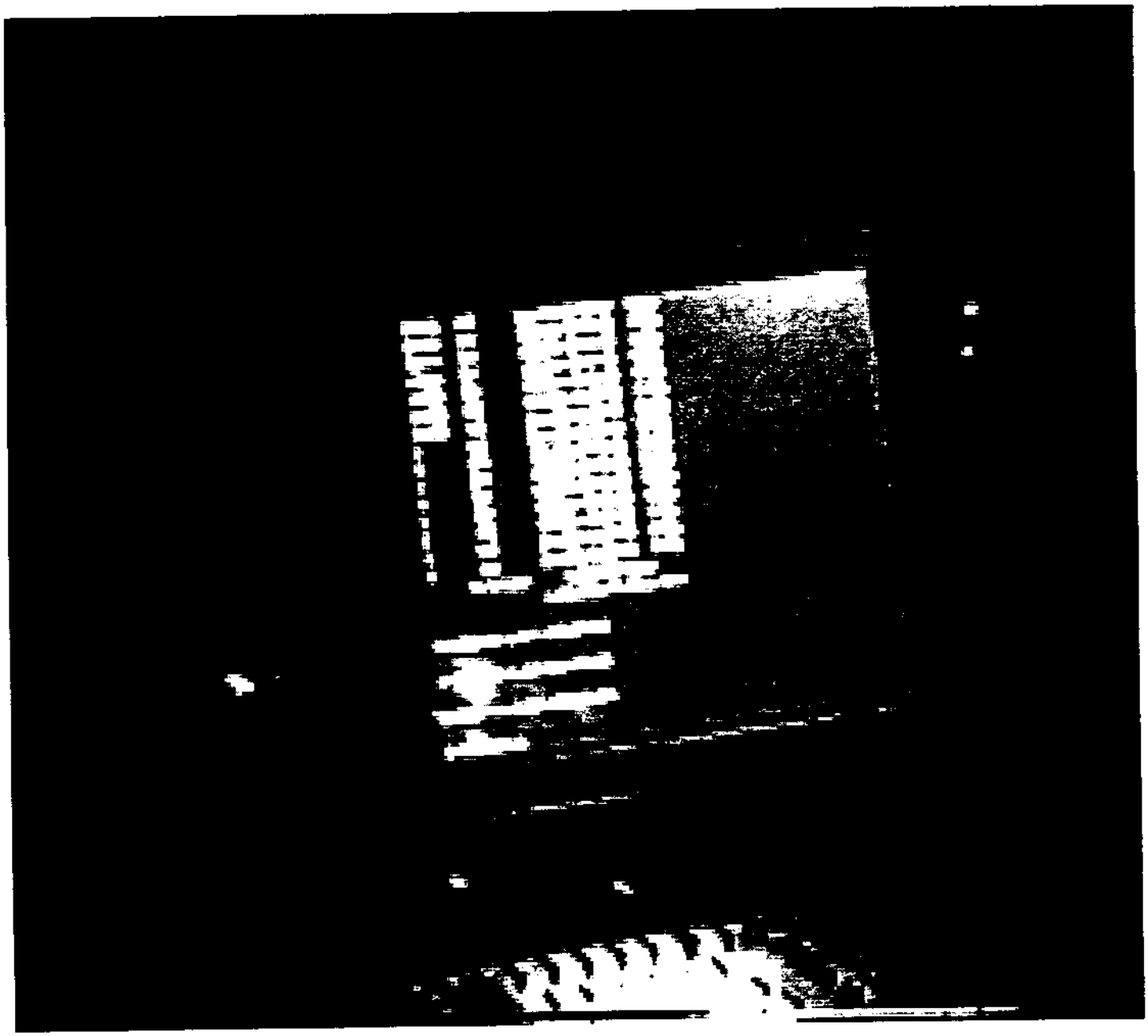

**Figure 4.11. Geophone data acquisition system (Delray Beach, FL)**

**IV- 9/10/1998 (Clearwater) Coastal Caissons**
Only one set was tested
The vibration was induced after 2 hr from construction
two pile were used 3D and 2D

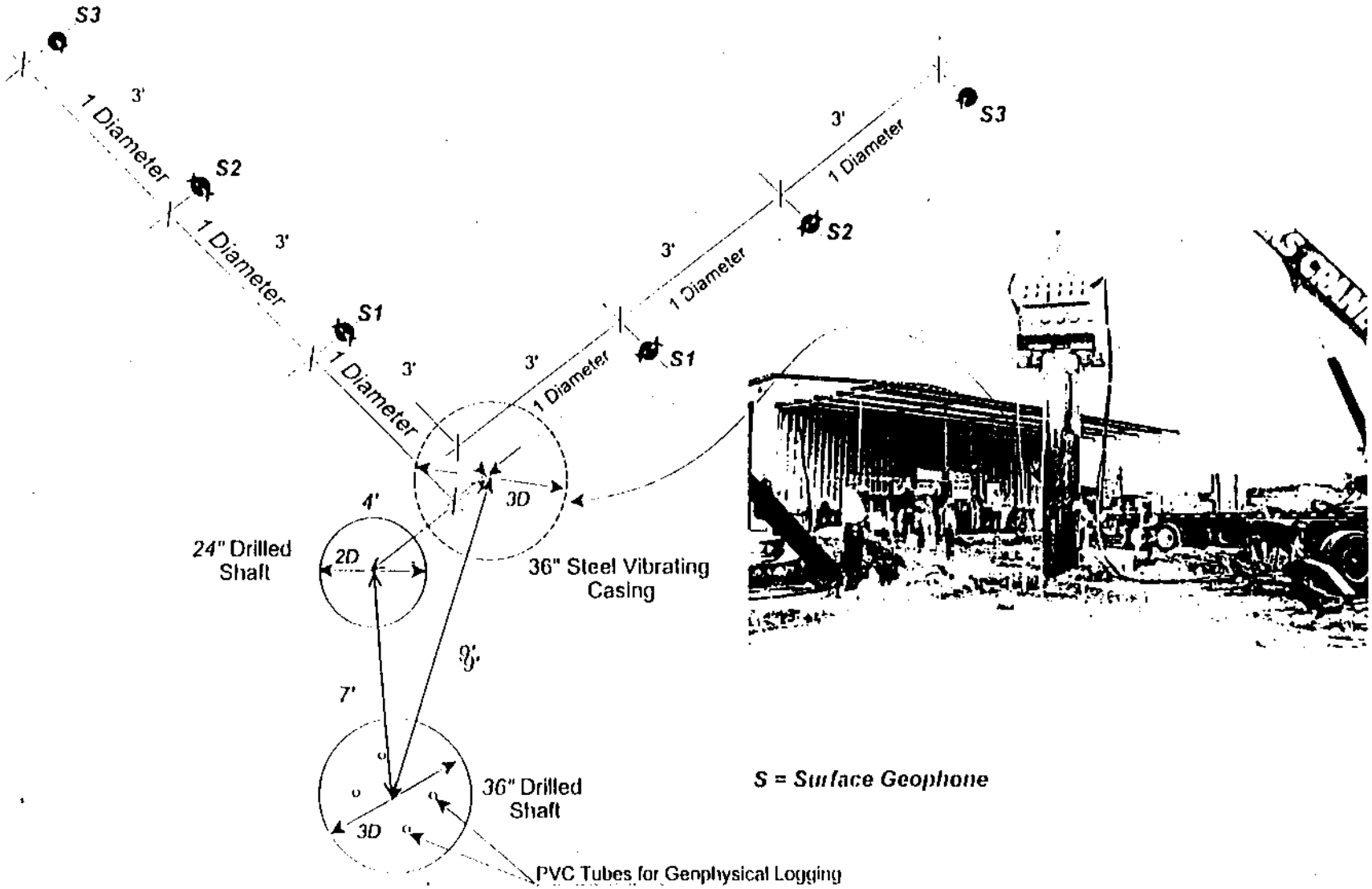


Figure 4.12 Layout at the Clearwater Test Site.

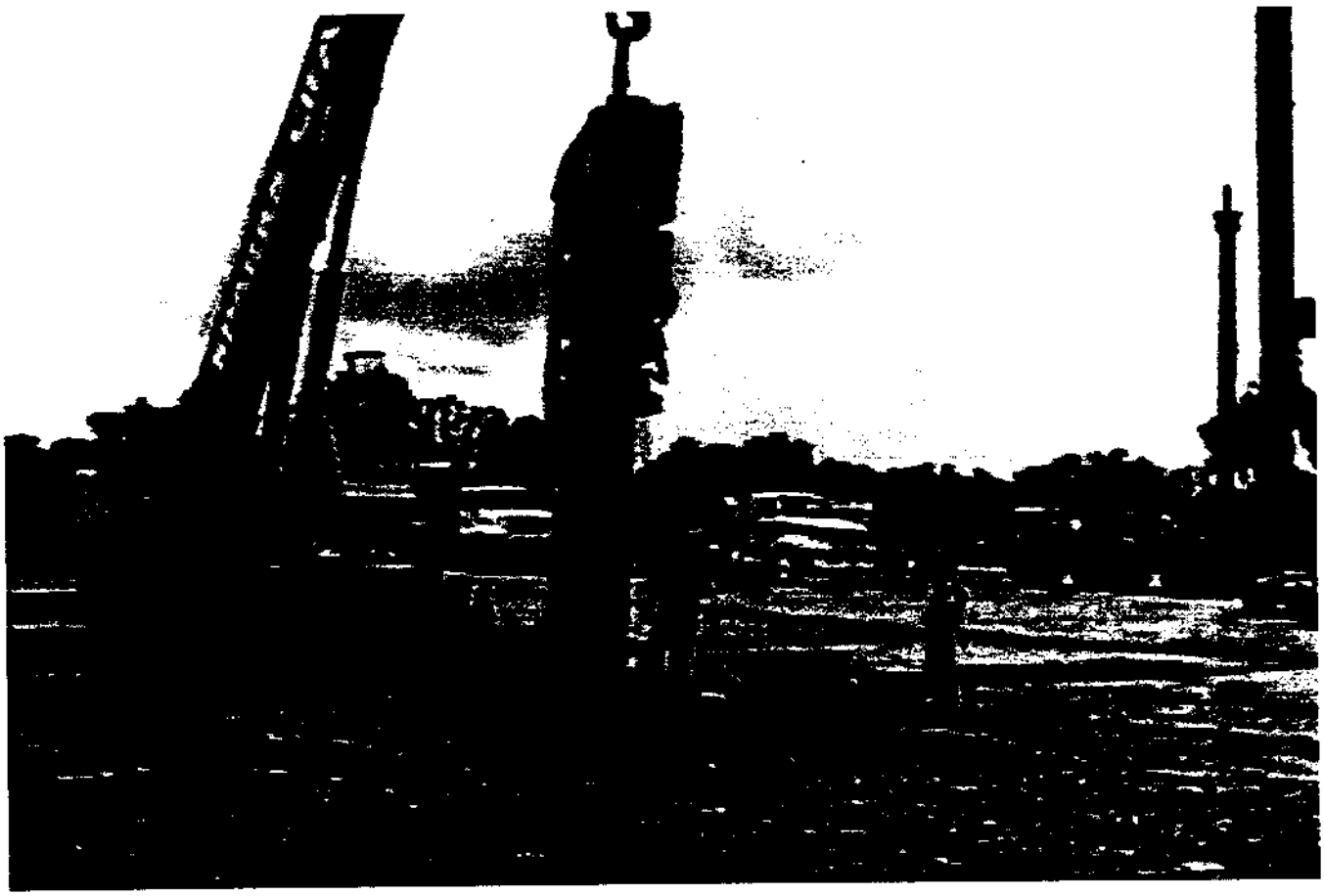

**Figure 4.13. Installation of the 24- inch diameter steel casing ( Clearwater, FL)**

**Figure 4.14. Installation of the 36-inch diameter steel casing ( Clearwater, FL)**

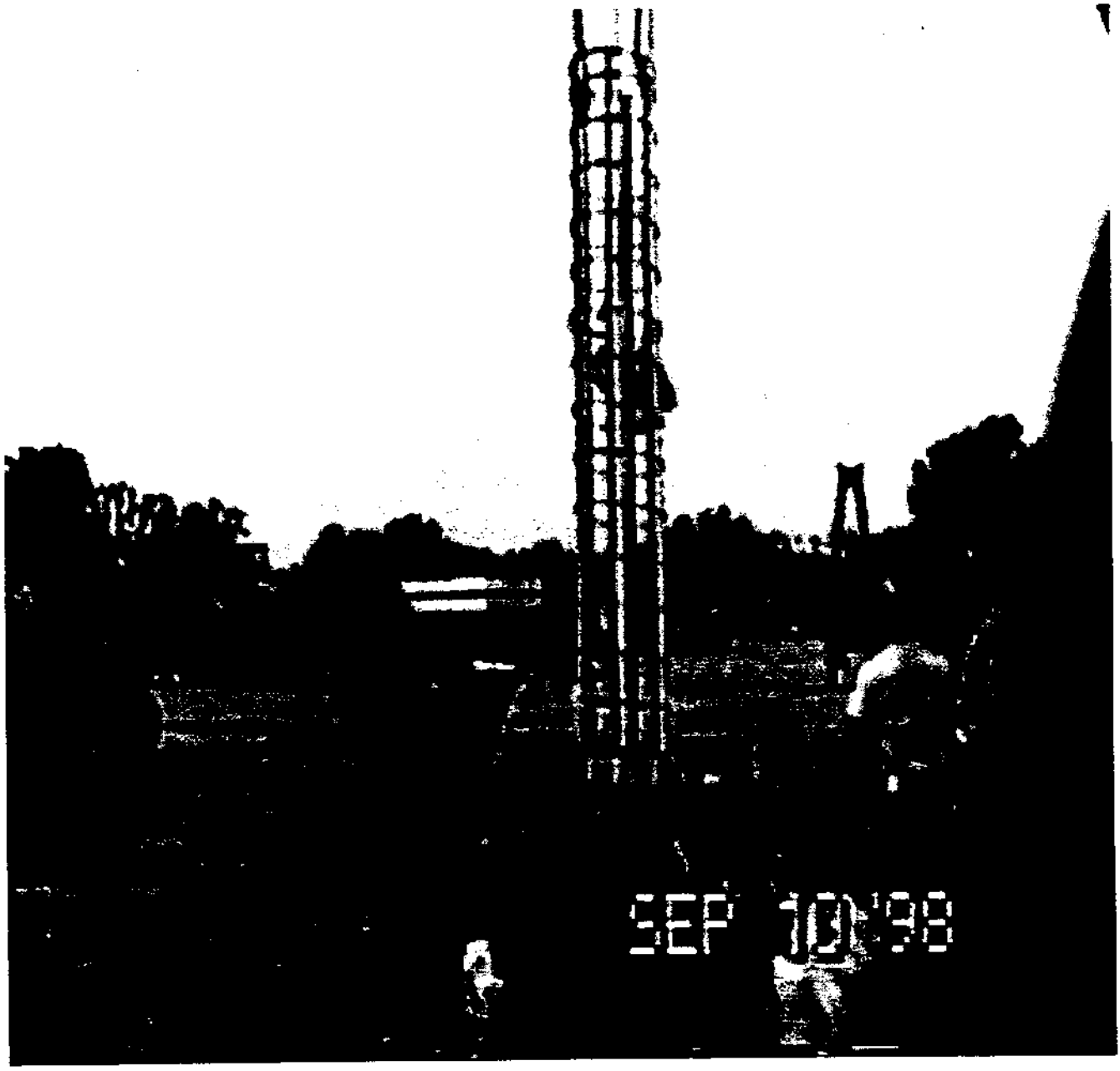


**Figure 4.15. Steel cage with geophone and cross-hole sonic logging instrumentation (Clearwater, FL).**

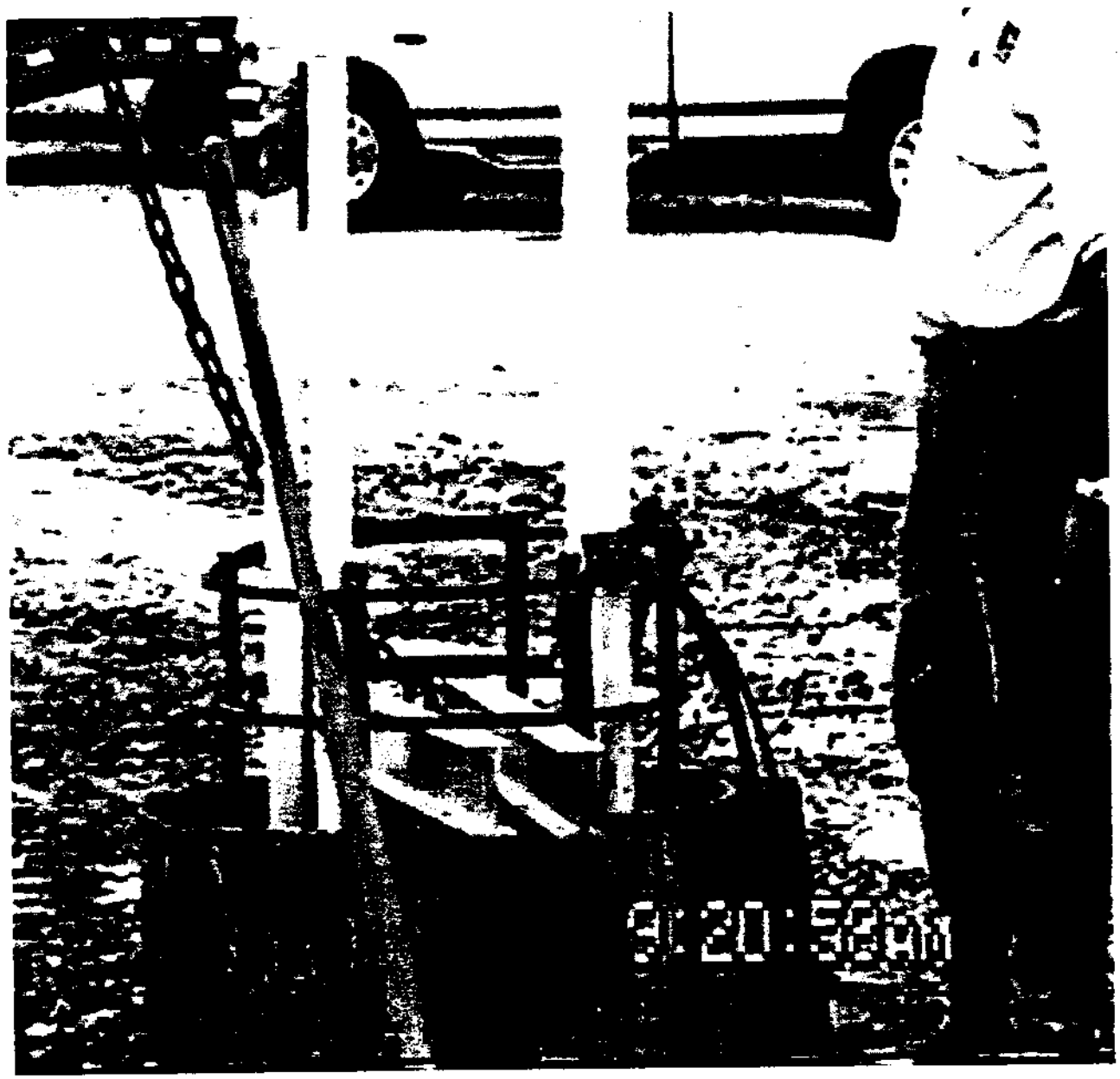

**Figure 4.16. Placing the steel cage in the drilled shaft ( Clearwater, FL).**

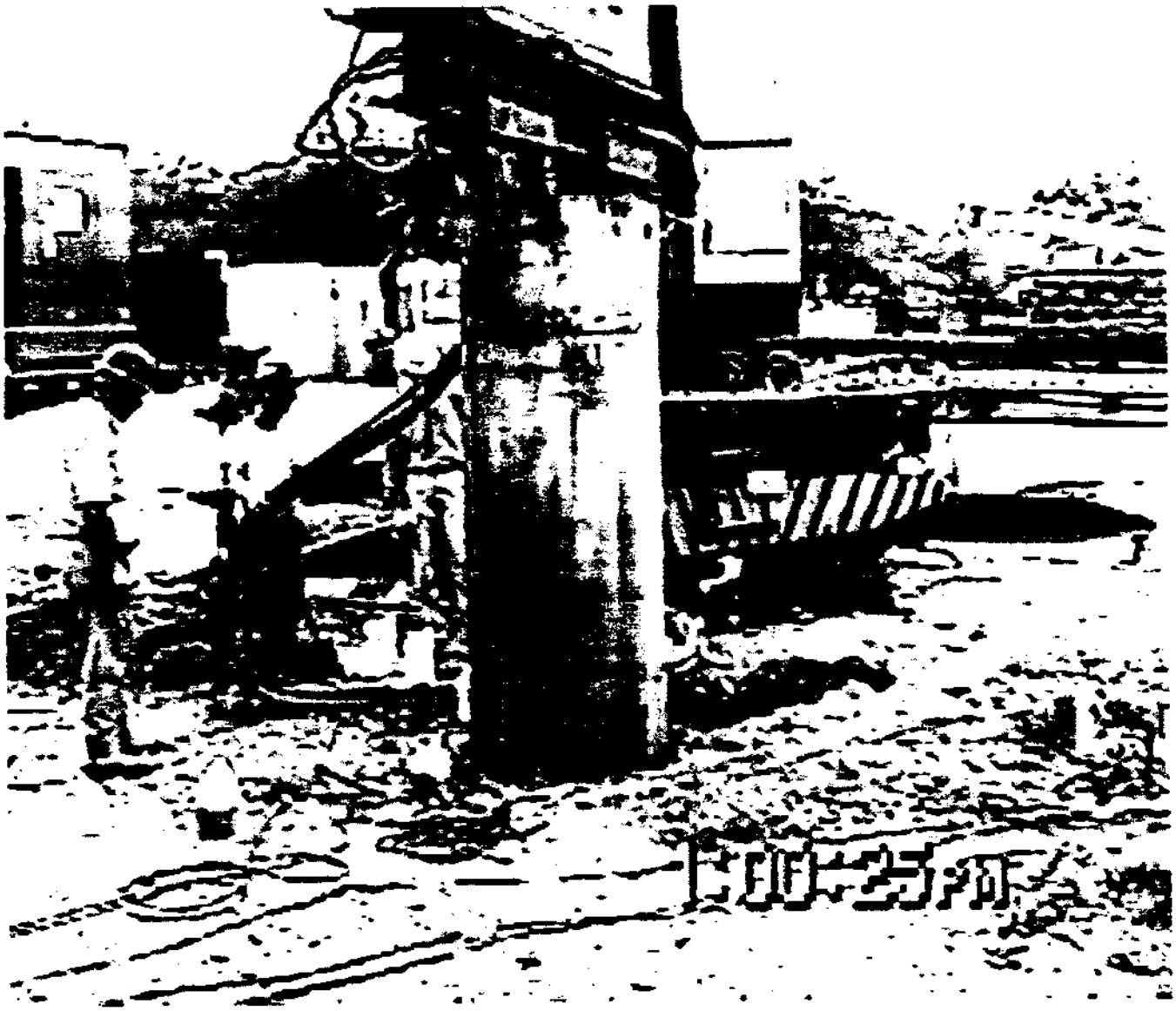

**Figure 4.17. Vibration of casing adjacent to freshly poured shafts (Clearwater, FL).**

**Figure 4.18. Surface placement of cylinders exposed to 2-hr vibration (Clearwater,FL)**

**Figure 4.19 PIT on shaft ( Clearwater, FL)**

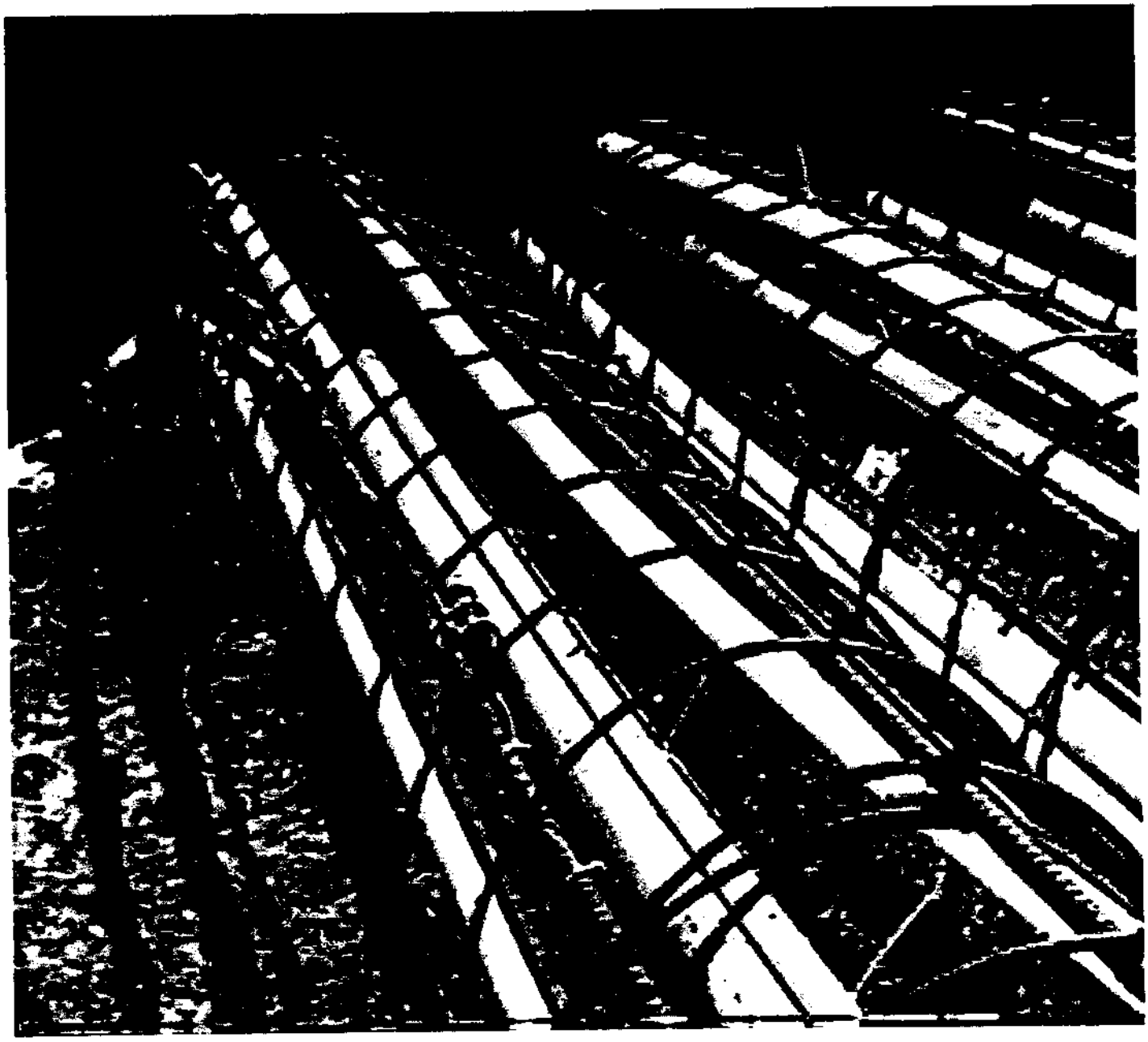

**Figure 4.20. CSL tubes and geophones in place on the steel reinforcing cage.**

**Figure 4.21. CSL recording equipment (Delray Beach, FL).**

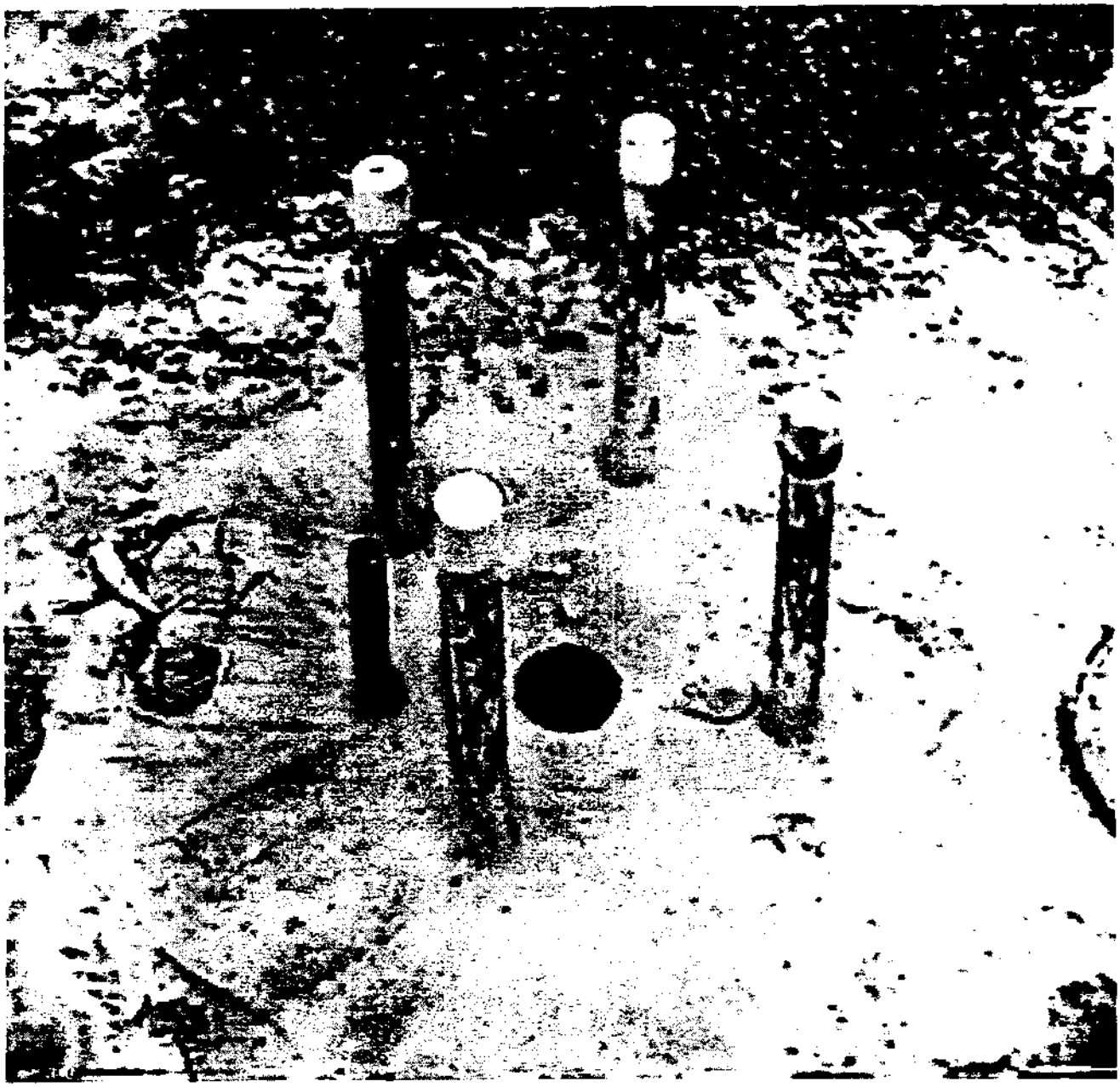

**Figure 4.22. Cored drilled shaft (Delray Beach, FL).**

# CHAPTER V

# ANALYSIS OF RESULTS AND DISCUSSION

## 5-1 Laboratory Test Results

Results from compressive strength tests showed considerable variations (**Figures 5.1 to 5.10** ). These variations may not be significant if the results from one set are compared with those obtained from other sets for the same vibration amplitudes. Concrete samples subjected to vibration amplitudes of 0.5 in./sec did not show any trend when the samples were vibrated at different time delay levels. As the amplitude exceeded 2.5 in./sec, a slight reduction was noticed in both the compression modulus and the compressive strength **(Figures 5.11 to 5.13).** The largest reductions in the stiffness and strength values were of concrete samples subjected to velocity amplitudes of about 7 in./sec. Data tables showing all the laboratory measurements of this segment are presented in **Appendix A.**

On a log-log scale, if tangents of the obtained function are extended, the intersection would produce a threshold velocity at which a noticeable change could be detected in the strength as well as the stiffness values. The threshold for the compressive strength was 6 in./sec and about the same value foe the compression modulus. Accordingly, variations of the compressive strength with the velocity amplitude can be estimated using the following relationship:

$$f'c_{vel} = (f'c) \cdot e^{-0.03\,v} \qquad (5.1)$$

where $f'_{cvel}$ = compressive strength at any velocity amplitude (psi)

f'c = compressive strength at 28 days (psi)

v = velocity amplitude (in./sec)

The following relationship represents a reasonable estimate for the variation in the compression modulus with velocity amplitude:

$$Ec_{vel} = (Ec).\ e^{-0.02\ v} \qquad (5.2)$$

where $E_{cvel}$ = compression modulus at any velocity amplitude (psi)

Ec = compressive strength at 28 days (psi)

v = velocity amplitude (in./sec)

However, it must be noted that the wave forms used in this phase of the testing program were compression waves. Thus, the velocity amplitudes in **Equations 5.1 and 5.2** represent the compression wave. In a real field situation, the modes of vibrations generated from a typical drilled shaft construction are predominantly shear waves (**Figure 5.14**). Therefore, the threshold velocities suggested in this study may not be attainable in the field since the generated shear waves are transferred to the adjacent freshly poured concrete through the shear friction displacement of the casing relative to the soil. Even if full contact was assumed between the soil and the adjacent casings, the amplitudes of the shear waves would have damped based on the material and geometrical damping of the soil surrounding the casings. This hypothesis was proved true during field testing on full scale drilled shafts.

## 5-2 Analysis of Field Results

### 5-2-1 FAU Field Test # 1

The first field testing at **Florida Atlantic University** took place on **December 3, 1997.** The objective for this segment of field testing was to drive a 36" diameter with 40 foot length steel casing into sandy soil layers in order to monitor the ground response. A total of seven holes



Time (hrs.)

Figure 5.1: Compressive strength of concrete samples subjected to acceleration of 0.25 g

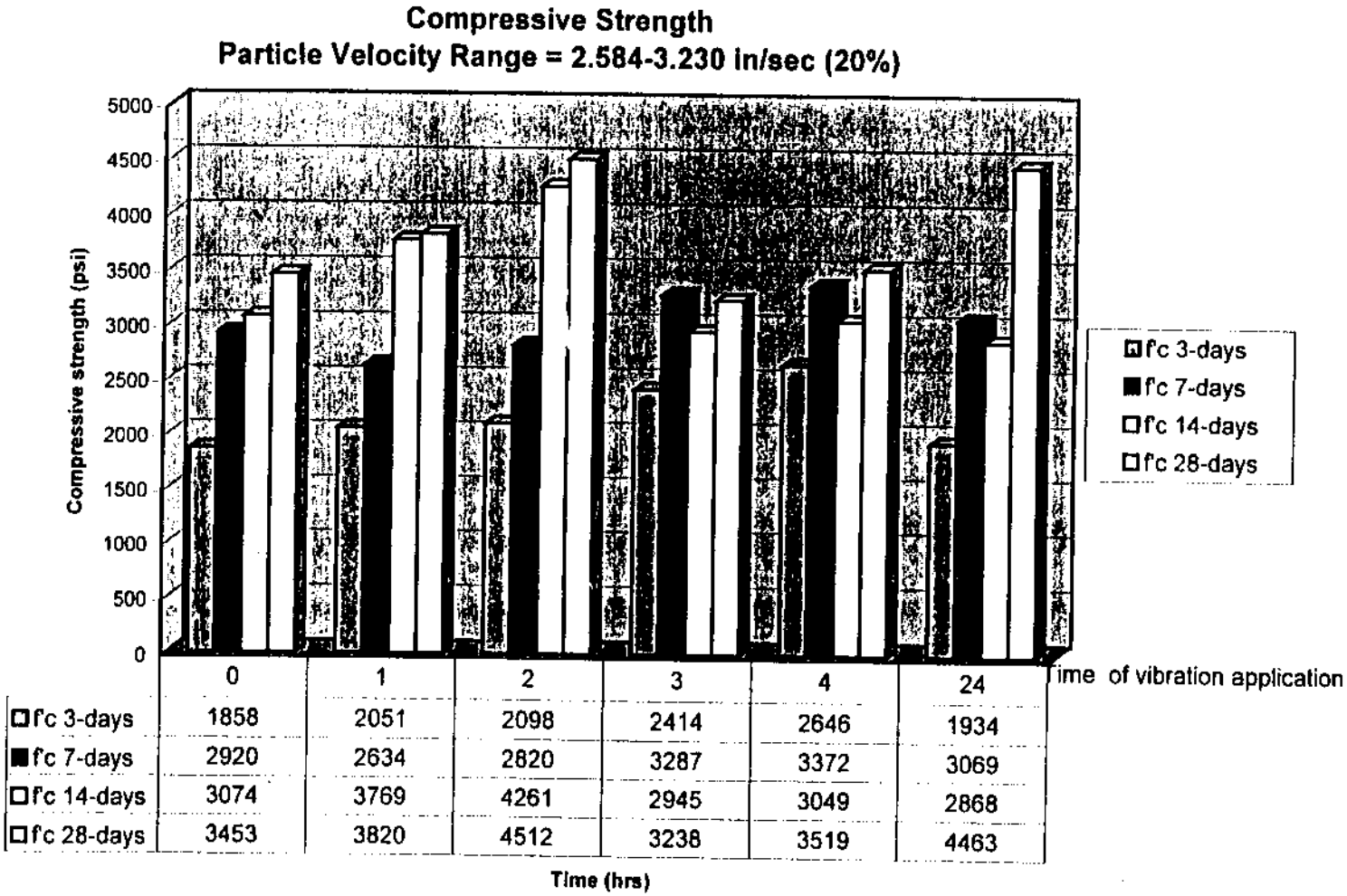


| | 0 | 1 | 2 | 3 | 4 | 24 |
|---|---|---|---|---|---|---|
| f'c 3-days | 1858 | 2051 | 2098 | 2414 | 2646 | 1934 |
| f'c 7-days | 2920 | 2634 | 2820 | 3287 | 3372 | 3069 |
| f'c 14-days | 3074 | 3769 | 4261 | 2945 | 3049 | 2868 |
| f'c 28-days | 3453 | 3820 | 4512 | 3238 | 3519 | 4463 |

Figure 5.2: Compressive strength of concrete samples subjected to acceleration of14 g.

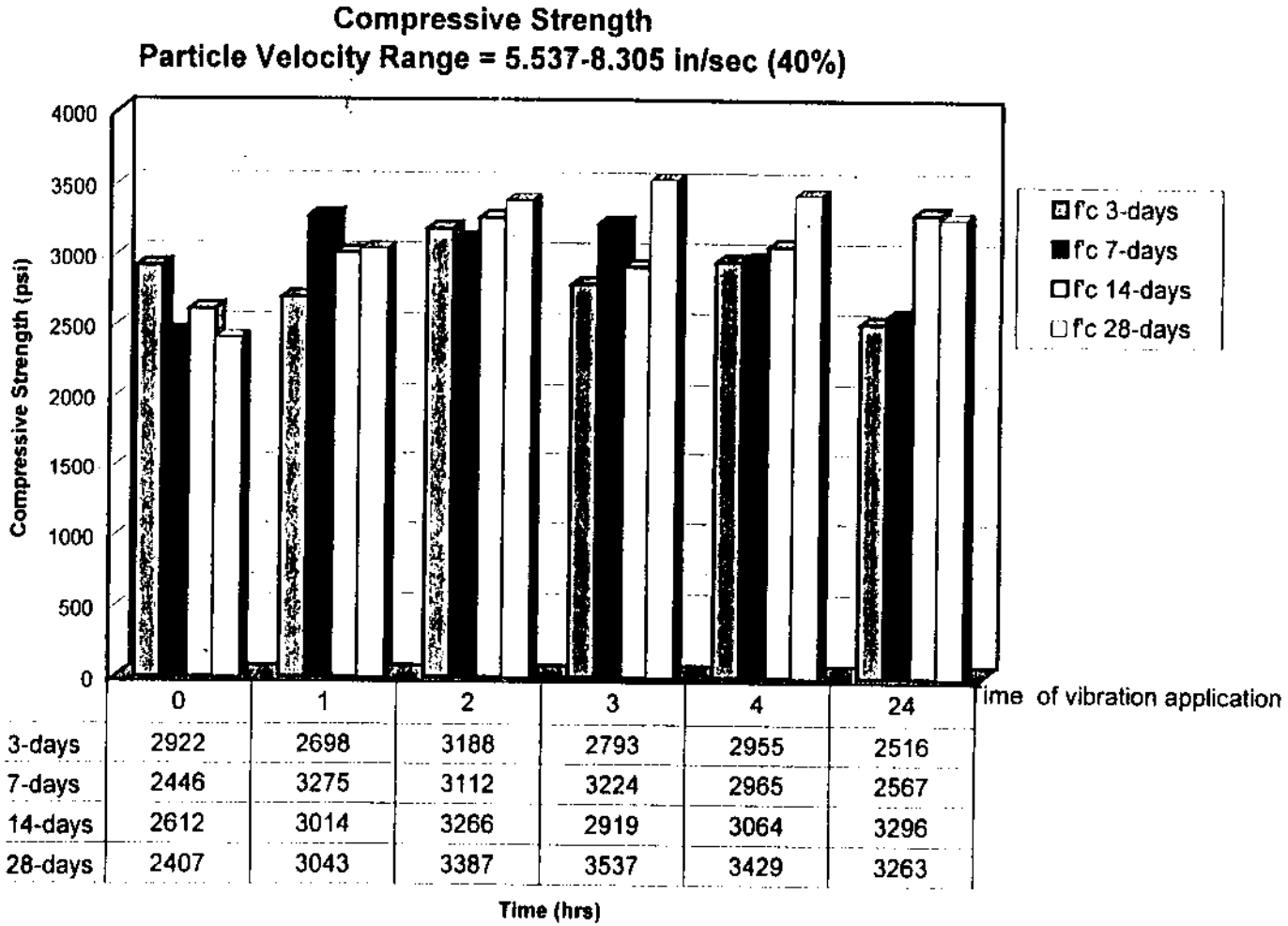


| | 0 | 1 | 2 | 3 | 4 | 24 |
|---|---|---|---|---|---|---|
| f'c 3-days | 2922 | 2698 | 3188 | 2793 | 2955 | 2516 |
| f'c 7-days | 2446 | 3275 | 3112 | 3224 | 2965 | 2567 |
| f'c 14-days | 2612 | 3014 | 3266 | 2919 | 3064 | 3296 |
| f'c 28-days | 2407 | 3043 | 3387 | 3537 | 3429 | 3263 |

Figure 5.3: Compressive strength of concrete samples subjected to acceleration of 30 g.

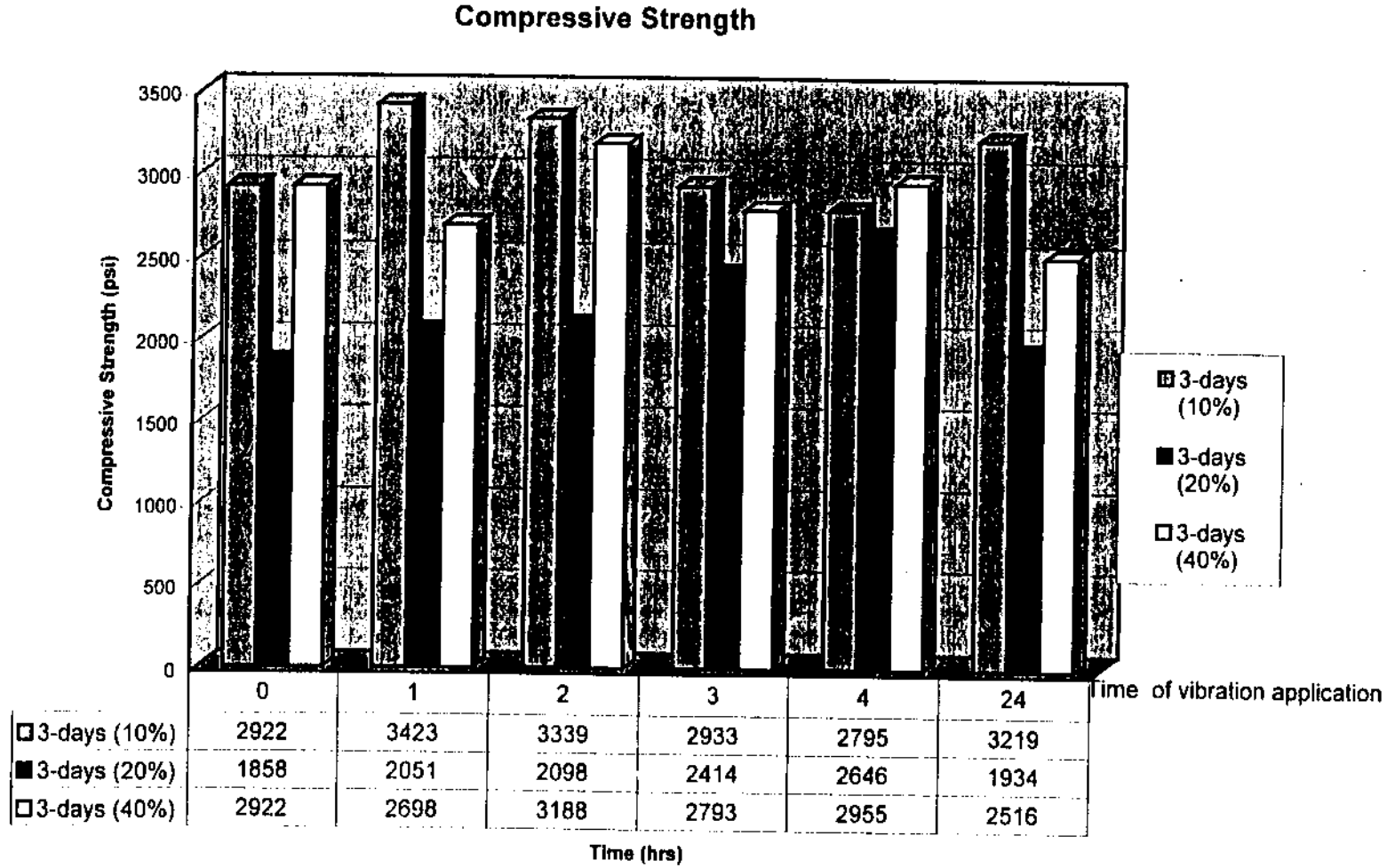


| | 0 | 1 | 2 | 3 | 4 | 24 |
|---|---|---|---|---|---|---|
| 3-days (10%) | 2922 | 3423 | 3339 | 2933 | 2795 | 3219 |
| 3-days (20%) | 1858 | 2051 | 2098 | 2414 | 2646 | 1934 |
| 3-days (40%) | 2922 | 2698 | 3188 | 2793 | 2955 | 2516 |

Figure 5.4: Compressive strength of concrete samples after 3 days

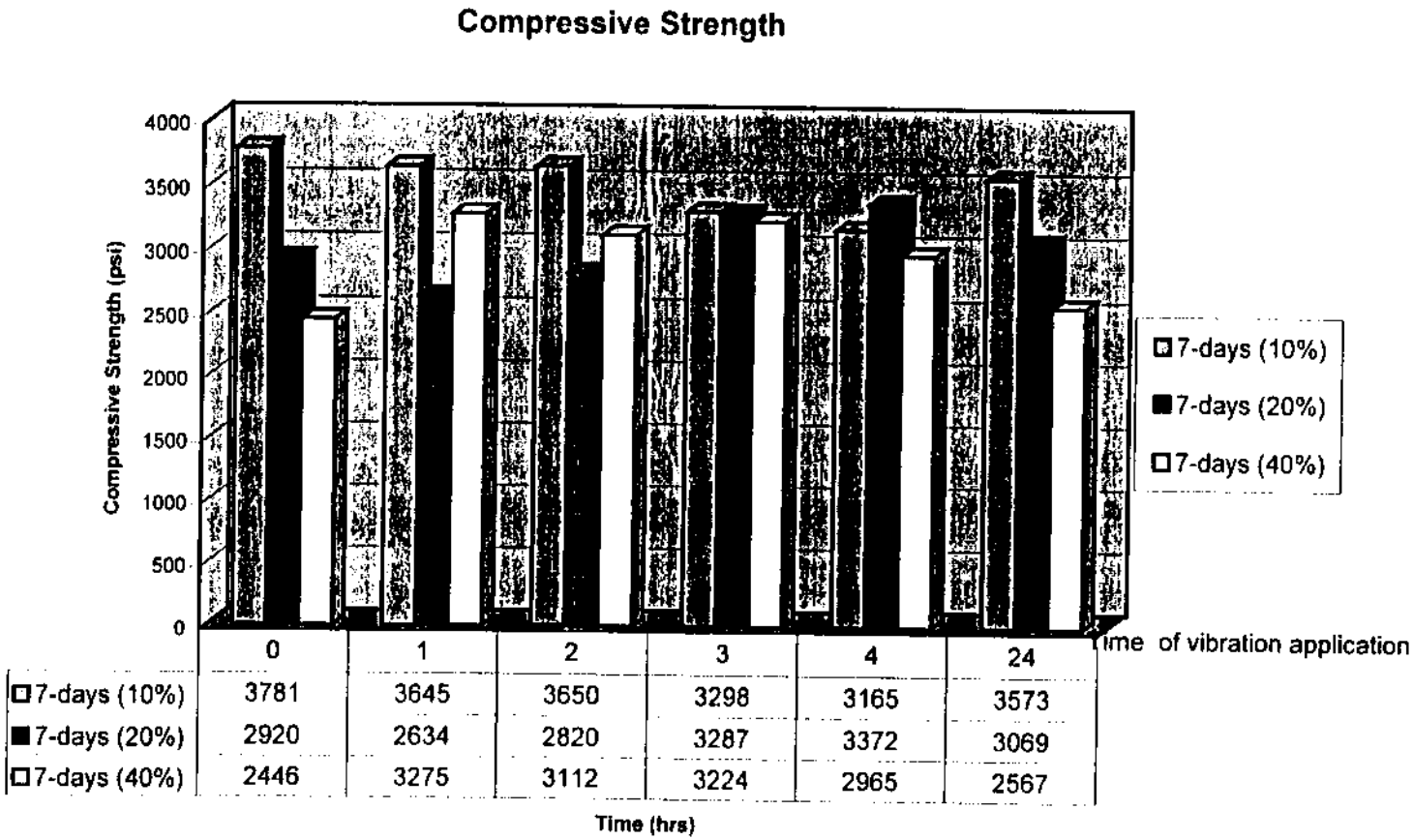


| | 0 | 1 | 2 | 3 | 4 | 24 |
|---|---|---|---|---|---|---|
| 7-days (10%) | 3781 | 3645 | 3650 | 3298 | 3165 | 3573 |
| 7-days (20%) | 2920 | 2634 | 2820 | 3287 | 3372 | 3069 |
| 7-days (40%) | 2446 | 3275 | 3112 | 3224 | 2965 | 2567 |

Figure 5.5: Compressive strength of concrete samples after 7 days

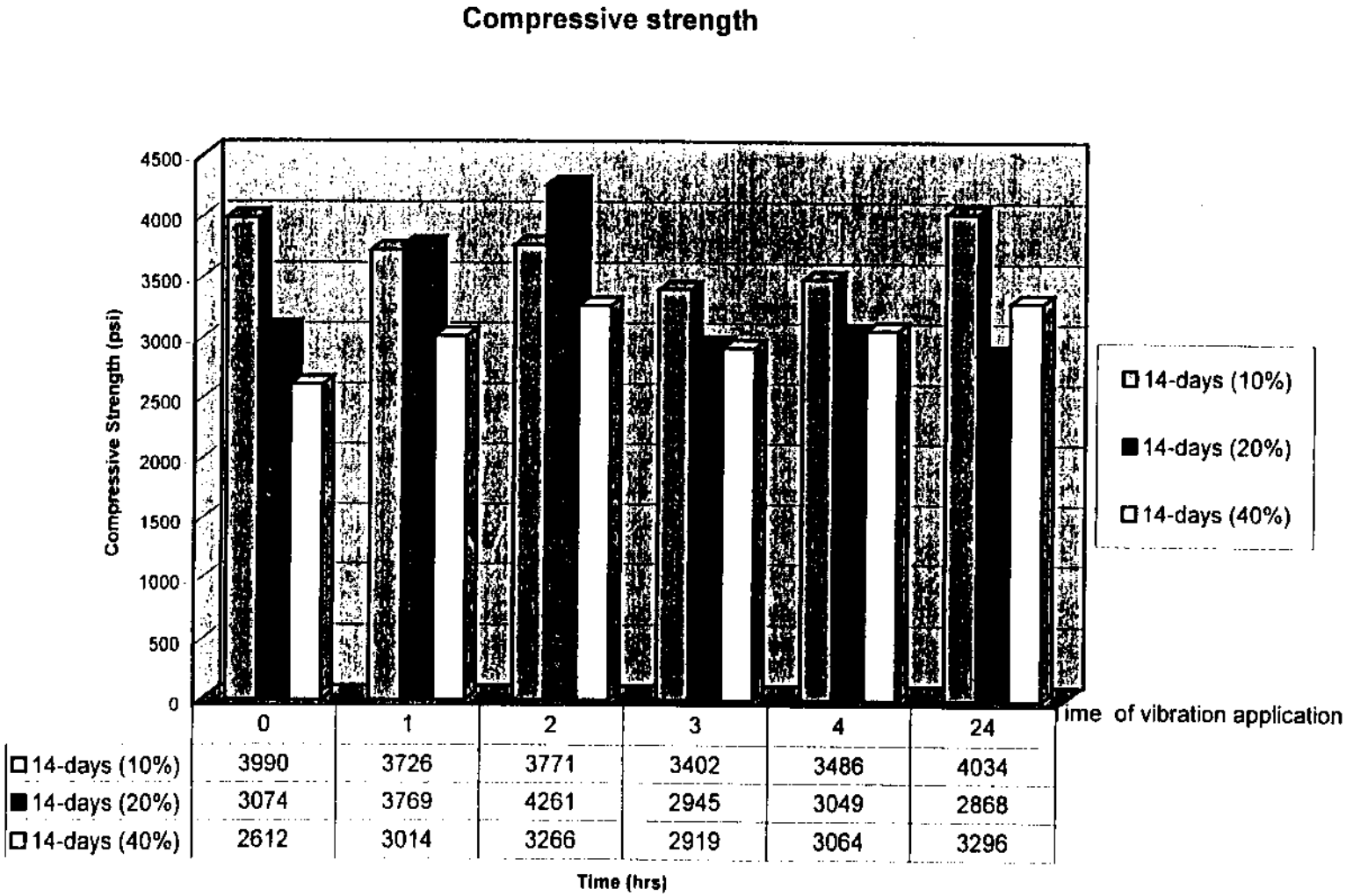


| | 0 | 1 | 2 | 3 | 4 | 24 |
|---|---|---|---|---|---|---|
| 14-days (10%) | 3990 | 3726 | 3771 | 3402 | 3486 | 4034 |
| 14-days (20%) | 3074 | 3769 | 4261 | 2945 | 3049 | 2868 |
| 14-days (40%) | 2612 | 3014 | 3266 | 2919 | 3064 | 3296 |

Figure 5.6: Compressive strength of concrete samples after 14 days

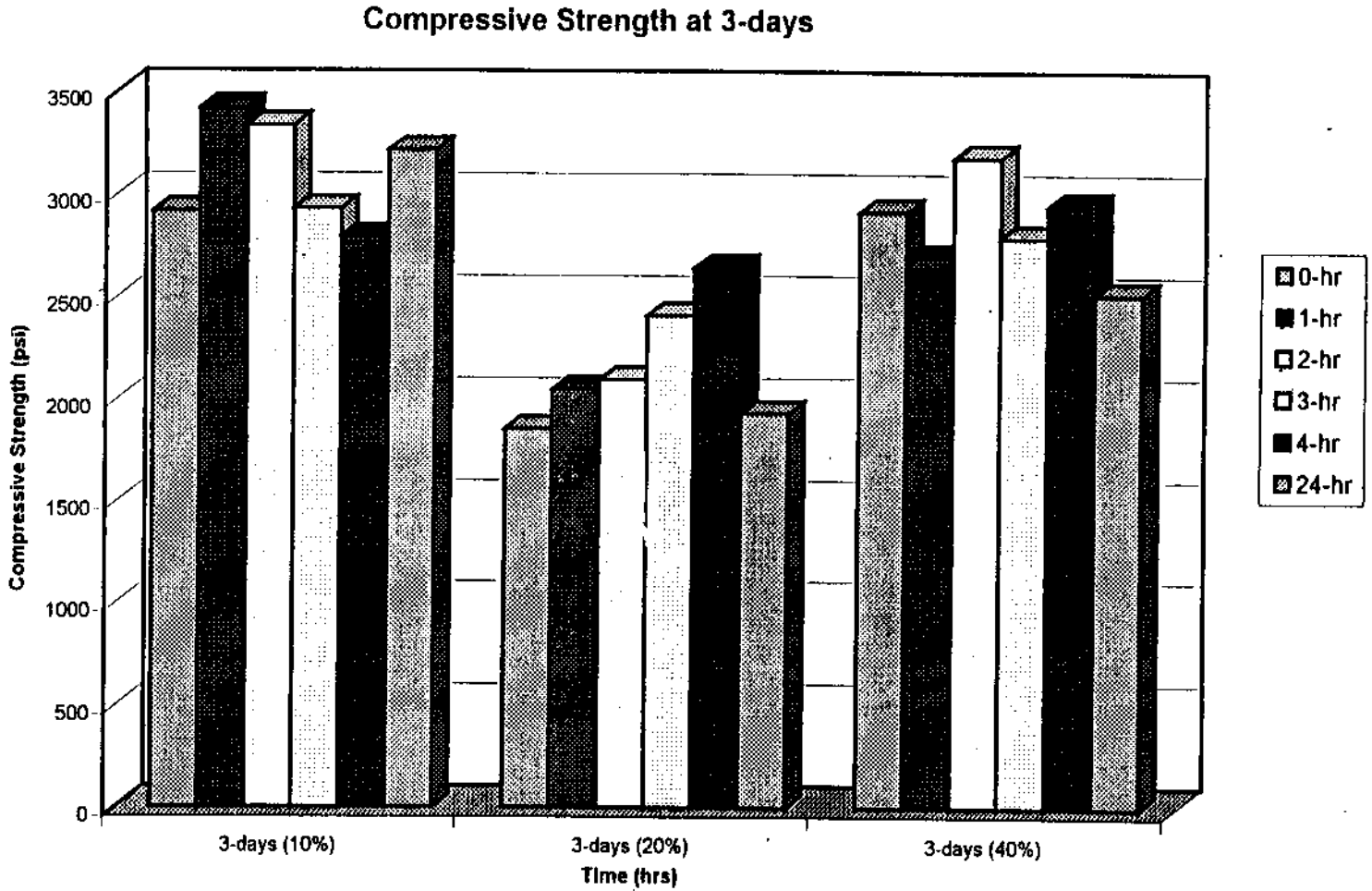


Figure 5.7: Compressive strength of concrete samples after 3 days; vibration amplitude = 30 g.

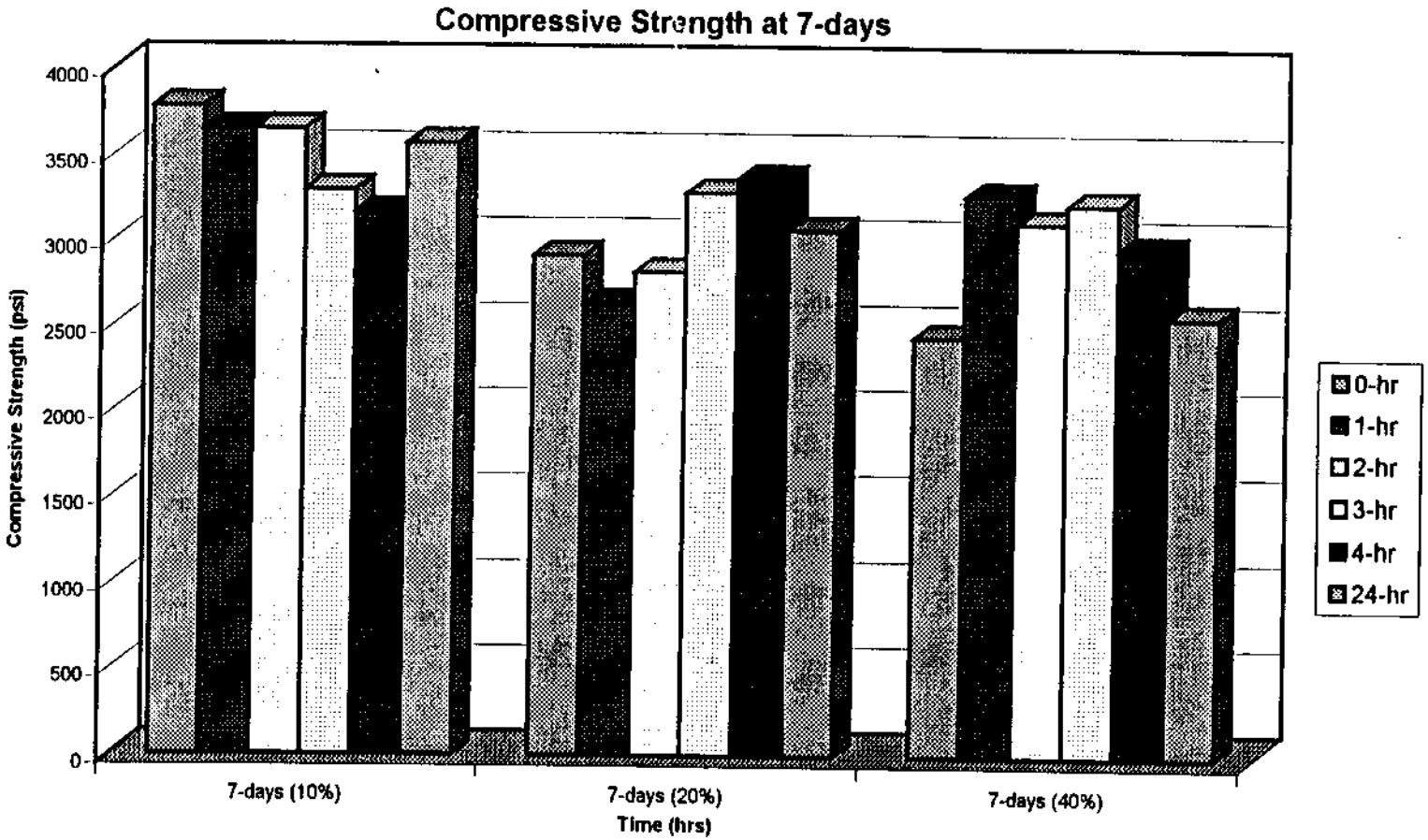


Figure 5.8: Compressive strength of concrete samples after 7 days; vibration amplitude = 30 g.

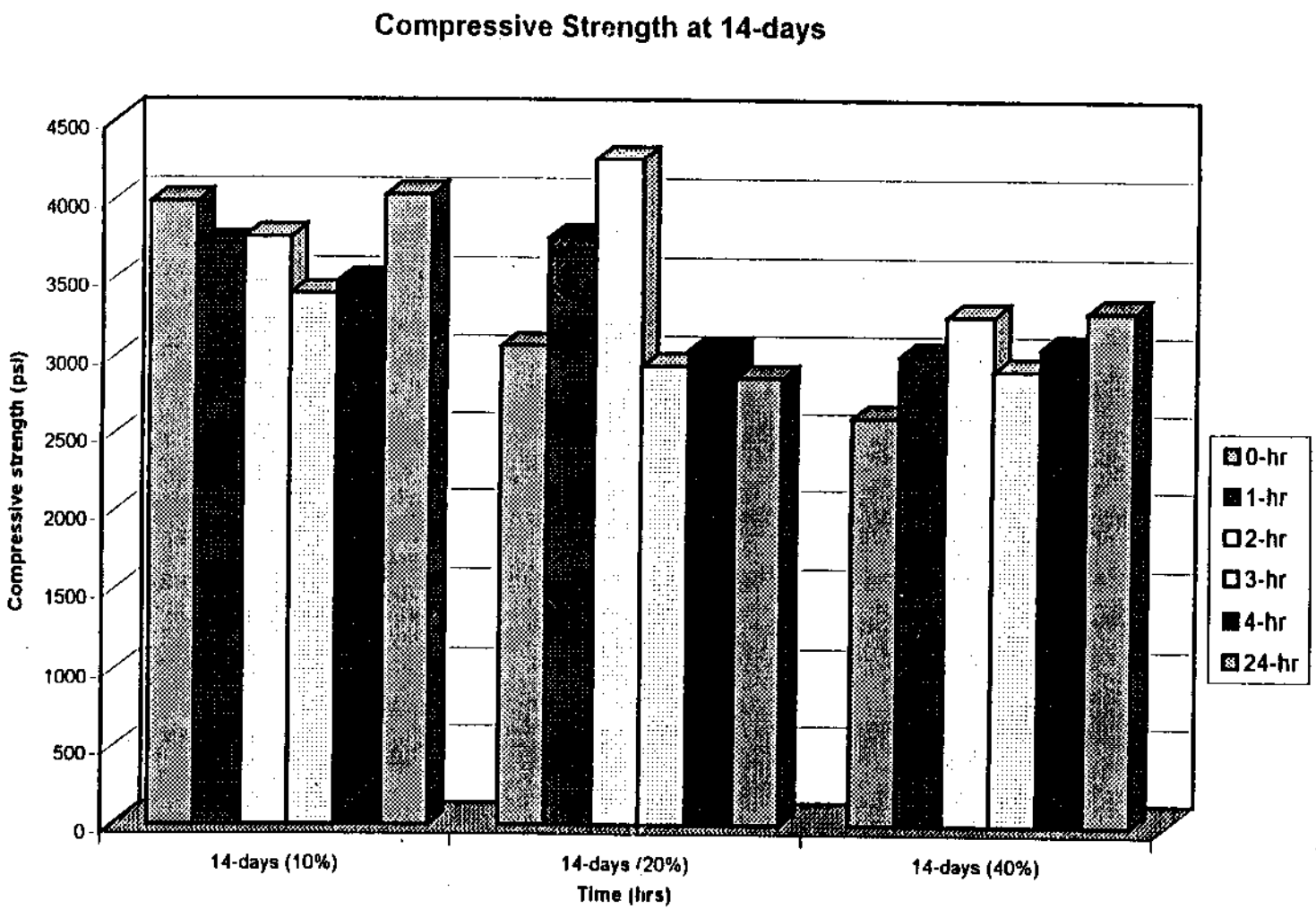


Figure 5.9 : Compressive strength of concrete samples after 14 days; vibration amplitude = 30g.

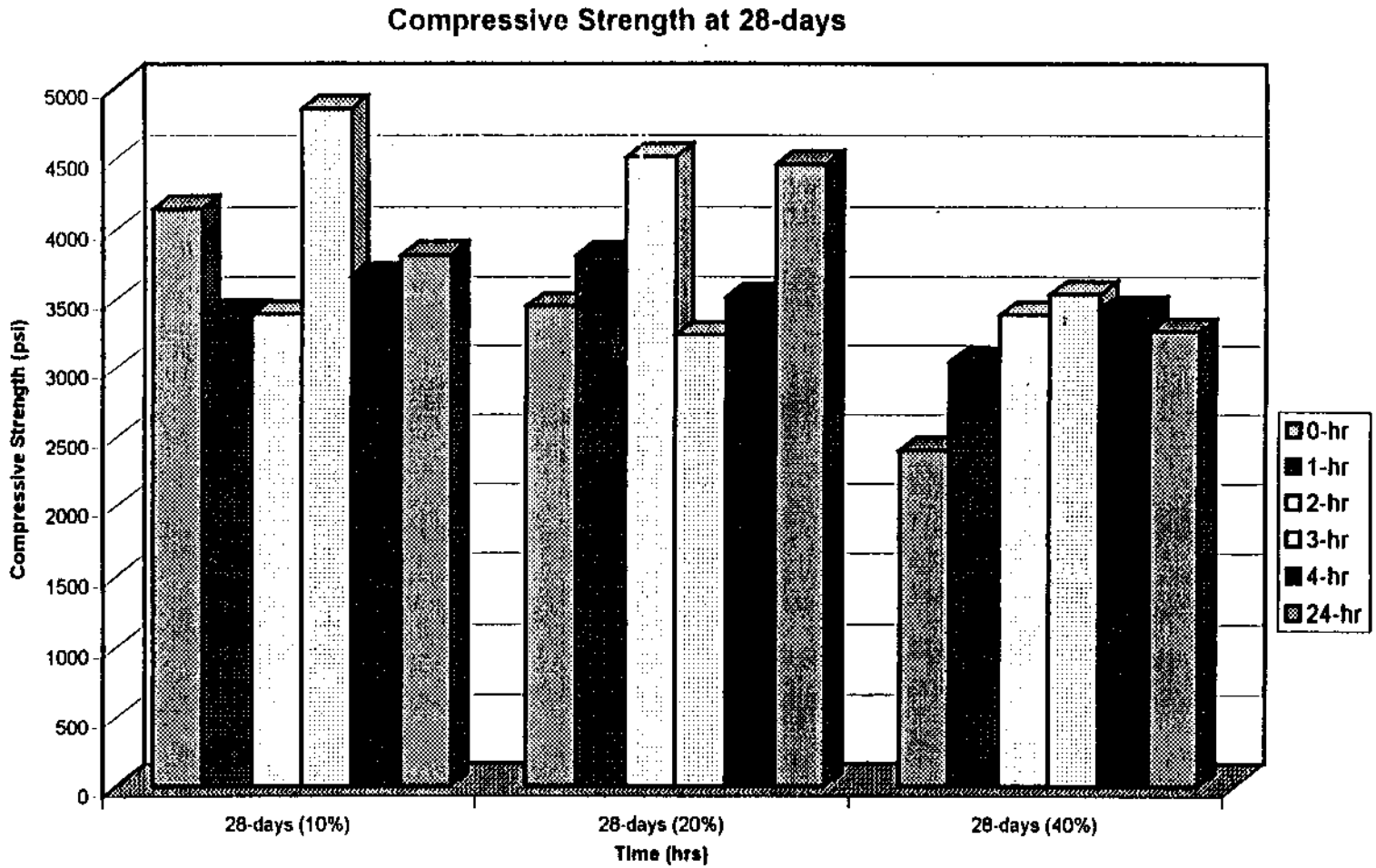


Figure 5.10 : Compressive strength of concrete samples after 28 days; vibration amplitude = 30g.

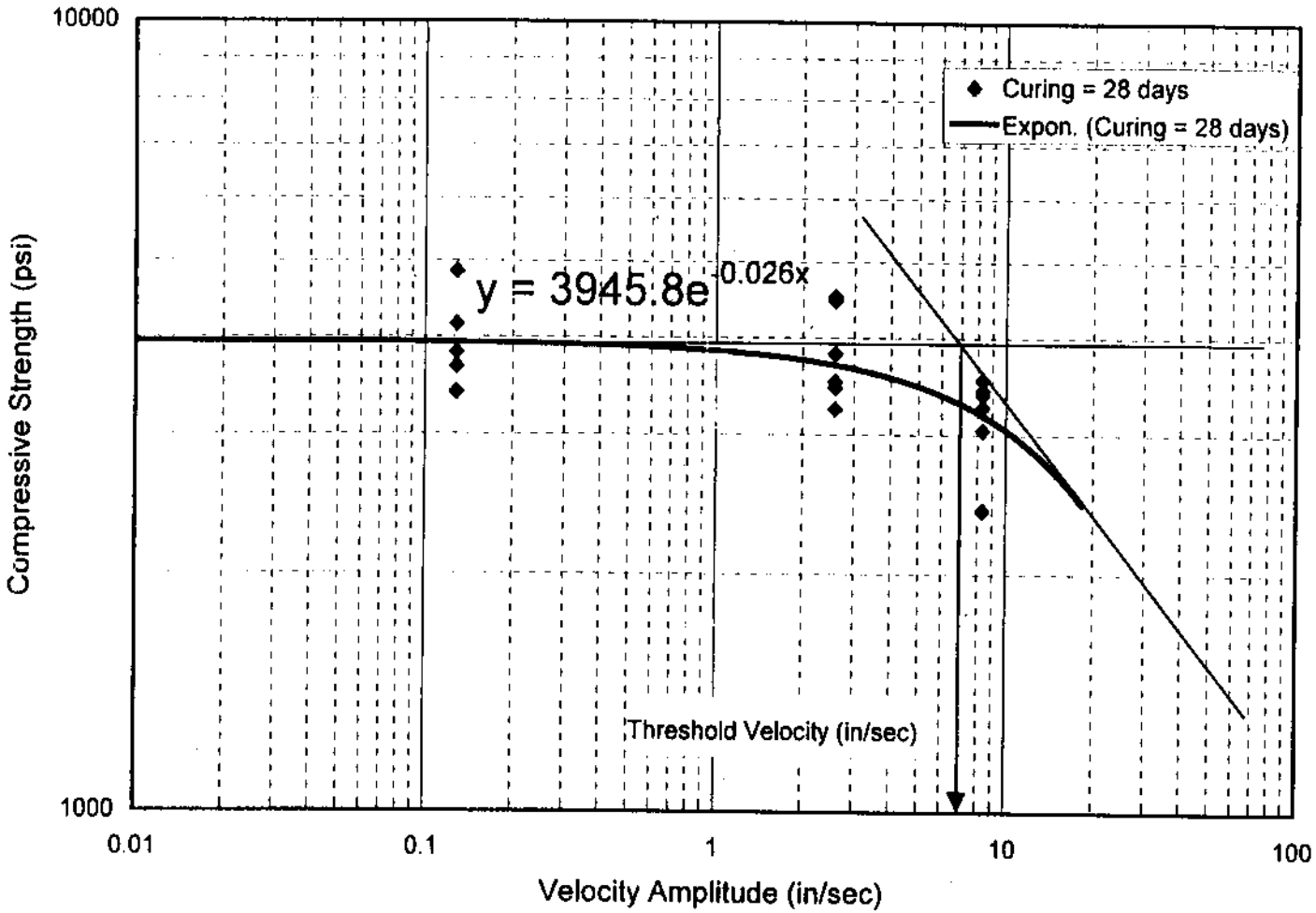


Figure 5.11: Compressive strength of concrete vs. velocity amplitude for all the tested samples

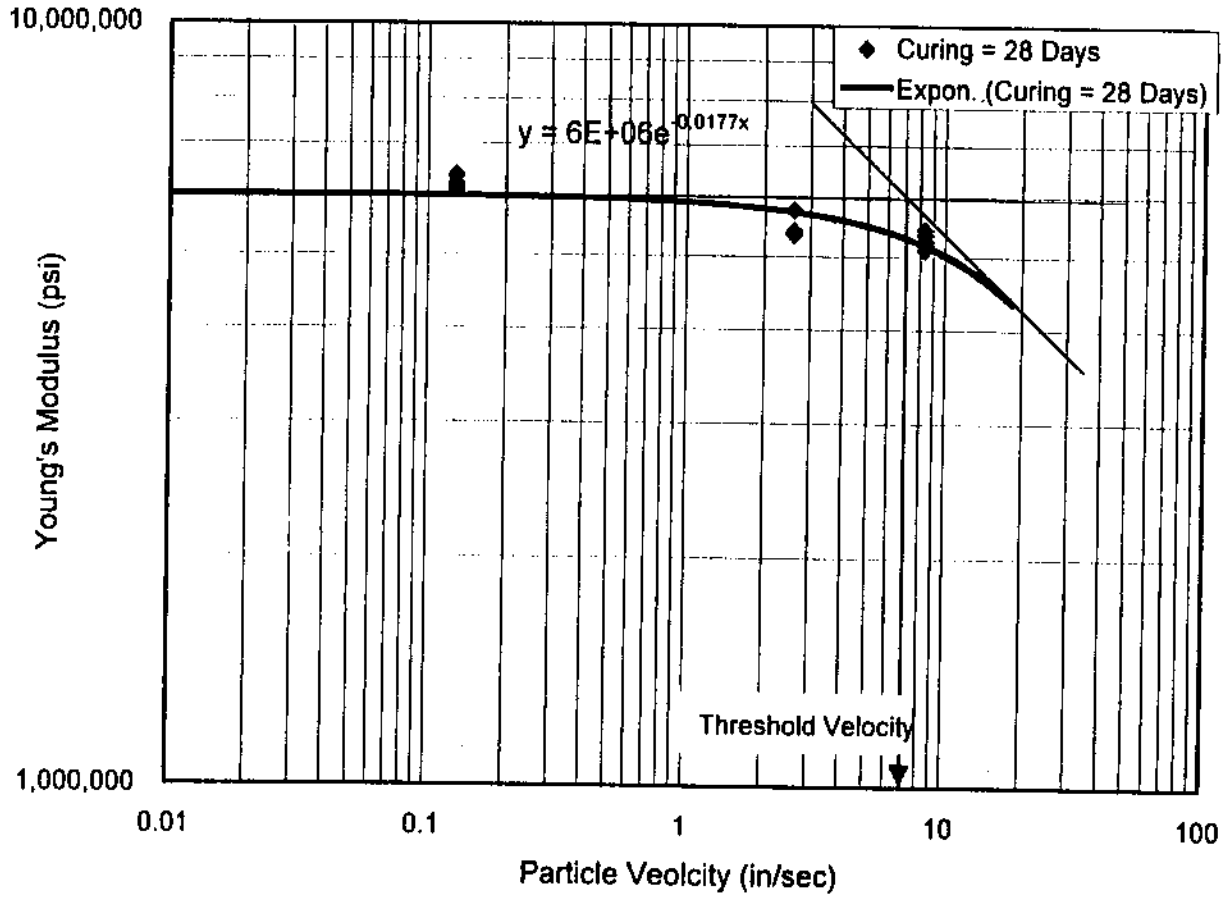


Figure 5.12: Compression modulus of concrete vs. velocity amplitude for all the tested samples

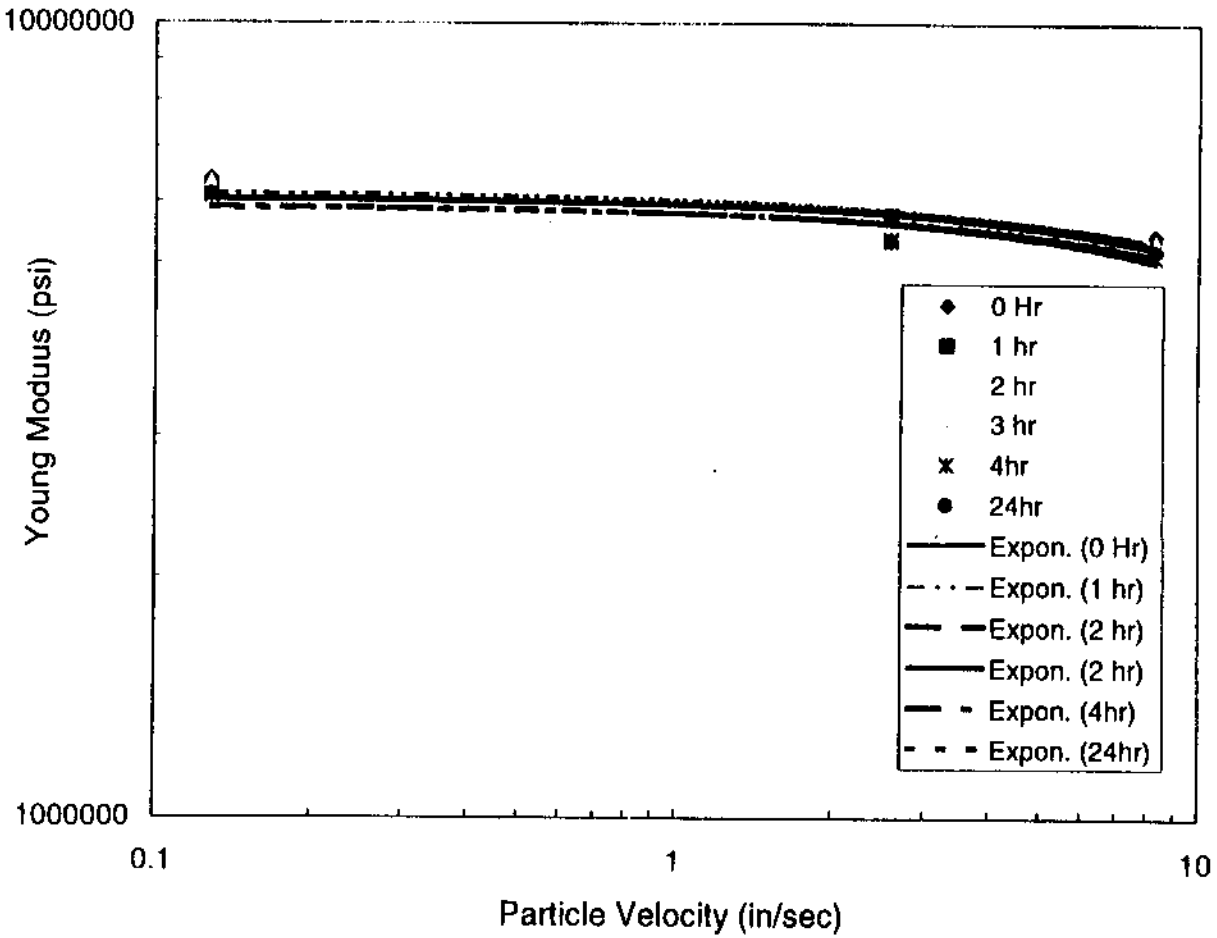


Figure 5.13: Compression modulus of concrete vs. velocity amplitude for the time delay used in testing

were drilled in the ground to monitor the generated vibrations. Two type of sensors were used in this phase. The first set of sensors consisted of two accelerometers. The first accelerometer was a triaxial one mounted on the steel casing directly using a metal stud to affix it firmly to the surface. The other two sensors were placed on 12 inch long steel rods driven into the ground. A wax adhesive was used to affix the accelerometers to the steel rods. Since the FFT analyzer used in the testing was capable of controlling two channels at the same time, the first channel was for the input vibration induced by the steel casing and the second channel for the ground accelerometer. The second accelerometer was located on the ground surface at three different distances from the casing, i.e. 5, 10, and 15 feet respectively. The triaxial accelerometer was first placed at 5 ft above the ground surface. While the casing was penetrating the soil, the accelerometer became closer to the ground. At that time the triaxial accelerometer was removed and placed again at a location of 5 feet above the ground. Thus, the second location was at 10 feet and third one at 15 feet from the tip of the casing (**Table 5.1**).

Results from this segment of testing indicated that velocity amplitudes generated from the driven steel casing were between 2 to 15 in./sec (**Figures 5.15 to 5.22**). The lower bound was for vibratory oscillation of 21Hz (1250 rpm). The upper bound was for 46 Hz (2750 rpm) oscillation. Unexpectedly, the waveforms recorded from the triaxial accelerometer showed that the signals were more random narrow band vibrations than harmonic sinusoidal ones. The reason was not precisely known for not getting typical sinusoidal waveforms despite the fact that the rotated masses inside the vibrator were moving systematically. However, one interpretation for such behavior by the steel casing might be related to the manner in which the vibrator was gripping the steel casing. The vibrator was gripping the casing only at one point causing what might be an uneccentric dynamic loading. This interpretation was confirmed from

Table 5.1: Florida Atlantic University Test Site

PERFORMED BY: FLORIDA STATE UNIVERSITY & LAW ENGINEERING

PART A: Data Organization

CH1: Accelerometer from FAU (PCB) mounted on steel casing

CH2: Accelerometer from DOT (Wilcox Research) mounted on the ground

| Casing | HP File name | | | | | |
|---|---|---|---|---|---|---|
| Depth (Ft.) | CH1 Vertical | CH2 Horizontal | CH1 Sensor Vertical Dist. | CH2 Sensor Horizontal Dist. | Hammer RPM | *Frequency Hz* |
| 1.5 | Trace1.dat | Trace2.dat | 5 ft. Sensor was 5' from edge | 5 ft. Sensor was 5' from the casing | 1250 | ***21*** |
| 5 | Trace3.dat | Trace4.dat | 5 ft. Sensor was 5' from edge | 5 ft. Sensor was 5' from the casing | 1800 | ***30*** |
| 8 | Trace5.dat | Trace6.dat | 10 ft. Sensor was 10' from edge | 10 ft. Sensor was 10' from the casing | 2000 | ***33*** |
| 10 | Trace7.dat | Trace8.dat | 10 ft. Sensor was 10' from edge | 10 ft. Sensor was 10' from the casing | 2500 | ***42*** |
| 12 | Trace9.dat | Trace10.dat | 15 ft. Sensor was 15' from edge | 10 ft. Sensor was 10' from the casing | 2750 | ***46*** |
| 13 | Trace11.dat | Trace12.dat | 15 ft. Sensor was 15' from edge | 15 ft. Sensor was 15' from the casing | 2750 | ***46*** |
| 13.75 | Trace13.dat | Trace14.dat | 15 ft. Sensor was 15' from edge | 15 ft. Sensor was 15' from the casing | 1500 | ***25*** |
| 14.75 | Trace15.dat | Trace16.dat | 15 ft. Sensor was 15' from edge | 15 ft. Sensor was 15' from the casing | 2000 | ***33*** |

Part B: Signal Analyzer Set-Up

The HP Signal Analyzer was set-up was as follows:

1. 20 averages using the time domain
2. Channel amplification was X10
3. The bandwith for the frequency doamin was from 0-6.4 KHz
4. The state (set-up) file name is FAU1.sta
5. Two channel data acquisition
6- Number of Points = 1024 at 400 Resolution
7- PCB accelerometer (on Casing ) = 100 mVolt/g, Wilcoxon Accelerometer on the ground = 517 mV/g

PART C: Steel Casing Dimmensions

The casing dimensions were as follows:

a. Thickness = 1/2 inch
b. Length = 40 ft.
c. Diameter = 36 inches

Table 5.2 Time and Frequency Domain Analysis of Particle velocity

| Record Type / Record # | RMS of the Velocity vs. Time | RMS from SDF |
|---|---|---|
| Trace 1 | 1.169 | 1.07 |
| Trace 5 | 1.270 | 1.182 |
| Trace 7 | 1.758 | 1.664 |
| Trace 11 | 3.820 | 3.556 |

SDF=Spectral Density Function

Table 5.3 Soil Properties of Samples Obtained From the FAU Site on 7/3
Tested by: Dr. Kamal Tawfiq

| Sample No. | Depth (ft) | $\gamma_{wet}$ ($gm/cm^3$) | $\gamma_{dry}$ ($gm/cm^3$) | wc (%) | Void Ratio e |
|---|---|---|---|---|---|
| 1 | 1.5 | 1.25 | 1.25 | 0 | 0.289 |
| 2 | 3 | 1.395 | 1.388 | 0.48 | 0.332 |
| 3 | 4.5 | 1.29 | 1.247 | 3.45 | 0.298 |
| 4 | 6 | 1.51 | 1.319 | 14.48 | 0.407 |
| 5 | 8 | 1.7 | 1.437 | 18.27 | 0.41 |
| 6 | 9 | 1.6 | 1.417 | 12.91 | 0.364 |
| 7 | 10.5 | 1.686 | 1.437 | 17.3 | 0.378 |
| 8 | 12 | 1.694 | 1.487 | 13.94 | 0.352 |
| 9 | 13 | 1.819 | 1.493 | 21.77 | 0.415 |
| 10 | 15 | 1.578 | 1.371 | 15.13 | 0.327 |
| 11 | 16.5 | 1.578 | 1.289 | 22.3 | 0.336 |
| 12 | 19 | 1.577 | 1.281 | 23.06 | 0.327 |
| 13 | 21.5 | 1.547 | 1.271 | 21.75 | 0.325 |
| 14 | 24 | 1.526 | 1.241 | 23 | 0.323 |
| 15 | 26.5 | 1.491 | 1.215 | 22.71 | 0.324 |
| 16 | 29 | 1.681 | 1.366 | 23.07 | 0.367 |
| 17 | 31.5 | 1.615 | 1.289 | 25.32 | 0.356 |

Soil is mostly loose fine light tan sand to dark tan fine sand

Water Table at 6.7 ft

Boring Termination = 41 ft

Table 5.4 : Determination of Damping characteristics (D) in the sandy soil layer in FAU Site
Samples were tested on 8/15/1997

| Depth (ft) | Unit Weight $Gm/cm^3$ | Effective Unit Weight psf | Void Ratio (e) | Vertical Effectiveness Stress (psf) | Shear wave Velocity ft/sec | Shear wave Velocity in./sec |
|---|---|---|---|---|---|---|
| 1.5 | 1.25 | 78 | 0.289 | 117 | 484.78 | 11634.72 |
| 3 | 1.395 | 87.0 | 0.332 | 261.14 | 579.02 | 13896.55 |
| 4.5 | 1.29 | 80.5 | 0.3 | 362.23 | 639.30 | 15343.14 |
| 6 | 1.51 | 94.2 | 0.4 | 565.34 | 676.42 | 16234.11 |
| 8 | 1.7 | 43.7 | 0.41 | 349.44 | 596.39 | 14313.25 |
| 9 | 1.6 | 37.4 | 0.364 | 336.96 | 606.40 | 14553.60 |
| 10.5 | 1.686 | 42.8 | 0.378 | 449.47 | 646.65 | 15519.50 |
| 12 | 1.694 | 43.3 | 0.352 | 519.67 | 680.25 | 16325.89 |
| 13 | 1.819 | 51.1 | 0.415 | 664.37 | 698.32 | 16759.66 |
| 15 | 1.578 | 36.1 | 0.27 | 541.01 | 718.05 | 17233.20 |
| 16.5 | 1.578 | 36.1 | 0.336 | 595.11 | 709.87 | 17036.96 |
| 19 | 1.578 | 36.1 | 0.327 | 685.28 | 738.96 | 17734.99 |
| 21.5 | 1.547 | 34.1 | 0.325 | 733.86 | 752.53 | 18060.80 |
| 24 | 1.526 | 32.8 | 0.325 | 787.74 | 765.98 | 18383.57 |
| 26.5 | 1.491 | 30.6 | 0.324 | 811.92 | 772.21 | 18533.07 |
| 29 | 1.681 | 42.5 | 0.367 | 1232.34 | 837.19 | 20092.67 |
| 31.5 | 1.615 | 38.4 | 0.356 | 1208.84 | 838.25 | 20117.95 |

Water table at 5.9 ft. to 6.7 ft.

Hardin and Richart 1963

Shear wave velocity = vs = $(170 - 78.2e)^* \sigma_o^{1/4}$ for $\sigma_o > 2000$ psf

Shear wave velocity = vs = $(119 - 56.0e)^* \sigma_o^{1/5}$ for $\sigma_o < 2000$ psf

Hardin and Richart (1963)
*For Sandy Soil:*

$v_s = (170 - 78.2\ e)\ \sigma_o^{1/4}$ For $\sigma_o \geq 2000$ lb/ft$^2$

$v_s = (119 - 56\ e)\ \sigma_o^{1/4}$ For $\sigma_o < 2000$ lb/ft$^2$

$\sigma_o$ = effective confining stress
e = void ratio

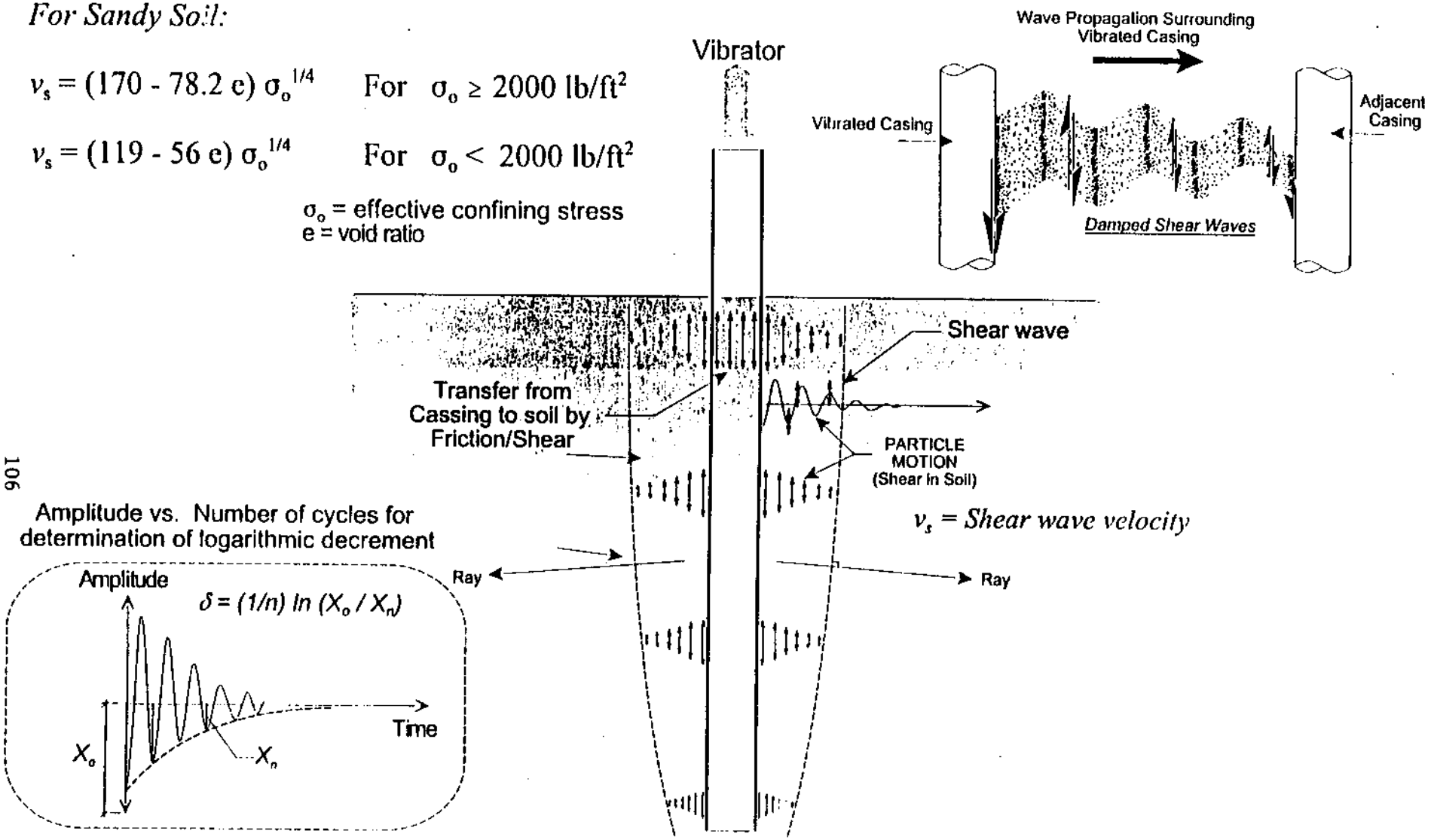


Figure 5.14. Vibratory drilled shaft casing generating shear waves in the surrounding soil.

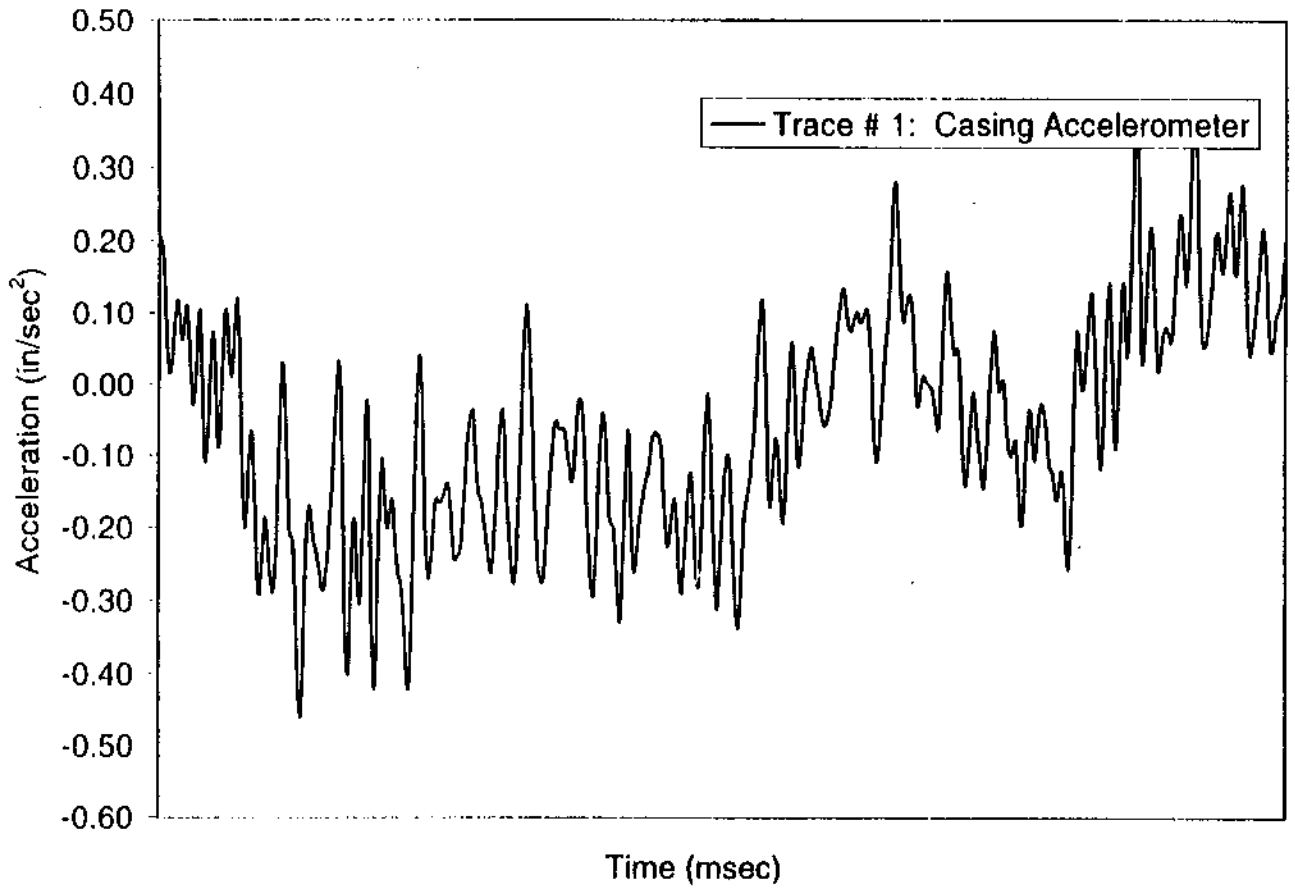


Figure 5.15 Time-history record of the steel casing at the accelerometer 5 ft. from the ground

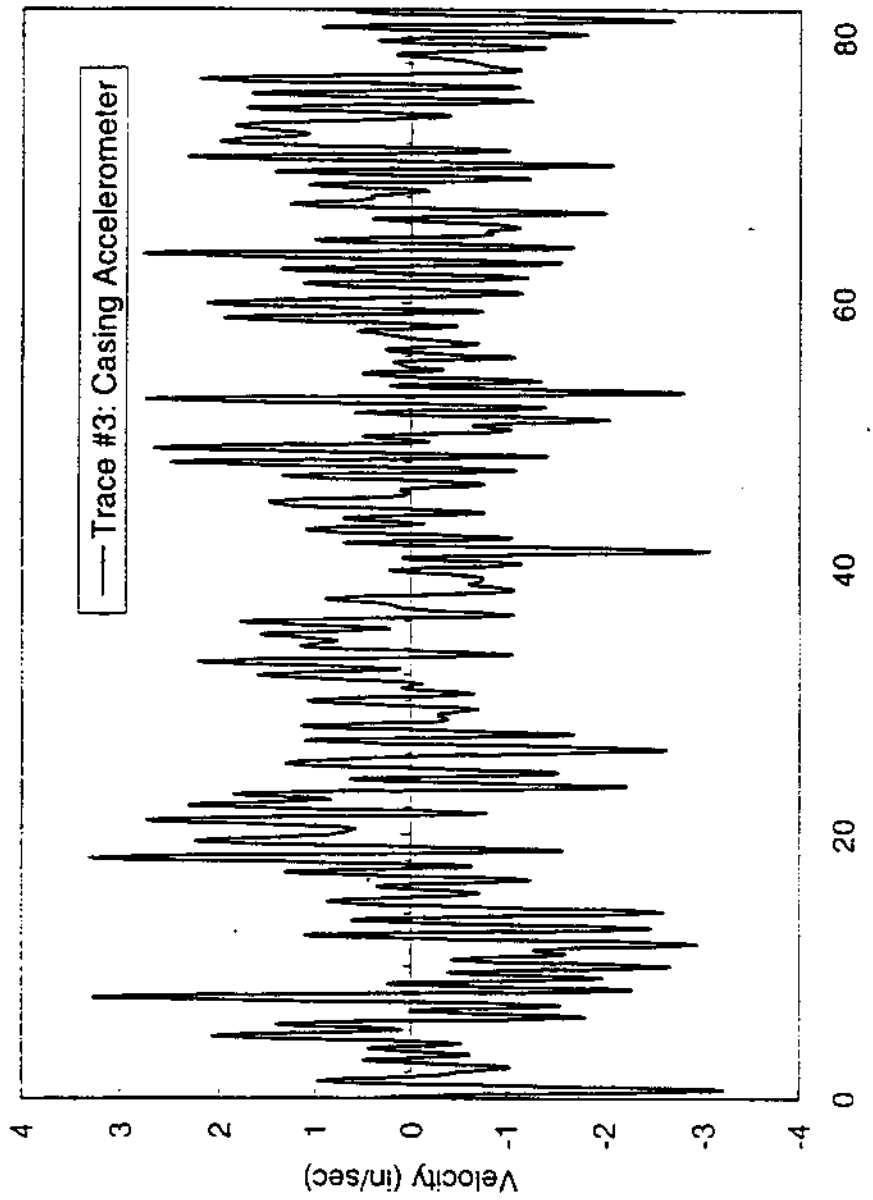


Figure 5.16 Time-history record of the steel casing at the accelerometer 5 ft from the ground

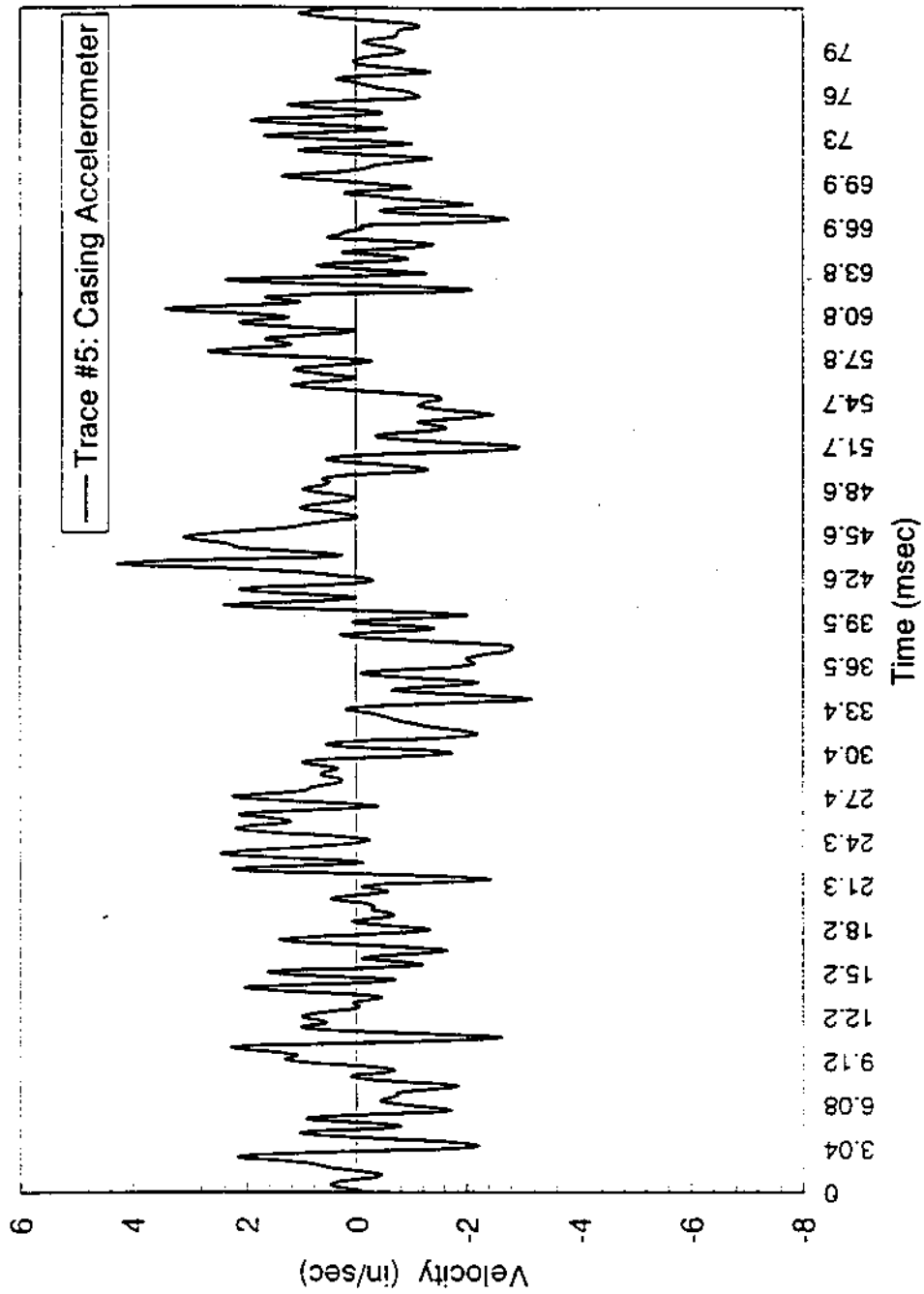


Figure 5.17 Time-history record of the steel casing at the accelerometer 5 ft from the ground

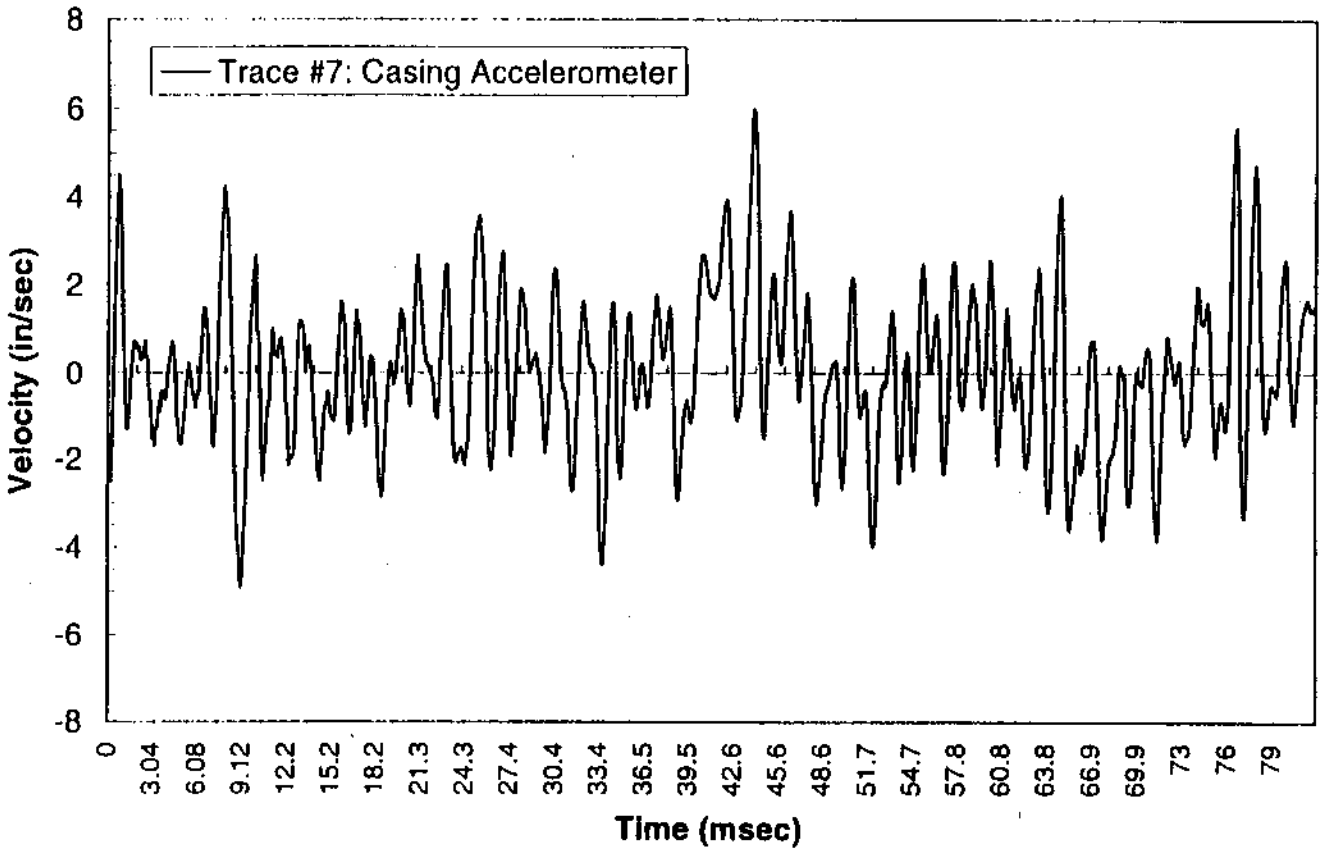


Figure 5.18 Time-history record of the steel casing at the accelerometer 5 ft from the ground

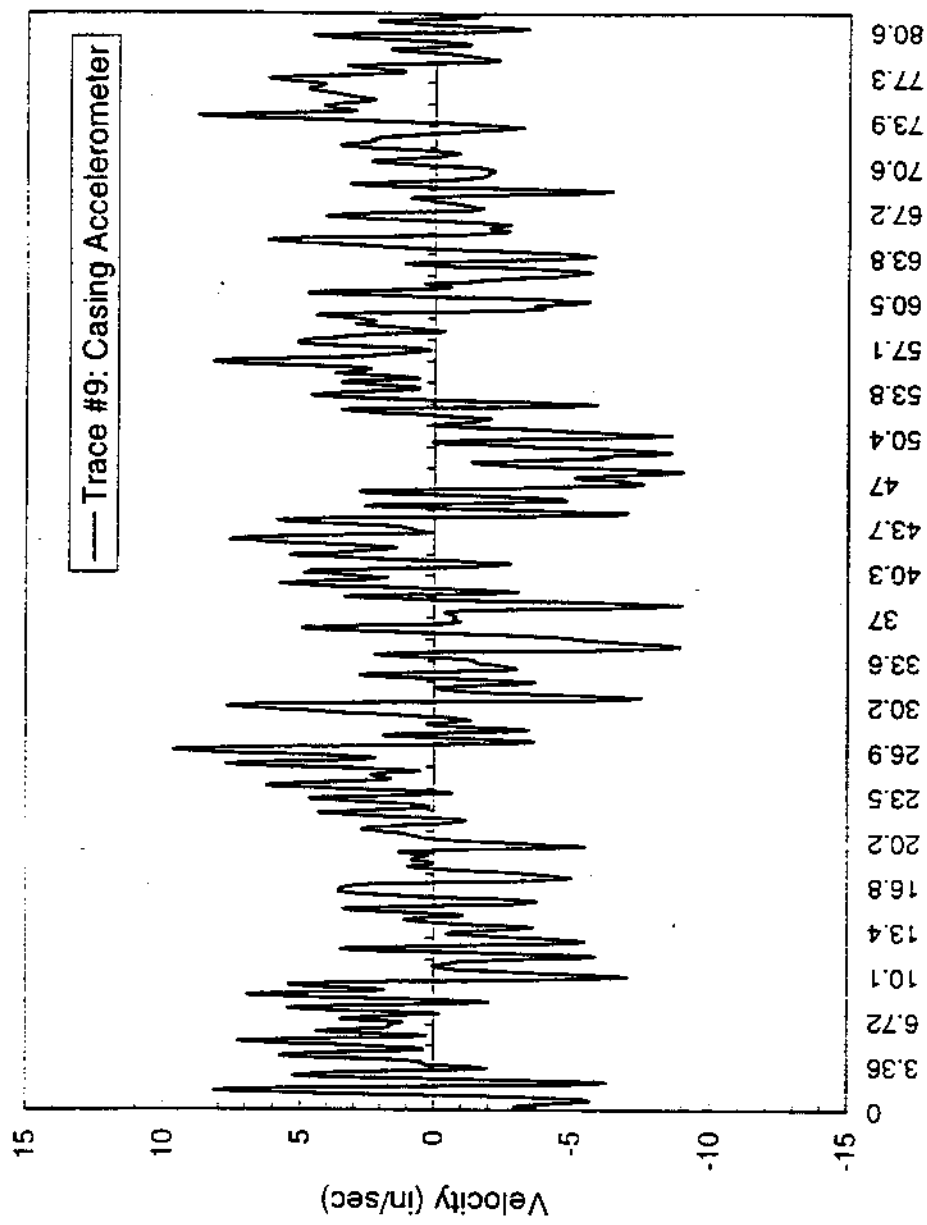


Figure 5.19 Time-history record of the steel casing at the accelerometer 5 ft from the ground

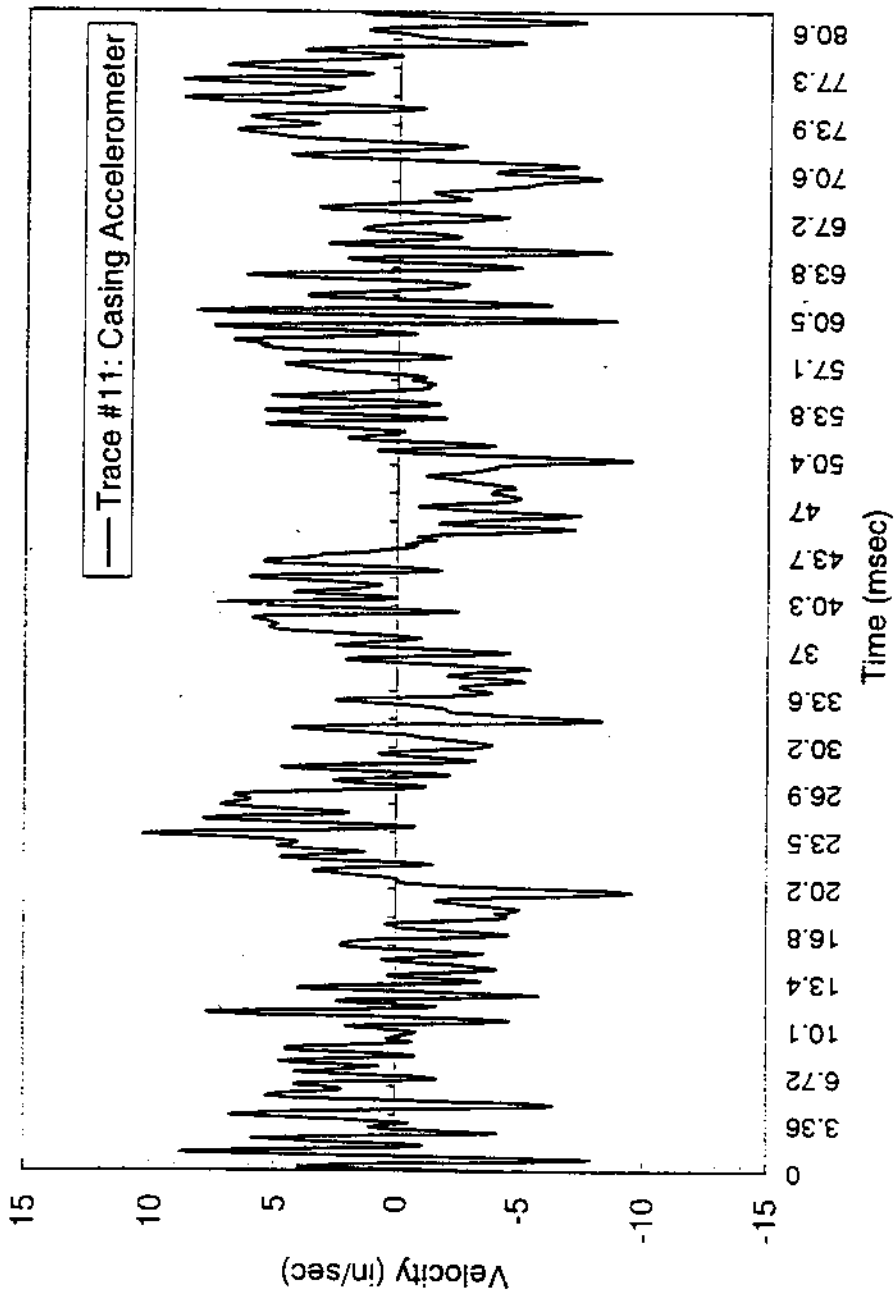


Figure 5.20 Time-history record of the steel casing at the accelerometer 5 ft from the ground

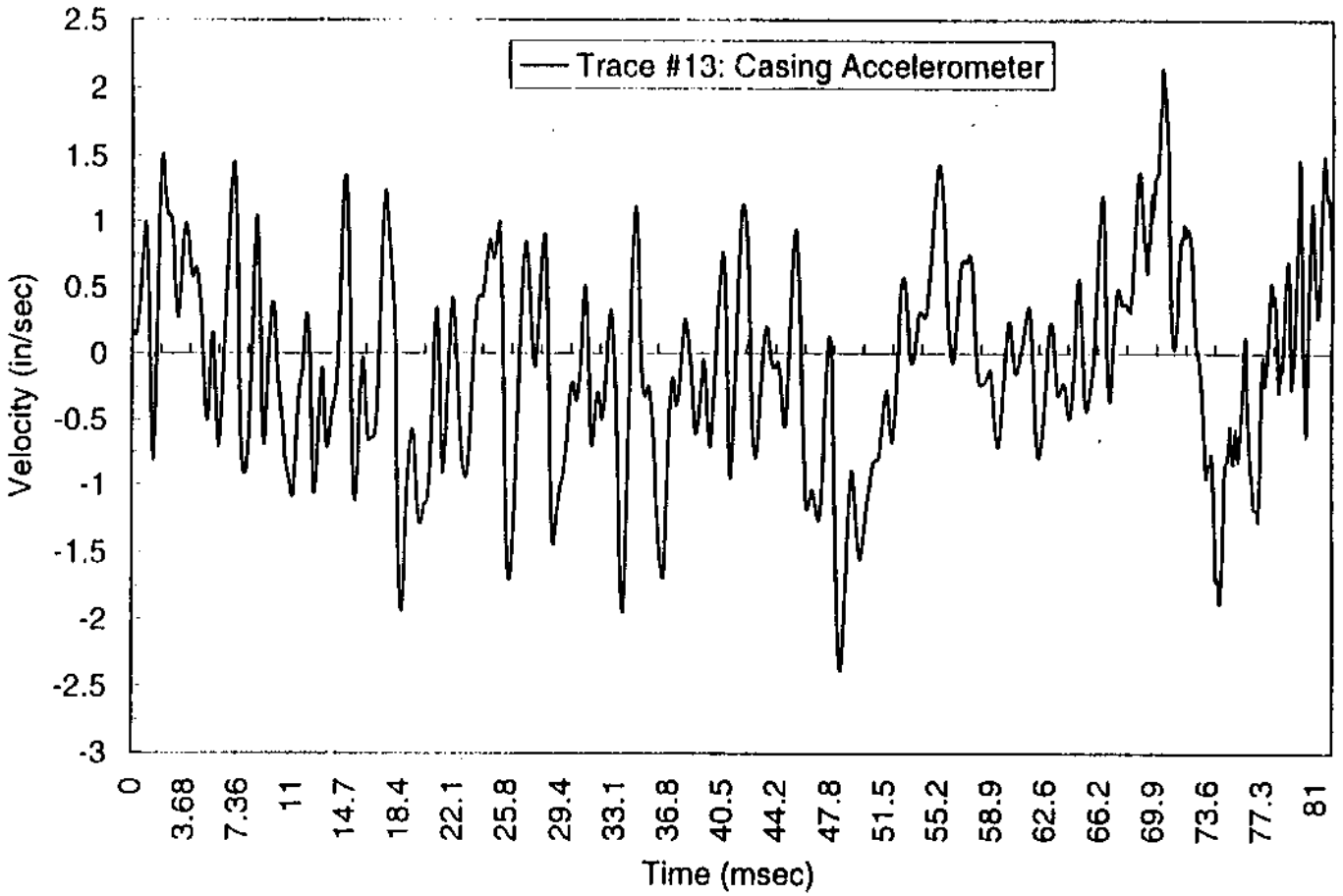


Figure 5.21 Time-history record of the steel casing at the accelerometer 5 ft from the ground

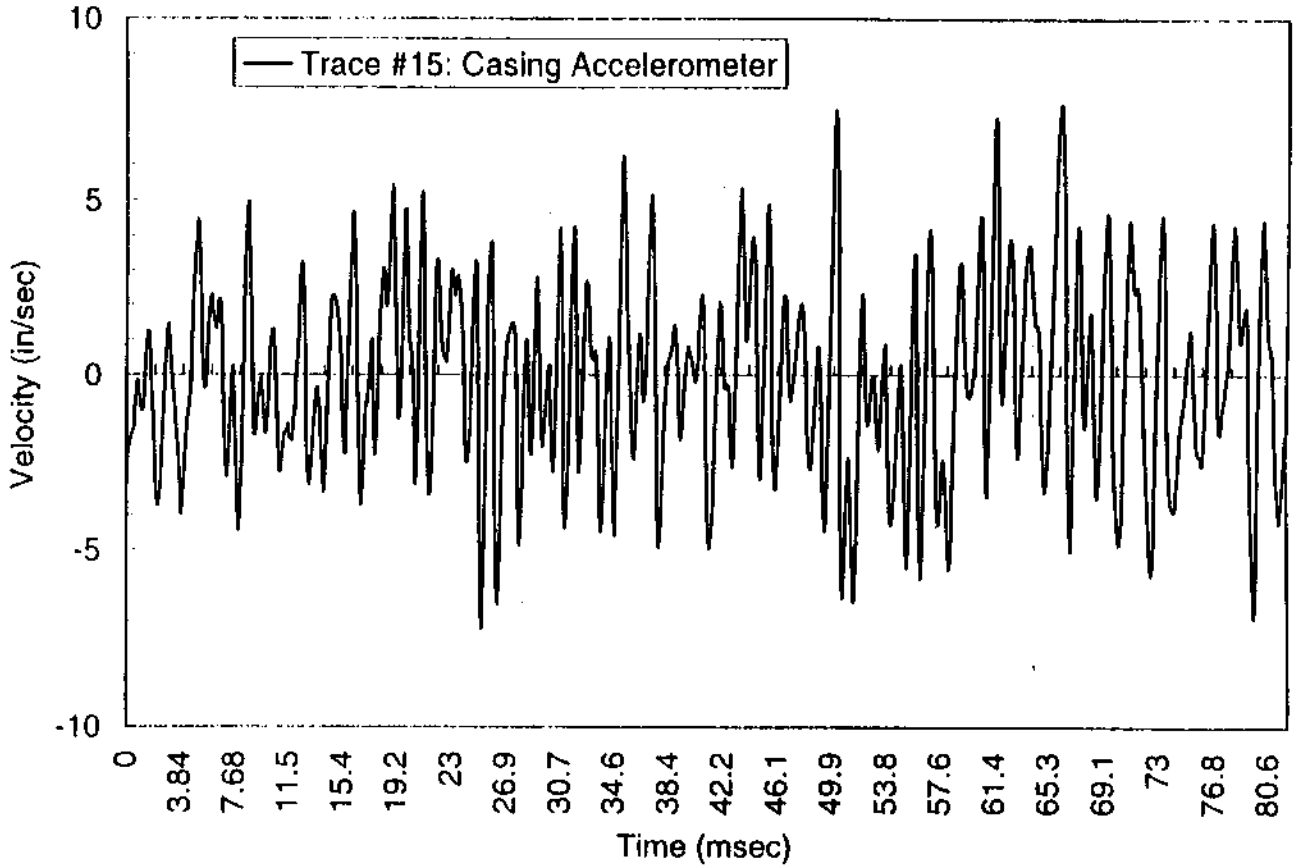


Figure 5.22 Time-history record of the steel casing at the accelerometer 5 ft from the ground

the records in the ground geophones at the second FAU field test site. These records showed vibration components that are larger than the vertical ones, although the intended motion was in the vertical direction.

The time-history records from the accelerometers were converted to velocity by using the direct integration method. If the vibrations are considered as narrow band responses, then the direct method will be inapplicable. In this case another method for determining the RMS velocity should be used. In this study it was decided to implement this technique and the casing vibrations were examined using the frequency response analysis. This analysis could be accomplished by integrating the spectral density function for the acceleration requiring the transformation of the time-history records from the time domain to the frequency domain (**Figures 5.23 to 5.26**). This transformation could be accomplished using the Fast Fourier Transform (FFT) algorithm.

For that purpose, an add-in program called FFTTOOLS was used along with a spreadsheet (Excel 4.0) that contained the acceleration records. Before converting the ASCII files collected during the field testing to acceleration records, it was necessary to establish a macro on the spreadsheet program to arrange the ASCII files and set the tables in a format that the FFTTOOLS could accept. Setting the required parameters for the FFT analysis, it was possible to obtain the frequency response function (FRF) and the spectral density function (SDF). The SDF was used to determine the RMS value of the acceleration and then integrated to obtain the SDF of the velocity. Accordingly, the RMS velocity could be obtained and compared with the RMS values from the direct integration of the time-history records. The RMS values from both methods are presented in **Table 5.2.**

As can be seen from **Table 5.2** the variation between the RMS values of the records using the two methods was expected. However, the small variations were an indication that using the

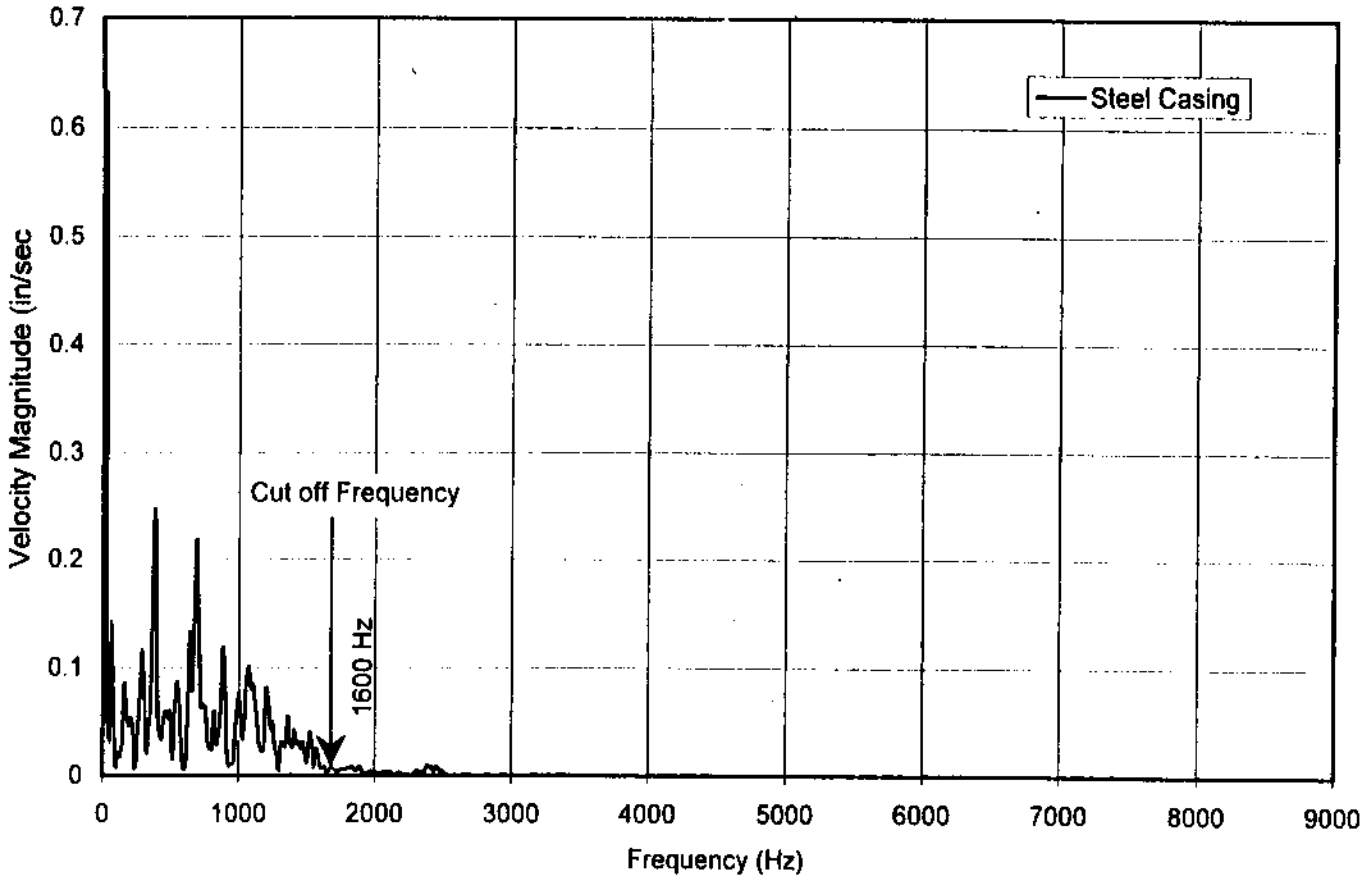


Figure 5.23: Frequency content of a 40 ft drilled shaft steel casing driven to 1.5 ft in sandy soil.

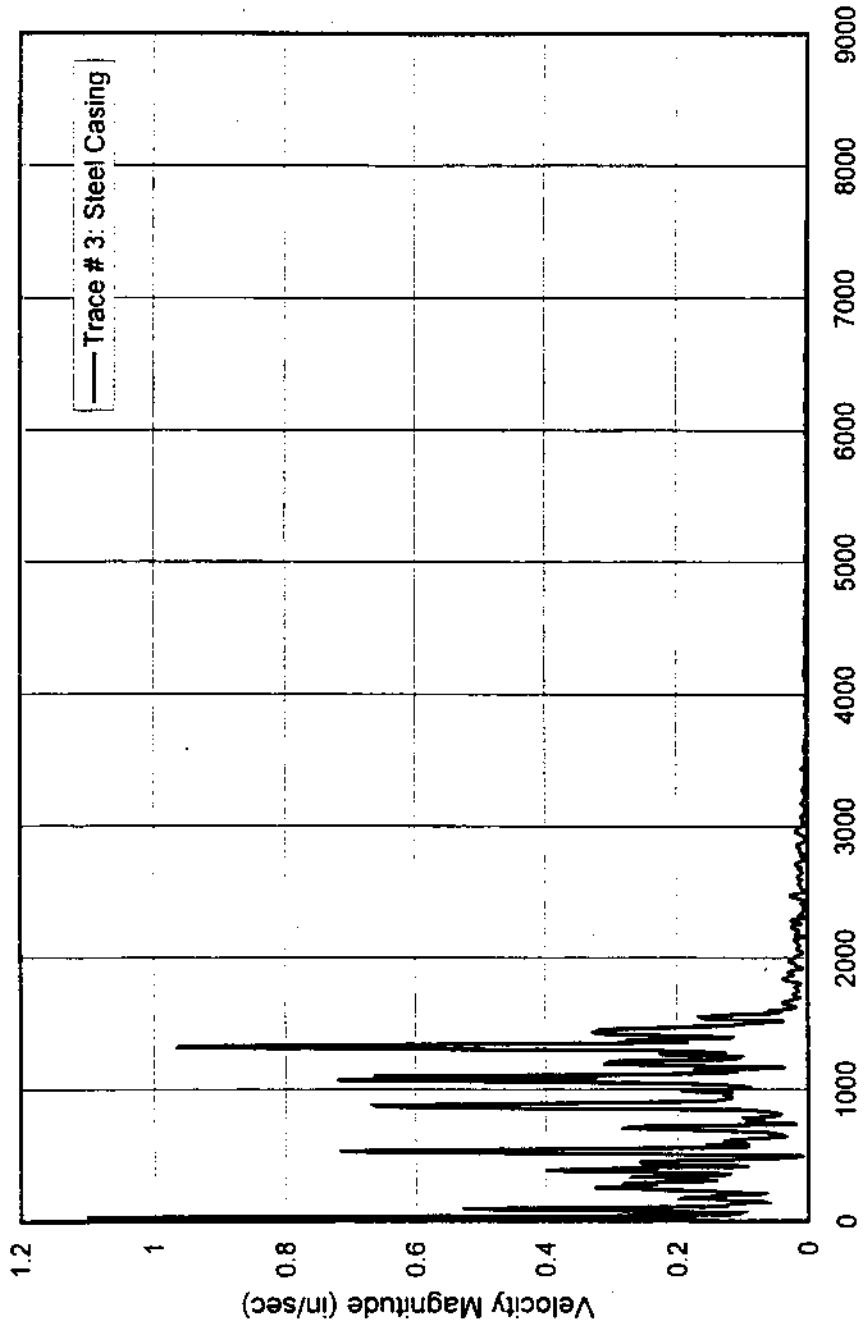


Figure 5.24: Frequency content of a 40 ft drilled shaft steel casing driven to5 ft in sandy soil

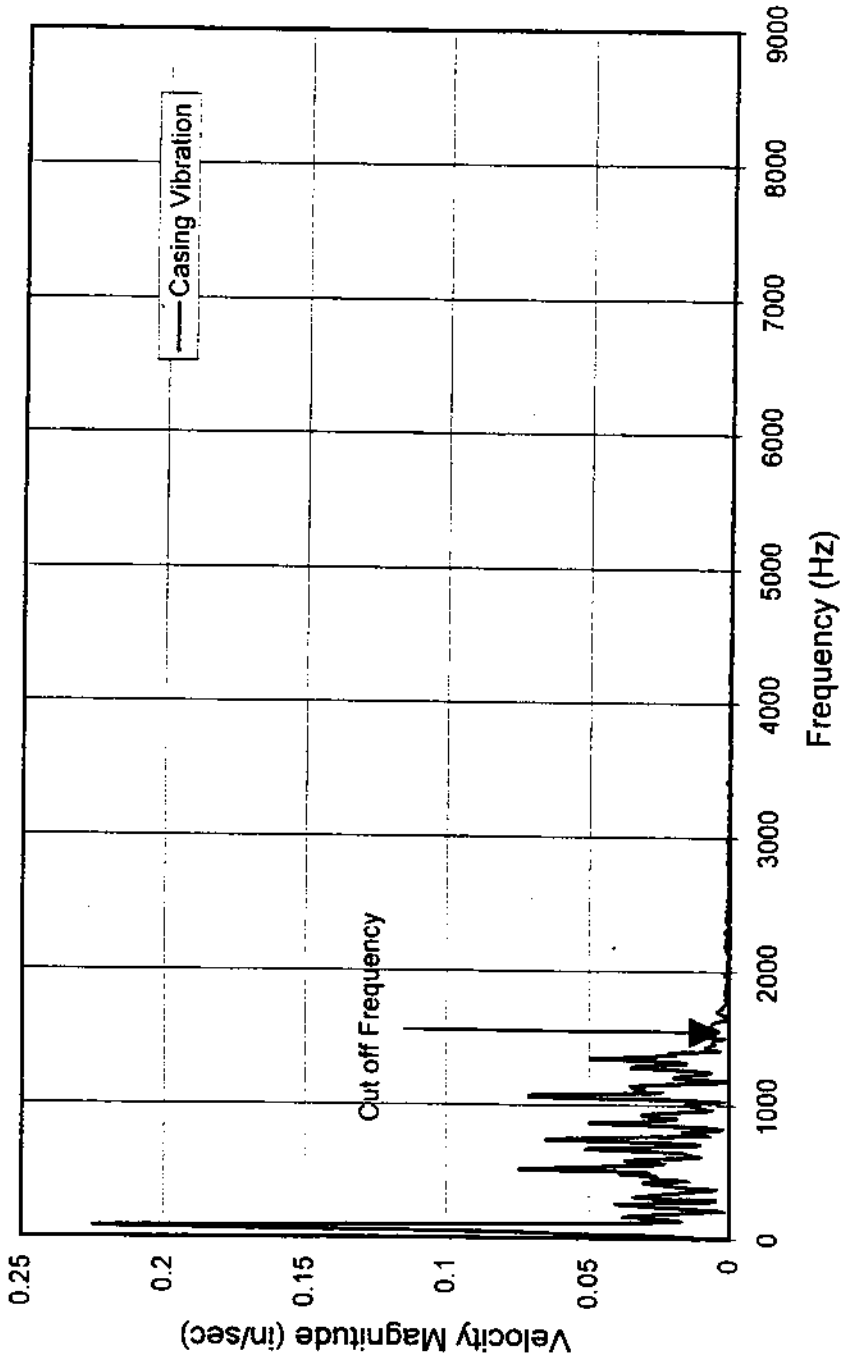


Figure 5.25: Frequency content of a 40 ft drilled shaft steel casing driven to 8 ft in sandy soil.

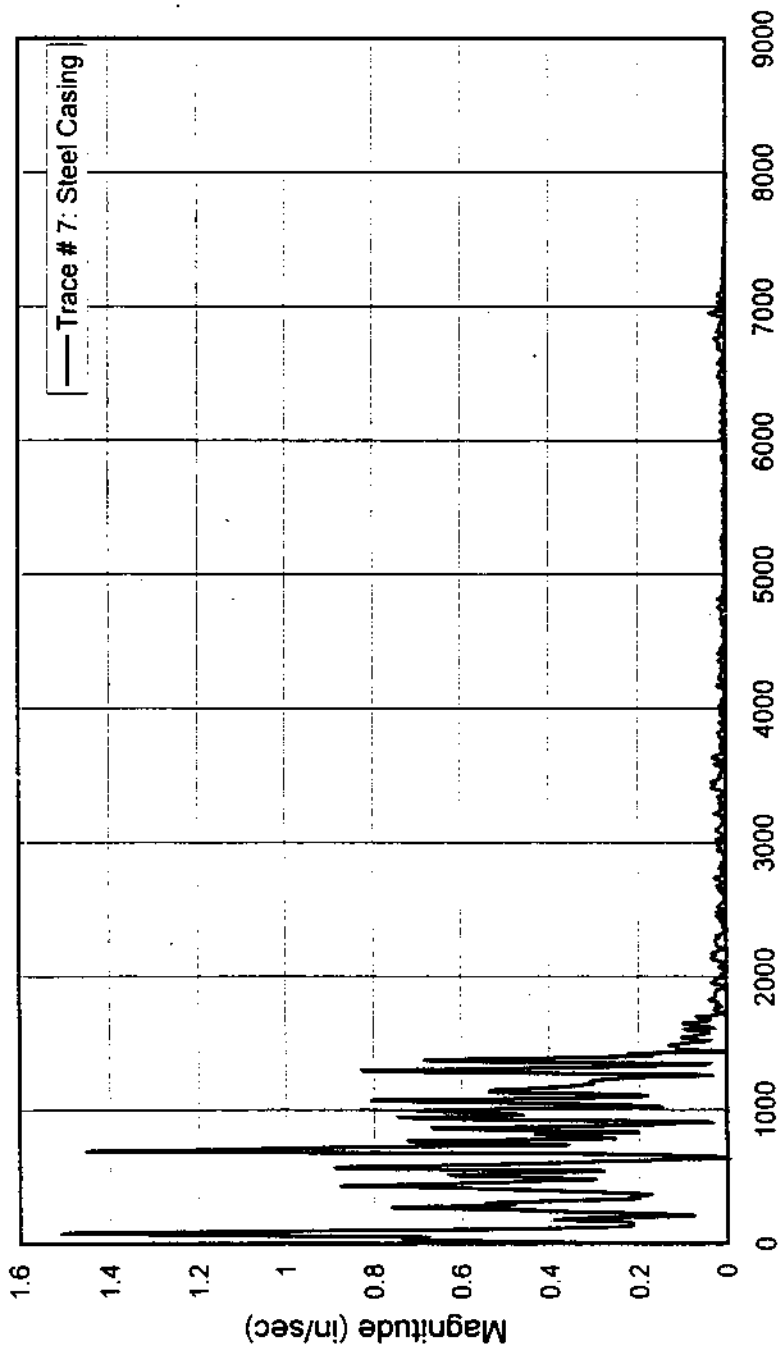


Figure 5.26: Frequency content of the steel casing due to 10 ft penetration.

direct integration method was an acceptable practice as determining the peak particle velocity from random vibration analysis is a laborious process that may deem the procedure impractical. On the other hand, with the advancements in hardware and software technologies make it easier to use the frequency domain analysis. The system parameters of the construction vibrations were determined by real time domain and frequency domain analysis in the present study. This approach, as compared with only frequency domain analysis, may provide field engineers with a broader knowledge of modal testing and analysis.

The frequency content of the casing vibration from the FRF was determined to be about 1500 Hz. When the RPM on the hydraulic pump was increased the frequency content reached 2000 Hz., the dominant frequency ranged between 16 Hz to 75 Hz **(Figures 5.27 to 5.30).** These values corresponded to the increase in the angular velocity of the mass rotation in the vibrator.

The surface accelerometer recorded particle accelerations that ranged from 0.5 in/sec$^2$ to 0.03 in/sec$^2$ for distances of 5 and 15 feet, respectively. The peak particle velocities of the ground response obtained by the direct integration method, ranged from 0.3 in/sec to 1 in/sec. It was noticed, that the surface response to the steel casing vibration exhibited higher velocities as the casing penetrated deeper in the ground. This observation was confirmed when the second field test at FAU was conducted with geophones inserted in the ground at certain depths. In general, the frequency content of the ground surface was about 300 Hz with the dominant frequency of about 32 Hz **(Figures 5.31 to 5.35)**.

### 5-2-2 FAU Field Test # 2

The second test at Boca Raton was on January 9, 1998 . The objectives were similar to the first field test, with the exception of that geophones were embedded in the ground and were used

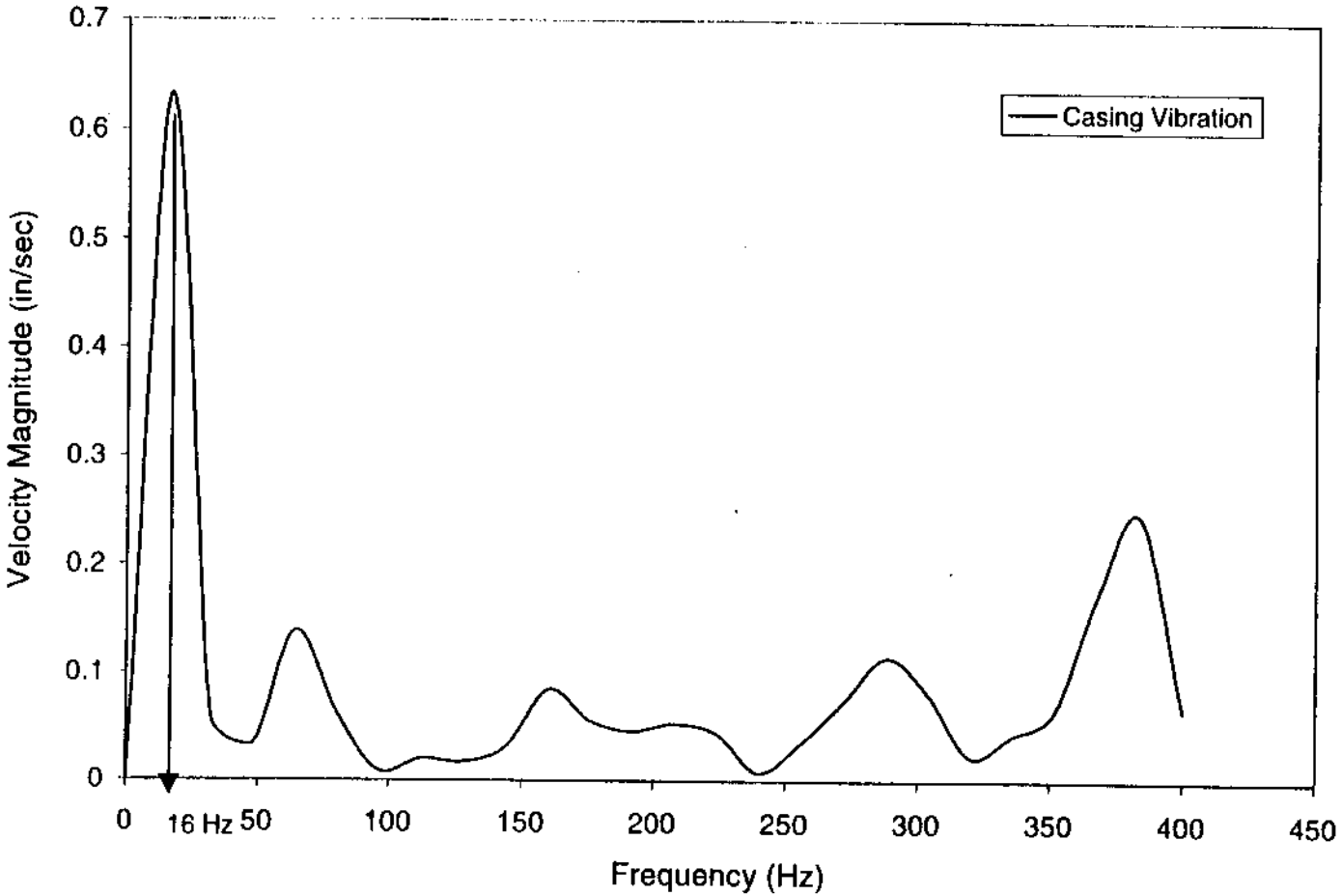


Figure 5.27: Dominant frequency of the steel casing at penetration depth of 1.5 ft

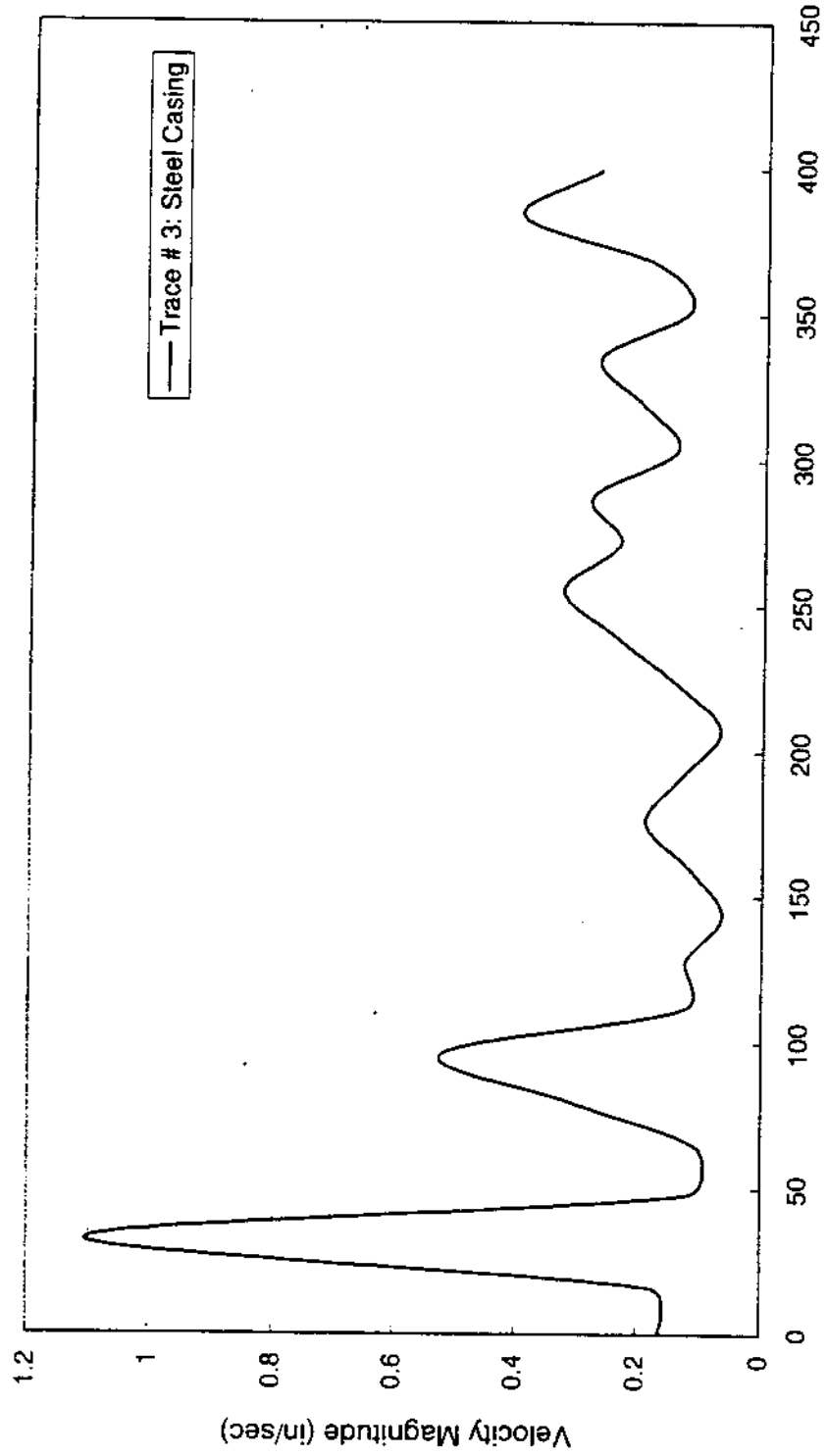


Figure 5.28: Dominant frequency of the steel casing at penetration depth of 5 ft

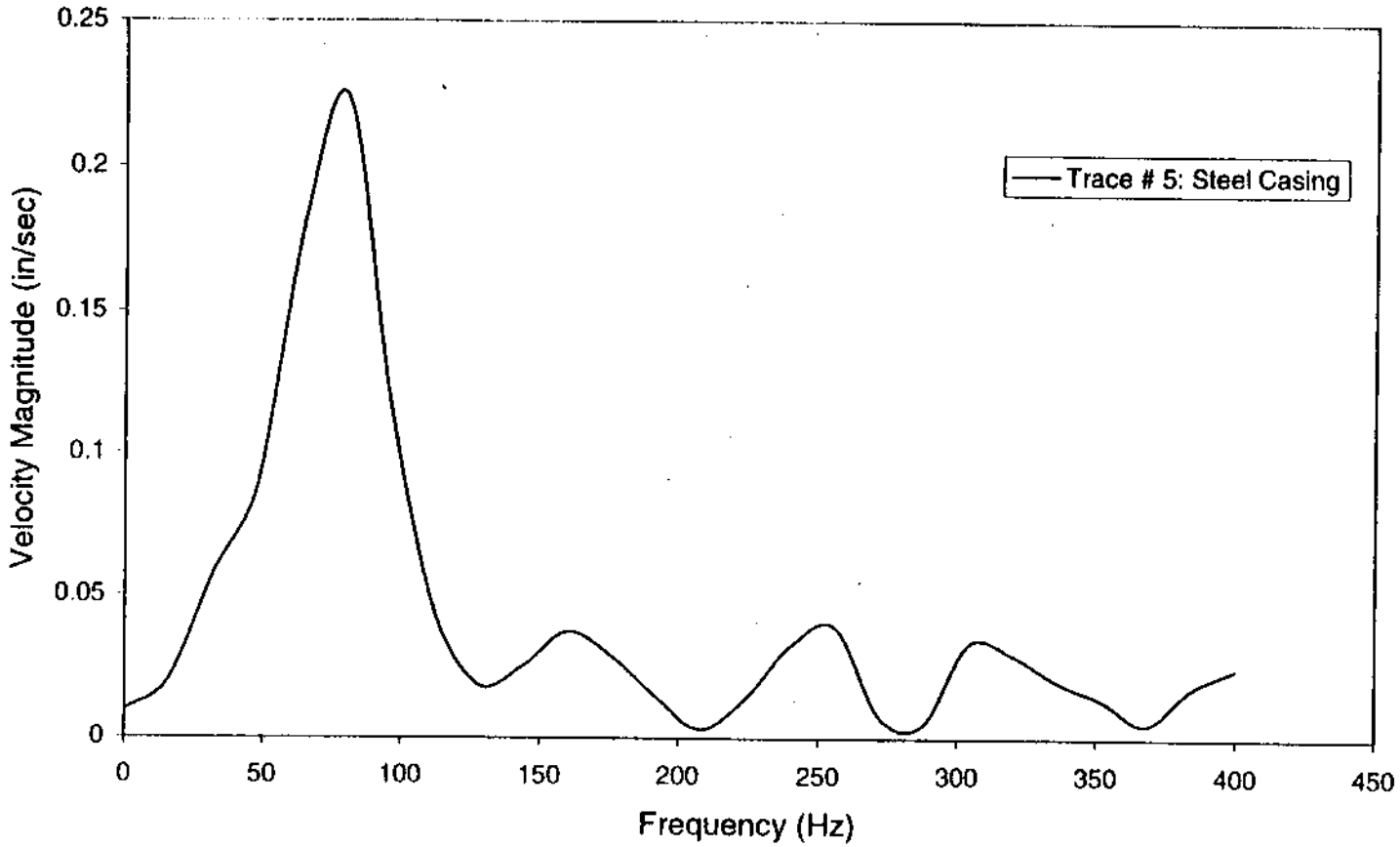


Figure 5.29: Predominant frequency of the steel casing at penetration depth of 8 ft.

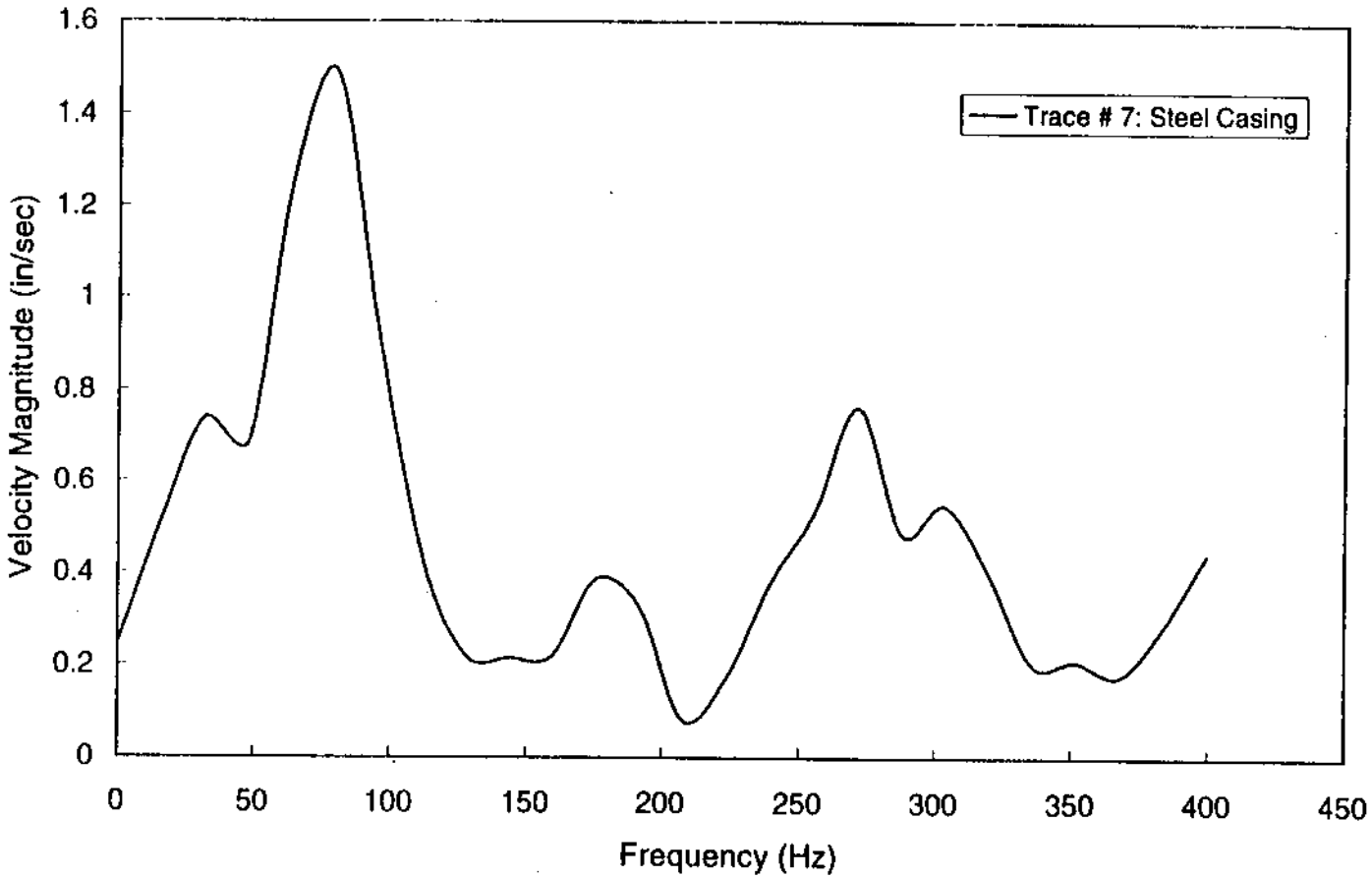


Figure 5.30: Predominant frequency of the steel casing due to a penetration depth of 10 ft in the ground

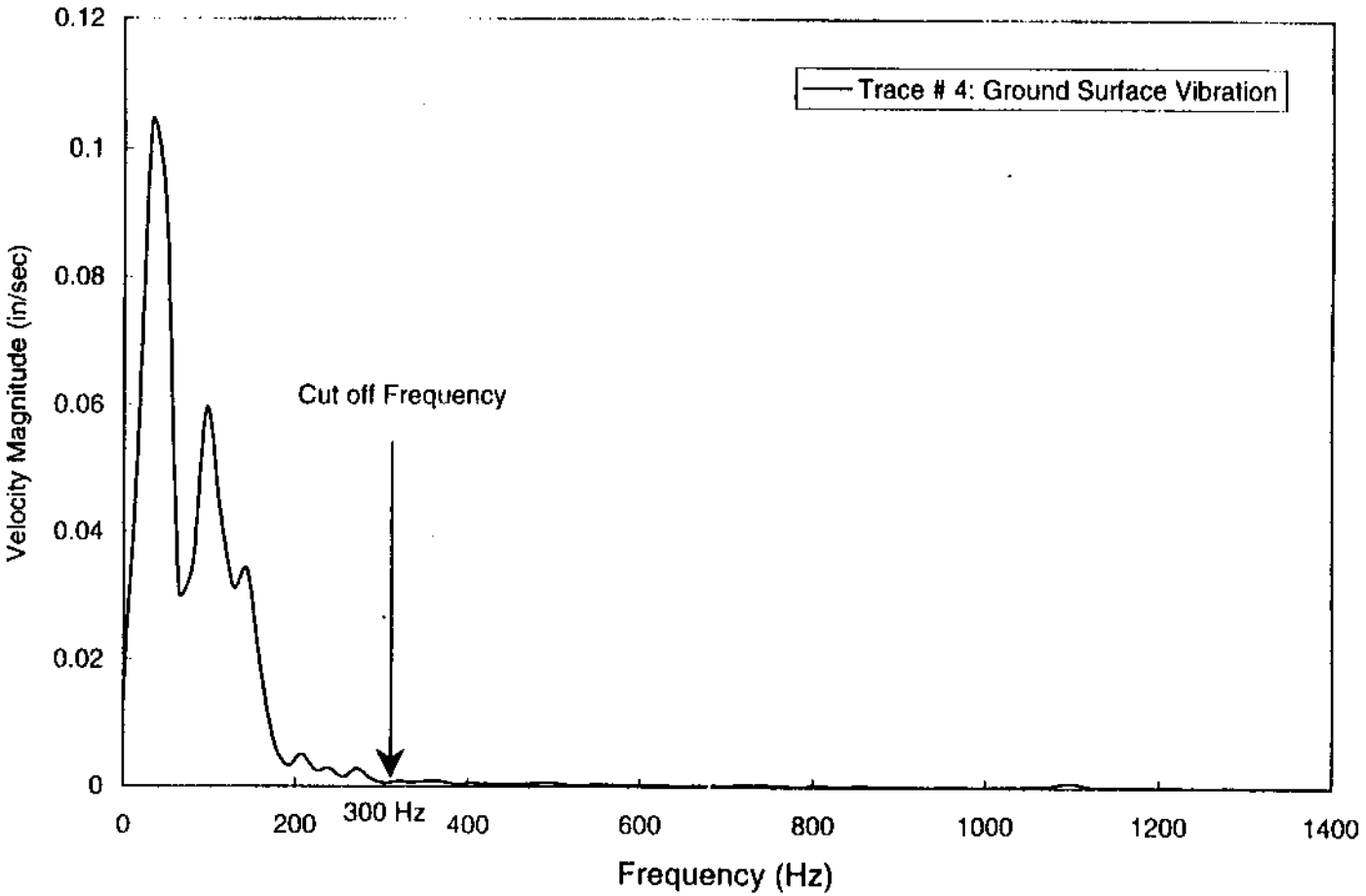


Figure 5.31: Frequency content of the ground surface vibration due to an 8 ft casing penetration

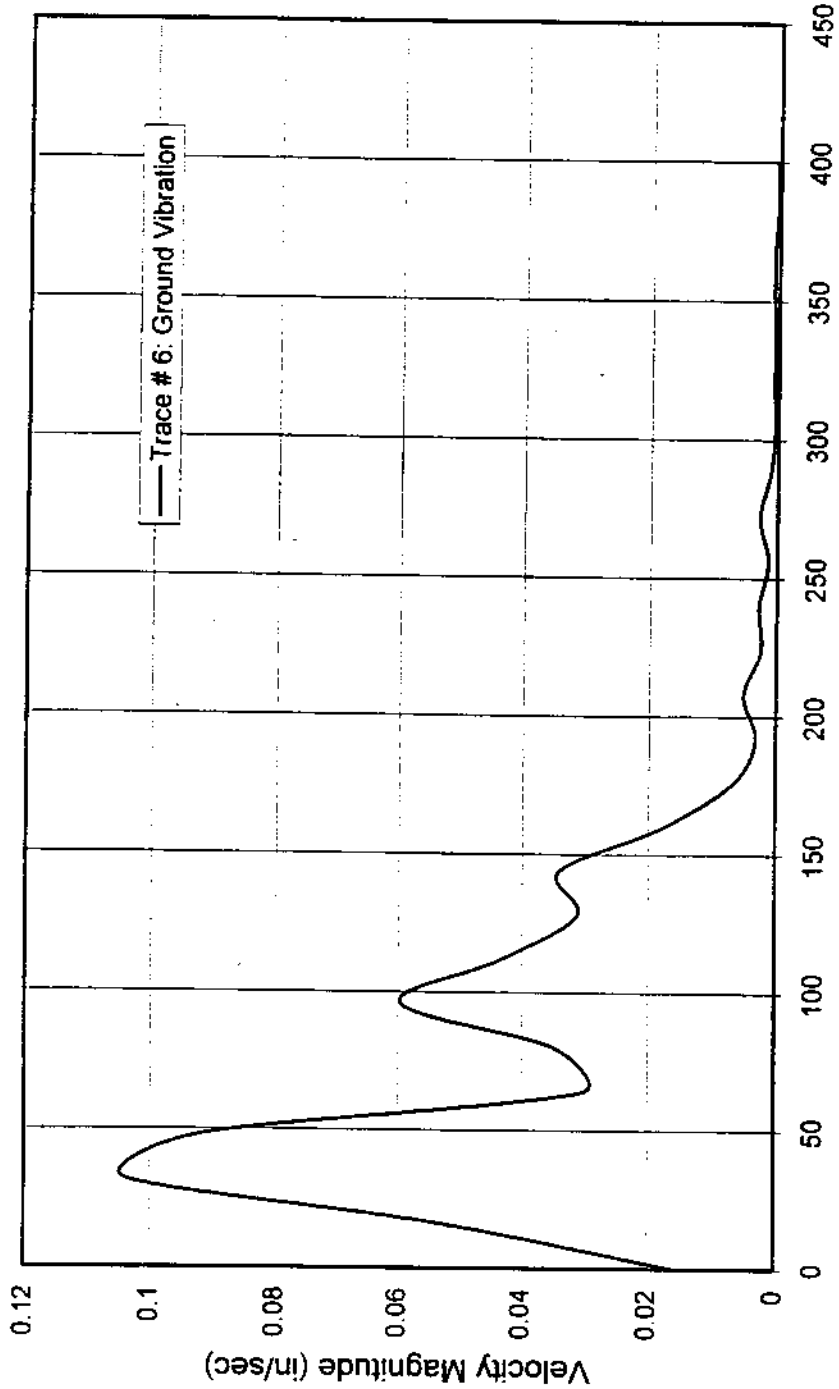


Figure 5.32: Dominant frequency of the ground surface due to 8 ft casing penetration.

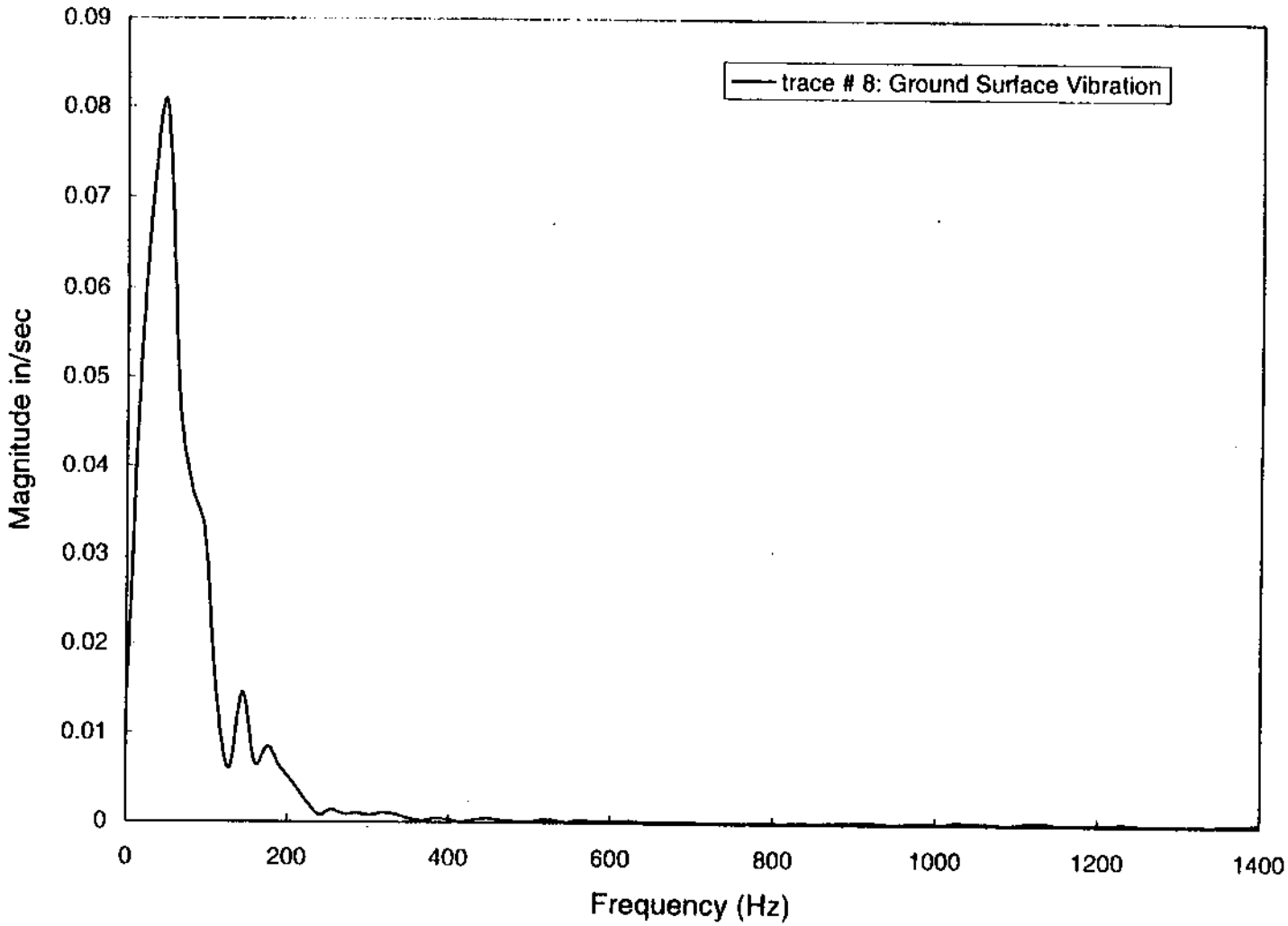


Figure 5.33: Frequency content of the ground surface due to a casing penetration of 10 ft.

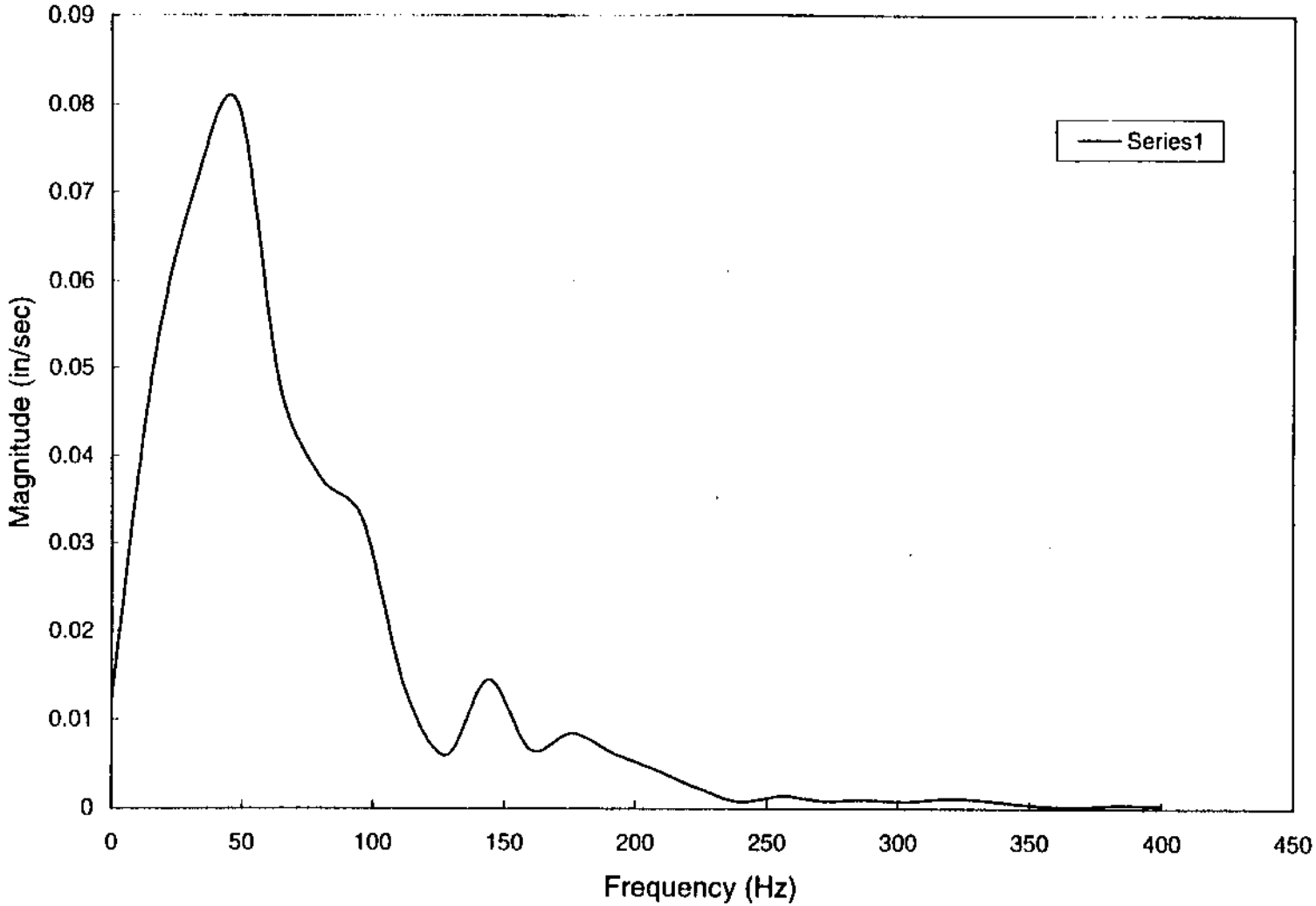


Figure 5.34 : Predominant Frequency of the ground surface due to a casing penetration of 10 ft.

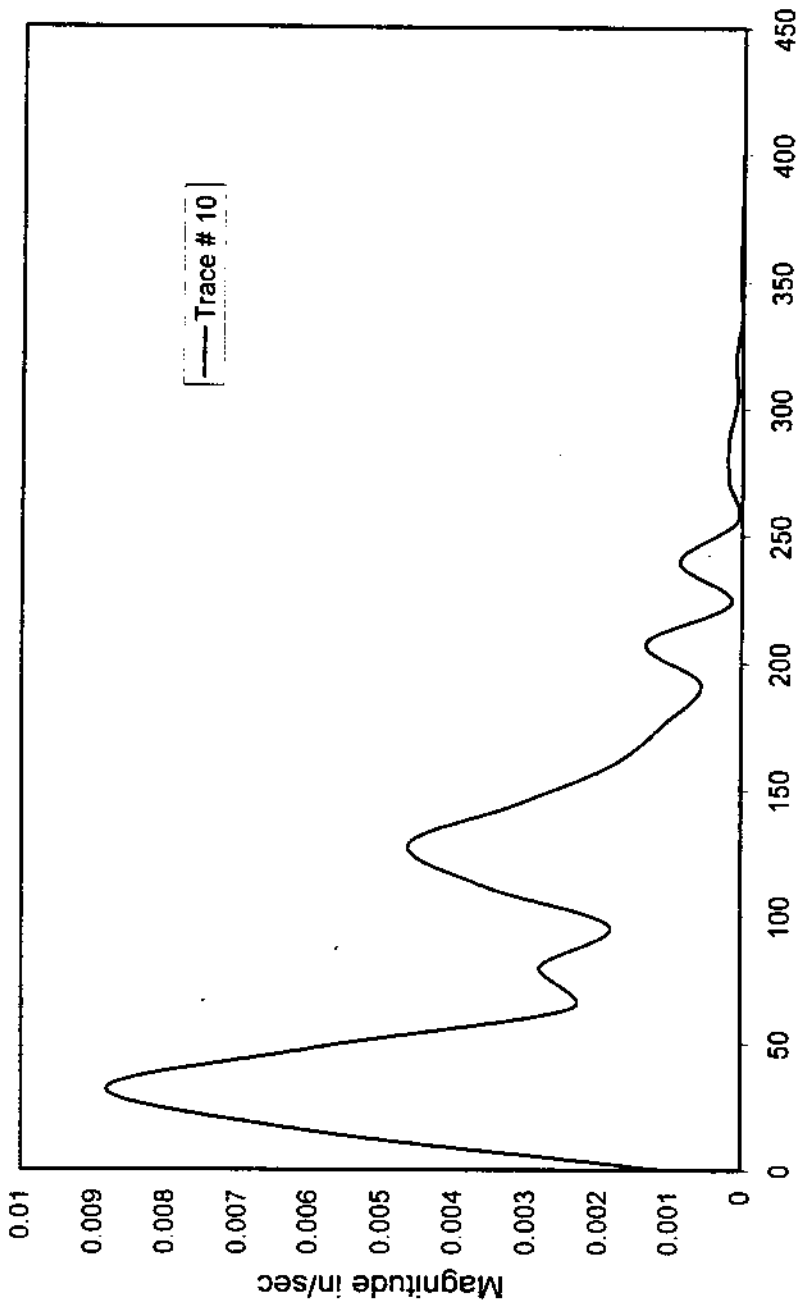


Figure 5.35: Dominant frequency of the ground surface due to 12 ft casing penetration.

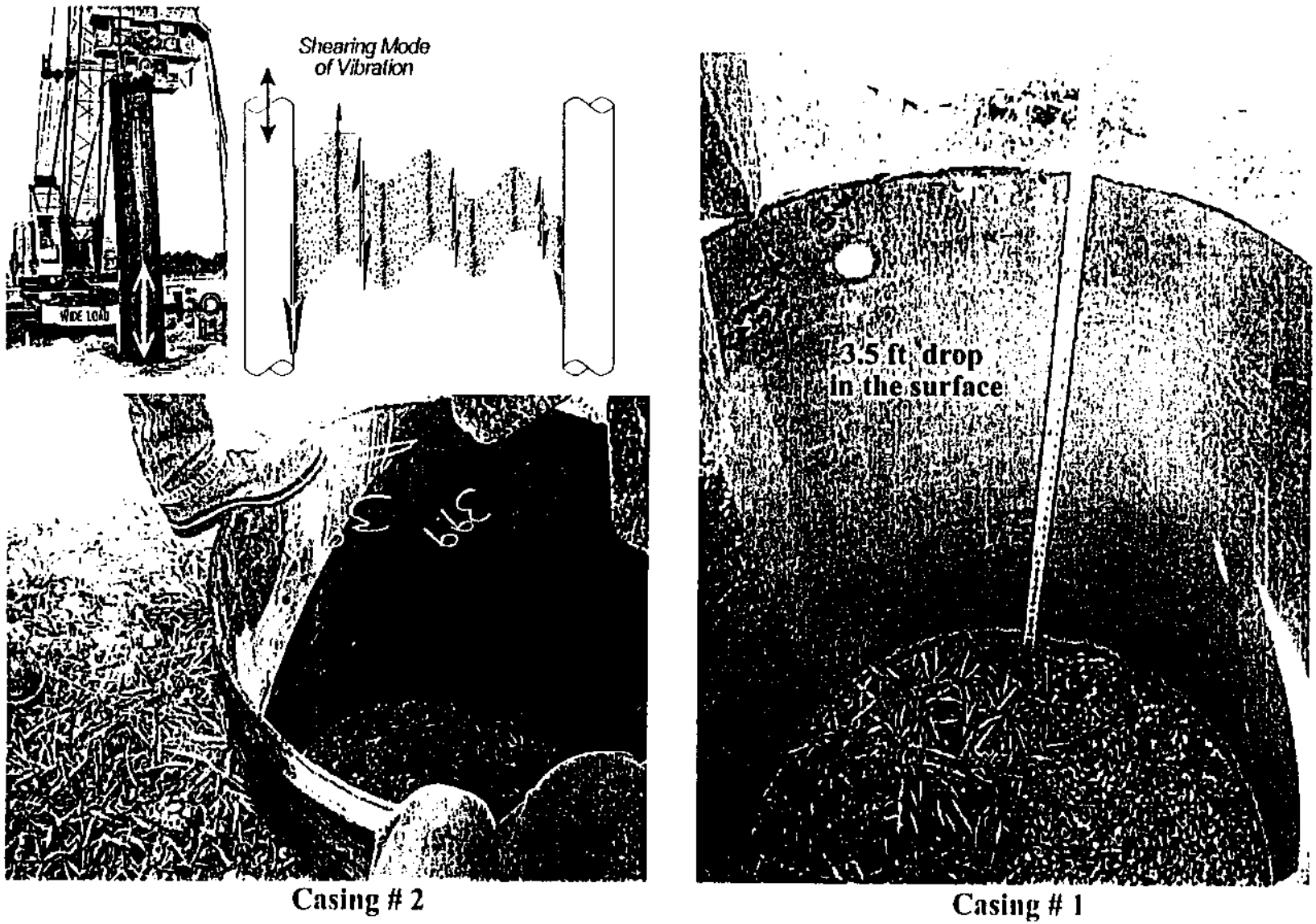


Figure 5.36. Drop in the ground level after completing the driving process.

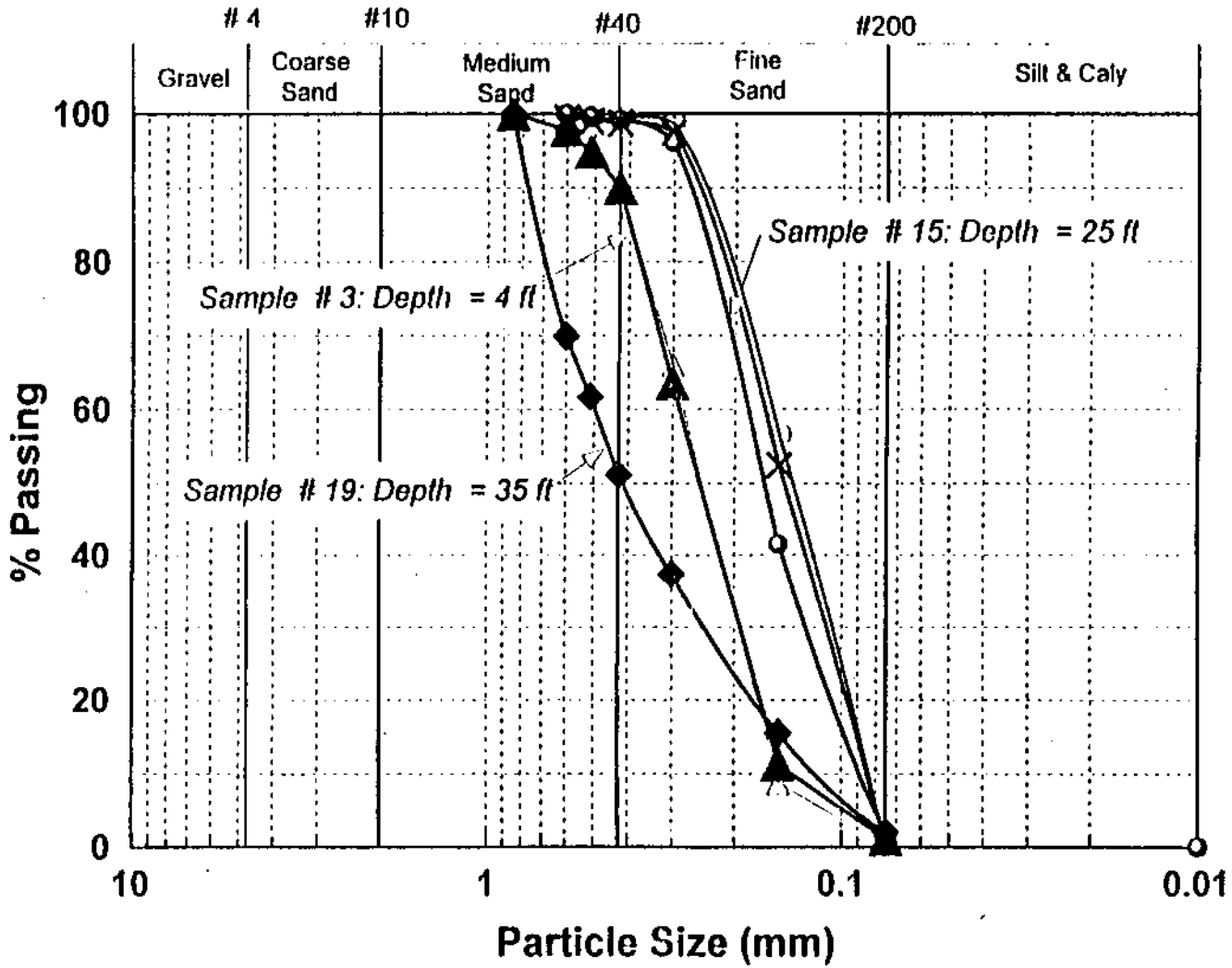


Figure 5.37. Grain size distribution of sand samples obtained from FAU Site.

to determine the peak particle velocities at different depths. Six of the eight geophones gave reasonable vibration measurements. The other two, embedded at 30 feet and 35 feet, malfunctioned. The geophones were placed in a circular pattern with the driven casing in the center and at a 9 feet radius. The needed measurements were collected by Law Engineering and the analysis was performed at Florida State University.

Peak particle velocities obtained from this field test indicated that some vibration components might dominate the maximum values. These components were in the longitudinal and the transverse directions. Most of the measurements, however, indicated that the vertical component prevailed. The reason for the escalation of the longitudinal and the transverse components could be due to the eccentric vibration that was applied on the steel casing by the vibrator. As it was explained in a previous section, the gripping of the steel casing was on one side only. The same was done when the casing was extracted. This eccentricity may have caused side vibrations in the casing which were manifested in large velocities in the L and T directions.

Selecting the vertical component (shear mode) of the peak particle velocity necessitated the re-examination of all the time-history records collected in the field. Such an examination was time consuming and can not be used for regular practice. It is customary to record, as a final result, the peak particle velocity from any of the three orthogonal directions. Any velocity that gives the maximum value is usually reported. Evaluation of the PPV values that are reported during construction vibration monitoring, may not indicate the mode of vibration that dominated the response.

In this study it was important to distinguish between these modes in order to assess the type of vibrations propagated through the system. For example, if the PPV was for the vertical mode then the conclusion is that the type of vibration would mostly be of a shear type. This is only true

for the driven steel casing. The reason is that the generated vibrations in the ground would predominantly be due to the friction between the casing surface and the surrounding soil. However, some kind of soil displacement may occur. This lateral displacement could give rise to the development of longitudinal vibration or compression vibrations. Since the lateral displacement in this case is very low, as compared to the large displacement caused by pile driving, the longitudinal and the transverse modes should be low accordingly.

Additional indication of the effect of vertical vibration on the surrounding soil was noticed in the first and the second field tests. After driving the full length of the casing, it was found that the ground level inside the casing was much lower than the one outside the casing (**Figure 5.36**). The drop between the two levels was about 3.5 feet.

The use of the PPV without knowing the mode of vibration would defeat the purpose of using the concept itself. One of the main objectives of specifying the particle velocities in monitoring construction vibration is to be able to relate to the strain levels that the vibrations induce in the system.. **Equation 2.4 in Chapter 2** showed that the strain amplitude can be determined from the particle velocity and the wave velocity through the system. If the compressive strain is of interest in monitoring the construction vibration, then the compression wave velocity has to be determined; accordingly the compression (V, L, or T) mode of the vibration should be used. If the shear strain is the critical response, then, all the shear components should be determined.

In this regard, soil samples obtained from the boring logs were analyzed to determine the shear wave velocities of the various layers at the site. Water contents, void ratios, and unit weight of about 52 samples were determined in the laboratory. Soil property measurements are presented in **Table 5.3**. Based on the obtained soil properties, the shear wave velocity at each

level was determined using the Hardin and Richart (1963) equations. According to Hardin and Richart, the shear wave velocity, $v_s$, can be determined as:

$$v_s = (170 - 78.2\ e)\ \sigma_o^{1/4} \qquad \textbf{For } \sigma_o > 2000 \text{ psf} \qquad (5.3)$$

$$v_s = (119 - 56\ e)\ \sigma_o^{1/5} \qquad \textbf{For } \sigma_o < 2000 \text{ psf} \qquad (5.4)$$

where $\sigma_o$ = octahedral effective stress

Values of the shear wave velocities are presented in **Table 5.4** and **Figure 5.38.** As can be seen from **Figure 5.38**, the effect of the ground water table was noticeable at a depth of 6.7 ft. Shear wave velocities dropped by 13 percent for the soil layer below the water table. At a depth of 12 ft, the shear wave velocity started to exceed the values at 6.7 ft.

Using the SPT results obtained from the two boring logs (**Figures 5.39 to 5.42**), one can notice the similarity in the variations of the wave velocities and the blow counts with depth. This similarity led to the use of **Equation 2.11** in **Chapter 2** to determine the shear wave velocity from the SPT blow counts. Shear wave velocities of the two boring logs at Delray site are also presented in **Figures 5.43 and 5.44**. Results from similar field studies are shown in **Figures 5.45 to 5.47**.

The peak particle velocities recorded by the geophones have shown that as the casing is driven deeply into the ground, the PPV values increased at all depths. For 5 ft casing penetration, the corresponding geophone at the same level (**G1 see Figure 4.2**) recorded PPV of about 0.18 in/sec. When the penetration depth of the casing reached 40 ft, readings from that geophone (**G1**) showed 2.0 in/sec. Also, at that penetration depth for the steel casing, the sixth geophone (**G6**) at 40 ft depth indicated a PPV values approximately equal to the values at the geophones above (**Figure 5.41**). **Table 5.5** presents all the measurements obtained from the FAU field test. These

measurements include PPVs during both driving and extracting the shaft casing. Additional readings are presented for **G1** and **G6** due the vibration of the second casing **(Figure 3.6)**.

From the obtained soil properties, the vertical effective stresses at various depths were calculated. These stresses were plotted against the PPV recorded from all the geophones. It should be mentioned here that the values of PPV were obtained manually, **Figures 5.50 to 5.52.**

$$v = \alpha \ e^{-\beta\sigma_o} \qquad (5.5)$$

where v = peak particle velocity (in/sec)

$\alpha$ and $\beta$= penetration depth factors

$\sigma_o$ = Effective vertical stress

$\alpha = -0.115\text{Ln}(D) + 0.7$

$\beta = 0.57e^{-0.105\,D}$

in which D = penetration depth (ft)

## 5.3 FIELD MONITORING OF INDUCED GROUND MOTION

The field work included monitoring of installation induced vibrations in the ground for sites 1 and 2. Assessment of vibration disturbances provides an insight into the source mechanism and the eventual dissipation of the energy transmitted to the subsurface during the installation of a steel casing. The data collected is presented to evidence the events monitored during this attempt to characterize the peak particle velocities of particles in the ground. However, the conditions are specific to this test and no attempt was made to relate the motions evaluated here with other soil types. This test was the first of its kind, and all the work in the tasks at FAU is considered exploratory.

The monitoring of induced vibrations during Field Tests Nos. 1 and 2 provided an insight into the actual inner working of the strata and the source mechanism. The data obtained was stored and analyzed on an HP Fast Fourier Transform Analyzer by LAW Engineering

(Jacksonville, FL).The results of which show a frequency content for the driven casing in the range of 2 - 2.2 kHz. **Figure 5.53** shows typical accelerations of the vibrating casing, with the attached accelerometer place five feet above the ground.

As expected, given the sandy conditions of the site, the energy dissipation from the driving of the casing significantly diminishes with increasing distance from the vibrating source. To show this energy dissipation, **Figure 5.54** is presented. The absolute values of the acceleration at 15 feet away from the source are significantly greater in magnitude than the values recorded at 10 feet.

More interesting data from this preliminary investigation is operated with the monitoring of vibrations in the subsurface. The virtual shaft discussed in Chapter IV shows what typical vibrations could be expected at varying locations at depth within the shaft. These vibrations are in fact those that can cause detrimental effects on the curing of the concrete in the shaft. With the geophones implanted, the vibrations generated during the installation procedure were recorded. A large volume of data was acquired during this exploratory phase. The sampling rate was 200 samples per second using the data acquisition system. The recordings were conducted in series, one geophone at a time in one-second interval.

As already indicated, a summary of the velocities observed during the installation has been presented in **Table 5.5**. The table shows the geophone numbers, their locations at depths and the average velocities of their recordings at varying driving ranges of the steel casing. The data is interpreted in **Figures 5.53 and 5.54**. The vibration levels at individual geophones during driving ranges is presented in **Figure 5.53**, in which a trend for each individual geophone is plotted. From the graph of the velocities at the location of each geophone during the stages of driving, it can be observed that the velocities increase as the tip of the steel casing penetrates to greater depth. Another presentation of the data is the recording of vibration levels during the installation as a function of the driving and the levels recorded by the geophones. **Figure 5.54** shows the results of the average recorded vibrations for the different stages of driving. These stages are representative of the tip elevation of the steel casing as it penetrated into the subsurface. From the graph it can be shown that for all but the last driving stage (30-40 feet), the vibration of the free end of the subsurface experiences the highest levels of vibrations. In other

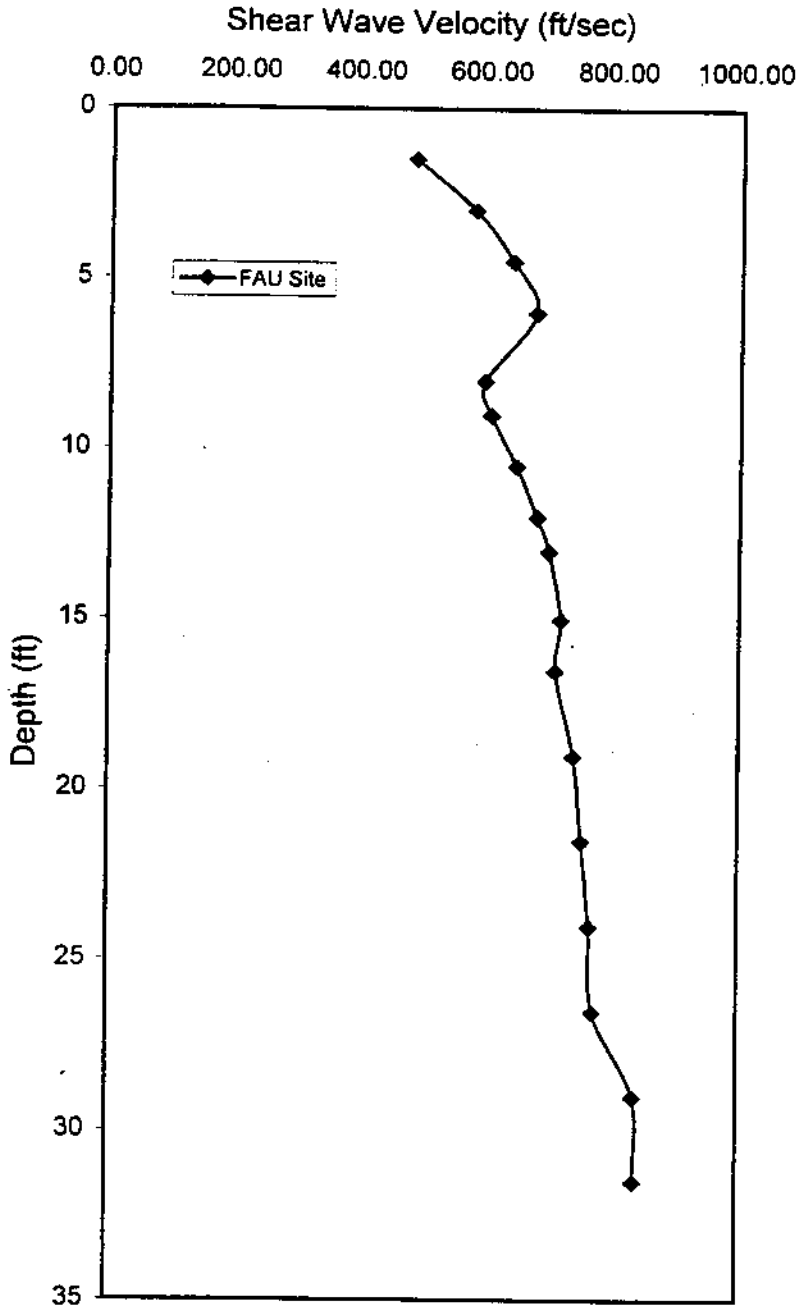


Figure 5.38: Shear wave velocity vs. depth at FAU Site

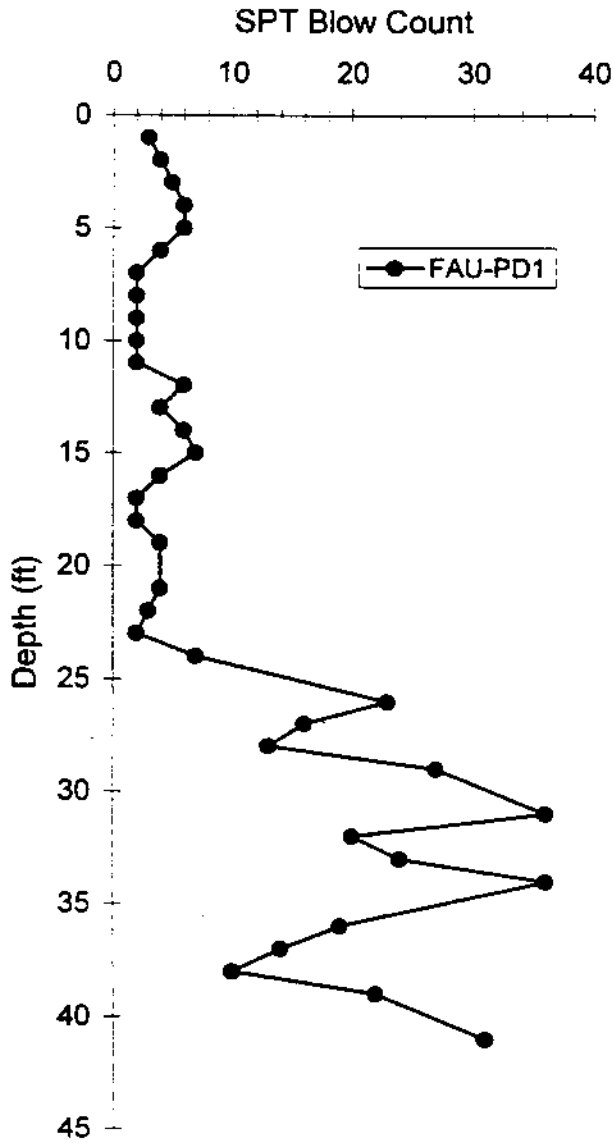


Figure 5.39: Standard Penetration Test results of boring # 1 at FAU site.

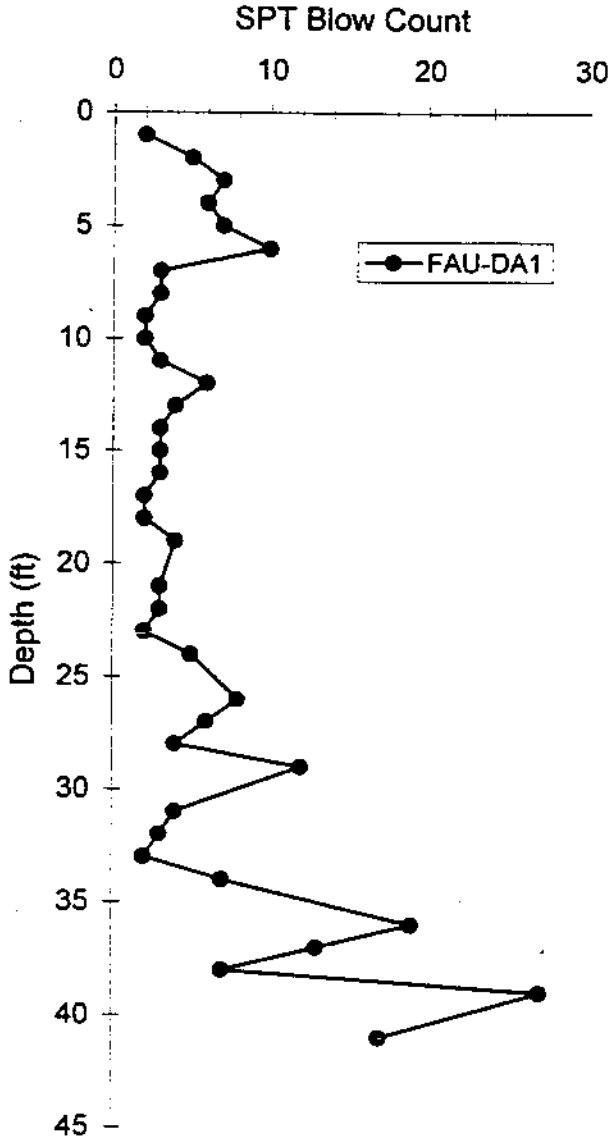


Figure 5.40: Standard Penetration Test results of boring # 2 at FAU site.

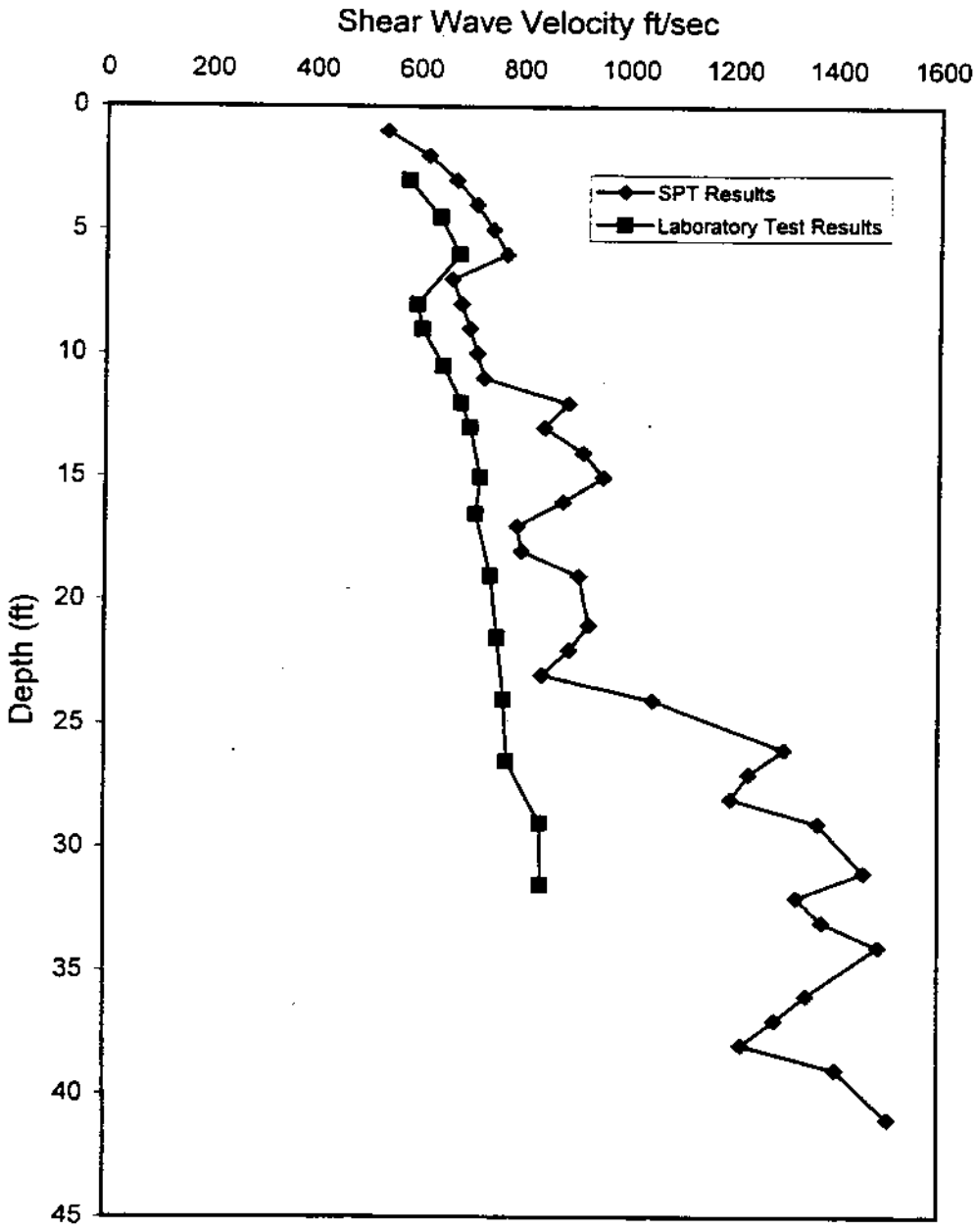


Figure 5.41: Shear wave velocity vs. depth using laboratory test results and SPT blow count values.

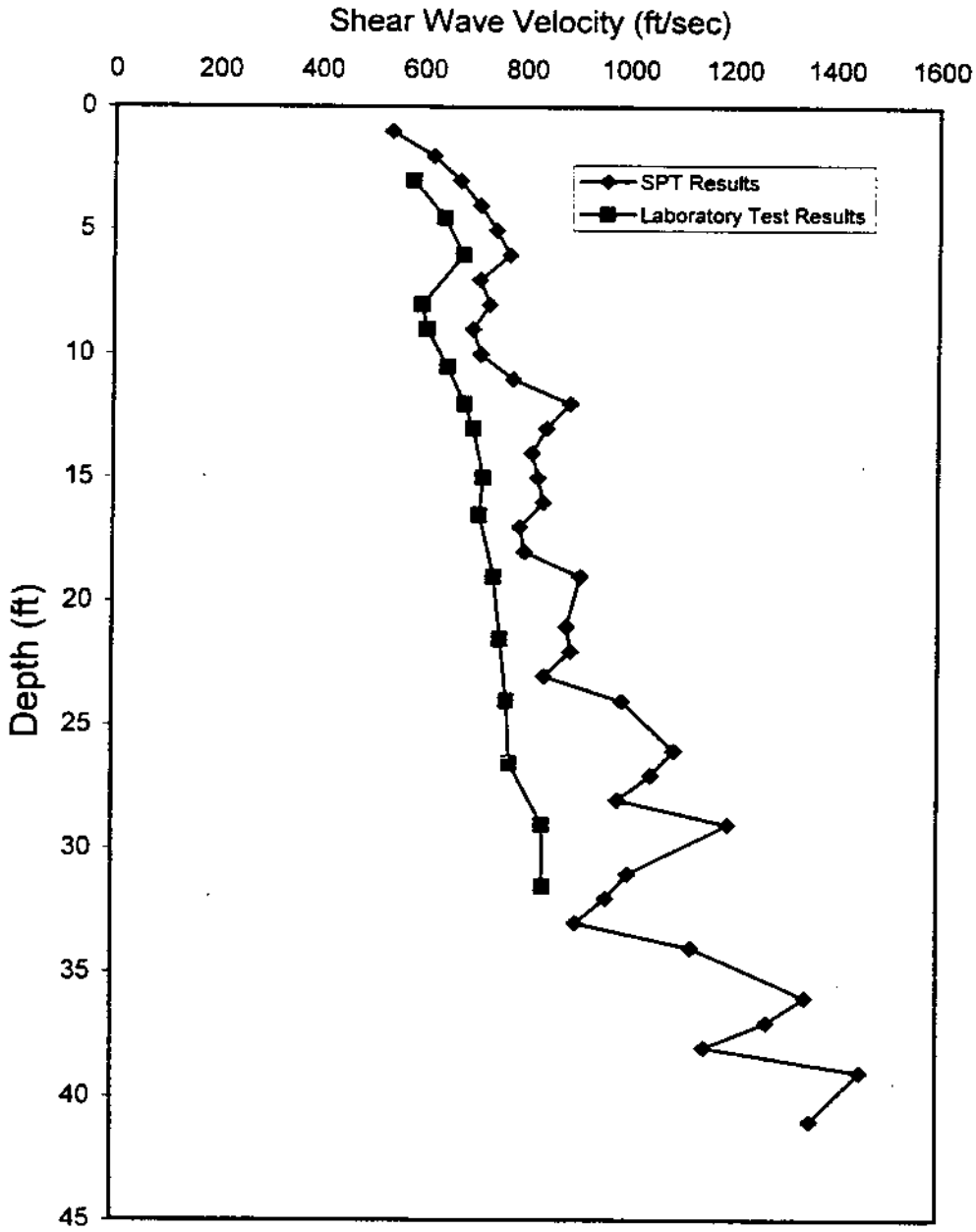


Figure 5.42: Shear wave velocity vs. depth using laboratory test results and SPT blow count values for the second boring log.

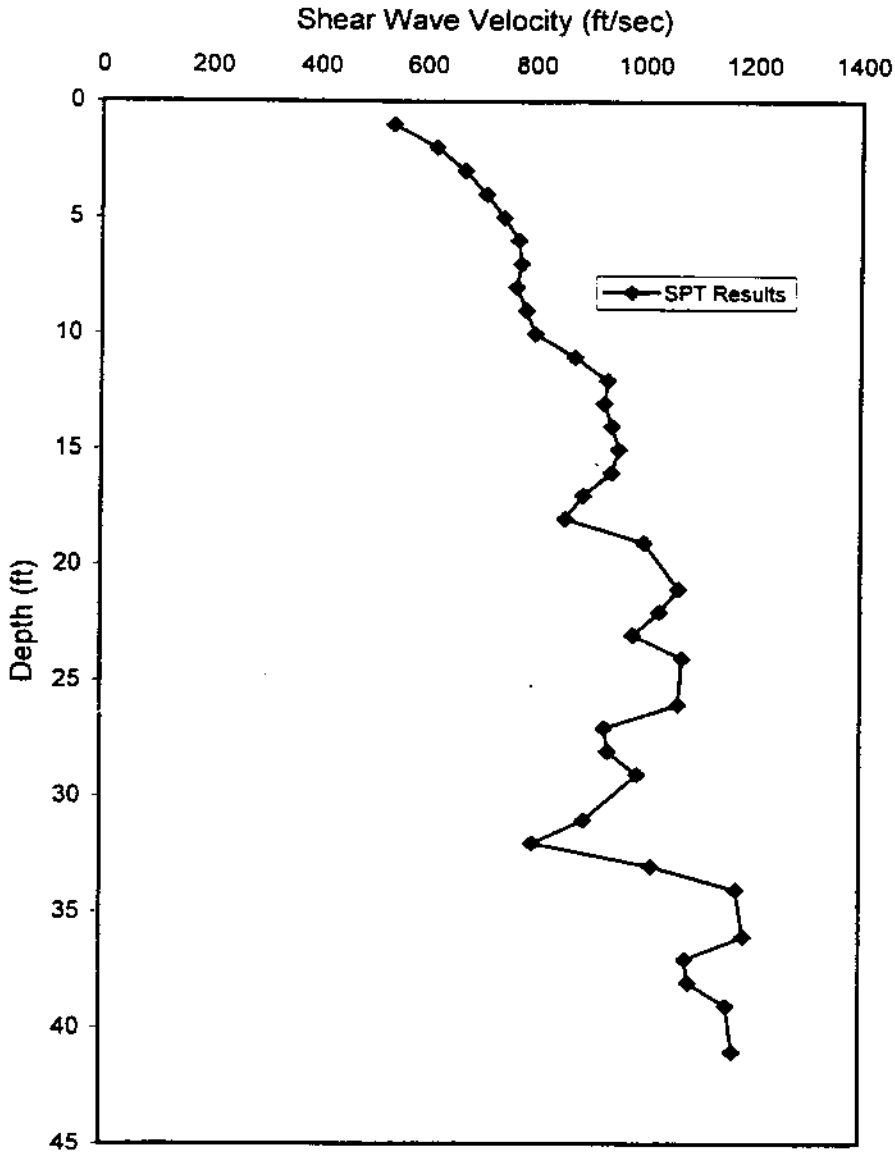


Figure 5.43: Shear wave velocity vs. depth using laboratory test results and SPT blow count values for the Delray Site.

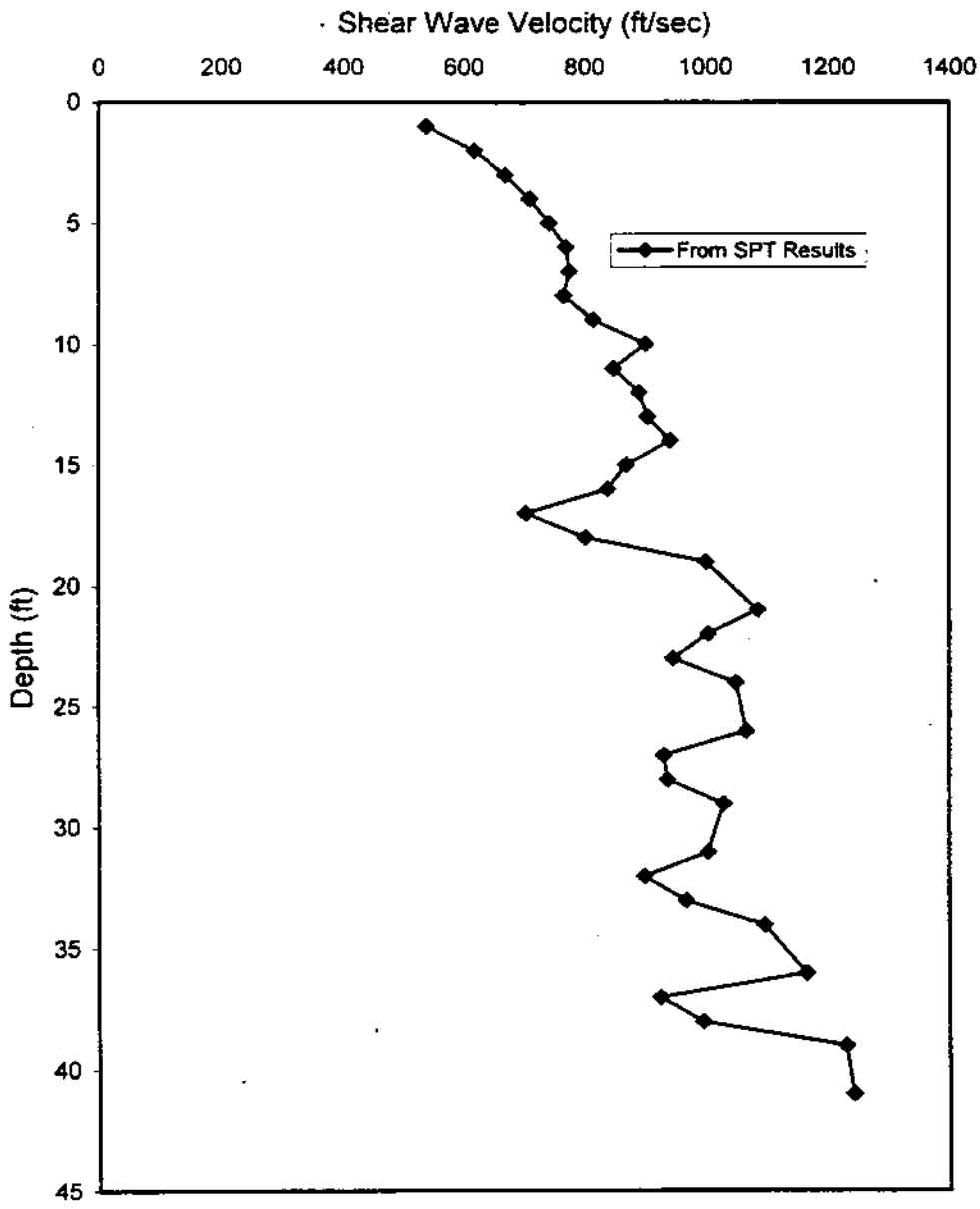


Figure 5.44: Shear wave velocity vs. depth using laboratory test results and SPT blow count values for the Delray Site Boring # 2.

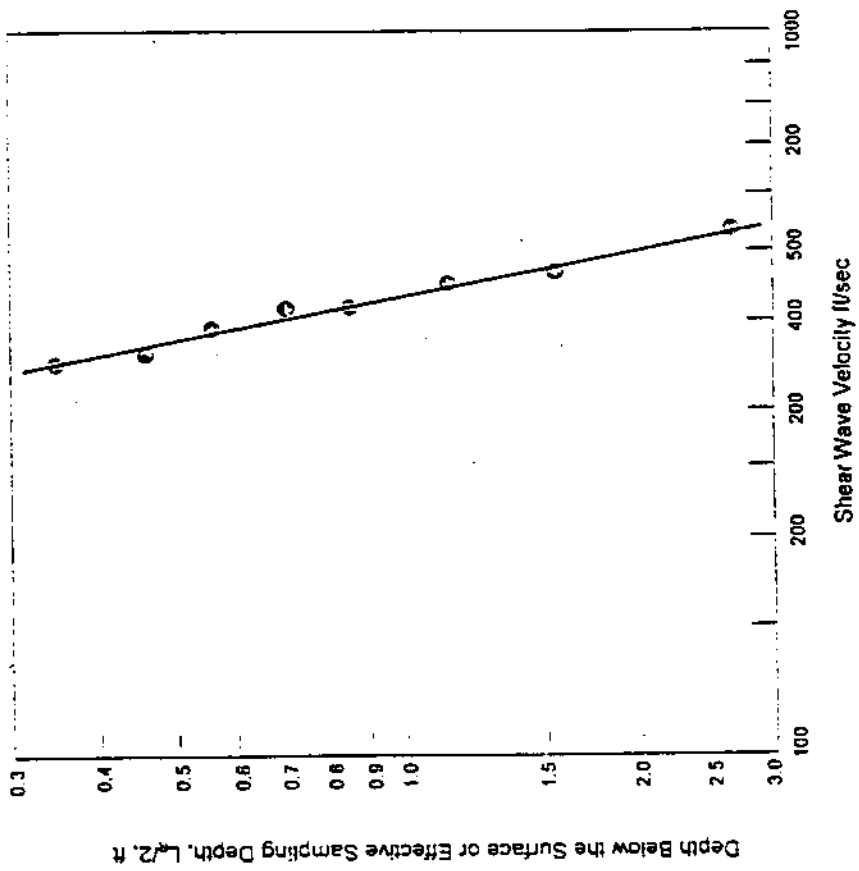


Figure 5.45 Shear wave velocity vs. Depth (Richart et al, 1970)

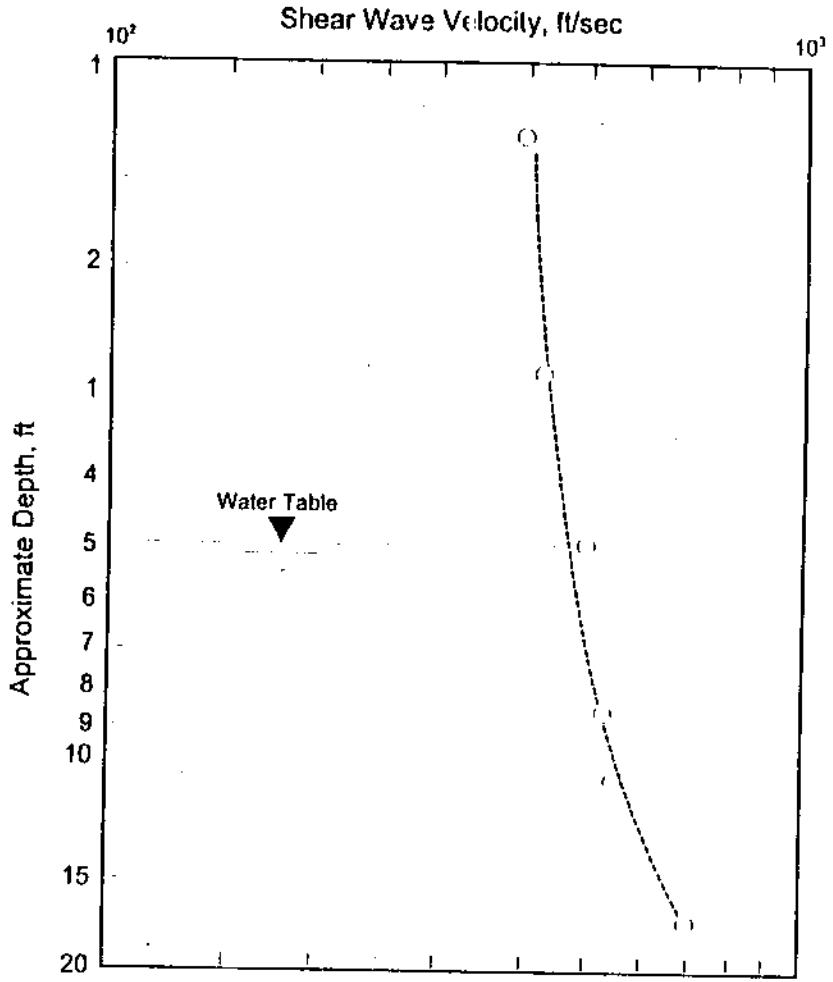


Figure 5.46. Shear wave velocity vs. Depth in uniform, fine sand
( after Ballard and Cassagrande, 1967)

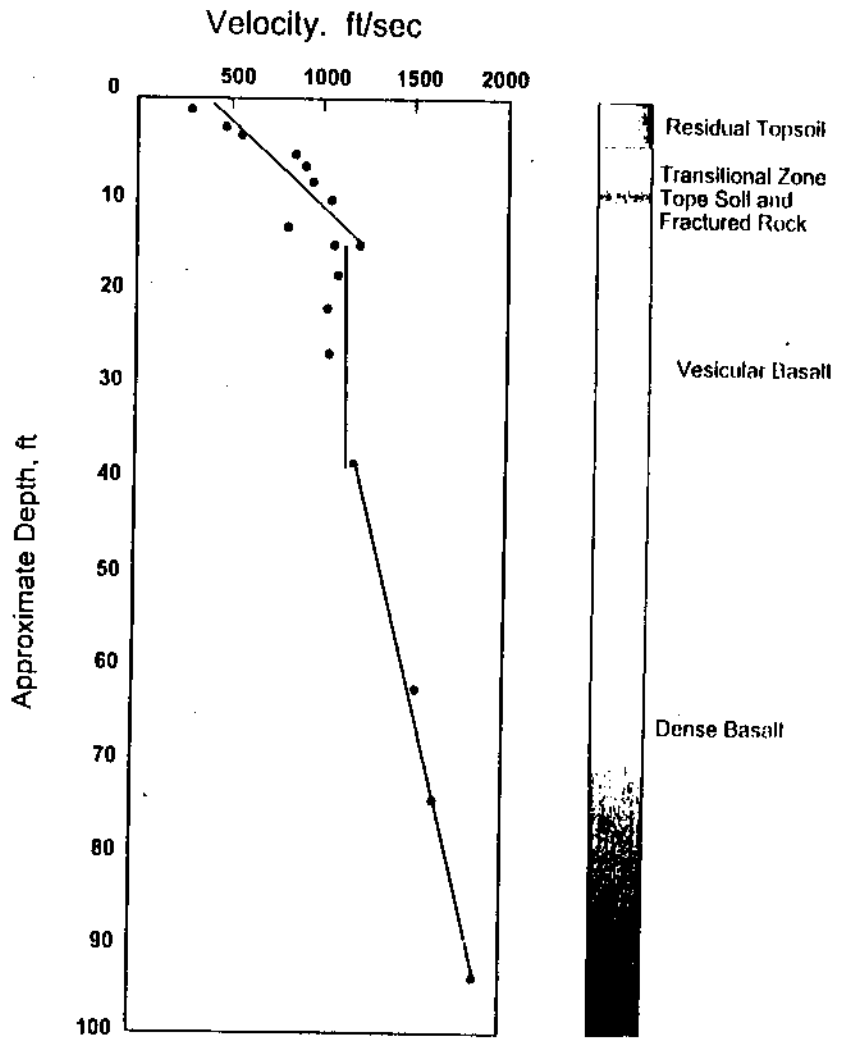


Figure 5.47. Shear wave velocity vs. Depth in rock profile ( after Fry, 1965)

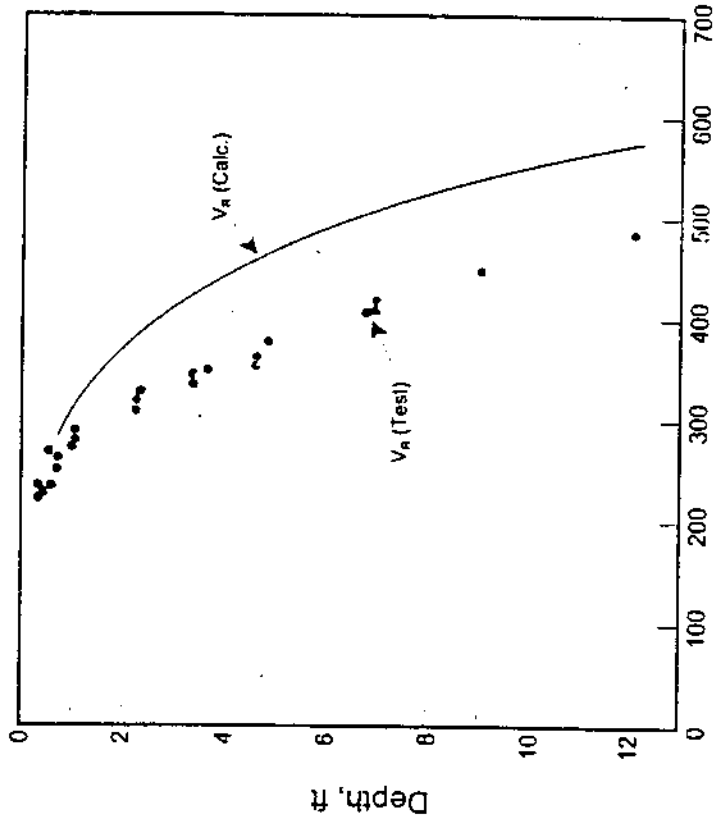


Figure 5.48. Variation of Rayleigh wave velocity with depth-Eglin Field Site (after Fry, 1963)

## Table 5.5: Particle Velocities vs. penetration depth and vertical effective stress

| Geophone No | Geophone Depth (ft) | Unit Weight (gm/cm3) | Effective Unit Weight (lb/ft3) | Effective Vertical Stress (lb/ft2) | Effective Vertical Stress (lb/in2) | Approx. Maximum Particle Velocity (in/sec) | Approx. Maximum Particle Velocity (ft/sec) | Penetration Depth |
|---|---|---|---|---|---|---|---|---|
| 1 | 5 | 1.51 | 94.224 | 471.12 | 3.27 | 0.189 | 0.023 | 0 to 5 ft |
| 2 | 10 | 1.686 | 42.8064 | 428.064 | 2.97 | 0.196 | 0.025 | |
| 3 | 15 | 1.578 | 36.0672 | 541.008 | 3.76 | 0.180 | 0.021 | |
| 4 | 20 | 1.547 | 34.1328 | 682.656 | 4.74 | 0.131 | 0.028 | |
| 5 | 25 | 1.526 | 32.8224 | 820.56 | 5.70 | 0.100 | 0.008 | |
| 6 | 40 | 1.615 | 38.376 | 1535.04 | 10.66 | 0.021 | 0.008 | |
| 1 | 5 | 1.51 | 94.224 | 471.12 | 3.27 | 0.23 | 0.025 | 5 to 10 ft |
| 2 | 10 | 1.686 | 42.8064 | 428.064 | 2.97 | 0.22 | 0.015 | |
| 3 | 15 | 1.578 | 36.0672 | 541.008 | 3.76 | 0.19 | 0.021 | |
| 4 | 20 | 1.547 | 34.1328 | 682.656 | 4.74 | 0.17 | 0.014 | |
| 5 | 25 | 1.526 | 32.8224 | 820.56 | 5.70 | 0.13 | 0.012 | |
| 6 | 40 | 1.615 | 38.376 | 1535.04 | 10.66 | 0.06 | 0.008 | |
| 1 | 5 | 1.51 | 94.224 | 471.12 | 3.27 | 0.24 | 0.023 | 10 to 15 ft |
| 2 | 10 | 1.686 | 42.8064 | 428.064 | 2.97 | 0.25 | 0.013 | |
| 3 | 15 | 1.578 | 36.0672 | 541.008 | 3.76 | 0.23 | 0.013 | |
| 4 | 20 | 1.547 | 34.1328 | 682.656 | 4.74 | 0.18 | 0.017 | |
| 5 | 25 | 1.526 | 32.8224 | 820.56 | 5.70 | 0.15 | 0.019 | |
| 6 | 40 | 1.615 | 38.376 | 1535.04 | 10.66 | 0.09 | 0.008 | |
| 1 | 5 | 1.51 | 94.224 | 471.12 | 3.27 | 0.25 | 0.025 | 15 to 20 |
| 2 | 10 | 1.686 | 42.8064 | 428.064 | 2.97 | 0.27 | 0.018 | |
| 3 | 15 | 1.578 | 36.0672 | 541.008 | 3.76 | 0.23 | 0.010 | |
| 4 | 20 | 1.547 | 34.1328 | 682.656 | 4.74 | 0.21 | 0.025 | |
| 5 | 25 | 1.526 | 32.8224 | 820.56 | 5.70 | 0.18 | 0.017 | |
| 6 | 40 | 1.615 | 38.376 | 1535.04 | 10.66 | 0.13 | 0.009 | |
| 1 | 5 | 1.51 | 94.224 | 471.12 | 3.27 | 0.29 | 0.025 | 20 to 30 |
| 2 | 10 | 1.686 | 42.8064 | 428.064 | 2.97 | 0.30 | 0.021 | |
| 3 | 15 | 1.578 | 36.0672 | 541.008 | 3.76 | 0.28 | 0.023 | |
| 4 | 20 | 1.547 | 34.1328 | 682.656 | 4.74 | 0.25 | 0.017 | |
| 5 | 25 | 1.526 | 32.8224 | 820.56 | 5.70 | 0.24 | 0.019 | |
| 6 | 40 | 1.615 | 38.376 | 1535.04 | 10.66 | 0.22 | 0.011 | |
| 1 | 5 | 1.51 | 94.224 | 471.12 | 3.27 | 0.35 | 0.025 | 30 to 40 |
| 2 | 10 | 1.686 | 42.8064 | 428.064 | 2.97 | 0.36 | 0.023 | |
| 3 | 15 | 1.578 | 36.0672 | 541.008 | 3.76 | 0.35 | 0.021 | |
| 4 | 20 | 1.547 | 34.1328 | 682.656 | 4.74 | 0.34 | 0.019 | |
| 5 | 25 | 1.526 | 32.8224 | 820.56 | 5.70 | 0.34 | 0.018 | |
| 6 | 40 | 1.615 | 38.376 | 1535.04 | 10.66 | 0.34 | 0.010 | |
| 1 | 5 | 1.51 | 94.224 | 471.12 | 3.27 | 0.65 | 0.010 | Extraction |
| 2 | 10 | 1.686 | 42.8064 | 428.064 | 2.97 | 0.48 | 0.010 | |
| 3 | 15 | 1.578 | 36.0672 | 541.008 | 3.76 | 0.35 | 0.010 | |
| 4 | 20 | 1.547 | 34.1328 | 682.656 | 4.74 | 0.7 | 0.010 | |
| 5 | 25 | 1.526 | 32.8224 | 820.56 | 5.70 | 0.7 | 0.010 | |
| 6 | 40 | 1.615 | 38.376 | 1535.04 | 10.66 | 0.6 | 0.010 | |
| 1 | 5 | 1.51 | 94.224 | 471.12 | 3.27 | 0.25 | 0.010 | 2nd Shaft |
| 6 | 40 | 1.615 | 38.376 | 1535.04 | 10.66 | 0.12 | 0.010 | |
| 1 | 5 | 1.51 | 94.224 | 471.12 | 3.27 | 0.32 | 0.010 | |
| 6 | 40 | 1.615 | 38.376 | 1535.04 | 10.66 | 0.15 | 0.010 | |
| 1 | 5 | 1.51 | 94.224 | 471.12 | 3.27 | 0.3 | 0.010 | |
| 6 | 40 | 1.615 | 38.376 | 1535.04 | 10.66 | 0.35 | 0.010 | |
| 1 | 5 | 1.51 | 94.224 | 471.12 | 3.27 | 0.32 | 0.010 | |
| 6 | 40 | 1.615 | 38.376 | 1535.04 | 10.66 | 0.6 | 0.010 | |

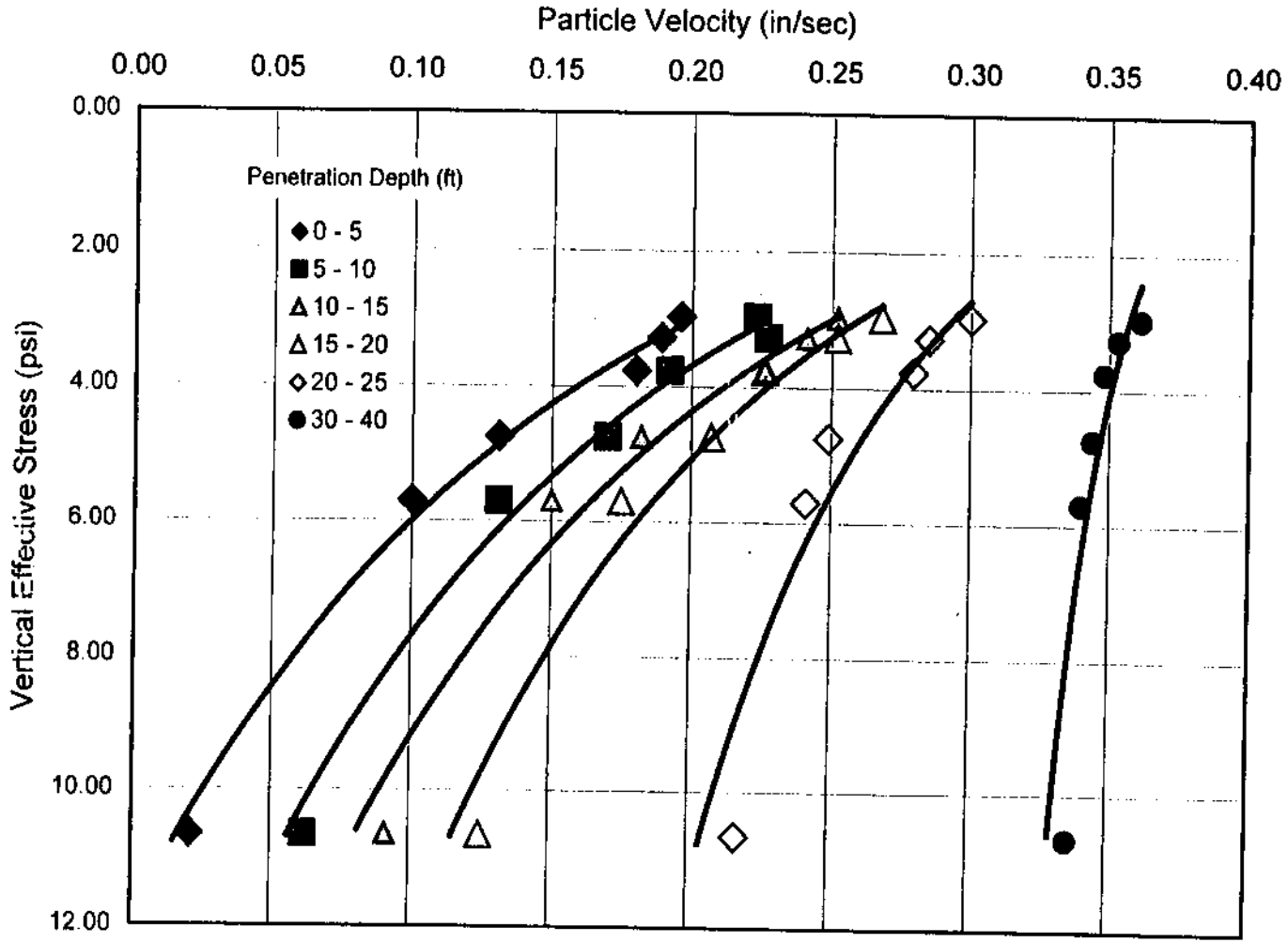


Figure 5.49: Particle velocity vs. Penetration depth of the steel casing

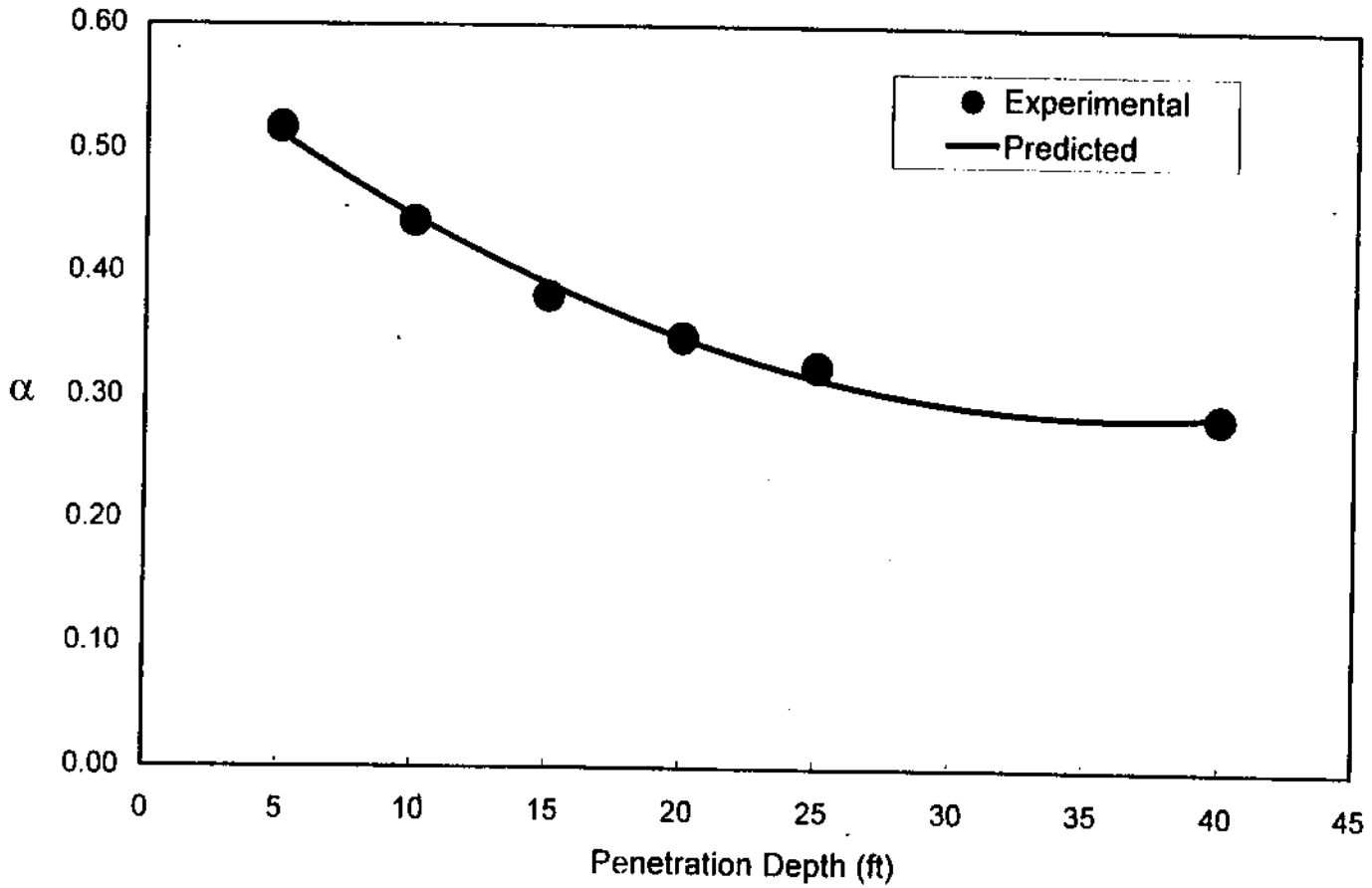


Figure 5.50: Factor α vs. Penetration Depth of the Drilled Shaft Casing

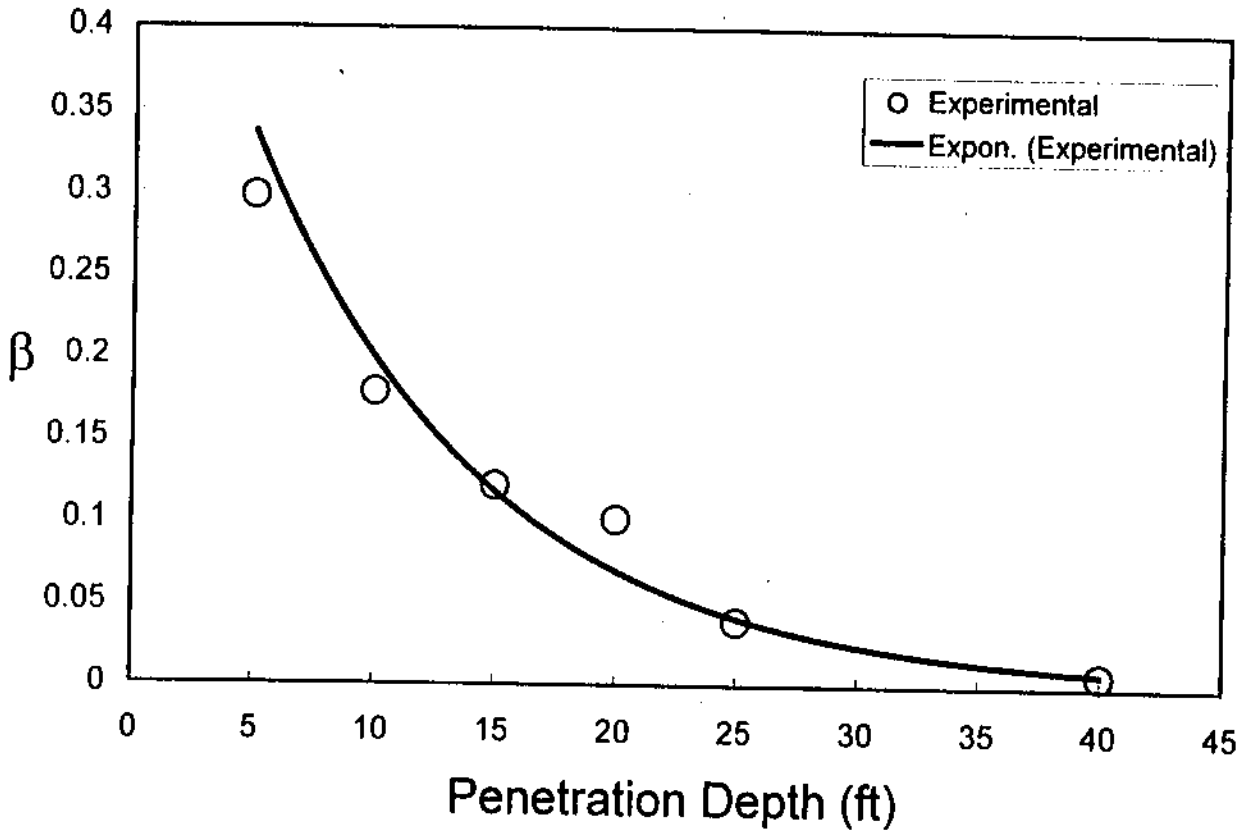


Figure 5.51: Factor β vs. Penetration Depth of the Drilled Shaft Casing

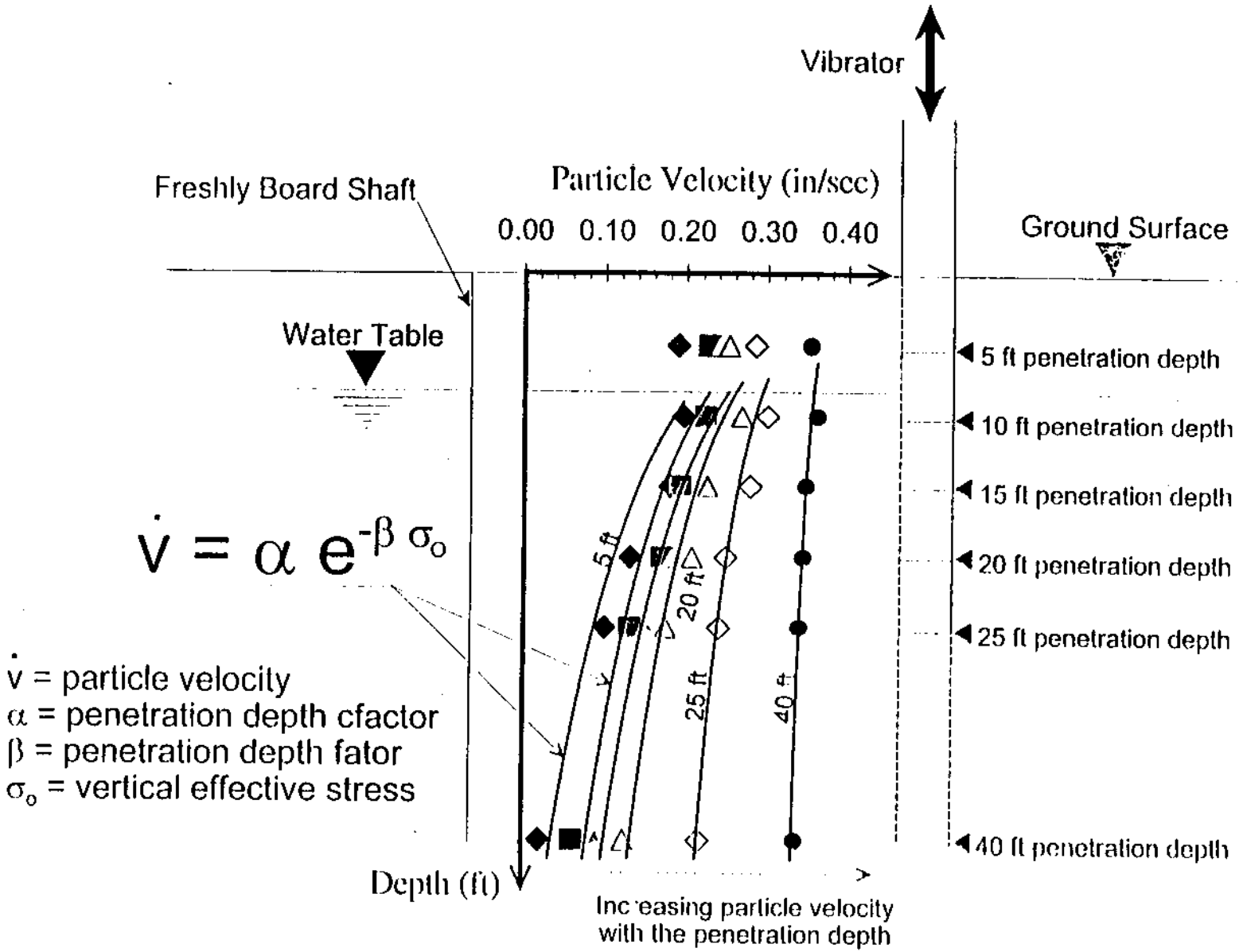


Figure 5.52 Change in the particle velocity with penetration depth of a drilled shaft casing.

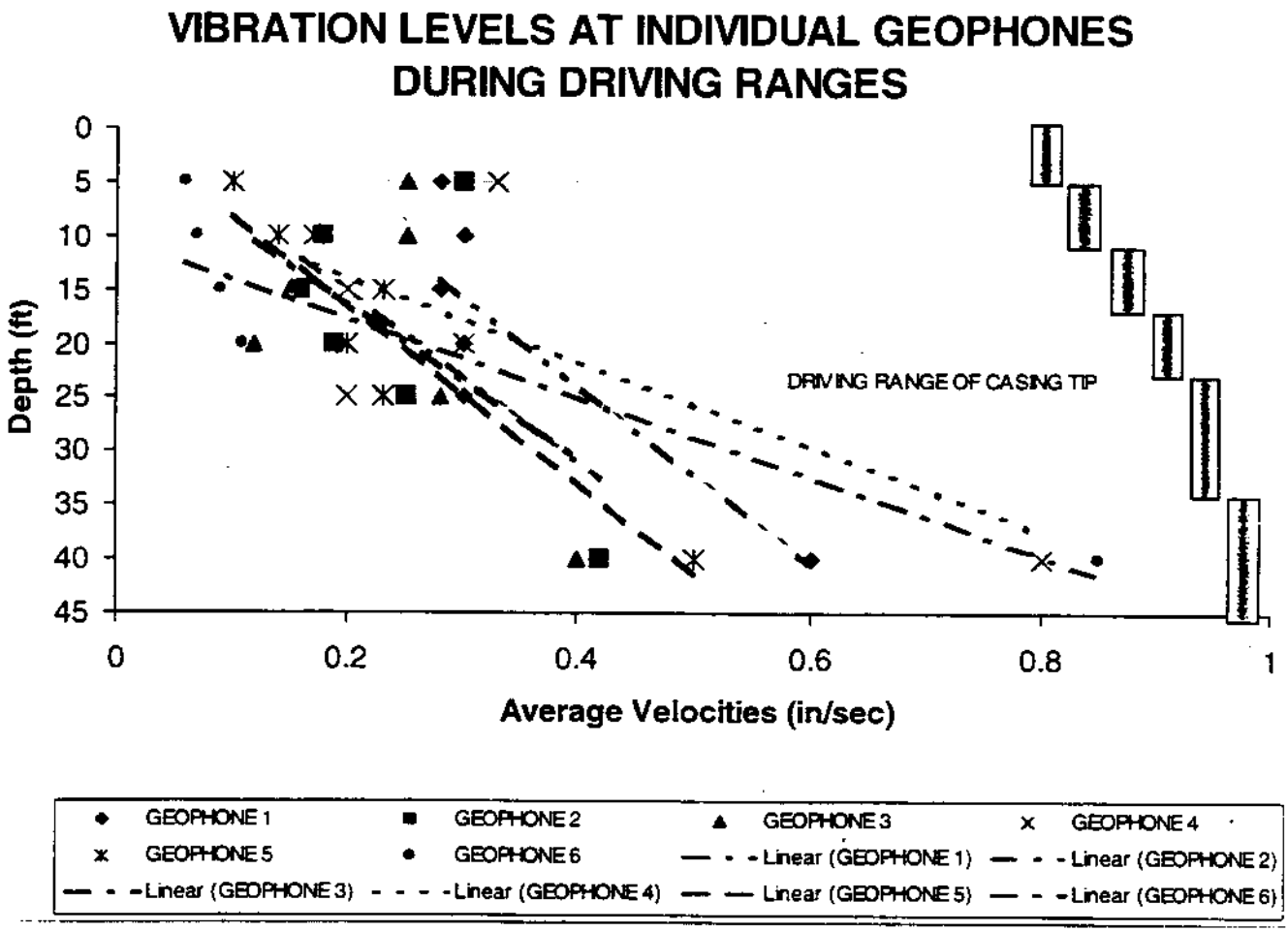


Fig 5.53. Vibration levels at individual geophones during driving ranges

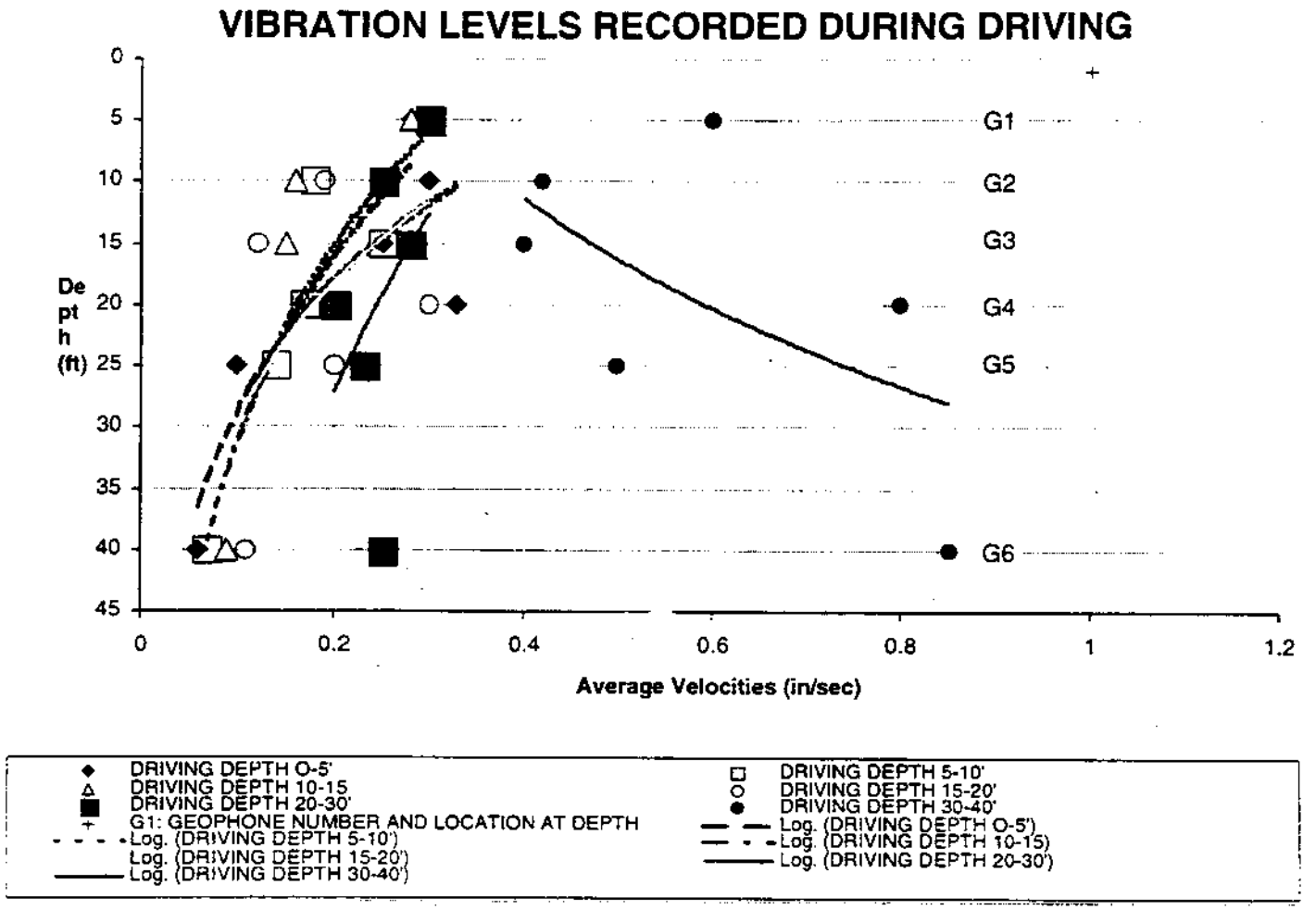


Fig 5.54. Average recorded vibration for different depths of driving

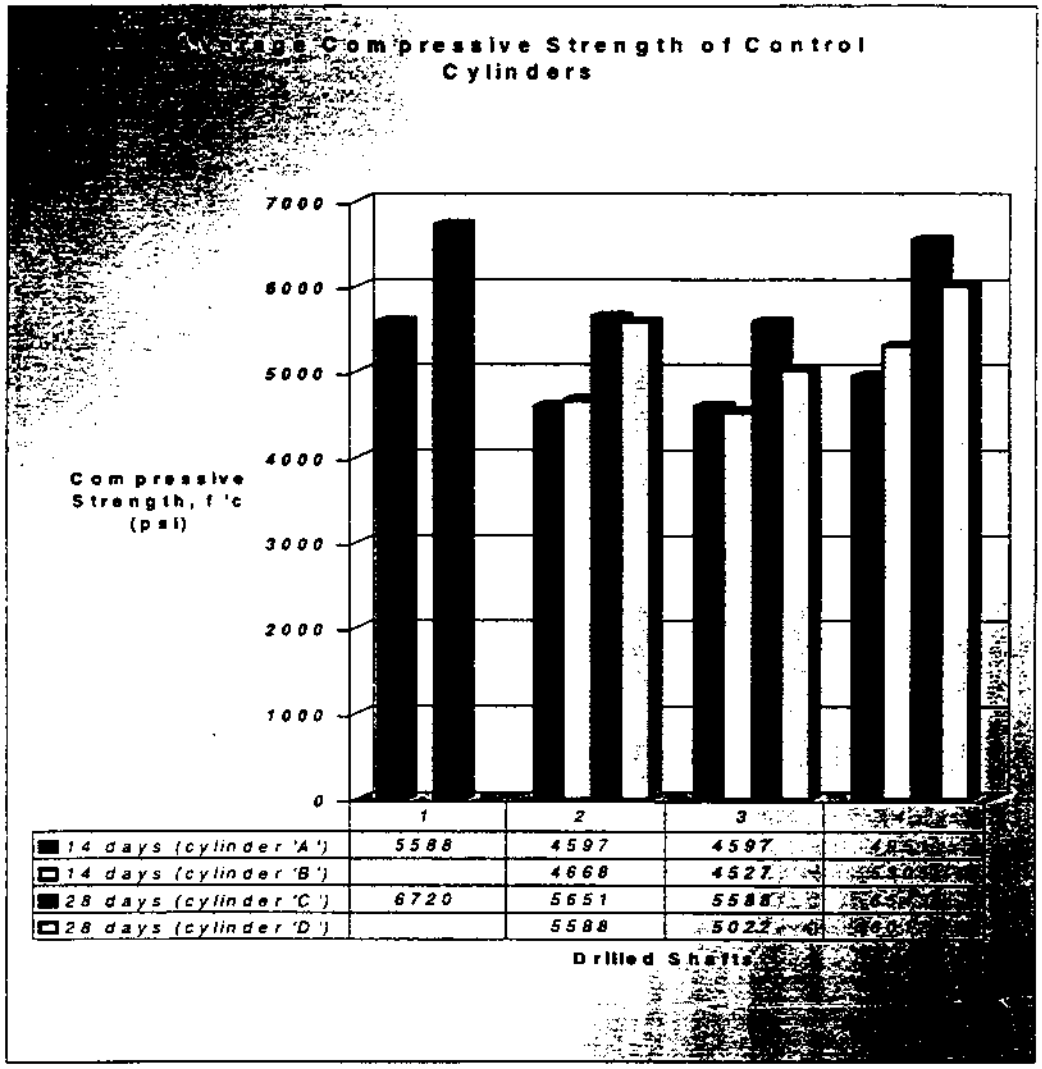


Figure 5.55. Compressive strength of control samples.

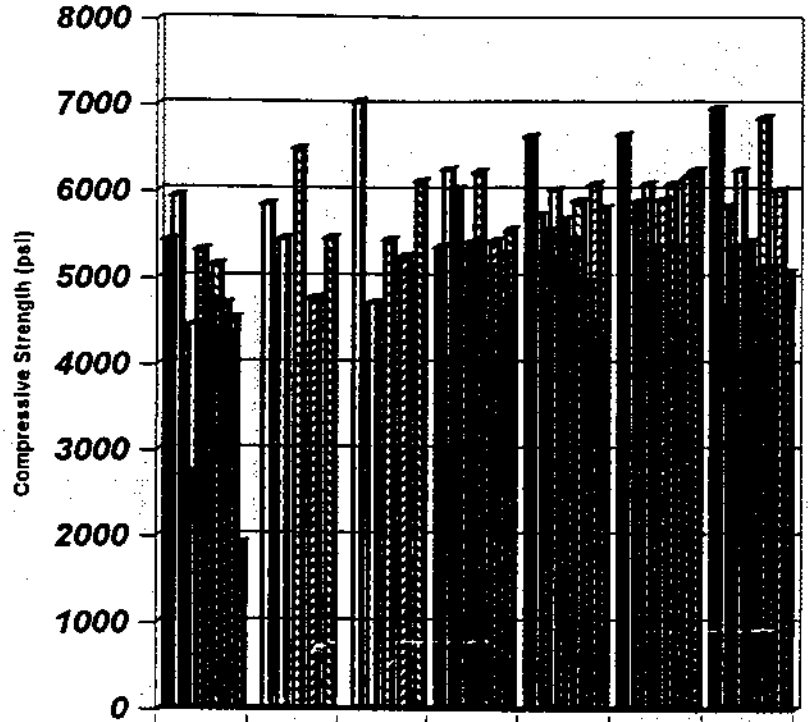


| | .25' | 4.5' | 5.0' | 10.0' | 10.5' | 13.5' | 14.5' |
|---|---|---|---|---|---|---|---|
| DS 1-2 | 5430 | 0 | 0 | 5350 | 6630 | 6650 | 6960 |
| DS 1-3 | 5940 | 5850 | 7040 | 6250 | 5720 | 5650 | 5820 |
| DS 2-2 | 2720 | 0 | 0 | 6030 | 5540 | 5880 | 5350 |
| DS 2-3 | 4450 | 5450 | 4710 | 5300 | 6010 | 6080 | 6240 |
| DS 3-2 | 5320 | 0 | 0 | 5410 | 5670 | 5350 | 5420 |
| DS 3-3 | 4730 | 6500 | 5440 | 6220 | 5440 | 5900 | 5088 |
| DS 4-2 | 5160 | 0 | 0 | 5130 | 5890 | 6080 | 6850 |
| DS 4-3 | 4700 | 4770 | 5250 | 5420 | 4960 | 5360 | 5120 |
| DS 5-2 | 4536 | 0 | 0 | 5269 | 6078 | 6159 | 6023 |
| DS 5-3 | 1910 | 5460 | 6114 | 5545 | 5806 | 6240 | 5069 |

Figure 5.56. Compression strength of cored samples.

words, the total amount of vibration exposure is greatest at ground elevation, with the exception of the final driving stage, where the trend indicates that the particles velocities at a point near the final destination of the driven casing is greatest. One more observation that can be made from **Figure 5.54** is that as the steel casing penetrates to greater depth, the percent difference of the readings between the geophones decreases. Notably, the loose sandy soils in which this test was conducted adversely affect the transmission of vibrations.

The peak particle velocities (PPV) recorded are within the ranges expected based upon review of similar data from other projects. However, the maximum PPV values are rather small, due to the nature of the soil. Therefore, it would be reasonable to suggest that the effects of these vibrations would not pose any damage to existing structures.

Laboratory tests on representative concrete samples were performed under controlled environmental and boundary conditions. Samples were prepared from the same mix design, and subjected to predetermined vibration amplitudes at certain frequency contents. The delay time of induced vibration were equal for all the sets. The main advantage of testing concrete samples under such controlled conditions was the reproducibility of the test procedure for a large number of samples. Although some researchers do not consider it as a weakness, the lack of reproducing the actual waveforms produced in the field restricts the material behavior obtained from laboratory testing as a function of the controlled loading conditions. It should be noted herein that the mode of dynamic loading in the laboratory was predominantly compression, while the actual waves propagated in the ground during drilled shaft construction were mainly shear waves. The effect of the mode of vibration was not one of the parameters that were covered in this study. The reason was the difficulty to separate the modes of vibrations in the field. The use of the triaxial geophones indicated that vibrations in the vertical, longitudinal, and transverse directions were recorded at different locations in the ground and in the freshly placed concrete. However, the vertical (shear) mode was, for most of the measurements, higher than the other two modes. At some locations when the steel casing was not fully penetrating the ground, the longitudinal and the transverse modes exhibited larger particle velocities than the vertical mode. An explanation for such behavior was that the interaction between the vibrator and the casing was not perfectly eccentric. Any small eccentricity at the grip between the vibrator and the casing can amplify the transverse or the longitudinal modes causing increased particle motions in these directions. Although too small, soil displacement during casing penetration would produce compression mode of loading in the longitudinal and the transverse directions. To control the predominancy of the vertical vibrations (shear) during casing vibration and at any

penetration depth is unrealistic. Therefore, one should expect that during casing higher particle velocities are recorded in directions other than the vertical direction.

# CONCLUSIONS

## I) Laboratory Test Results :

Construction vibrations that produce particle velocities less than 8 in./sec would not have any effect on the compressive strength or compression modulus of the concrete aged between the time of placement to the first 24 hours.

1) All concrete samples, subjected to vibration amplitudes of 8in./sec, after three to four hours from placement, showed noticeable surface voids on the concrete surface. Traces of microcracks were also noticed on some samples, subjected to large vibration amplitudes, i.e. 8.3 in./sec. after three to four hours from placement. The presence of the microcracks was not as common as the surface voids in samples of this category. Therefore, a final conclusion on the development of microcracking at this age of concrete is not definitive. Further investigations, using a Scanning Electron Microscope(SEM), may be needed to clarify such occurrences. No voids were induced inside the samples.

## II) Field Test Results:

1. The testing conducted to establish the integrity of the shafts included Pile Integrity Testing (PIT), Crosshole Sonic Logging (CSL),Gamma-Gamma, Neutron-Neutron, and coring to obtain an actual indication of the compressive strength. The geophysical methods used, when combined, provided a subsurface profile of the shaft.
2. Crosshole Sonic Logging (CSL) tests showed continuity across the cross-sectional areas of the shafts with the exception of the 2-hour, 36-inch shaft. However, the PVC access tubes were stressed during the passing of a hurricane, which was the most likely reason for the deviation from the other shafts.

3. Pile Integrity Testing (PIT) showed a definite reflection of the transmitted wave from the shaft tip, indicating no structural damage in the shaft length.

4 Gamma-Gamma logging of the drilled shafts showed lower density profiles for the upper parts relative to the bottom ones.

5 Neutron-Neutron logging showed that the porosity within the shafts is relatively unchanged by the vibration.

6 The geophysical data obtained can be compared in relative terms to conclude the following: the upper 1/3 or 5 feet of the shafts showed some relatively reduced concrete properties. The relative weakness of the upper shaft sections was further evidenced by the compressive strengths of the cored concrete samples, Fig 5.56. This can be attributed only to the segregation of the aggregate during vertical pouring of concrete, since the field velocities of 2.5 in./sec are much below the threshold value of 8.3 in./sec that can affect the strength.

7 The geophysical data only served to show relative performance within each individual shaft, and no comparisons were established with the other shafts, as no trend could be established in the correlation of the values between the compressive strength and the geophysical data. Nevertheless, the data shows that shaft integrity was not adversely affected, and though within each shaft relative weakness existed in the upper sections, it was not an indication of poor concrete.

8 These findings however have limitations. Primarily, the data is true only for the subsurface conditions tested, i.e. loose soils. The loose soil condition aided to a great extent in the attenuation of the vibrations induced, and consequently diminished the transfer of the higher peak velocity across the interface between the stratum and shaft.

9 Peak particle velocities activated during travel of the stress waves, (i.e. 2.5 in./sec) were well below the threshold values of 8in./sec known to cause damage in concrete structures.

III) Comprehensive Evaluation:

The concept of particle velocity is used to control construction vibrations for almost all types of projects in civil engineering. Although the concept is helpful as a quality control factor during construction, particle velocities should not be used alone to assess the impact of the construction vibration on the surrounding structures. For a meaningful assessment, particle velocities should be translated into strain amplitudes. A value of 8 in/sec particle velocity would produce different strain amplitudes in different materials and in different structures. Even for the same construction material, but with different moduli values, the same particle velocity would result in different strain amplitudes and hence different effects. For example, "green concrete" would have lower compression and shear moduli as compared to aged concrete. Therefore, the effect of PPV on the same material at different time levels may vary since the induced strain amplitudes are different.

It is important to conduct a preliminary assessment of the effect of vibration before construction of deep foundations. Such an assessment requires the following:

a) **Determining the physical and mechanical properties of the in-situ soil layers**

b) **Predicting generated waveforms**

c) **Assessing the PPV based on the generated waveforms**

d) **Determining the shear or compression wave velocity of the in-situ layers.**

e) **Field testing for Part (c ).**

f) **Determining the damping ratios of the soil layers**

g) **Determining the strain amplitudes at critical locations.**

**h) Predicting the damage due to the obtained strain amplitudes.**

The concept of the PPV is very helpful to estimate the impact of construction vibration. However, the PPV concept is a transposition from mining engineering, where the applications are limited to certain practices. In Civil Engineering applications, the sources of vibrations are numerous. The types of vibrations range from natural to man-made vibrations. Also, the waveforms range from deterministic to non-deterministic.

# REFERENCES


Alemo, J., and Grandas, J.A., (1989) "Optimal vibreringsinstats for anlaggningsbetong," (optimum amount of concrete vibration in dam construction), Vattenfall, Stockholm,

Forssblad, Lars and Sallstorm, Stig, "Concrete Vibration – What's Adequate?," Concrete International: Design & Construction, September 1, 1995, V.17, No. 9, pp. 42-48

Hardin, B.O., and Black, W.L., (1968), "Vibration Modulus of Normally Consolidated Clays," Proc. ASCE, JSMFD, Vol.92, No. SM2, pp. 27-42

Hardin, B.O., and Drnevich, V.P., (1972), "Shear Modulus and Damping in Soils: Design Equations and Curves," Proc. ASCE, JSMFD, Vol.98, SM7, pp. 667-692.

Hardin, B.O., and Drnevich, V.P., (1970), "Shear Modulus and Damping in Soils: Design Equations and Curves," Journal of the Soil Mechanics and Foundations Division, ASCE, Vol.98, No. 5M7.

Hardin, B.O., and Richart, F.E., Jr. (1963), "Elastic Wave Velocities in Granular Soils," Journal of the Soil Mechanics and Foundations Division, ASCE, Vol. 89, No.SM1, Feb. 1963, pp. 33-65.

Howes, E.V., (1979) "Effects of Blasting Vibrations on Curing Concrete," Proceedings of the 20th United States Symposium on Rock Mechanics, University of Texas, Austin, TX, pp. 455-458.

Hulshizer, A.J., Acceptable Shock and Vibration Limits for Freshly Placed and Maturing Concrete, Rayheon Engineers & Constructors, Inc., Philadelphia, Pennsylvania.

Hulshizer, A.J., and A.J. Desai, "Shack Vibration Effects on Freshly Placed Concrete," Journal of Construction Engineering Management, ASCE, Vol. 110, NO. 2, Paper 18892 (June 1984).

Hulshizer, A.J., Acceptable Shock and Vibration Limits for Freshly Placed and Maturing Concrete, ACI Materials Journal, November- December 1996, No. 93-M59, pp. 524-533.

Iwasaki, T., Tatsuoka, F. and Takagi, Y. (1976), " Dynamic Shear Deformation Properties of Sand for Wide Strain Range," Report of Civil Engineering Institute, No. 1085, Ministry of Construction, Tokyo, Japan.

Kokusho, T. (1980), "Cyclic Triaxial Test of Dynamic Soil Properties for Wide Strain Range," Soils and Foundations, Japanese Society of Soil Mechanics and Foundation Engineering, Vol. 20, No. 2, June.

Krizek, R.J., Mclean, F.G. and Giger, M.W.(1974), "Effect of particle characteristics on wave velocity," Journal of the Geotechnical Engineering Division, American Society of Civil Engineers, Vol. 100, No. GT1.

L'Hermite, R., and Tournon, G., "Vibretion of Fresh Concrete (La vibration du beton frain)," *Annales*, Institut Technique du Batiment et des Travaux Publics (Paris), 1948.

Marshall, L.S., (1981), "Load, Deformation and Strength Behavior of Soils Under Dynamic Loadings," Proceedings International Conference on Recent Advances in Geotechnical Earthquake Engineering and Soil Dynamics, University of Missouri-Rolla, St. Louis, pp. 873-895

Massarsch, K. R., and Westerberg, E., "Frequency - Variable Vibrators and Their Application to Foundation Engineering," Deep Foundation Institute 20th Annual Member's Meeting and Seminar, Charleston, South Carolina October, 1995.

Meissner, H.S., "Compacting Concrete by Vibration," ACI JOURNAL, *Proceedings* V. 34, No. 10, June 1953, pp 885-892

Olsen, Mikael, P. J. "Energy Requirements for Consolidation of Concrete During Internal Vibration," *Consolidation of Concrete*, SP-96, American Concrete Institute, Detroit, 1987, pp. 179-196.

Oriard, L.L., and Coulson, J.H. (1980), "TVA Blast Vibraton Criteria for Mass Concrete," Minimizing Detrimental Construction Vibrations, ASCE Preprint 80-175, ASCE, New York, pp. 101-123.

Prakash, S and Puri V. K. (1981), "Dynamic Properties of Soils from In-Situ Tests," Journal of the Geotechnical Engineering Division, American Society of Civil Engineers, Vol. 107, No. GT7, July

Ohta, Y. and Goto, N. (1976), "Estimation of S-wave Velocity in Terms of Characteristic Indices of Soil," Butsuri-Tanko, Vol. 29, No. 4, 1976, pp. 34-41 (in Japanese).

Richart, F.E., Jr., J.R. Hall, Jr., And R.D. Woods, Vibrations of Soils and Foundations, Prentice-Hall, Englewood Cliffs, N.J. (1970), 412 pp.

Richart, F. E., Jr., Hall, J. R., Jr. and Lysmer, J. (1962), "Study of the Propagation and Dissipation of 'Elastic' Wave Energy in Granular Soils," University of Florida Report to Waterways Experiment Station, Corps of Engineers, U.S. Army, Contract DA-22-070-eng-314, Sept. 1962.

Seed, H. Bolton and Idriss, I. M. (1970), "Soil Moduli and Damping Factors for Dynamic Response Analyses," Report No. EERC 70-10, Earthquake Engineering Research Center, University of California, Berkeley, California.

Shibata, T. and Soelarno, D. S. (1975), "Stress-Strain Characteristics of Sands Under Cyclic Loading," Proceedings, Japanese Society of Civil Engineers, No. 239, July.

# PART II

## EFFECTS OF SOUND INDUCED DURING THE INSTALLATION OF PILES

# PILE DRIVING NOISE MITIGATION THROUGH USE OF AN ACOUSTIC CURTAIN

## 1.1 Background

During the installation of driven piles, the noise level becomes a critical parameter due to the low threshold of human perception. In particular, construction noises from this type of foundation installation becomes a concern when the site is near office buildings or residential areas. Common pile hammers often exceed the noise limits set by state transportation projects, thus requiring an alternate method of installation to be sought. This project focused on the use of an acoustic curtain constructed of a combination of absorptive and reflective materials to provide a complete enclosure of the source to mitigate the propagation of the inherent noise.

## 1.2 Laboratory Testing

### 1.2.1 Test Setup

A reduced scale experiment was conducted to determine the Sound Pressure Level (SPL) reduction through the use of an acoustic curtain in a laboratory chamber, which represented open field conditions with no reverberation. An omni-directional noise to represent the hammering of a shaft was provided by dropping a hammer onto a steel tube of rectangular cross-section, which provided a sharp single point source. The noise was measured as a SPL in dB (ref. $2x10^{-5}$ $N/m^2$) and was taken as an average of 20 hammer blows. The test setup is shown below and the results indicate a SPL reduction of about 16.5 dB.

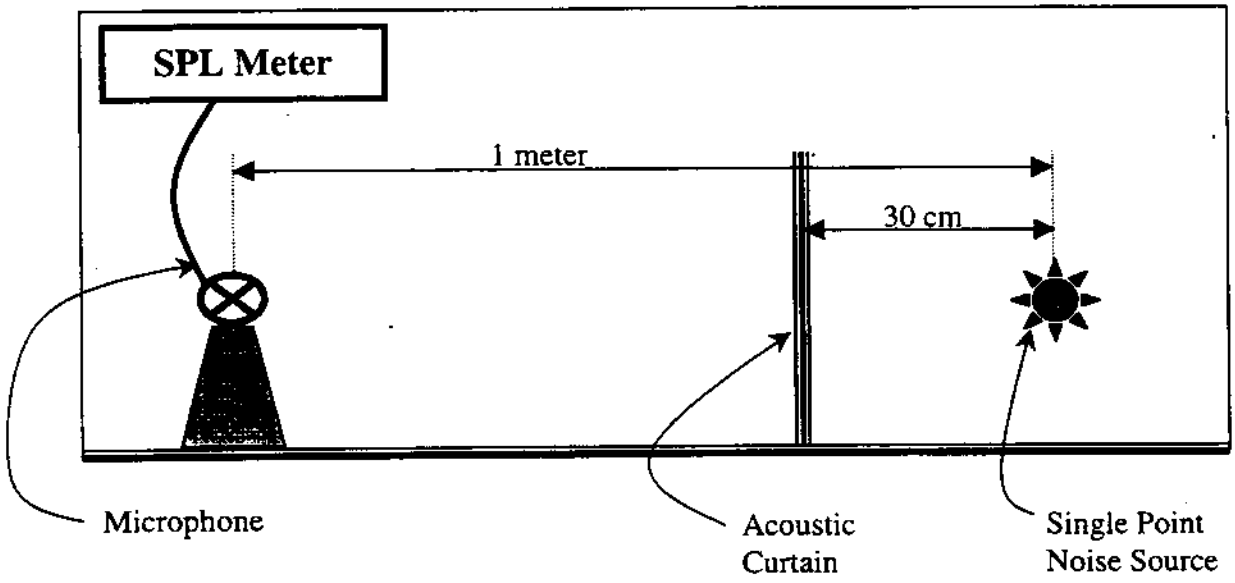


**Figure 1. Enclosed chamber with no reverberation**

### 1.2.2 Test Results

- Without curtain - Average SPL = **118.1 dB**
- With curtain - Average SPL = **101.6 dB**
- Noise reduction obtained with curtain = ***16.5 dB***

These results indicate that the acoustic curtain provides significant reduction in sound pressure levels when placed around a single-point, Omni-directional noise source. In a practical sense, a 16.5 dB reduction is almost equivalent to heavy construction noises being reduced down to the sound of average street traffic (a 20 dB reduction).

## 1.3 Field Testing

A full-scale field-test was conducted to determine the actual sound pressure level (SPL) reduction through the use of an acoustic curtain in a true on-site application. An industrial diesel hammer was used to drive 12 inch square concrete piles 20 ft in length to accurately replicate true construction field practice. The noise was measured as a sound pressure level at various heights and distances from the source and an octave band analysis was performed at a specified location to identify the pertinent frequencies. When compared to the lab results, higher SPL reductions (up to 20 dB) were achieved in the field. A detailed description of the companies involved and the experimental test setup is included on the following pages.

### 1.3.1 Field Test Setup

Commencement of the field test took place on the north of the FAU Boca Raton campus in the field just east of Parking Lot #5 (see Figure 2). The site was chosen to be the same as for the first phase of the project (drilled shafts) because the required permits were still valid through FAU Facilities Planning and the soil type was already known. Standard Penetration Tests (SPT) performed prior to the drilled shaft phase indicated sandy soil conditions down to depths greater than would be reached by the 20' pile. Locally known as "sugar sand," the soil provided ideal pile driving conditions and easy pile extraction. It was also noted that the water table was no more than 5' below the surface and no bedrock or any other underground obstruction was encountered.

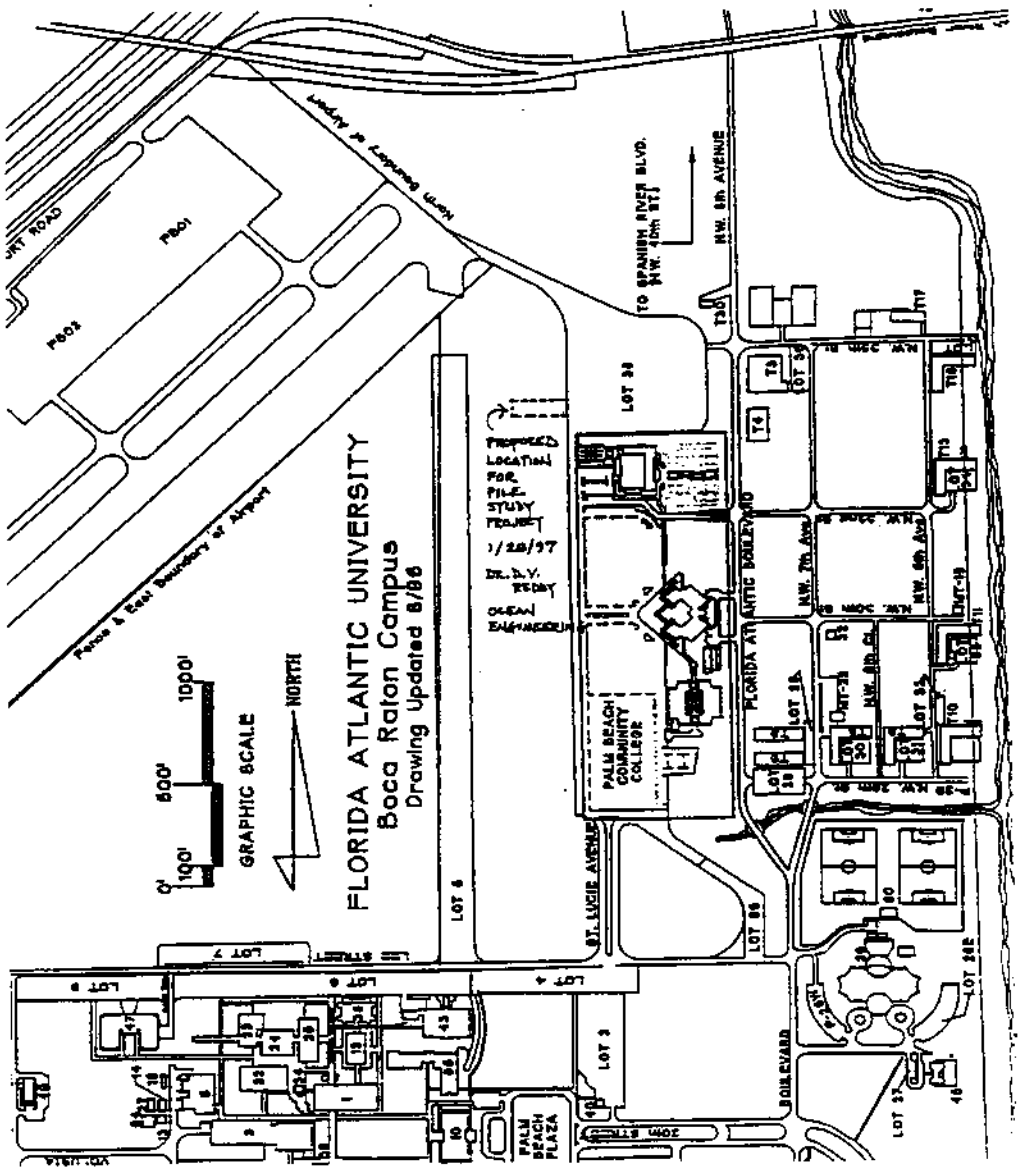


**Figure 2. Site selection**

The noise measurements were taken at seven distinct recording stations as shown in Figure 3. Three stations provided sound pressure levels at 10' above the ground for radial distances of 50, 100, and 300 ft. Three separate stations were also setup to take measurements at the same radial distances, but only 5' off the ground. As per the recommendation of Dr. Kenneth Campbell, FDOT Noise Specialist, the 5' and 10' measurement poles were set in different radial directions 45° apart to ensure that the meters would measure the true spread of the noise. The seventh station was located at a radial distance of 100 ft and provided a real-time octave band analysis to determine all the inherent sound frequencies at 5' above grade.

In total, four piles were driven and extracted, and noise levels were measured for two piles driven in the standard manner, and for two driven with the acoustic curtain in place. Figure 3 shows a plan view of the field test setup depicting the location of the noise source, the acoustic curtain, and the seven measuring stations.

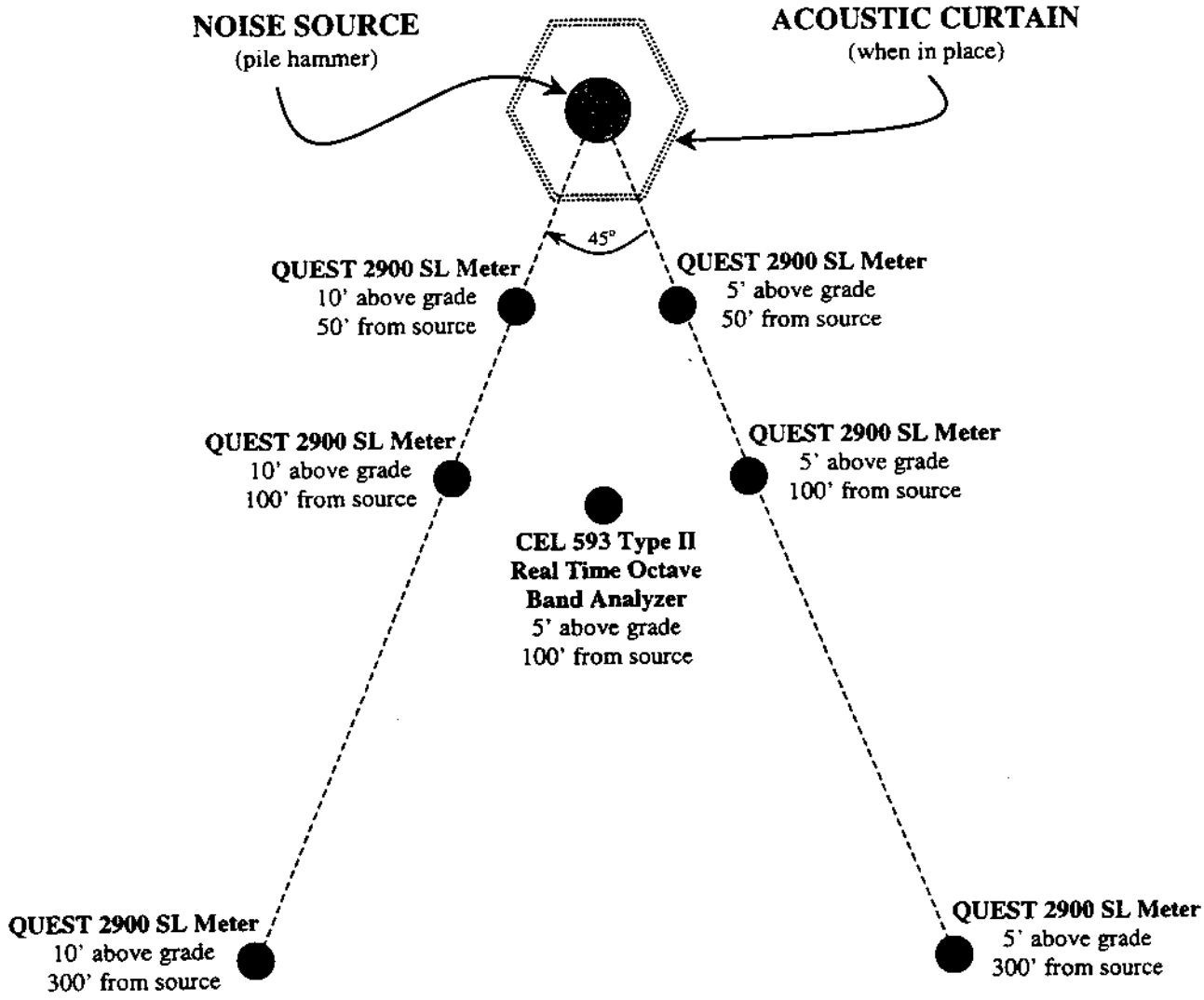


**Figure 3. Field test setup**

### 1.3.2 Pile Driving

Curry Industries, a specialist in pile driving and precast concrete, provided all material, labor and equipment necessary to install and extract the concrete piles used in the full-scale field-test. The piles were 12"x12"x20' commercial grade prestressed concrete with a 5000 psi 28-day strength, and were driven with a standard Delmag D-12 diesel pile hammer. In total, the piles were driven and extracted four times, twice in the

standard manner and twice with the acoustic curtain enclosing the hammer. Upon completion of the project, Curry Industries extracted the piles and removed all the equipment, leaving the site in the natural state it was prior to commencement. Figure 4 shows the piles, installation, and extraction.

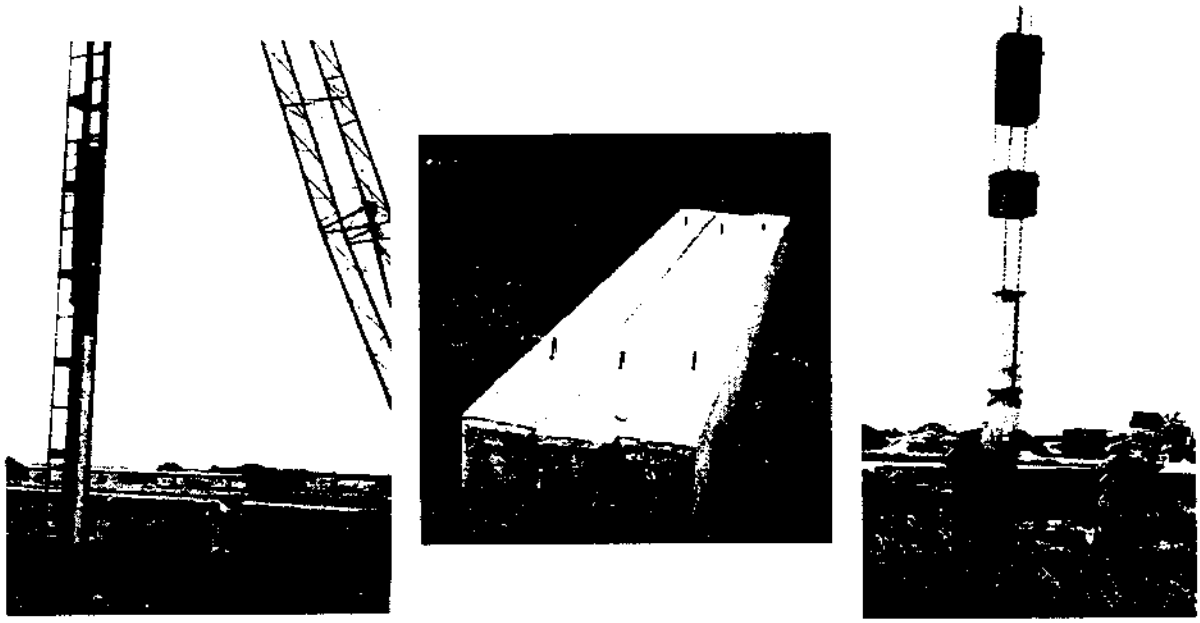

(a) (b) (c)

**Figure 4. (a) Pile driving, (b) 20 ft concrete piles, and (c) pile extraction**

### 1.3.3 Noise Measurements

A pile driver noise impact and insertion loss analysis was conducted by LAW Engineering & Environmental Services to determine the dB reduction achieved through the use of an acoustic curtain. Six Quest 2900 Type II Sound Level Meters were used to measure the sound pressure levels (in decibels) in conjunction with a CEL 593 Type II Real Time Octave Band Analyzer to identify the frequency ranges omitted by the source and mitigated by the curtain. In total, noise measurements were taken at 7 stations: 3 at 10 ft above the ground for radial distances of 50 ft, 100 ft, and 300 ft from the source, 3 at 5 ft above the ground for the same radial distances, and the last (octave band analysis) at 5 ft above ground 100 ft from the source. Pictures of the sound pressure level measuring devices and setup are shown below in Figure 5. ( The Details of report is presented in Appendix-1).

(a) (b) (c)

**Figure 5. (a) Setting up for noise measurements at 50 ft, (b) Quest 2900 SL meters, (c) 10 ft measurement pole with meter**

### 1.3.4 Acoustic Curtain

The acoustic curtain used in this study was provided by Environmental Noise Control, a Division of Dynamic Services, Inc. and was made of 400 square feet of Acoustical STC-18 High NRC Blanket, which is a combination of absorptive and reflective materials designed for industrial applications. It is made from a (400 $ft^2$, 1 $lb/ft^2$) . Reinforced poly-vinyl chloride outs shell for added mass with a specially developed inner lining of 2 in. thick fiber glass acoustical insulation(1.5 $lb/ft^2$). A clear vinyl strip was included as a window for the hammer operator to view the pile's progress. The blanket was connected to the specially designed frame shown in Figure 6, which was then attached to the crane with steel leads and slowly erected into place.

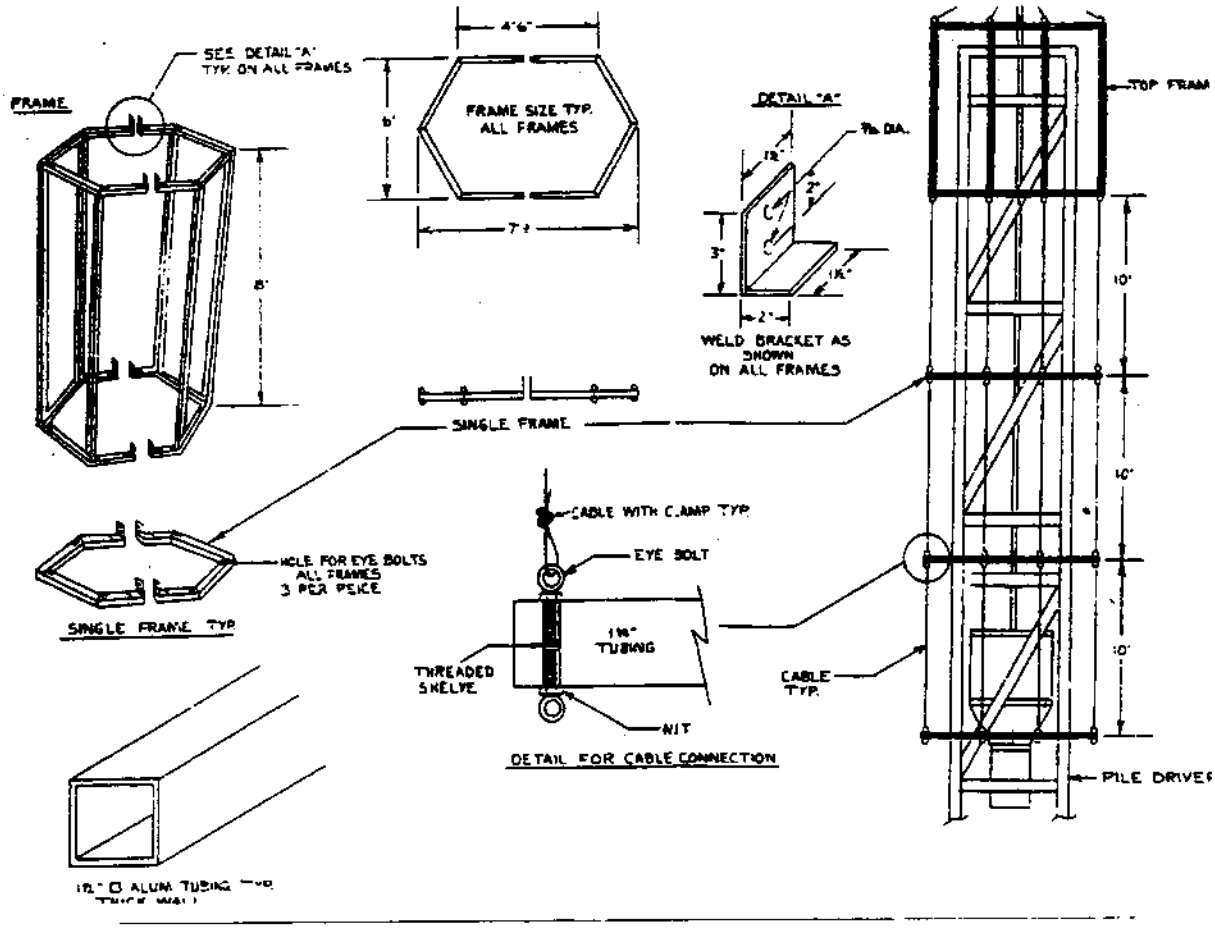


**Figure 6. Curtain and frame assembly (courtesy of ENC)**

The curtain was allowed to swing open one side so that new piles could be easily slipped in under the pile hammer, and the curtain was pulled closed when the pile was in place to ensure total closure and maximum noise absorption. Figure 7 shows a picture sequence outlining the procedure followed to secure the curtain around the pile driving apparatus.

**Figure 7(a). Assembling the curtain from rectangular panels connected together by Velcro and rope**

**Figure 7(b). Attaching the completed curtain to the crane with steel leads to the frame**

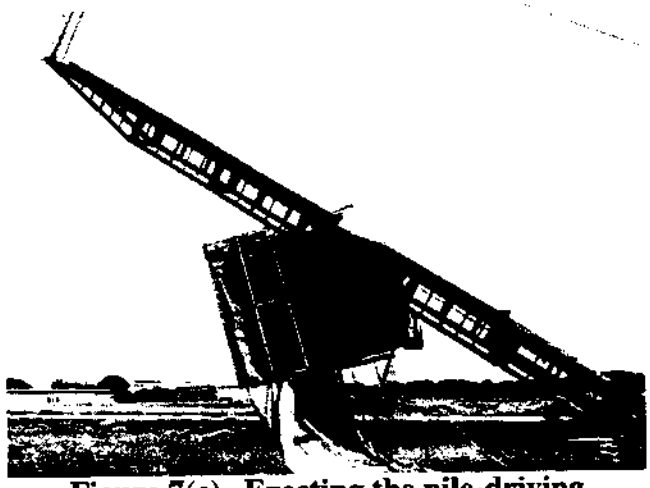

**Figure 7(c). Erecting the pile-driving frame with the curtain attached**

**Figure 7(d). Adjusting the frame to ensure the pile will be driven vertically and at the proper location**

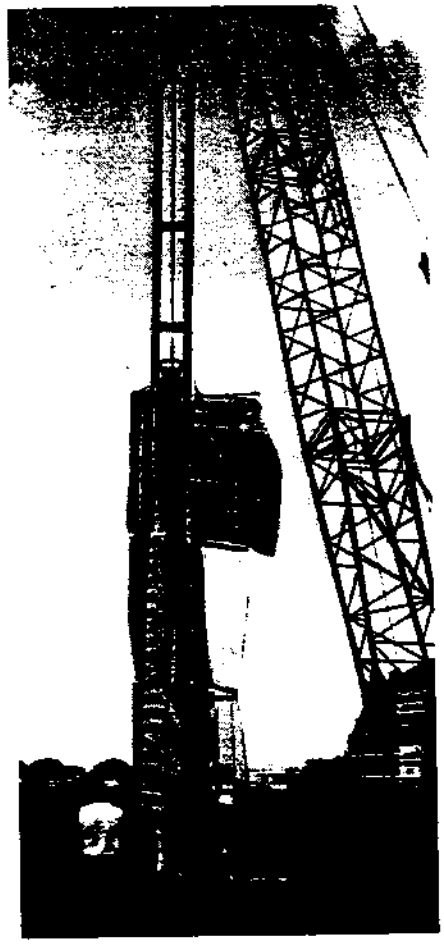

**Figure 7(e). Curtain swung open for pile installation and setup**

**Figure 7(f). Attaching the skirt to the bottom of the curtain to minimize sound propagation along the ground**

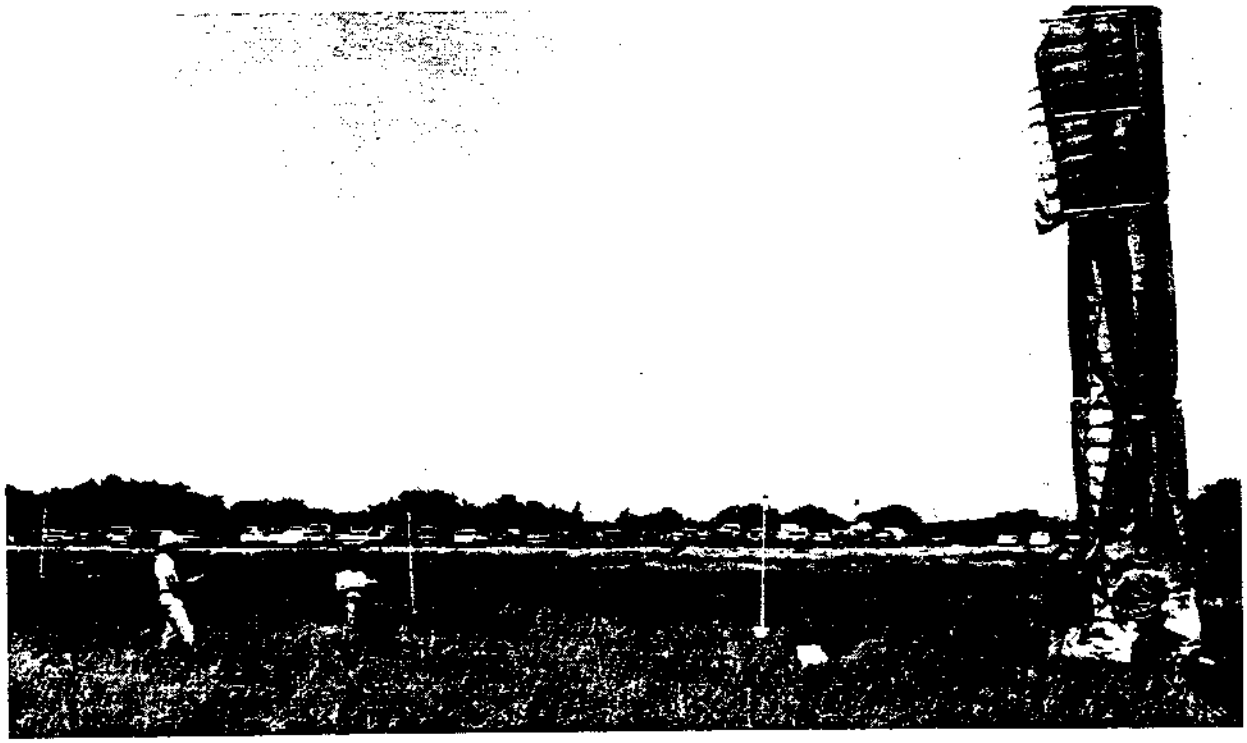

**Figure 7(g). Final field-test setup showing noise measurement poles and the acoustic curtain completely enclosing the pile driving apparatus**

### 1.3.5 Discussion and Conclusions

Based on a very limited study, it appears that the acoustic curtain provides approximately a 20 decibel reduction when total enclosure is achieved. This project has opened the doors to new area of research in the field of construction noise reduction. Through the use of practically designed curtains, FDOT can achieve a greater volume of work without adding to noise pollution, which becomes bothersome to local residents as a result of traditional construction practices. Further research should include: driving in varied soil conditions, testing different curtain materials and designs, testing with larger pile hammers and louder noise sources such as steel piles, and providing a practical method of attaching the curtain to the crane, with a design that allows for rapid installment of new piles so that the job schedule is not slowed down.

**References**

Dowding, C.H., Construction Vibrations, Prentice Hall, 1996.